NASA Technical Paper 1640

The Stratcom VIII Effort

APRIL 1980

NASA

NASA Technical Paper 1640

The Stratcom VIII Effort

Edith I. Reed, *Editor*
Goddard Space Flight Center
Greenbelt, Maryland

National Aeronautics
and Space Administration

**Scientific and Technical
Information Office**

1980

All measurement values are expressed in the International System of Units (SI) in accordance with NASA Policy Directive 2220.4, paragraph 4.

PREFACE

The Stratcom program has been conducted around the concept of a multiparameter study of the stratosphere using various sensors and platforms as appropriate. The Stratcom VIII effort concentrated on photochemical problems and included many types of instruments on the ground, on balloons, on rockets, and on aircraft. This effort was conducted in the vicinity of Holloman Air Force Base, New Mexico, in late September 1977.

The introductory sections of this publication provide information on Stratcom VIII objectives, operations, and related engineering and meteorological data, with the main body of the report composed of papers specific to each experiment. This report supersedes two earlier publications: "Stratcom VIII Scientific Objectives and Mission Organization" (Reed, 1977) and "Stratcom VIII Data Workshop, April 13–14, 1978" (Reed, 1978), including most of the information in these and much additional data. Appreciation is expressed to the U.S. Army, White Sands Missile Range, New Mexico, for the photographs on pages 28, 29, 35, 36, 129, 159, 160 and 187.

CONTENTS

ELECTRONS, IONS, AND AEROSOLS

PAYLOAD ENVIRONMENT

HIGHLIGHTS OF THE STRATCOM VIII RESULTS

Edith I. Reed
NASA, Goddard Space Flight Center
Greenbelt, Maryland 20771

INTRODUCTION

The primary objective of the Stratcom program is the study of stratospheric photochemistry. The 1977 effort took place in late September in the vicinity of Holloman Air Force Base, New Mexico. Emphasis was placed on the ozone–nitrogen oxides–ultraviolet flux interactions. Secondary objectives were the study of the balloon and payload environment, the comparison of independent measurements of ozone and nitrogen oxides, and the development of new sensor systems.

The platforms included two large balloons, a U–2 aircraft, several scientific rocket payloads, and numerous meteorological rockets and balloons. The Stratcom VIII–A large balloon carried instruments from several laboratories with emphasis on in situ observations; released from its payload were three parachute–supported packages. The Stratcom VIII–B large balloon carried the payload assembled by D. Murcray and his colleagues from the University of Denver; this payload was primarily for the observations of the infrared solar absorption spectra during sunset. The U–2 aircraft from the Ames Research Center carried an infrared spectrometer, the SAS–II instrument for NO, NO_2 and O_3, and aerosol collectors. Rocket payloads were for ozone content, conductivity, and ion mobility.

It should be noted that the Stratcom VIII effort was a cooperative program with the Atmospheric Sciences Laboratory providing leadership and, jointly with NASA, integration and launch. Each experimenter was responsible for obtaining funds for his institutional support, instrumentation, travel, and data analysis. Appreciation is expressed to each participant for making the details of his results available so that a better understanding of these phenomena may be obtained.

OZONE MEASUREMENTS

The Stratcom VIII effort included 18 sensors for the observation of ozone as described in Table 1. Of the 18 instruments, four provided no useful data on ozone: two because the tape recorder in the dropsonde failed, one of the Rhodamine–B instruments on the A–balloon was erratic for unknown reasons, and various objects in the field of view excessively degraded the data from the balloon–borne Recoz photometer. The low sampling rate and the noise level of the back–up telemetry system on the B–balloon payload did not permit interpretation of the infrared spectra in terms of ozone. Data from the U–2 infrared spectrometer and from one of the ultraviolet instruments have not yet been analyzed in terms of ozone content. Data from the Dasibi instrument was limited by

Table 1
Ozone Instruments

Instrument	Platform	Principle	Status of Data
Overburden measurements			
Dobson spectrophotometer	Ground	UV	Final
SenTran filter photometer	Ground	UV	Final
Spectrometer	U-2	IR	Not Reduced
Rocoz photometer	Super Loki	UV	Final
Filter photometer	Dropsonde	UV	No data
Spectrometer	B-balloon	IR	Noisy telemetry
Spectrometer	A-balloon	UV	Final
Spectroirradiometer	A-balloon	UV	Final
Filter photometer	A-balloon	UV	Not reduced
Rocoz photometer	A-balloon	UV	Final
In situ measurements			
ECC	small balloon	Electrochem. cell	Final
MAST	small balloon	Electrochem. cell	Final
SAS-II	U-2	Chemilum(NO)	Final
Chemiluminescent	Arcas	Rhodamine-B	Final
Chemiluminescent	Dropsonde	Rhodamine-B	No data
Chemiluminescent (2 instruments)	A-balloon	Rhodamine-B	Final; one failed
Dasibi	A-balloon	UV cell	Preliminary

intermittent pump operation. The investigators themselves question the ozone data from the Rhodamine-B instrument above 40 km. Not all of the remaining observations are independent, in that the MAST calibration factor was normalized so that total column ozone matched the Dobson observations, and the Rhodamine-B profiles were normalized to match the MAST profile in the 20 to 25 km region.

Table 2 lists an analysis of the available data as taken from the sections by Randhawa, Simeth, Manion, Ainsworth, Sellers, et al., Mentall and Zak, Krueger et al., and Loewenstein, et al., representing data from 11 systems on 6 different platforms.

Table 2
Ozone Data from the Stratcom VIII Effort

		Ozone Density (molecules/meter^3)				
Source	Total O_3 (atm-cm)	20 km	25 km	30 km	35 km	40 km
Dobson	0.279					
SenTran	0.282					
ECC	0.280	3.95	4.30	2.74	1.40	
MAST		2.3 (18)	4.0 (18)	2.6 (18)		
Dasibi						4.06(17)
Chemilum (A-balloon)						
Ascent		3.7 (18)	4.0 (18)	2.6 (18)	1.3 (18)	5.0 (17)
Descent					0.92(18)	6.3 (17)
Chemilum (Arcas)		2.8 (18)	4.0 (18)	2.0 (18)	1.3 (18)	6.7 (17)
UV spectrometer					1.3 (18)	6.2 (17)
UV spectroirradiometer		2.8 (18)	5.4 (18)	2.9 (18)	1.5 (18)	8 (17)
ROCOZ (Super-Loki)		3.14(18)	5.19(18)	3.84(18)	1.91(18)	6.77(17)
SAS-II		3.0 (18)				
Average	0.280	3.1 (18)	4.5 (18)	2.8 (18)	1.4 (18)	6.1 (17)
US Standard (1976)	0.345	4.77(18)	4.28(18)	2.52(18)	1.40(18)	6.07(17)
Max/Min	1.01	1.7	1.4	1.9	2.1	2.0

PAYLOAD ENVIRONMENT

Some properties of the atmosphere appear to be disturbed by the presence of the balloon and payload, making in situ measurements representative of the atmosphere possible only during relatively rapid ascent and descent rates, such as were achieved in the small meteorological balloons and parachute dropsondes, and as was planned for the Stratcom VIII-A payload. This is strikingly evident in the data for water vapor (Goodman) which show values of 0.3 to 6 ppmw in the 20 to 40 km region when observed from a rapidly descending dropsonde. But a sensor on the apex of the Stratcom VIII-A balloon during its relatively slow ascent provided values of about an order of magnitude higher. The sensors near the Stratcom VIII-A principal payload indicated that the water vapor content in the immediate vicinity of the payload was generally several orders of magnitude greater than ambient, but decreasing as a function of time.

The air temperature sensors on the Stratcom VIII-A principal payload (Ballard, Ainsworth) all indicated temperatures similar to those measured by meteorological sondes up to about 20 km. During the day, the air temperature at 40 km near the payload was 10 to 20 K warmer than meteorological sonde temperatures; during the slow descent near sunset the temperatures became nearly equal; in the early morning hours, near 30 km, temperatures near the payload became less than those indicated by meteorological sondes. This behavior of the air around the balloon and payload is consistent with that observed during earlier Stratcom efforts and can be associated with surface temperatures of the balloon.

ADDITIONAL RESULTS

1. The nitric acid column density between 30° and 40°N latitude is consistent with observations at higher and lower latitudes (Murcray and Barker).

2. Young aerosols, as indicated by a bimodal distribution of aerosol sizes, are not restricted to tropical latitudes as previously thought (Farlow, et al.).

3. Water vapor in the stratosphere is layered and in the range of 0.3 to 6 ppm (Goodman).

4. A 20 percent perturbation in the ozone content at about 37 km during sunset was observed by one sensor (Randhawa).

5. The orography of mountainous terrain affects air flow to altitudes of at least 40km (Freeman).

6. The enhancement of ion mobilities by Krypton lamp illumination could not be attributed solely to NO; alternative explanations are being explored (Hale and Croskey).

7. The observations of CO_2 emissions and air temperature are being used for the development of improved algorithms for the conversion of CO_2 emission to air temperatures at stratospheric altitudes (Murcray et al.).

8. The Stratcom–VIII experience was a key factor in the development of several observing systems which have since been used successfully:

- A dropsonde for the chemiluminescent measurement of NO (Shaw).
- A filter photometer for the ground–based measurement of total ozone (Simeth).

THE STRATCOM PROGRAM

Frank P. Hudson
Environmental Research
Department of Energy
Washington, D.C. 20545

Harold N. Ballard
Atmospheric Sciences Laboratory
U.S. Army Electronics Command
White Sands Missile Range
New Mexico 88002

ABSTRACT

The Stratcom series of balloon flights, initiated in 1968 with a 30-kg payload for the measurement of stratospheric temperature, pressure, ozone, and winds, has evolved into a multiplatform effort for measurement of more than 20 parameters of interest to stratospheric studies. This overview of the 10-year program, outlines the goals, organization, modus operandi, and accomplishments of the series.

INTRODUCTION

Stratcom (Stratospheric Composition) is a long-term, multi-purpose program for integrated, correlated measurements of stratospheric parameters related to composition, thermodynamics, and radiative balance. It is a joint undertaking of several laboratories whose combined scientific, engineering, and field capabilities make possible an extensive program of multiple related measurements in the very complex and variable stratosphere. It emphasizes correlated in situ measurement of critical parameters, because measurements of related parameters under the same conditions facilitate sound interpretations leading to a better understanding of atmospheric processes and their roles.

Balloon platforms are used because they are well-suited for carrying complex payloads into the altitude region of interest and remaining there for a period of time. The series of flights were planned to cover the 10 to 50 km (33,000 to 164,000 ft) altitude range, from 10° to 65°N latitude, at all seasons of the year. Changes in measurements as a function of altitude and at sunrise/sunset are of particular interest. Longer term flights are launched during the stratospheric wind turnaround periods in spring and fall.

Other modes of measurement and platforms are included to permit better altitude and regional coverage. This includes remote sensors and ground, aircraft, rocket, parachute, and satellite platforms.

The principal reason for combining the talents and resources of the several laboratories is to make the required complex operation possible, but some secondary benefits are of considerable importance: (1) the value of each experiment is enhanced because of the availability of measurements, at the same time and place, of related parameters; (2) the unification of operational and engineering needs to serve a number of experiments at one time permits a large saving in both time and money; (3) the recoverable, reusable system provides a common background for later similar experiments under other selected conditions of altitude, latitude, and season for comparative purposes; and (4) a body of data, acquired under common conditions, is available for direct use in developing and validating models in contrast to the usual use of statistical means of disparate data, thus providing insight into the balance between photochemical equilibrium and dynamic processes.

PURPOSES

In addition to the goals requiring data from many sensors, there are goals unique to each participating laboratory. These range from pure science to development of the operational methods. There is much overlapping of goals and many degrees of mutual support. Included are:

1. Measurements of species densities, solar ultraviolet flux, and thermodynamic properties for basic understanding of atmospheric processes.

2. Development and validation of photodissociation and chemical kinetic models of the stratosphere.

3. Determination of natural variations of parameters, and relationship to altitude, latitude, time-of-day, season-of-year, and other time cycles.

4. Development of understanding of meteorology of the stratosphere.

5. Study of parameters important to stratospheric pollution from aircraft, fluorocarbon chemicals, and other sources.

6. Development and calibration of instruments for rocket and parachute payloads can be extended to potential satellite instrumentation.

7. Study of the perturbed atmosphere for defense studies.

8. Development of instrumentation, platforms, and field operational methods for defense oriented studies.

9 Development of methods for meso-scale pollution studies in the troposphere.

HISTORY

The sequence of Stratcom experiments was initiated in 1968 by the Army's Atmospheric Sciences Laboratory (ASL), White Sands Missile Range (WSMR), under the direction of Harold N. Ballard. The eight flights in the Stratcom Program were as follows:

Flight	Date	Location	Purpose
I	September 11, 1968	HAFB, New Mexico	T, P, O_3, winds
II	September 22, 1969	HAFB, New Mexico	T, P, O_3, winds
III	September 18, 1972	HAFB, New Mexico	many parameters
IV	October 19, 1973	Palestine, Texas	H_2O and NO
V	May 22, 1974	HAFB, New Mexico	H_2O and NO
VI	September 24, 1975	HAFB, New Mexico	many parameters
VII	September 27, 1976	HAFB, New Mexico	many parameters
VIII	September 28, 1977	HAFB, New Mexico	many parameters

The first flight in September 1968 carried a payload of 30 kg (66 lb) of instrumentation at an altitude of 50 km, the top of the stratosphere. The principal goals were the study of atmospheric motions, diurnal temperature variations, thermodynamics, and ozone density. A similar flight, with upgraded instrumentation, was made in September 1969 (References 1, 2, 3, and 4). The Aerospace Instrumentation Laboratory, Balloon Branch, of the Air Force Cambridge Research Laboratory provided balloon design, launch operations, and flight control. The WSMR facilities provided necessary range support.

In 1971, the AEC's Sandia Laboratories, Albuquerque, New Mexico (SLA), was invited to participate. Experimentally this added mass spectrometry and ultraviolet spectroscopy; and, of fundamental importance, this made available the extensive instrumentation development and field experimentation experience and facilities of Sandia. At this point, the correlated multi-instrument approach, backed by theory and modeling, was initiated. The September 1972 flight, Stratcom III, carried 17 instruments with a payload weight of 118 kg (260 lb) to 48.7 km altitude for 9 hrs of measurement with all instruments functioning successfully (References 5, 6, and 7).

Stratcom IV and V, October 1973 and May 1974, were special-purpose flights dedicated to the use of Bell Telephone Laboratory's tunable spin-flip Raman laser for the measurement of stratospheric H_2O and NO (References 8 and 9). Stratcom IV was launched at Palestine, Texas with the support of the National Scientific Balloon Facility.

The Stratcom VI operation, September 24 to 26, 1975, returned to the multi-parameter approach. For the first time, other platforms were included in the effort: a second large balloon, the U-2 aircraft, and research payloads on rockets. Several laboratories added instruments; the relationship with other measurement programs was enlarged. An ideal flight profile was realized on the major balloon; about 85 percent instrumentation success was obtained; and an excellent, highly adaptable

system usable for future flights at other altitude ranges, latitudes, and seasons of the year was developed and proved.

The Stratcom VI-A Balloon was launched from Holloman AFB, New Mexico (32°N., latitude), at 2357 on September 23, 1975. Peak altitude of 38.7 km was attained at about 0300 on September 24. The instruments were turned on intermittently during ascent, and continuously for a period of 1 hr before to 1 hr after sunrise. Periodic measurements were made at float altitude and during a slow descent initiated at about 1100. A 2-hr measurement period through sunset at about 25 km altitude was followed by an ascent to 36.6 km for a 2-hr sunrise measurement period on September 25. The scientific payload was brought down by parachute from 1000 to 1035 with all instruments turned on. Recovery of the intact payload in excellent condition was near Springeville, Arizona. Balloon VI-B was launched at 1500 on September 26 to provide infrared absorption measurements through sunset. The U-2 aircraft flight pattern was at 18.3 and 21.3 km, under Balloon VI-A, on September 24 (References 10, 11, 12, and 13).

The Stratcom VII operation, September 28 to 29, 1976, was again a broadly based series of measurements including the flight of two large balloons and several closely related rocketsondes. This series of measurements was especially interesting because the ascent and descent portions of the Balloon VII-A flight occurred under contrasting conditions of vertical wind, providing data on two quite different stratospheric regimes. Balloon VII-A, carrying 26 instruments, was launched at 0730 MST on September 28 from Holloman Air Force Base.

The peak altitude of 39 km was reached before noon for a series of measurements at that altitude. The principal measurements were made during a slow descent to 18 km, with measurements at that altitude during sunset. The payload rose to 23 km during the night for a series of measurements at sunrise on September 29 and during the 40-minute parachute descent after cutdown at 1030. The payload was successfully recovered about 20 km north of the launch site. All instruments operated as planned. Balloon VII-B carrying the infrared spectrometer and a Fourier-transform interferometer spectrometer, was launched on September 30 for measurements through sunset. Rocketsonde measurements of ozone, temperature, pressure, and electrical conductivity were made on September 28 in the altitude range of 60 to 10 km.

The Stratcom VIII operation followed a somewhat similar pattern, but with additional ozone sensing systems (ground, aircraft, rocket and balloon; remote and in situ) so as to provide a broad comparison of techniques. The effort and the preliminary results are the subject of the remaining sections of this document. A list of papers, reports, and presentations related to the entire Stratcom program is given in the Bibliography section.

CONCLUSION

The Stratcom program has been conducted around the concept of a multiparameter study of the stratosphere using various sensors and platforms as appropriate. In addition to the scientific results from these flights, these efforts have been invaluable for the training of new experimenters and for the development of new measurement systems.

REFERENCES

1. Randhawa, J. S., "Ozone Measurements from a Stable Platform near the Stratopause Level," *J. Geophys. Res.*, **74**, 1969, pp. 4588–4590.

2. Ballard, H. N., N. J. Beyers, M. Izquierdo, and J. Whitacre, "A Constant-Altitude Balloon Experiment at 48 km," *J. Geophys. Res.*, **75**, 1970, pp. 3501–3512.

3. Randhawa, J. S., "Ozone Measurements near Sunrise," *Nature* (Phys. Sci.) **233**, 1971, p. 101.

4. Ballard, H. N., N. J. Beyers, B. T. Miers, M. Izquierdo, and J. Whitacre, "Atmospheric Tidal Measurements at 50 km from a Constant-Altitude Balloon," *J. Appl. Met.*, **11**, 1972, pp. 1138-1149.

5. Ballard, H. N., M. Izquierdo, C. McDonald, and J. Whitacre, "Atmospheric Temperatures Measured Near 48 km by Balloon-Borne Thermistors," Proceedings, Eighth AFCRL Scientific Balloon Symposium, 30 September to 3 October 1974, AFCRL-TR-74-0393, A. S. Carten, Jr., Editor, pp. 401–416.

6. Ballard, H. N., F. P. Hudson, "Stratospheric Composition Balloon-Borne Experiment, 18 September 1972," ECOM-5554 U.S. Army Electronics Command, Fort Monmouth, N.J., January 1975, AD-A008021, 112 pp.

7. Randhawa, J. S., and M. Izquierdo, "Ozone Measurements at 48 km," *J. Photochemistry*, **6**, 1976, p. 148.

8. Patel, C. K. N., E. G. Burkhardt, and C. A. Lambert, "Spectroscopic Measurements of Stratospheric Nitric Oxide and Water Vapor," *Science*, **184**, 1974, pp. 1173–1176.

9. Burkhardt, E. G., C. A. Lambert, and C. K. N. Patel, "Stratospheric Nitric Oxide: Measurements During Daytime and Sunset," *Science*, **118**, 1975, pp. 1111–1113.

10. Williams, W. J., J. J. Kosters, A. Goldman, and D. G. Murcray, "Measurements of Stratospheric Fluorocarbon Distributions Using Infrared Techniques," *Geophys. Res. Lett.*, 3, 1976, pp. 379-382.

11. Ballard, H. N., and F. P. Hudson, "Stratospheric Composition Balloon-Borne Experiment, 23-26 September 1975," ECOM-5830, U.S. Army Electronics Command, Fort Monmouth, N. J., October 1977, 119 pp., AD-A049030.

12. Collins, Jerry L., "Stratcom-Related Photodissociation Rates and Solar Flux Intensities," ECOM 77-1, U.S. Army Electronics Command, Fort Monmouth, N. J., February 1977, 32 pp., AD-A037644.

13. Ballard, H. N., J. M. Serna, and F. P. Hudson, "Calculation of Selected Atmospheric Composition Parameters for the Mid-Latitude, September Stratosphere," ECOM 5818, U.S. Army Electronics Command, Fort Monmouth, N. J., May 1977, 41 pp., AD-A041081.

THE STRATCOM VIII EFFORT

Edith I. Reed
NASA, Goddard Space Flight Center
Greenbelt, Maryland 20771

Harold N. Ballard
Atmospheric Sciences Laboratory
U.S. Army Electronics Command
White Sands Missile Range
New Mexico 88002

Miguel Izquierdo
Electrical Engineering Department
University of Texas at El Paso
El Paso, Texas 79968

ABSTRACT

The Stratcom VIII objectives were to measure a number of parameters of interest to photochemical studies, to study the payload environment, to compare various sensor systems for ozone and for nitric oxide, and to provide a platform for development of new sensor systems. In all, more than 40 instruments were included for the observations of about 30 parameters and involved the cooperation of at least 20 organizations. General descriptions of the major payloads (two large balloons) are given, showing sensor location and providing engineering data. The description of launch operations gives times, locations, and peak altitudes for the many small balloon and rocket launches and the detailed flight paths for the large balloons and the U-2 aircraft.

INTRODUCTION

The Stratcom program was conceived as a multifaceted program for the study of phenomena in the stratosphere. Some of the objectives require correlation of data from diverse sensor systems; other objectives are related to theoretical descriptions of the stratosphere; yet others are strictly engineering.

The organizers of the Stratcom VIII effort, Harold Ballard and Frank Hudson, in consultation with the Upper Atmospheric Research Office at NASA Headquarters, have tried to ensure that certain parameters critical to the understanding of stratospheric structure and photochemistry are well defined; that sensor systems are complementary, being neither unduly duplicative nor grossly unrelated;

and that there is some room for the unanticipated, for serendipity. These sensor systems were deployed on a variety of platforms: two large balloons, three parachute drops, several small balloon and rocket payloads, and two U-2 flights. In addition, there are numerous meteorological sondes and various ground-based observations.

The following discussion of the Stratcom VIII effort outlines the objectives of the effort, the instruments and observations as related to these objectives, and information pertaining to field operations including vehicle parameters and flight paths.

OBJECTIVES

Photochemistry

The art of modeling photochemical phenomena in the stratosphere has made rapid progress in the past few years, largely due to concern about the effects of pollutants in the stratosphere. However, the content of the important trace constituents is highly variable, with atmospheric transport affecting those species that require a long time to reach photochemical equilibrium, and with the diurnal changes in solar radiation affecting those that have a short time constant. The prime objective of the Stratcom VIII effort was to measure a substantial number of important trace species during a single day, obtaining altitude profiles wherever feasible together with spectral measurements of the ultraviolet flux. The planned use of the platforms is shown in Figure 1.

The planned strategy was as follows:

(1) On the morning of the first day, during the ascent of Balloon VIII-A, obtain data on ozone, both in-situ and overburden, and on the UV flux, both the direct solar component and the diffuse sky flux. Continue these measurements throughout the daylight portions of the 33-hour flight of the VIII-A Balloon and continue the in-situ ozone measurements at night.

(2) Just before Balloon VIII-A reaches its maximum altitude of about 40 km in the late morning, drop two separate parachute supported payloads: First, a chemiluminescent NO and O_3 sonde with a UV filter photometer for ozone overburden and another filter photometer for Earth albedo; second, a Krypton lamb-Gerdien condenser, also sensitive to the NO content of the atmosphere. An hour or so later, near noon, drop a third parachute-supported package which includes an Al_2O_3 water vapor sensor.

(3) After Balloon VIII-A reaches float altitude, launch two scientific rocket payloads for ozone altitude profiles: the ASL in-situ chemiluminescent ozone sonde and the Rocoz filter photometer for ozone overburden. At various times fly the Mast and ECC balloon ozone sondes.

(4) Observe parameters related to ion and electron content by means of two more scientific rocket payloads. One is a Gerdien condenser and the second a blunt probe. Simultaneously,

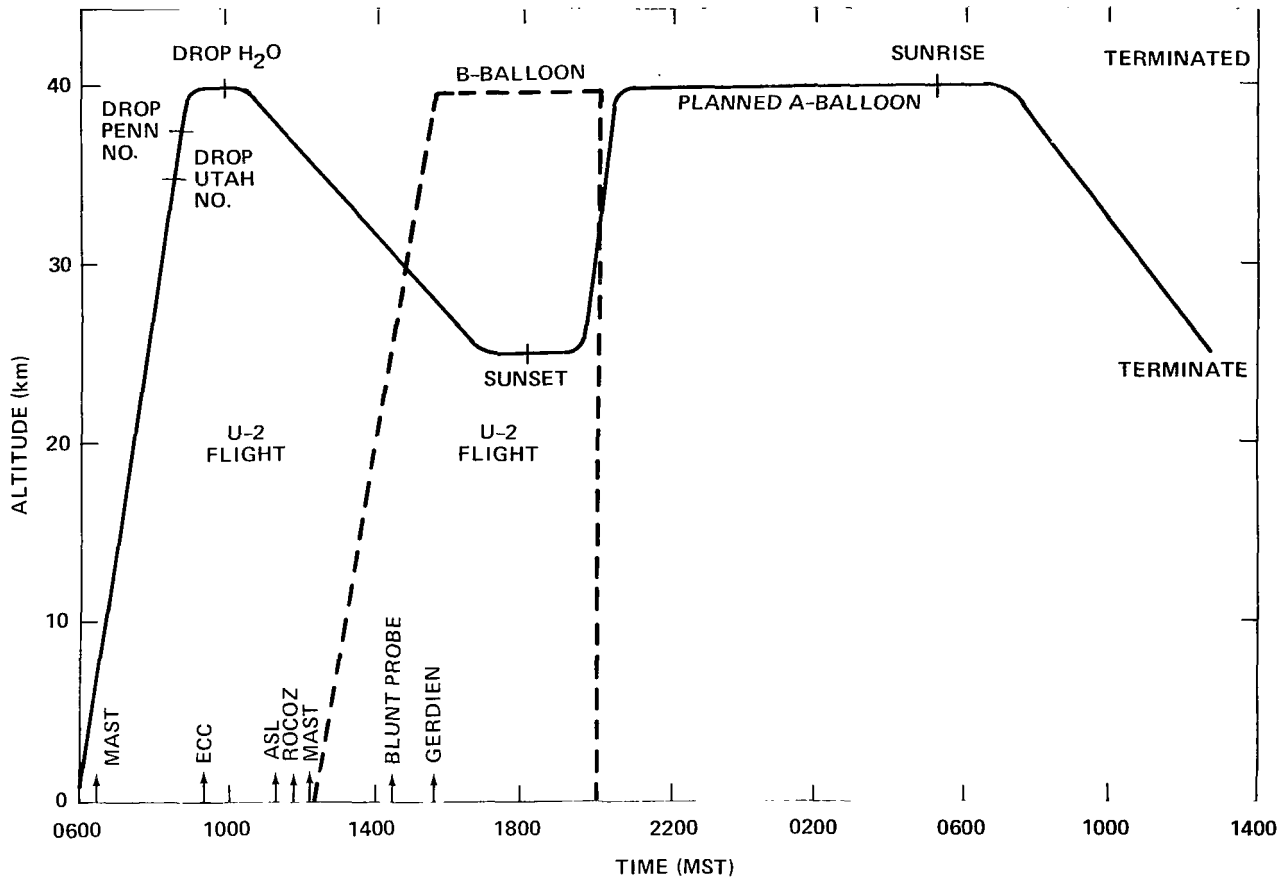

Figure 1. Planned Stratcom VIII effort involving two large balloons (A and B), U-2 flights, and, as indicated by the short arrows, several small balloon and rocket flights.

use similar instruments on the Balloon VIII-A and, from the ground, the partial reflection and the C-3 ionosondes.

(5) Observe structural parameters (pressure, air temperature, and winds) from Balloon VIII-A by temperature and pressure sensors, from Balloon VIII-B by pressure and two types of temperature sensors, and by means of meteorological rockets and balloons.

(6) Observe the radiative balance in the visible and IR regions with broad spectrum pyranometers at the top of the balloon, below the gondola, and on the ground.

(7) In the early afternoon, open helium valves at the top of Balloon VIII-A to permit it to descend slowly to about 25 km. During the descent, collect seven air samples by means of a cryogenic sampler for later analysis of fluorocarbons (CFM's) N_2O, CO, CO_2, CH_4, H_2, and H_2O. Simultaneously, use an on-board gas chromatograph to provide data on halogen compounds: CCl_4, CH_3Cl, chloroforms, and CFM's. If the gas chromatograph is not ready for this flight, fly a second cryogenic sampler, increasing the total number of air samples to 14.

(8) Meanwhile, also in the afternoon of the first day of Balloon VIII-A, launch Balloon VIII-B, so that the altitude profile of various constituents may be observed remotely during sunset. The spectral range to be observed is chosen to provide data for NO, NO_2, N_2O, HNO_3, O_3 and possibly on N_2O_5 and $ClONO_2$.

(9) If the flights occur before October 1, as Balloon VIII-A nears 40 km fly one and possibly two U-2 aircraft containing stratospheric sensors at altitudes near 20 km in the vicinity of White Sands Missile Range (WSMR) for a period of about 1 hour. The IR spectrometer on the U-2 covers a spectral range chosen to obtain data on HNO_3, CH_4, CFM's, and N_2O. Additional sensors will be used to observe water vapor and to collect aerosols for later examination. A chemiluminescent sensor (SAS-II) for NO, NO_2, and O_3, and a cryogenic sampler to collect air samples for later analysis for N_2O, CFM's, CCL_4, and possibly $CHCl_3$ and CH_3CCl_3 may also be flown.

(10) After sunset, permit Balloon VIII-A to rise to well above 30 km by the release of ballast. Continue to observe ozone with the two in-situ systems. Just prior to sunrise of the second day, again turn on the solar UV instruments to provide data on the UV flux and the ozone overburden. Descend in mid-morning, with the gas chromatograph again providing data on a number of halogen compounds.

The set of data resulting from this strategy should be highly valuable for checking the ability of a photochemical model to produce altitude profiles of the various trace species consistent with the observed UV fluxes and trace species, over the diurnal cycle. A model expressly for this purpose, that is, for the computation of the distributions of trace species for specific places and times, has been constructed by F. Hudson for use with these data.

Much, but not all, of this plan was carried out from September 28 to 30 from the Holloman Air Force Base and the White Sands Missile Range. Both large balloons were launched, Balloon VIII-B on the afternoon of September 28, and Balloon VIII-A the next morning. On Balloon VIII-A, a second cryogenic sampler replaced the gas chromatograph. This balloon did not descend as planned (neither the helium valves nor ballast release were operable) so that the samplers obtained data on the extent of contamination near the gondola rather than on the stratospheric trace species. Most of the ozone sensors provided data. Telemetry terminated after 24 hours, precluding daylight observations during the second day of flight. The cryogenic sampler and the H_2O sensors did not fly on the U-2, but water vapor data are available from the third parachute drop. Data were obtained from the rocket flights of the two types of ozone sensors and from the blunt probe, but not from the Gerdien condenser. Both the Mast and the ECC balloon ozone sondes provided data. One U-2 made two flights, about 12 hours apart, obtaining aerosol samples, ozone content, and, on the second flight, infrared spectra.

Those aspects of photochemistry relating to ultraviolet emissions, O_3, HO_x (H_2O, CH_4), and NO_x (HNO_3, N_2O, and possibly NO_2) may make use of the Stratcom VIII observations on these species. Disappointingly, none of the four sensors planned for NO observations provided useful data, nor will there be data on the chlorine compounds. Of particular interest was the unexpected bimodal distribution of aerosol sizes hitherto found only in tropical regions (a "dry" stratosphere with water vapor

on the order of 1 ppmv from 25 to 38 km), and the further evidence that solar radiation at wavelengths corresponding to the 220 nm atmospheric window varies with solar activity.

Balloon Environment

Two aspects of the balloon environment are important to experimenters: (1) the orientation and thermal history and (2) composition and temperature perturbations to the atmosphere in the immediate vicinity of the balloon.

The payload of Balloon VIII-A was designed to minimize perturbations to the environment by the use of pressure-tight containers, nonporous surfaces, and the avoidance of the excessive use of foamed materials and adhesive tapes. During its planned 33-hour flight, the balloon and payload would experience diurnal changes in radiation and several planned changes in altitude. The strategy for environmental studies is as follows:

(1) Include temperature sensors in several of the experimental packages, on the frame of the gondola, and on the balloon film near its apex. The packages have varying surface finishes, insulation, and internal heat dissipation.

(2) Include a pyranometer at the top of the balloon to measure thermal energy coming from above, and also on the base of the gondola to measure energy coming from below.

(3) Include a levelness indicator on the top of the balloon to monitor its variations in tilt.

(4) Include a 3-axis anemometer in the main payload to sense air motions relative to the payload both during altitude changes and at float.

(5) Measure air temperatures at the top of the balloon and just below the main payload.

(6) Measure water vapor content at the top of the balloon near the payload and a short distance below the payload. Compare these data with the water vapor profiles as measured by the sonde dropped from the payload.

The data on package temperatures and energy input can be used in thermal studies. The data on air temperatures and water vapor content may be used in developing and confirming a model at Langley Research Center (R. Davis) describing the behavior of the boundary layer associated with the balloon.

During the flight of Balloon VIII-A, these data were obtained from the main payload for 24 hours, from the package at the top of the balloon for 3 hours, and from the water vapor dropsonde. Because the planned mid-flight descent rate was much less than planned, analysis of the cryogenically collected air samples provided information on the nature and density of the trace gases associated with the payload.

Comparison of Techniques

The Stratcom VIII effort was unique in the large number of platforms, (balloons, rockets, aircraft, and ground-level) planned for use in a short period of time, limited primarily by the availability of telemetry frequencies, ground stations, and tracking capabilities. This effort provided the opportunity for the comparison of techniques, some well proven, some in the infancy of their development. Prime emphasis was given to techniques for the measurement of ozone and included several that have been widely used. Several systems for NO were included, all with relatively short histories of experience. The results of two cryogenic air sampling systems, prepared and analyzed by different groups, and the results from a balloon-borne gas chromatograph for many of the same species were planned to be complementary to each other.

Ozone

The VIII-A Balloon was the principal platform for ozone sensors and included three in-situ (two identical chemiluminescent sondes and the Dasibi ozone monitor) and four remote (the CSU/GSFC filter photometer, the USU filter photometer, the Panametrics filter photometer, and the Sandia/GSFC spectrometer) sensors. A second type of remote measurement of ozone can be obtained from the IR solar absorption spectrometer of the VIII-B Balloon; during ascent the ozone is deduced from the change in overburden, and during sunset, from the absorption as a function of elevation angle. The U-2 aircraft included the SAS-II chemiluminescent sensor and infrared observations of ozone overburden. Auxiliary launches provided additional vertical profiles and range. The parachute-dropped NO sonde included a USU filter photometer for ozone and an engineering model of the chemiluminescent ozone sonde. Standard meteorological-type rocket payloads, one with the chemiluminescent ozone monitor and one with the UV filter photometer, were flown. These rockets extended the altitude range well above the balloon maximum altitude of about 40 km. The Mast and the ECC balloon-borne ozone sondes provided additional profiles of ozone in the troposphere and lower stratosphere. Finally, the total ozone was monitored from the ground with the Dobson spectrophotometer and an engineering model of a UV filter photometer. There was a faint possibility that the Nimbus-4 BUV ozone spectrometer would obtain data in the vicinity of the Stratcom VIII flights. There have been previous "fly-offs" among sondes for meteorological balloons, among rocket sondes, and among satellite instruments, but none with the heavy emphasis on the balloon systems in the stratosphere.

Of the 18 ozone sensors, almost all provided data as needed for the comparison of techniques. Only those on the first parachute drop (a chemiluminescent sonde and a UV filter photometer) did not result in data. However, similar instruments on the main gondola did provide data. The Mast balloon sondes provided a tropospheric ozone profile on September 29 and a profile up to 10 mb (millibar) in the stratosphere on September 30. Nimbus-IV, with the BUV instrument, did not happen to be near HAFB during the days of flight.

Nitric Oxide

The remote sensing of NO with an infrared spectrometer (Balloon VIII-B) has been done for several years; likewise, the U-2 aircraft-borne SAS-II chemiluminescent instrument has had considerable

flight experience. The parachute-dropped chemiluminescent sonde is a new system. The potential of the Krypton lamp-Gerdien condenser system for NO observations is not yet well understood. In the Stratcom VIII flights, simultaneous observations by the various systems would permit comparison of data from three different techniques and would be a major step in the engineering and proof of the parachute drop system. The comparison of NO techniques was not successful: there was more noise than expected in the infrared spectra from Balloon VIII-B; on one U-2 flight the cryogen system for the IR spectrometer malfunctioned; the SAS-II instrument had an electronics problem in the NO system; the tape recorder on the chemiluminescent dropsonde failed; and the Krypton lamp-Gerdien condenser rocket failed to reach its expected altitude.

Cryogenic Samplers and In-Situ Gas Chromatography

These systems on Balloon VIII-A and the U-2 are comparable in the sense that, for both, gas chromatography is used in the analysis of the contents of the collected samples; hence, both techniques provide values on the CFM's, N_2O, CCl_4, and some other species. Because one sampler and the gas chromatograph were planned for Balloon VIII-A, collecting in the 25- to 40-km range, and the other on the U-2, at least 5 km lower, the data would not be simultaneous in place; the U-2 data may be used to extend the balloon data to a lower altitude. The balloon-borne version of the gas chromatograph is new; this flight should have confirmed the considerable engineering accomplishment. However, the gas chromatograph was not ready and was replaced by a second cryogenic sampler. The U-2 cryogenic sampler was not flown because only one U-2 was available.

Engineering and Exploratory

There were some instruments in the Stratcom VIII effort which were included for engineering and exploratory purposes. Two infrared radiometers, at the 4.3- and 15-μm emission lines of CO_2, were flown in order to obtain data for use in developing better inversion techniques for air temperatures. Data from these radiometers will be compared with balloon and rocket-borne in-situ temperature measurements. A Lyman-alpha sensor (121.6 nm) was flown as part of the Top Package on Balloon VIII-A. If, perchance, it should observe substantial Lyman-alpha emission, the other data from the Stratcom VIII flights would be needed to define the circumstances under which such emissions can penetrate to balloon altitudes. Both a blunt probe and a Gerdien condenser are included for conductivity measurements; there have been some little understood changes in conductivity near sunset/sunrise which need study.

The engineering experience gained by the participation in this effort is proving valuable. Although the chemiluminescent dropsonde provided no data during this effort, its next flight was successful. The limits of the usefulness of a simple inversion algorithm for the 15-μm CO_2 radiation to air temperature have been demonstrated, and the more complete algorithm is now being developed and confirmed.

INSTRUMENTATION AND INTEGRATION

A concise summary of the parameters to be measured and the instruments for each is found in Figure 2. Table 1 provides more information about each element of the Stratcom VIII effort. It is to be

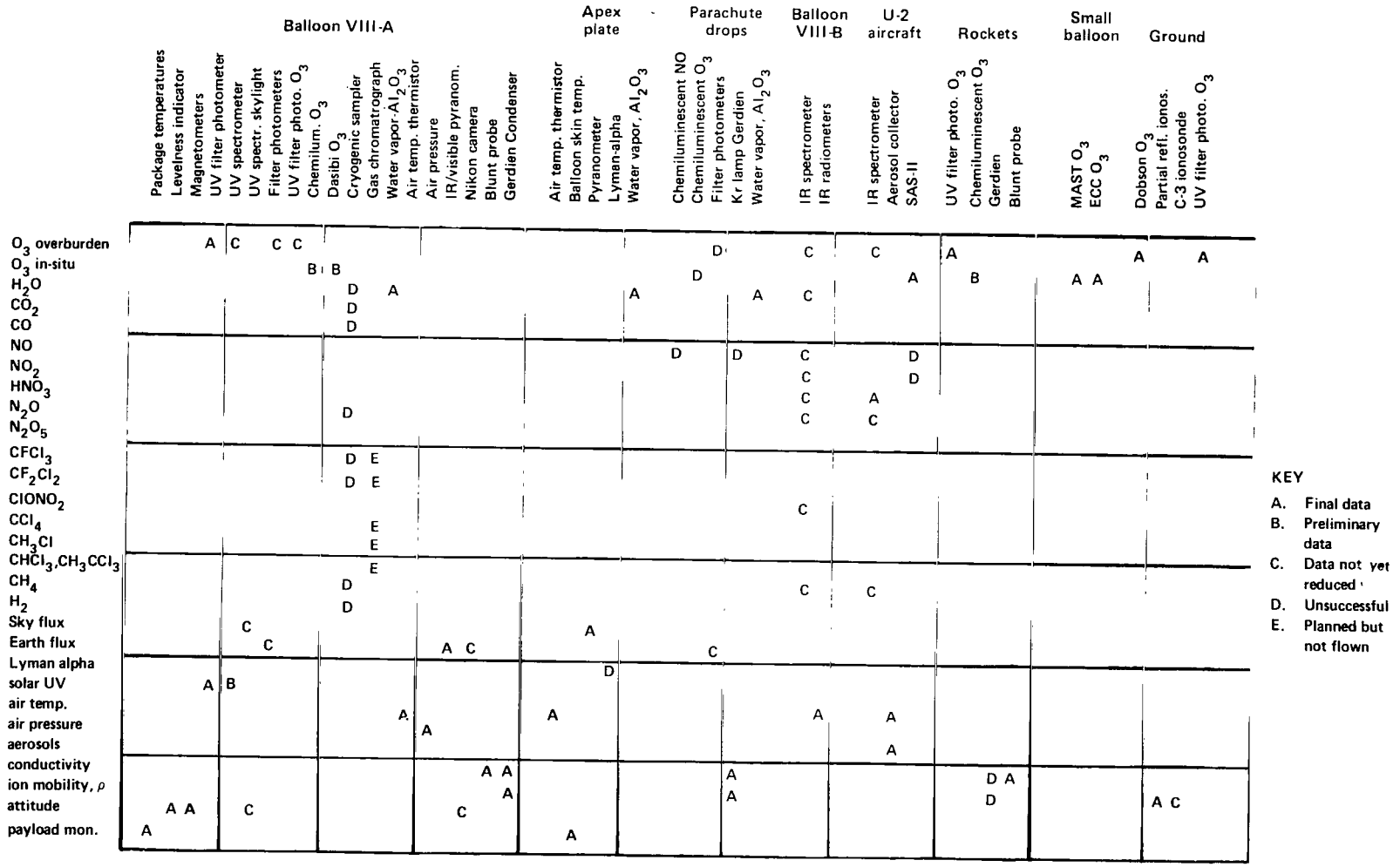

Figure 2. Parameters and instruments planned for the Stratcom VIII effort.

Table 1a
Systems, Instruments, Investigators, and Organizations

Platform	System/Instrument	Person	Organization
Stratcom VIII-A Balloon Basic System:	Balloon Design	Arthur Korn, Code LCB	AFGL
	Balloon	James Gray	NASA/WFC
	Flight Control	Duke Gildenberg	AFGL/HAFB
	Balloon Launch support	Joseph Koehly	AFGL/HAFB
	Mechanical structure	Hector Carrasco Gustavo Cordova Joseph Whitacre	UTEP
	Payload integration	Miguel Izquierdo Svi Salpeter Preston Herrington	UTEP Sandia Lab.
	Control and telemetry	Miquel Izquierdo Preston Herrington	UTEP Sandia Lab.
	Power Supply	Claude Tate	ASL
	Payload monitors Package temperature Levelness indicator Magnetometers Other monitors	Preston Herrington	Sandia Lab.
Experiments:	UV filter photometer	Bach Sellers	Panametrics, Inc.
	UV spectrometer	Bernard Zak James Mentall	Sandia Lab.
	UV spectrometer (skylight)	Rex Megill K. D. Baker Larry Jensen Jagir Randhawa	USU ASL
	Filter photometers (2)	Rex Megill	USU
	UV filter photometer ozone sonde	Arlin Krueger David Wright Peter Simeth	CSU/GSFC NASA/GSFC SenTran Co.
	Chemiluminescent ozone sonde (2)	Jagir Randhawa	ASL
	Dasibi ozone monitor	John Ainsworth	NASA/GSFC
	Cryogenic sampler	Richard Lueb Leroy Heidt	NCAR

Table 1a (Continued)

Platform	Instrument/System	Person	Organization
Experiments: (continued)	Gas chromatograph	Robert Woods Leroy Heidt Richard Lueb	Sandia Lab. NCAR
	Water vapor sensors (Al_2O_3)	Philip Goodman	Panametrics, Inc.
	Air temperature sensors	Harold Ballard	ASL
	Air pressure sensors	Harold Ballard	ASL
	IR Pyranometer (nadir)	Robert Rubio	ASL
	Visible Pyranometer (nadir)	Robert Rubio	ASL
	Nikon camera (nadir)	Robert Rubio Claude Tate	ASL
	Blunt Probe Kr Lamp Gerdien Condenser	Jack Mitchell Leslie Hale	UTEP Penn State Univ.
	Anemometer	Carlos McDonald	UTEP
	Apex plate payload: Air Temperature sensor Balloon skin temperature Lyman-alpha intensity Levelness indicator	Carlos McDonald	UTEP
	Pyranometer, IR and visible	Robert Rubio	ASL
	Water vapor sensor (Al_2O_3)	Philip Goodman	Panametrics, Inc.
	Parachute drop No. 1 Chemiluminescent NO sonde	Rex Megill Alan Shaw	USU
	Filter photometers, O_3 and albedo	Rex Megill	USU
	Chemiluminescent ozone detector	Jagir Randhawa	ASL
	Parachute drop No. 2 Krypton lamp-Gerdien Condenser	Leslie Hale Charles Croskey	Penn State Univ.
	Parachute drop No. 3 Al_2O_3 water vapor sensor	Philip Goodman	Panametrics, Inc.

Table 1a (Continued)

Platform	Instrument/System	Person	Organization
Stratcom VIII-B Balloon	IR spectrometer	David Murcray John Williams	U. Denver
	IR radiometers (air temp)	David Murcray Don Snider Robert McClatchey	U. Denver ASL AFGL
	Air temperature sensors	Harold Ballard	ASL
	Structure, telemetry, integration, power	David Murcray	U. Denver
U-2 Aircraft:	Senior contact	Leo Poppoff	NASA/ARC
	IR spectrometer	David Murcray	U. Denver
	Aerosol impact collector	Neil Farlow Guy Ferry Ken Snetsinger	NASA/ARC
	SAS-II (NO, NO_2, O_3)	Max Loewenstein Walter Starr	NASA/ARC
Super Loki rocket:	UV filter photometer ozone sonde	Arlin Krueger David Wright Charles Manion	CSU/GSFC NASA/GSFC NASA/WFC
Arcas rocket:	Chemiluminescent ozone sonde	Jagir Randhawa	ASL
Arcas rocket:	Gerdien condenser	Jack Mitchell	UTEP
Super Loki rocket:	Blunt probe	Jack Mitchell	UTEP
Data sonde rocket:	Meteorological data	Stan Kubinski	ASL
Radiosonde balloon:	Meteorological data	Stan Kubinski	ASL
Small balloon:	Mast ozone sonde	Jagir Randhawa	ASL
Small balloon:	ECC ozone sonde	Charles Manion	NASA/WFC
Ground:	Dobson ozone spectrophotometer	Jagir Randhawa	ASL
	Filter UV photometer	Peter Simeth	SenTran Co.

Table 1a (Continued)

Platform	Instrument/System	Person	Organization
	Pyranometer–visible	Robert Rubio	ASL
	Partial reflection ionosonde C–3 Ionosonde	Robert Olsen	ASL
	Meteorology, forecasting	Duke Gildenberg	AFGL/HAFB
	Meteorology, post flight analysis	John Freeman	UST
	Tracking	Alton Duff Tillman Powell	ASL
	Data acquisition and reduction	Miguel Izquierdo Edward Avila George Holmack	UTEP WSMR
	Missile Range support	Robert Jones Leland Robertson	WSMR ASL
	Photochemical modeling	Frank Hudson Jose Serna	DOE PSL
	Model, balloon environment	Richard Davis	NASA/LaRC
	Scientific publications	Edith Reed David B. Friedman	NASA/GSFC
	Overall management	Harold Ballard	ASL

Table 1b
Organizational Acronyms

AFGL	Air Force Geophysics Laboratory Hanscom Air Force Base, Massachusetts 01731
AFGL/HAFB	Detachment 1, Balloon Branch Air Force Geophysics Laboratory (AFCS) Holloman Air Force Base, New Mexico 88330
ASL	Atmospheric Sciences Laboratory U.S. Army Electronics Command White Sands Missile Range, New Mexico 88002
CSU	Department of Atmospheric Sciences Colorado State University Fort Collins, Colorado 80523

Table 1b (Continued)

DOE	Environmental Research Department of Energy Washington, D.C. 20545
NASA/ARC	Space Sciences Division Ames Research Center Moffett Field, California 94035
NASA/GSFC	Goddard Space Flight Center Greenbelt, Maryland 20771
NASA/LaRC	Langley Research Center Hampton, Virginia 23665
NASA/WFC	DO-PMOB-PMS (ASRP) Wallops Flight Center Wallops Island, Virginia 23337
NCAR	National Center for Atmospheric Research P.O. Box 3000 Boulder, Colorado 80303
Pan	Panametrics, Inc. 221 Crescent Street Waltham, Massachusetts 02154
Penn	Ionosphere Research Laboratory Pennsylvania State University University Park, Pennsylvania 16802
PSL	Physical Sciences Laboratory New Mexico State University Las Cruces, New Mexico 88001
Sandia	Division 9226 Sandia Laboratories Albuquerque, New Mexico 87185
SenTran	SenTran Company 2705 de la Vina Street Santa Barbara, California 93105

Table 1b (Continued)

UDenver	Department of Physics University of Denver Denver, Colorado 80208
UTEP	Electrical Engineering Department University of Texas at El Paso El Paso, Texas 79968
UST	Institute for Storm Research University of St. Thomas Houston, Texas 77006
USU	Center for Atmospheric and Space Sciences Utah State University Logan, Utah 84322
WSMR	White Sands Missile Range New Mexico 88002

noted that this was a cooperative effort, in that many of the investigators were responsible for obtaining their own funding for instrumentation and data analysis; the Atmospheric Sciences Laboratory and NASA provided facilities and coordination.

The Stratcom VIII-A Payload

The most complex of the various payloads was that for the VIII-A Balloon. Mechanical and electrical integration as well as telemetry and command systems were under the cognizance of the University of Texas at El Paso.

Payload Layout

The instruments were in several packages: a small package at the top of the balloon to observe the balloon environment and incoming radiation, the main payload including a large number of sensors, and three sondes dropped from the main payload for vertical profiles of specific parameters. The gross physical characteristics of these are given Table 2. The top package and the three dropsondes are described in further detail in separate articles. (See "Measurements from the Apex of the Stratcom VIII-A Balloon", "A Dropsonde for Nitric Oxide and Ozone", "Electrical Structure and Ionizable Constituent Measurements", and "Water Vapor Measurements with Aluminum Oxide Sensors".)

Table 2
Physical Characteristics of the Stratcom VIII-A Packages

Package	Dimensions	Weight
Top	0.48 high X 0.43 m dia.	14.5 kg
Main	2.84 m long X 2.69 m wide X 1.22 m high	491 kg
Drop No. 1	1.75 m long X 0.51 m wide X 0.58 m deep	60 kg
Drop No. 2	0.61 m long X 0.30 m dia.	3.6 kg
Drop No. 3	0.61 m long X 0.20 m dia.	4.5 kg

The layout of the main payload is shown in Figure 3. Side views are shown in the photographs in Figures 4 and 5. The telemetry can and the battery pack were on adjustable mounts so that the telemetry could be used to make balance corrections about the x-axis and the battery pack about the y-axis. The levelness indicator showed that the payload was 0.25° from horizontal at launch and stayed within 1° throughout the flight.

The structure was designed so that the large dropsonde fitted into a recess located at the center of gravity of the overall structure. Sliding guides permitted this sonde to be deployed, leaving its parachute canister within the structure. The two smaller sondes offset each other about the x-axis and had a minimal effect about the y-axis. During the prelaunch checks it was noticed that the large dropsonde might collide with the antennas and the temperature sensors during its deployment. Therefore, it was decided to lift up the antennas and sensors to a minimum distance below the platform. The RF checks and command checks made at this time indicated no difficulty.

The solar UV sensors were mounted on the uppermost part of the frame. Thus, the USU Sky Photometer had a totally unobstructed field of view while the other three UV instruments were obstructed, at times, by the support cables and the several balloon reflection shields. The size and positioning of these instruments and their shields are shown in Figure 6.

Electrical Systems

A block diagram of the principal components of the power, control, and telemetry systems for the main payload is given in Figure 7.

The telemetry system consisted of two P-band transmitters, one at 230.4 MHz (Figure 8) and the other at 239.4 MHz (Figure 9). Each was modulated by 14 FM IRIG VCO channels, thus forming an FM/FM system. Three of the channels used 30-bit fast-time multiplexing pulse amplitude modulation (PAM) with three of the bits being used for sync and calibration, leaving 27 bits for information. Hence the telemetry system for the downlink data information had a combined capability of 109 data channels.

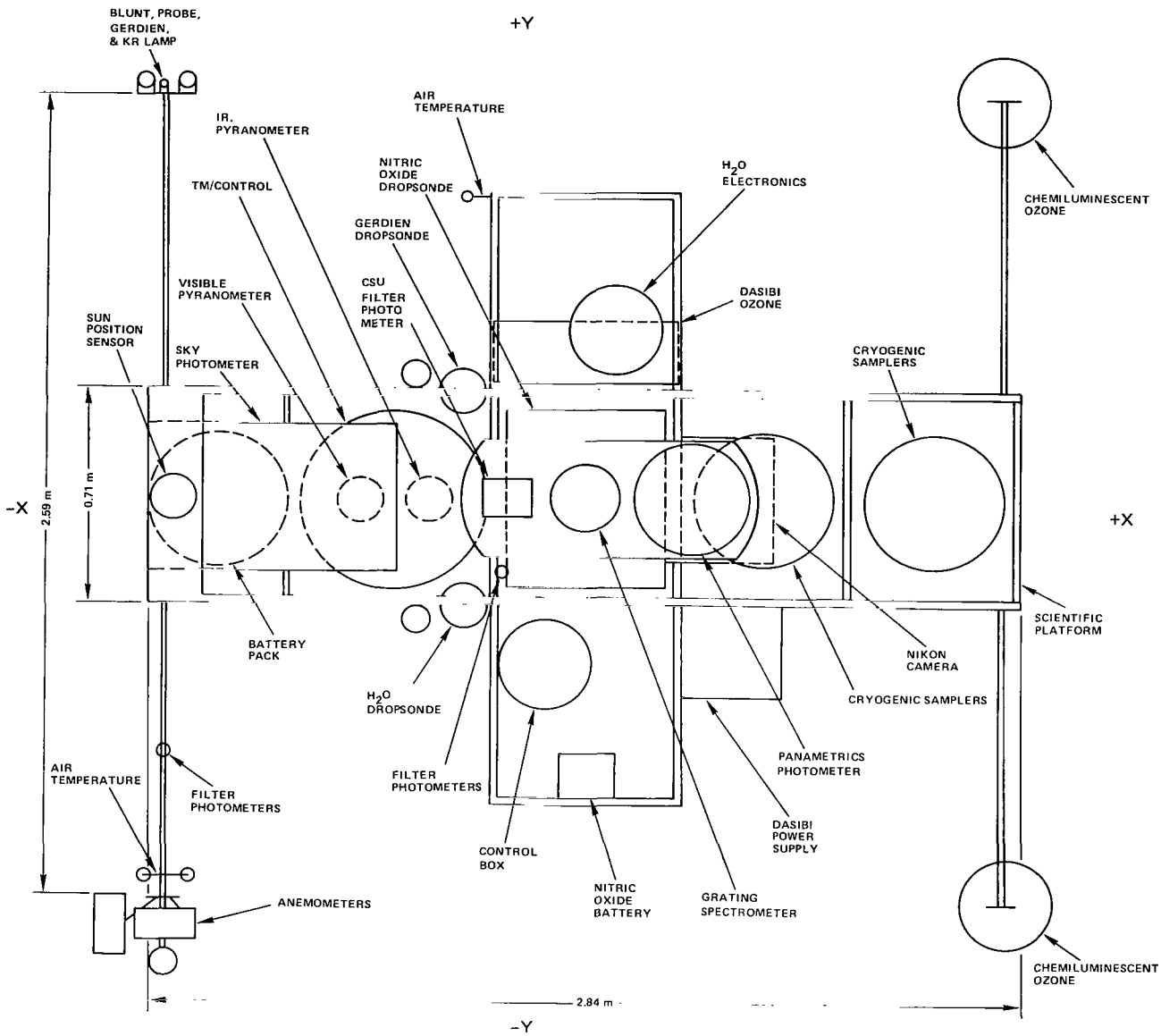

Figure 3. Layout of the Main payload for Balloon VIII-A.

The control system included a command receiver set at 416.6 MHz feeding a 60-command FSK (frequency shift keying) decoder whose output per command was an open collector. The fire module supplied 24 different low-impedance power commands with only three commands from the open collector decoder.

The power system consisted of three separate 28-V battery banks which could be selected by command, dc-to-dc converters that transformed the 28-V supply to +15, -15, +5, +6, and +24 V, and a bank of latching relays to distribute power and to perform other functions for individual instruments.

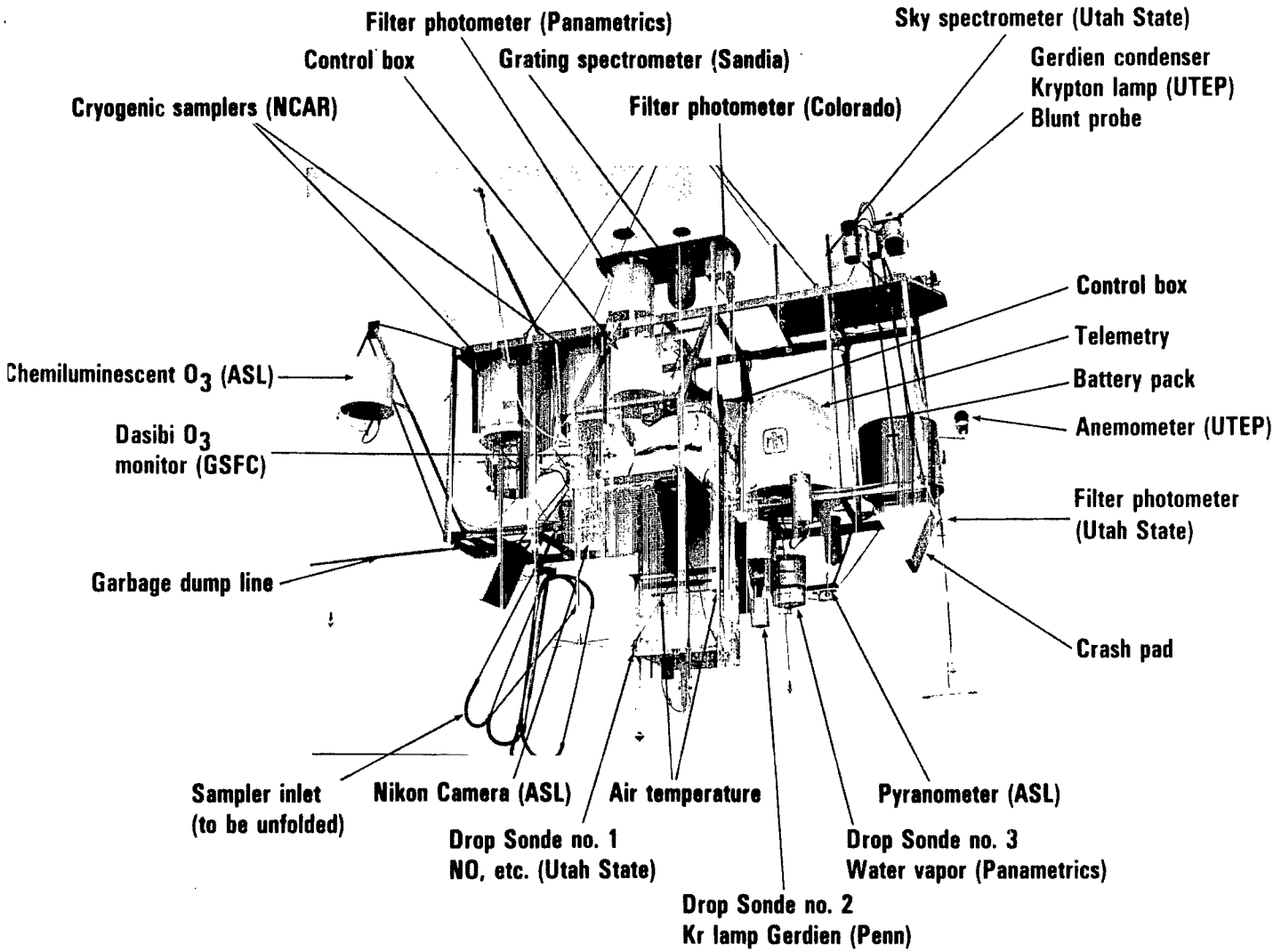

Figure 4. The +Y side of the main payload

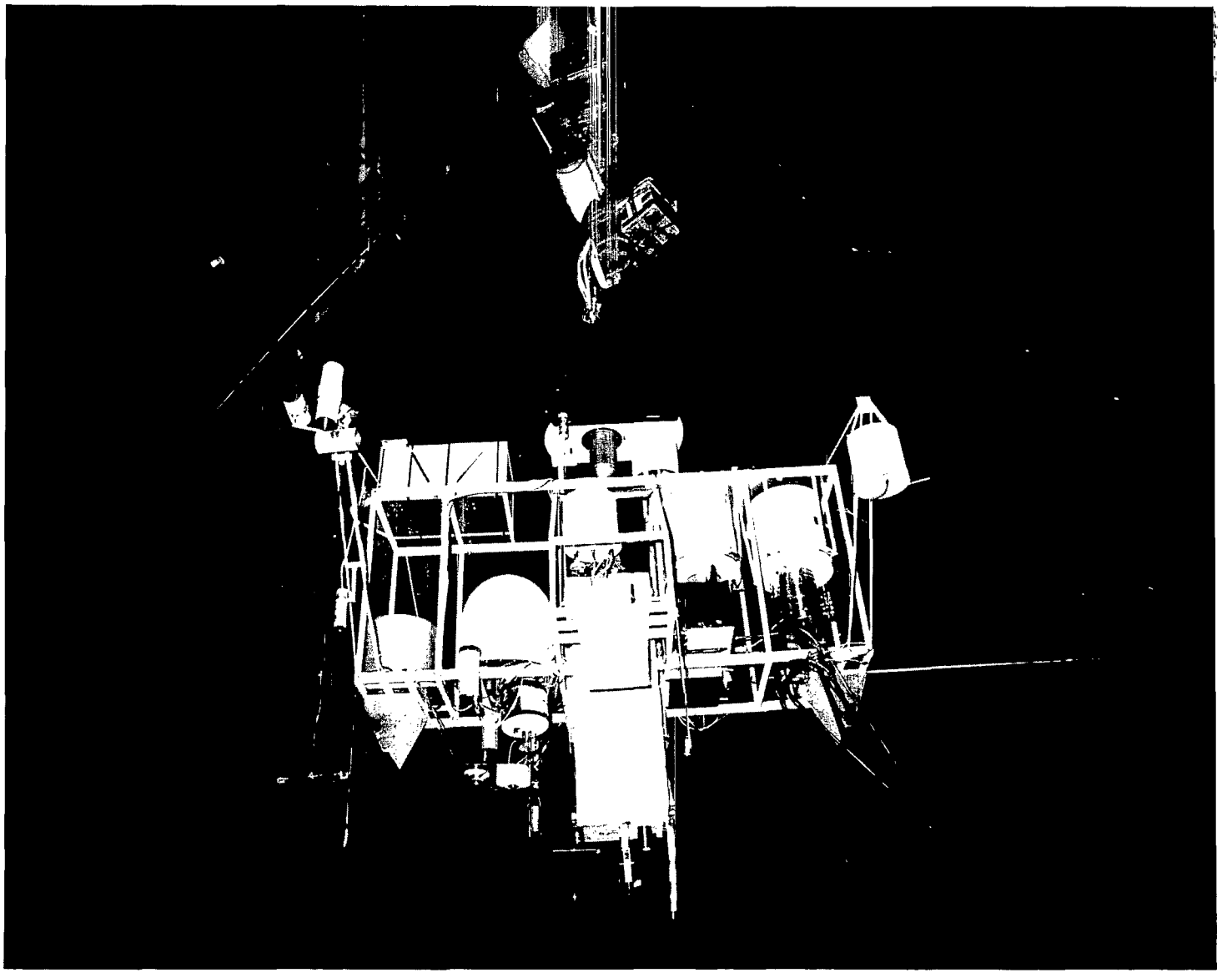

Figure 5. The -Y side of the main payload for Balloon VIII-A.

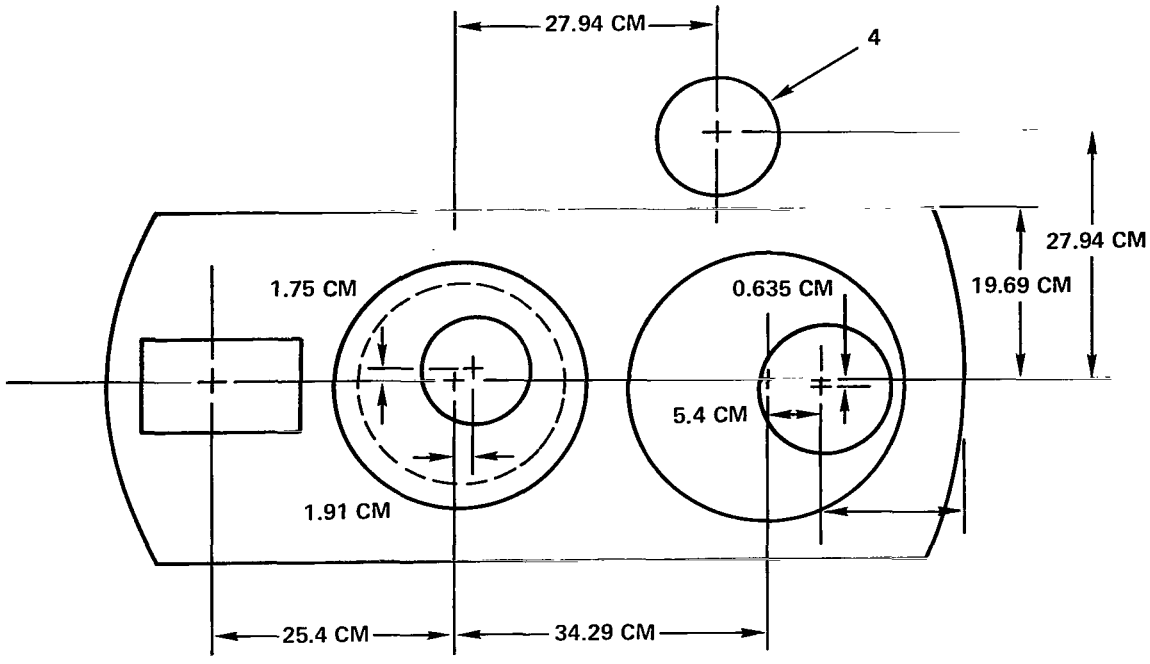

1. FILTER PHOTOMETER (PANAMETRIC)
2. GRATING PHOTOMETER (SANDIA)
3. FILTER PHOTOMETER (CSU)
4. FILTER PHOTOMETER (UTAH ST.)

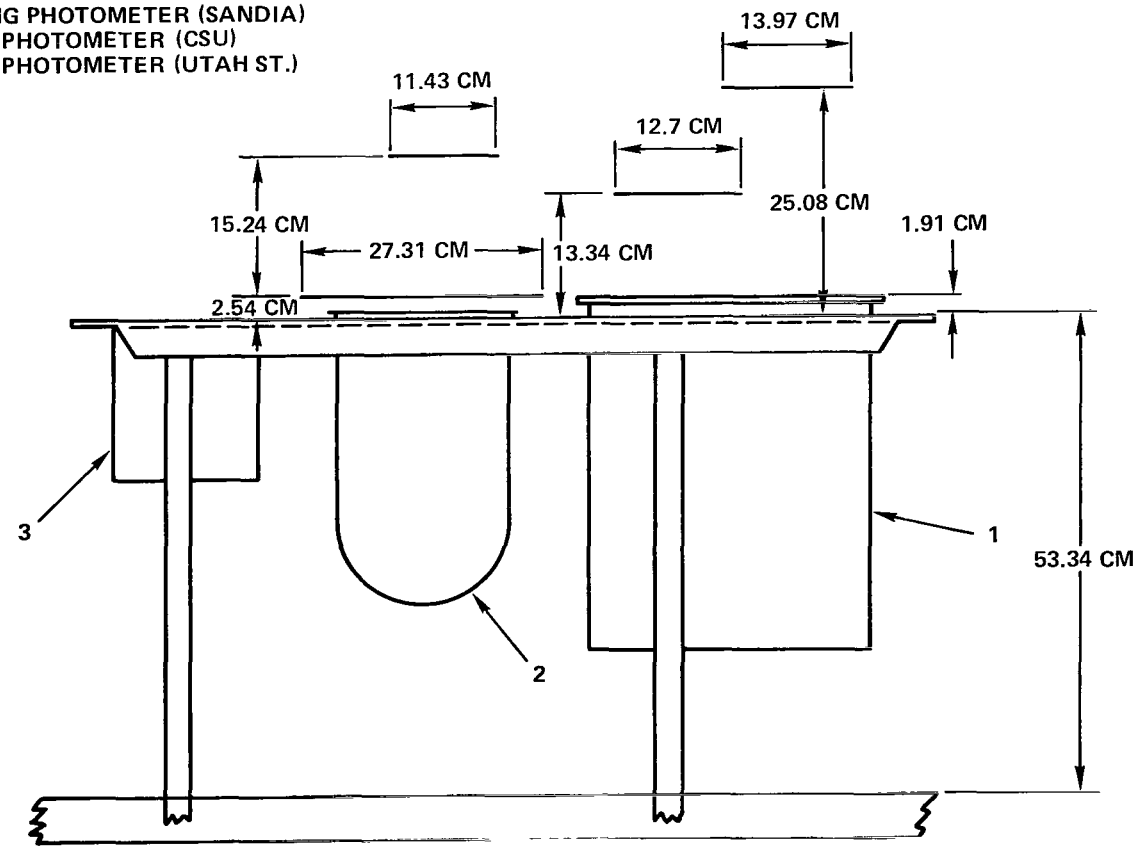

Figure 6. Location of the UV instruments and their sheilds.

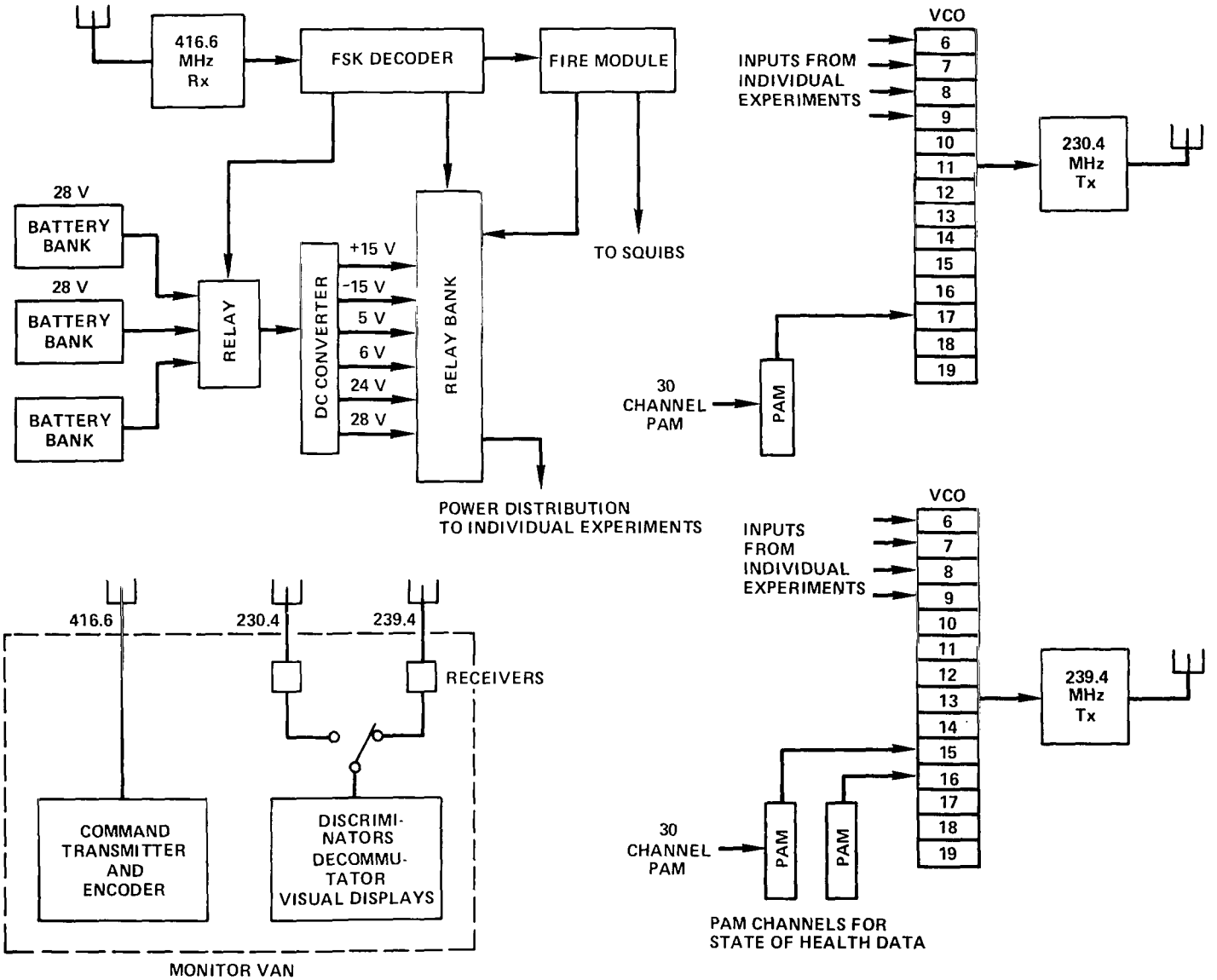

Figure 7. Outline of the power, control and telemetry systems for the main payload of Balloon VIII-A.

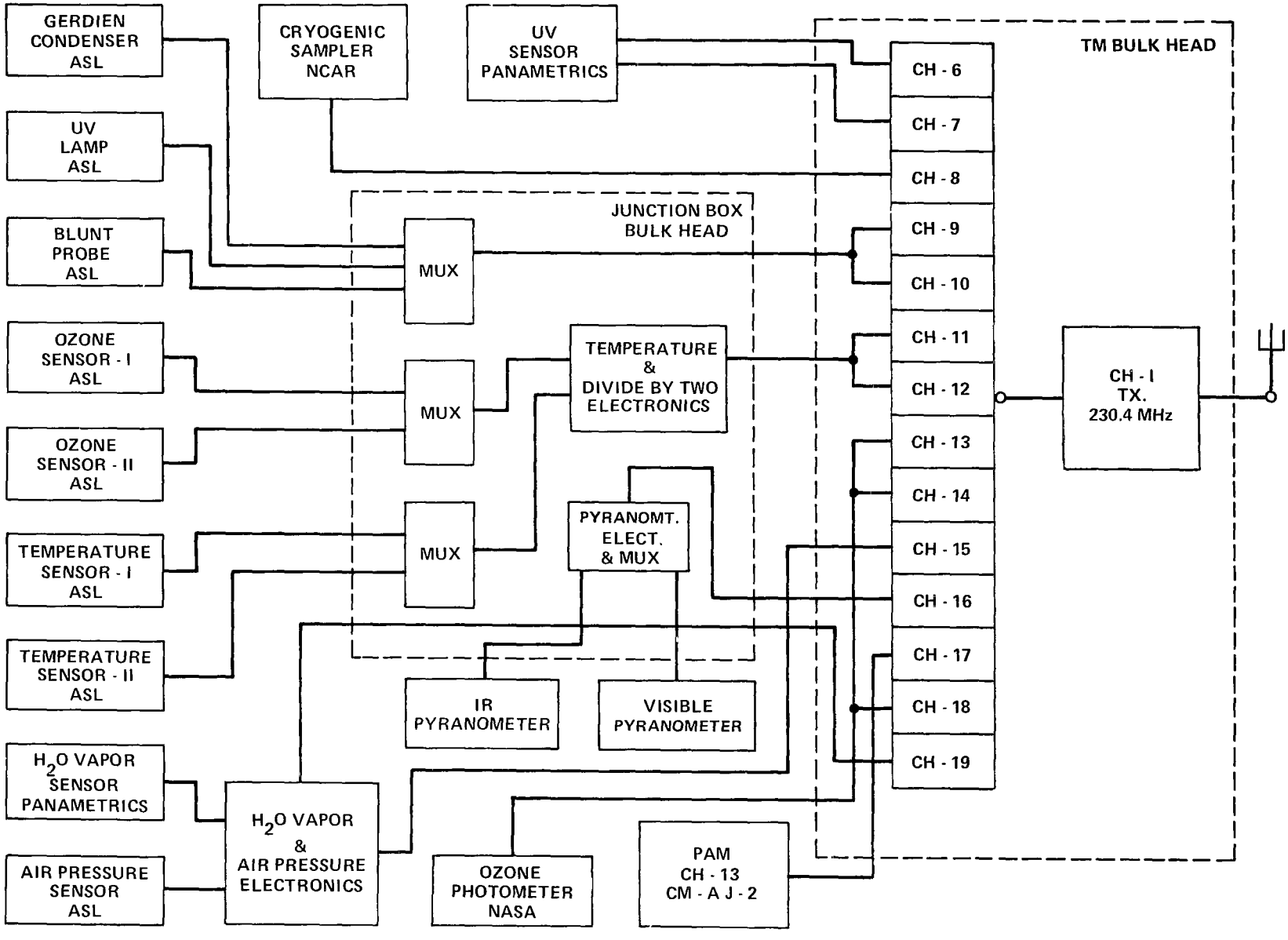

Figure 8. Distribution of channels for the 230.4 MHz telemetry link.

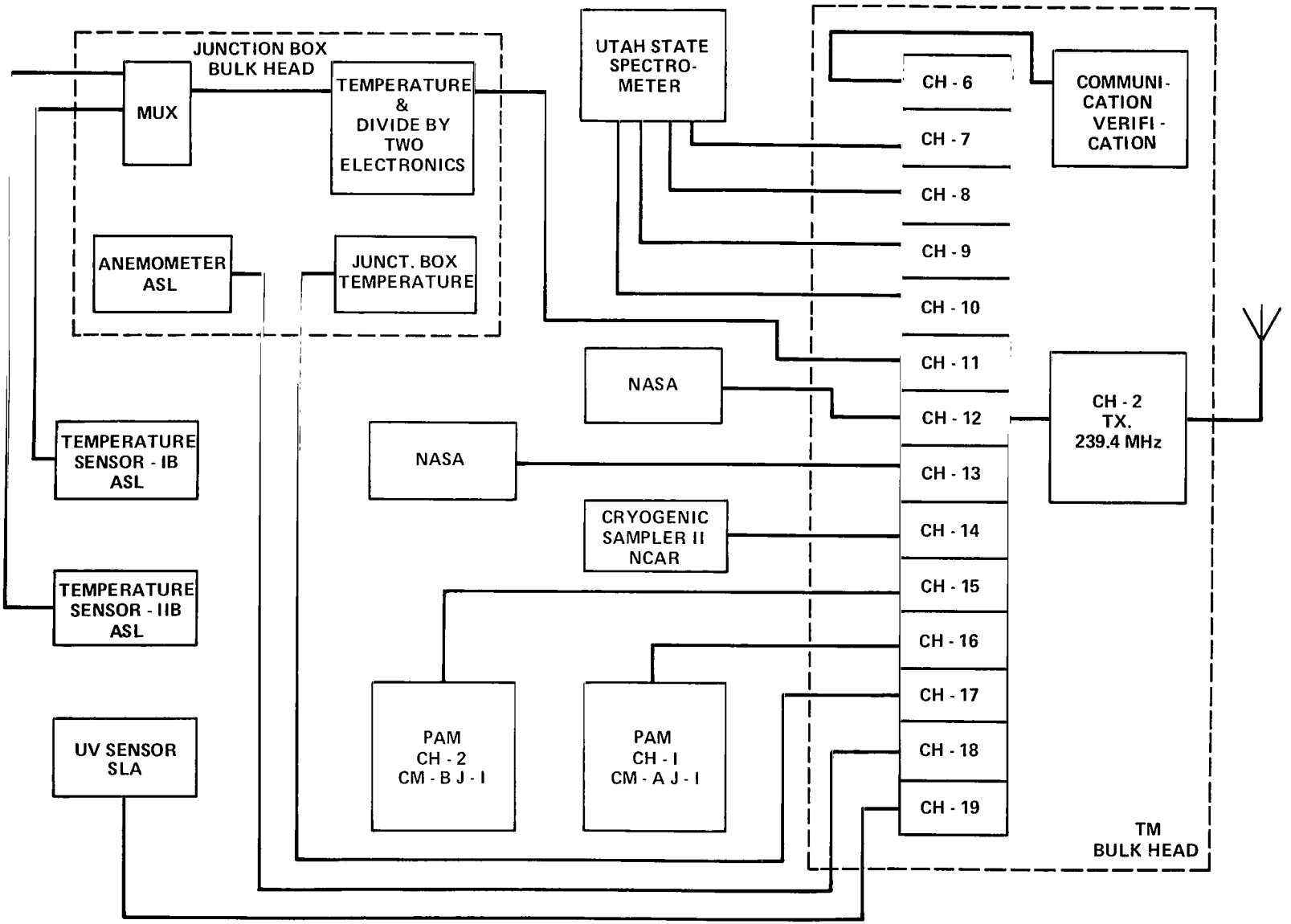

Figure 9. Distribution of channels for the 239.4 MHz telemetry link.

A portable monitor van was used during integration, preflight checks and flight operations to monitor the various telemetry channels and to send commands to the main payload. In the van were two P-bank receivers with yagi antennas, one bank of IRIG channel discriminators, and one PAM decommutator. The command system in the van included a 416.6-MHz transmitter with either 50- or 100-W power capability and an end fire helix antenna. The transmitter was modulated by an FSK encoder with 60 commands.

Further details on the electronic systems prepared by the University of Texas at El Paso may be found in their report on this flight (Reference 1).

The Stratcom VIII-B Payload

The payload prepared by D. G. Murcray and his colleagues at the University of Denver supported several types of infrared measurements. A view of this payload during launch preparations is shown in Figure 10. The gondola was constructed of brazed conduit and configured to keep the center of gravity low. The floor of the gondola was reinforced with aluminum I-beams. The rectangular design makes mounting the various components into the gondola much easier and helps keep the unit upright on impact. This type of construction has been used successfully on a number of past programs. The gondola is suspended from the corners by aircraft cables. Crash pads of crushable paper honeycomb reduce the accelerations on the instruments during impact after the flight.

The prime instrument is a 1-1/4 m Czerny-Turner IR grating spectrometer with an azimuth pointing control (at the top of its four-line suspension) and a mirror arrangement so as to observe the setting Sun. The two horizon-pointing radiometers on the left portion of the payload were for observations of the 4.3 μm and the 15 μm CO_2 thermal emission bands. Another view of this same payload, shortly before release, is shown in Figure 11. The small package extending to the side of the payload is a standard meteorological sonde.

OPERATIONS

The Stratcom VIII operation was conducted by Harold Ballard of the Atmospheric Sciences Laboratory, assisted by the staff and facilities of Holloman Air Force Base and the White Sands Missile Range. The large balloon launches were conducted by the Balloon Branch of the Air Force Geophysics Laboratory. The following section provides data concerning the balloon train, flight paths, and summaries of the related small balloon and rocket operations.

The Stratcom VIII-B Balloon

The Stratcom VIII-B Balloon, prepared by D. G. Murcray and his colleagues at the University of Denver, was the first of the large balloons to be flown, being launched from Holloman Air Force Base at 1251 MST, September 28, 1977. Range availability and weather considerations led to the

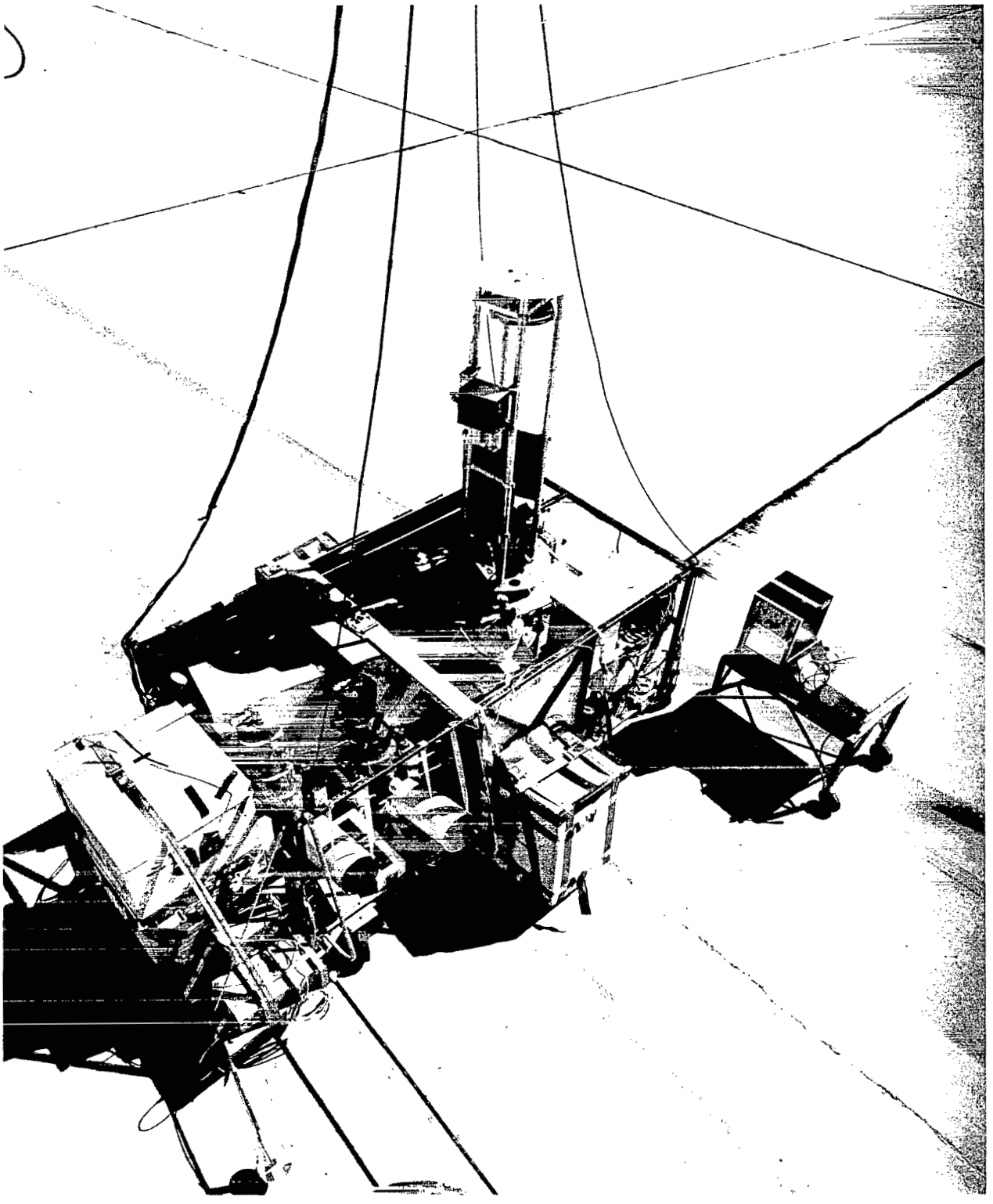

Figure 10. The Stratcom VIII-B payload during preparation at the launch site.

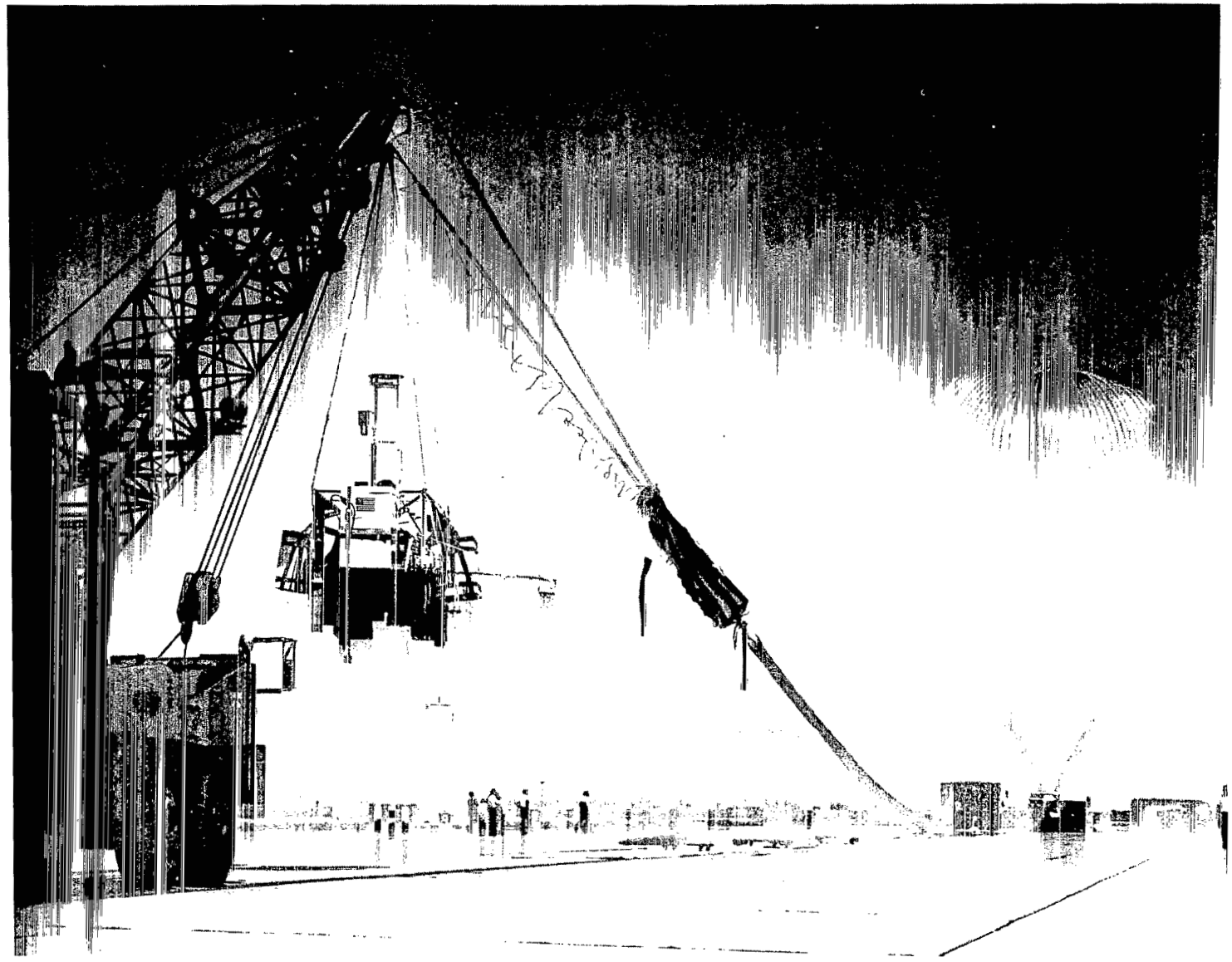

Figure 11. The Stratcom VIII-B payload prior to release.

launching of the VIII-B Balloon on the afternoon prior to the launch of the VIII-A Balloon, instead of afterwards, as originally planned.

Engineering data for the VIII-B Balloon and its payload are given in Table 3. The data system included on-board digital tape recorders, and, for the first time in the long history of this payload, a telemetry system. The latter proved to be invaluable; for the parachute system failed and the payload, including the digital tapes, burned upon impact.

Table 3
Engineering Data for Balloon VIII-B and Its Payload

Balloon:		Payload:	590 kg (1300 lb)
Material:	Stratofilm, 0.5 mil; 0.9 mil cap		
Manufacturer:	Wizen	Parachute:	
Diameter:	97.3 m (319 ft)	Quantity:	2
Volume:	3.29×10^5 m^3 (11.6×10^6 ft^3)	Type:	flat, circular
Length:	130.5 m (428 ft)	Diameter:	19.5 m (64 ft)
Weight:	568 kg (1252 lb)	Length:	27.4 m (90 ft)
		Weight:	38 kg (83.5 lb)
Ballast:	90.7 kg (200 lb)		

The VIII-B balloon followed a vertical trajectory as shown in Figure 12 and a horizontal path as shown in Figure 13. The balloon remained near its float altitude of 39 km from about 1521 MST through sunset (1822 MST) until termination at 1914 MST. The U-2 aircraft, Flight No. 77-157, flew from Moffett Field, California, to the vicinity of the VIII-B Balloon. The aircraft altitude as a function of time is shown in Figure 12, and its horizontal flight path in Figures 13 and 14.

The Stratcom VIII-A Balloon

The Stratcom VIII-A Balloon included experiments from a number of organizations, as indicated in the previous sections. Engineering data for this balloon and its payload are given in Table 4.

The Stratcom VIII-A Balloon was launched at 0607 MST, September 19, 1977, about 11 hours after the termination of the VIII-B Balloon. Figure 15 shows the vertical flight path of the VIII-A Balloon, release times for the three dropsondes, and launch times for the small balloons and rockets associated with this effort. Since the control system for the helium valves at the top of Balloon VIII-A and for ballast release became inoperable, it was not possible to descend as had been planned (see Figure 1). The variations in the altitude of the balloon that did occur are due to the changes of temperature (and density) of the helium in the balloon.

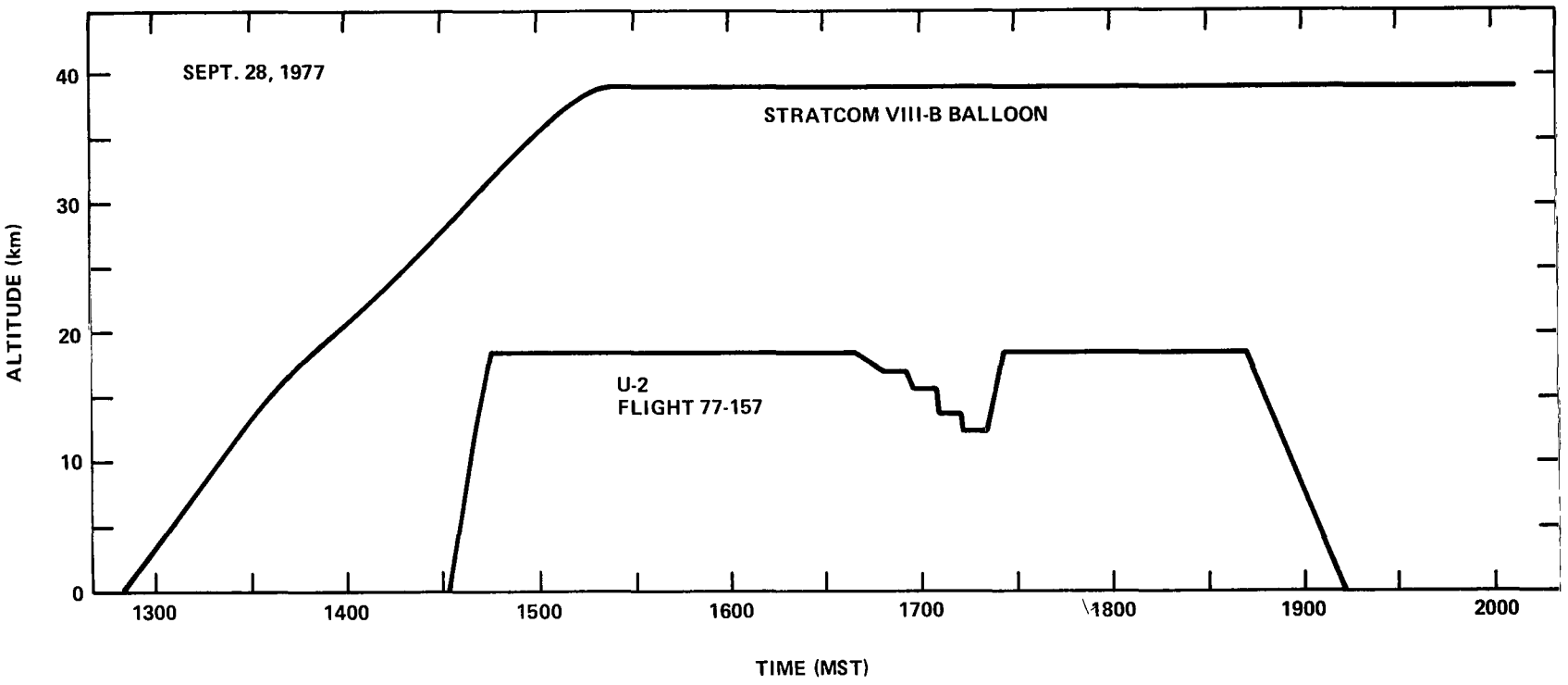

Figure 12. Vertical flight paths of Balloon VIII-B and the U-2 aircraft.

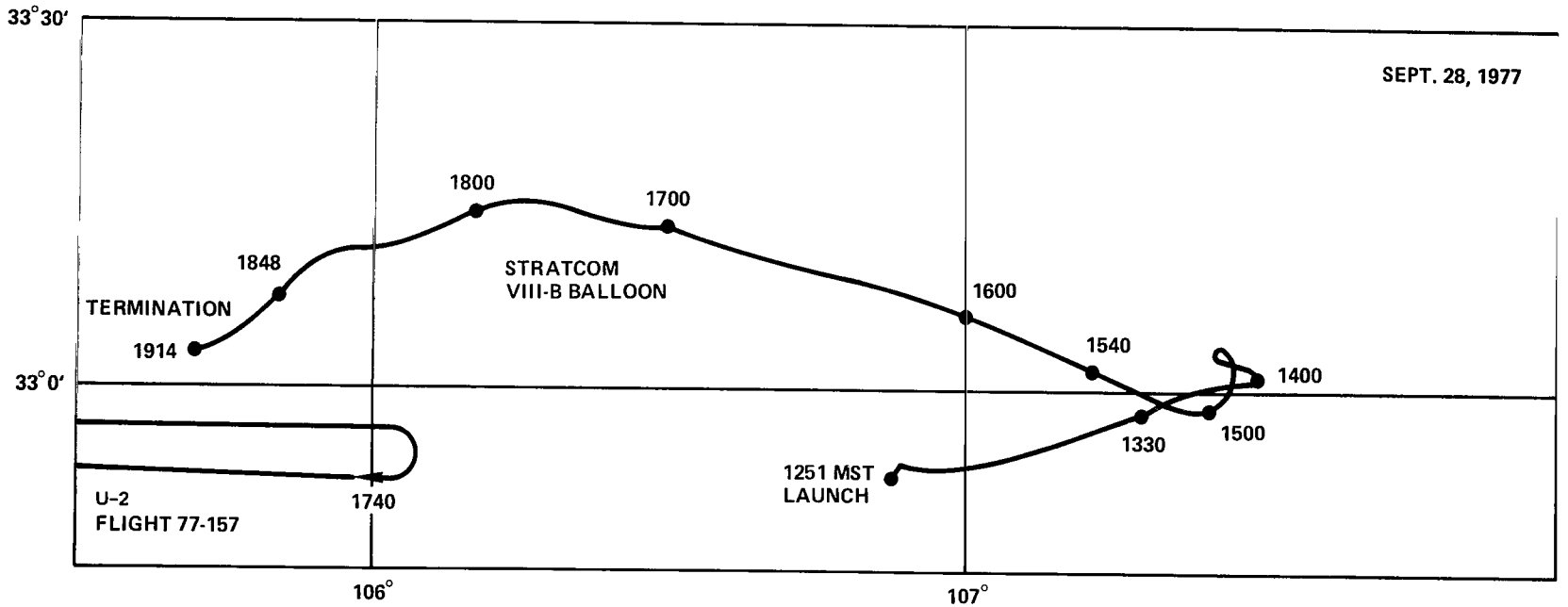

Figure 13. Horizontal flight path of Balloon VIII-B and the U-2 aircraft.

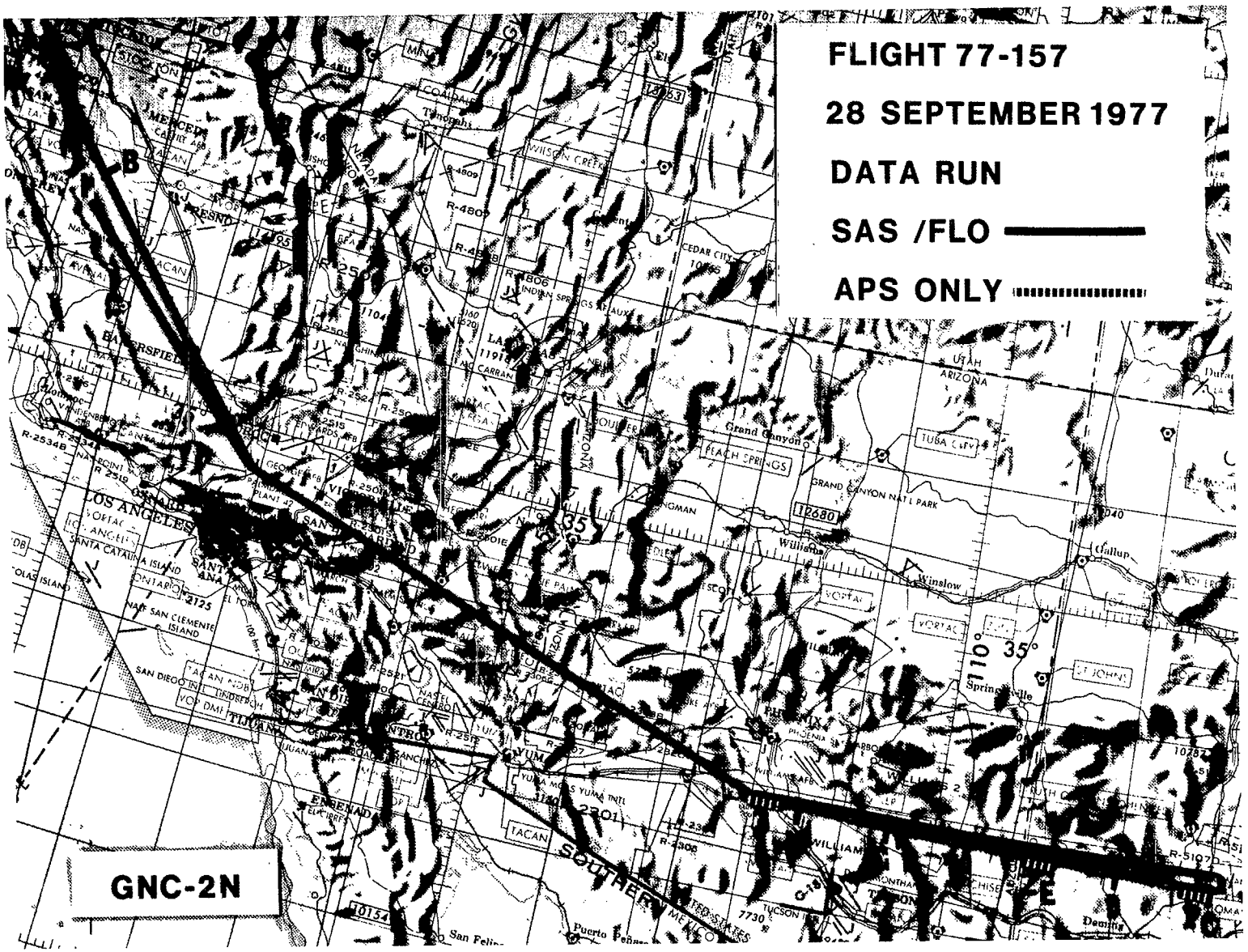

Figure 14. Flight path for U-2 flight 77-157.

Table 1b (Continued)

UDenver	Department of Physics University of Denver Denver, Colorado 80208
UTEP	Electrical Engineering Department University of Texas at El Paso El Paso, Texas 79968
UST	Institute for Storm Research University of St. Thomas Houston, Texas 77006
USU	Center for Atmospheric and Space Sciences Utah State University Logan, Utah 84322
WSMR	White Sands Missile Range New Mexico 88002

noted that this was a cooperative effort, in that many of the investigators were responsible for obtaining their own funding for instrumentation and data analysis; the Atmospheric Sciences Laboratory and NASA provided facilities and coordination.

The Stratcom VIII-A Payload

The most complex of the various payloads was that for the VIII-A Balloon. Mechanical and electrical integration as well as telemetry and command systems were under the cognizance of the University of Texas at El Paso.

Payload Layout

The instruments were in several packages: a small package at the top of the balloon to observe the balloon environment and incoming radiation, the main payload including a large number of sensors, and three sondes dropped from the main payload for vertical profiles of specific parameters. The gross physical characteristics of these are given Table 2. The top package and the three dropsondes are described in further detail in separate articles. (See "Measurements from the Apex of the Stratcom VIII-A Balloon", "A Dropsonde for Nitric Oxide and Ozone", "Electrical Structure and Ionizable Constituent Measurements", and "Water Vapor Measurements with Aluminum Oxide Sensors".)

Table 2
Physical Characteristics of the Stratcom VIII-A Packages

Package	Dimensions	Weight
Top	0.48 high X 0.43 m dia.	14.5 kg
Main	2.84 m long X 2.69 m wide X 1.22 m high	491 kg
Drop No. 1	1.75 m long X 0.51 m wide X 0.58 m deep	60 kg
Drop No. 2	0.61 m long X 0.30 m dia.	3.6 kg
Drop No. 3	0.61 m long X 0.20 m dia.	4.5 kg

The layout of the main payload is shown in Figure 3. Side views are shown in the photographs in Figures 4 and 5. The telemetry can and the battery pack were on adjustable mounts so that the telemetry could be used to make balance corrections about the x-axis and the battery pack about the y-axis. The levelness indicator showed that the payload was 0.25° from horizontal at launch and stayed within 1° throughout the flight.

The structure was designed so that the large dropsonde fitted into a recess located at the center of gravity of the overall structure. Sliding guides permitted this sonde to be deployed, leaving its parachute canister within the structure. The two smaller sondes offset each other about the x-axis and had a minimal effect about the y-axis. During the prelaunch checks it was noticed that the large dropsonde might collide with the antennas and the temperature sensors during its deployment. Therefore, it was decided to lift up the antennas and sensors to a minimum distance below the platform. The RF checks and command checks made at this time indicated no difficulty.

The solar UV sensors were mounted on the uppermost part of the frame. Thus, the USU Sky Photometer had a totally unobstructed field of view while the other three UV instruments were obstructed, at times, by the support cables and the several balloon reflection shields. The size and positioning of these instruments and their shields are shown in Figure 6.

Electrical Systems

A block diagram of the principal components of the power, control, and telemetry systems for the main payload is given in Figure 7.

The telemetry system consisted of two P-band transmitters, one at 230.4 MHz (Figure 8) and the other at 239.4 MHz (Figure 9). Each was modulated by 14 FM IRIG VCO channels, thus forming an FM/FM system. Three of the channels used 30-bit fast-time multiplexing pulse amplitude modulation (PAM) with three of the bits being used for sync and calibration, leaving 27 bits for information. Hence the telemetry system for the downlink data information had a combined capability of 109 data channels.

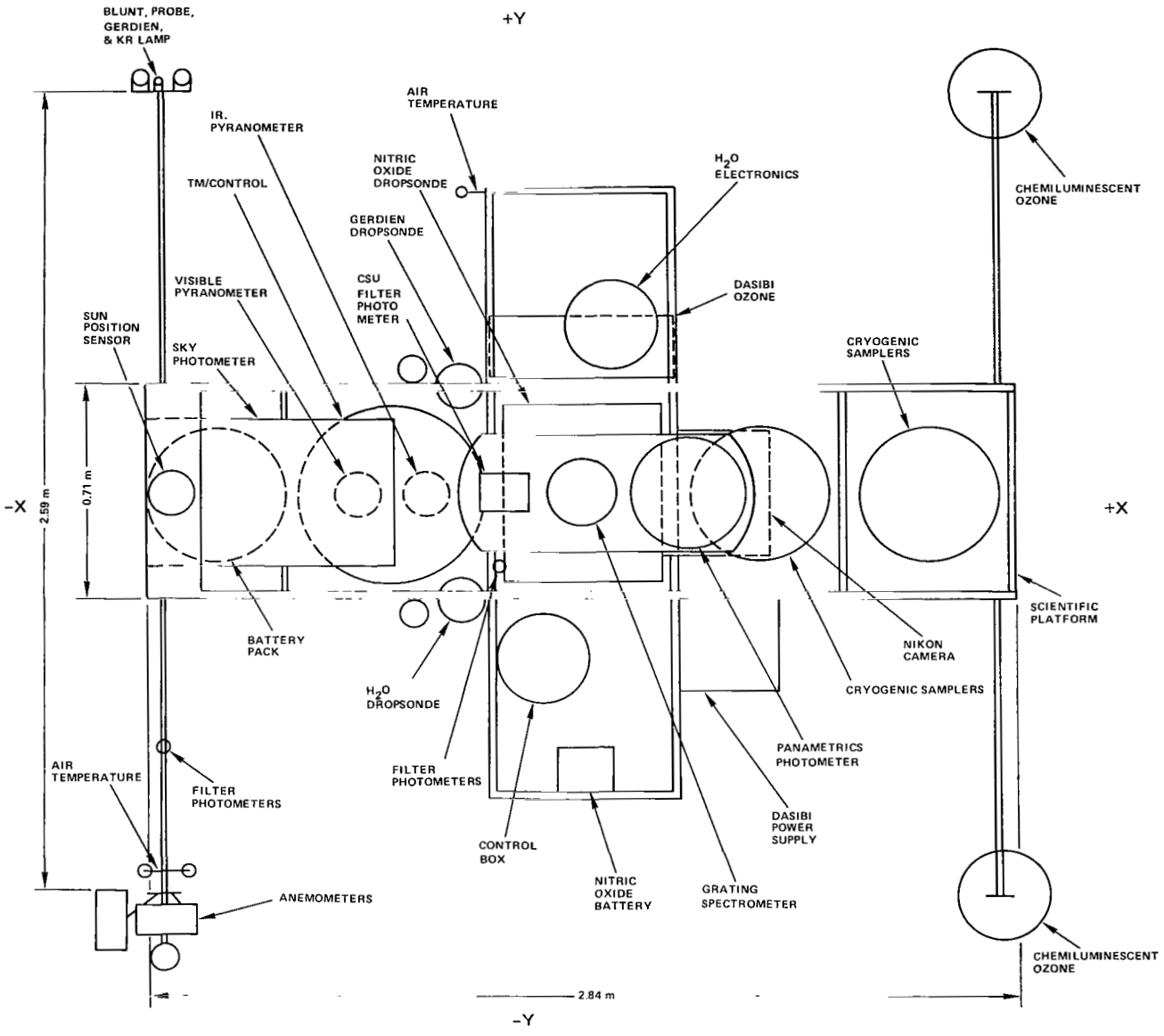

Figure 3. Layout of the Main payload for Balloon VIII-A.

The control system included a command receiver set at 416.6 MHz feeding a 60-command FSK (frequency shift keying) decoder whose output per command was an open collector. The fire module supplied 24 different low-impedance power commands with only three commands from the open collector decoder.

The power system consisted of three separate 28-V battery banks which could be selected by command, dc-to-dc converters that transformed the 28-V supply to +15, -15, +5, +6, and +24 V, and a bank of latching relays to distribute power and to perform other functions for individual instruments.

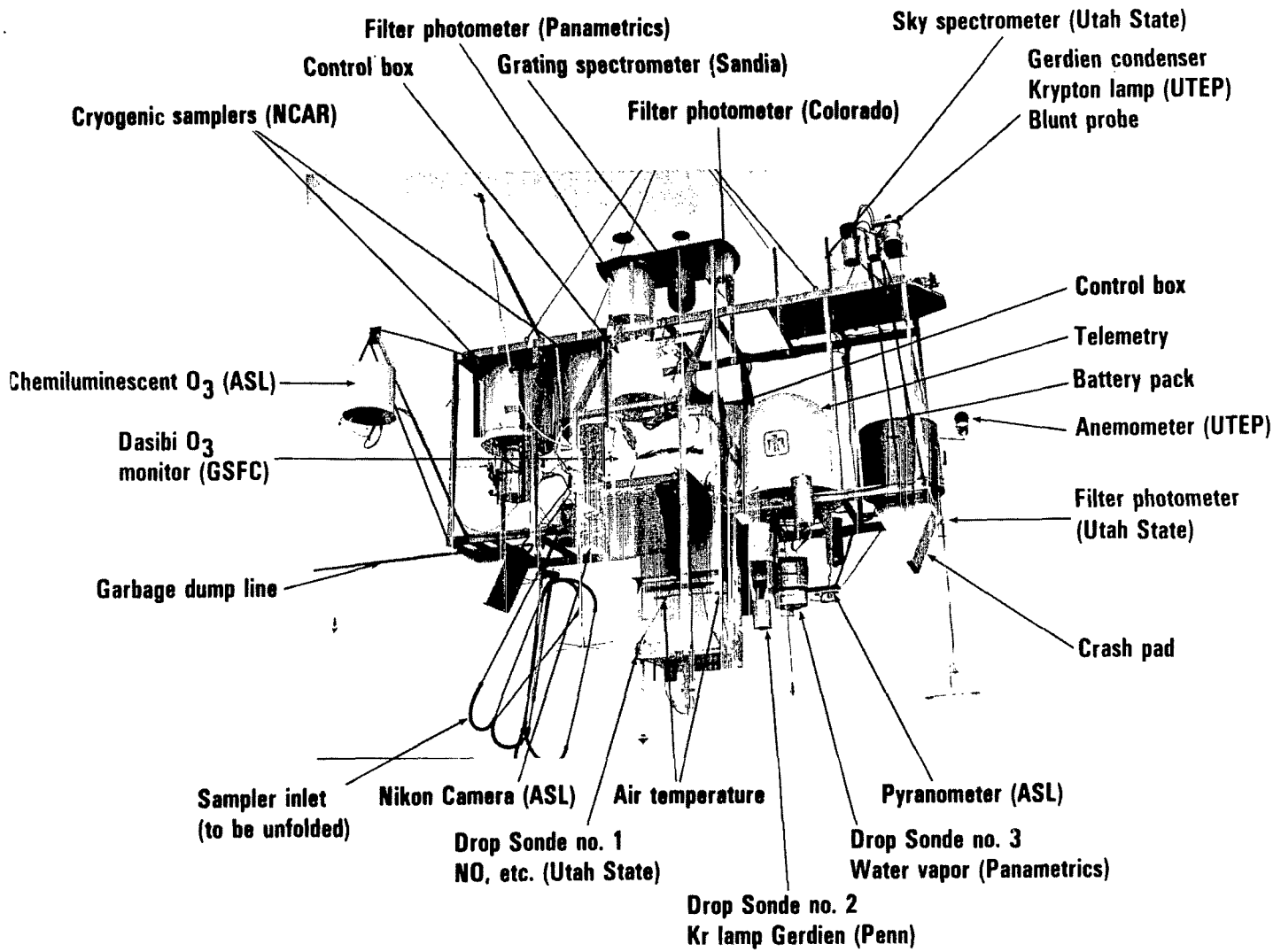

Figure 4. The +Y side of the main payload

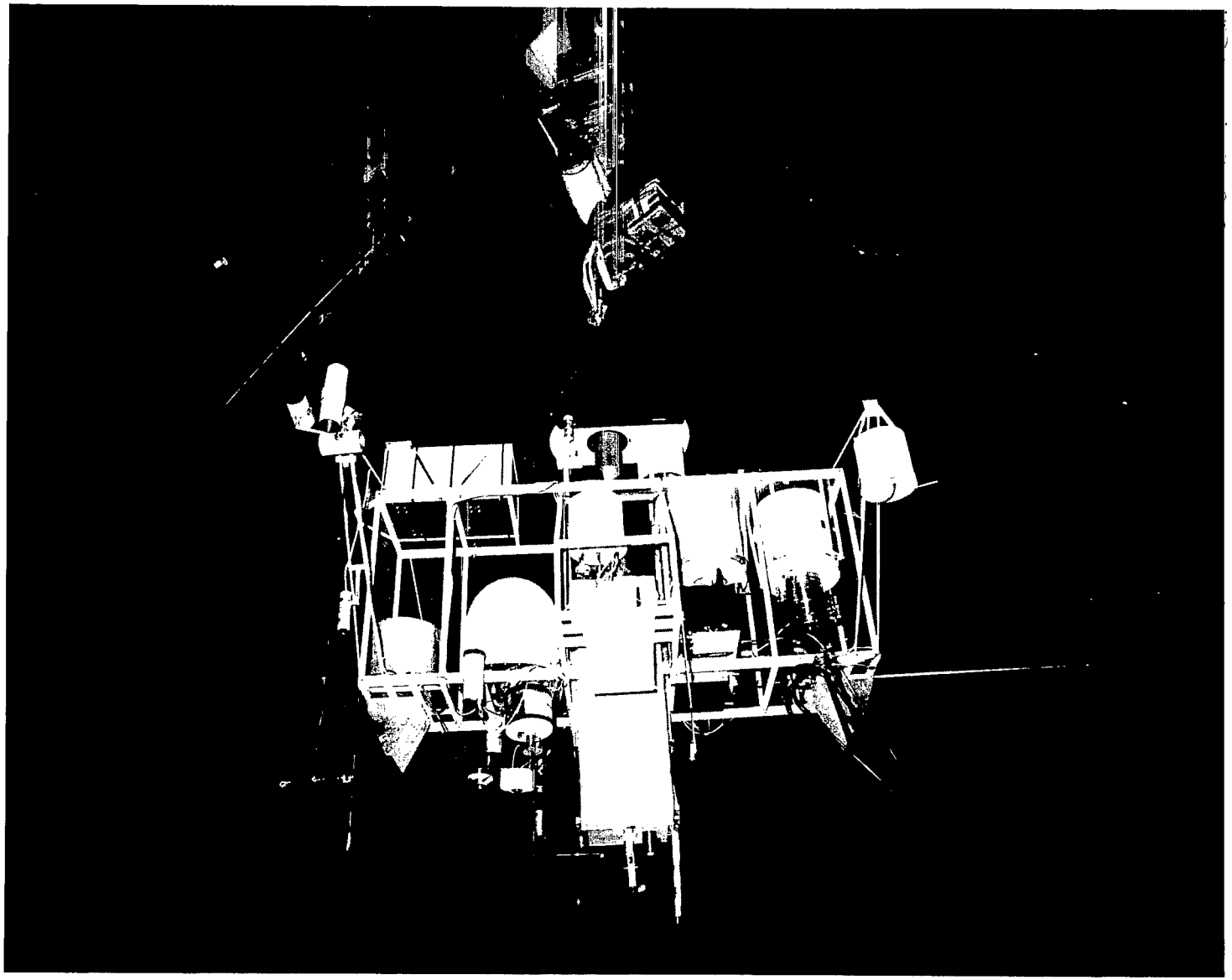

Figure 5. The -Y side of the main payload for Balloon VIII-A.

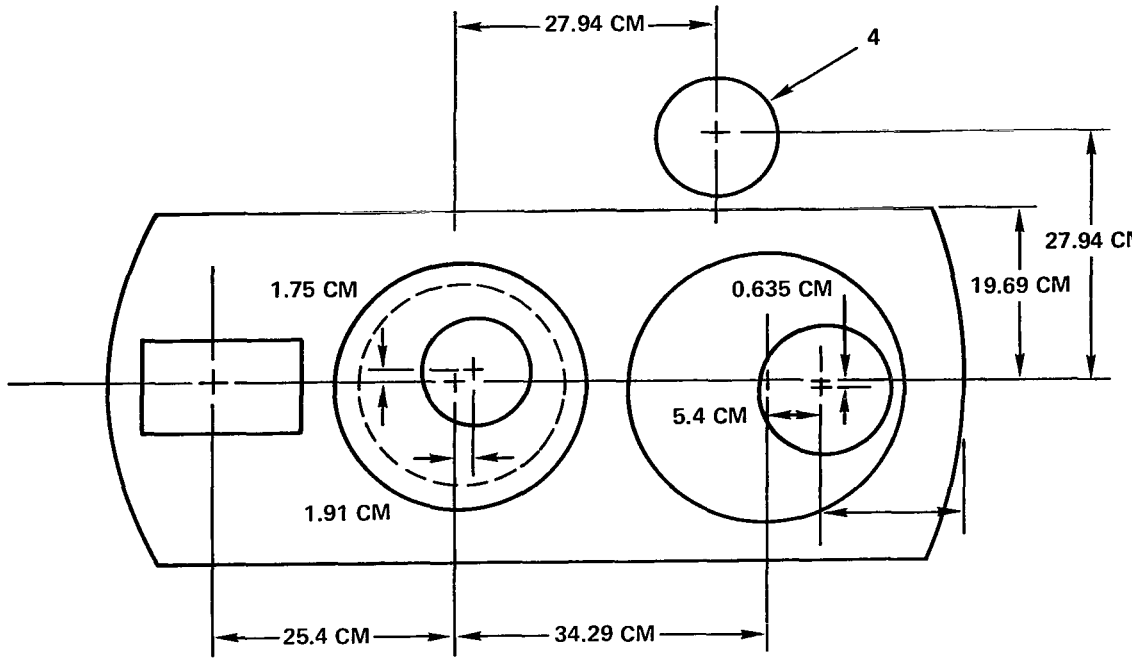

1. FILTER PHOTOMETER (PANAMETRIC)
2. GRATING PHOTOMETER (SANDIA)
3. FILTER PHOTOMETER (CSU)
4. FILTER PHOTOMETER (UTAH ST.)

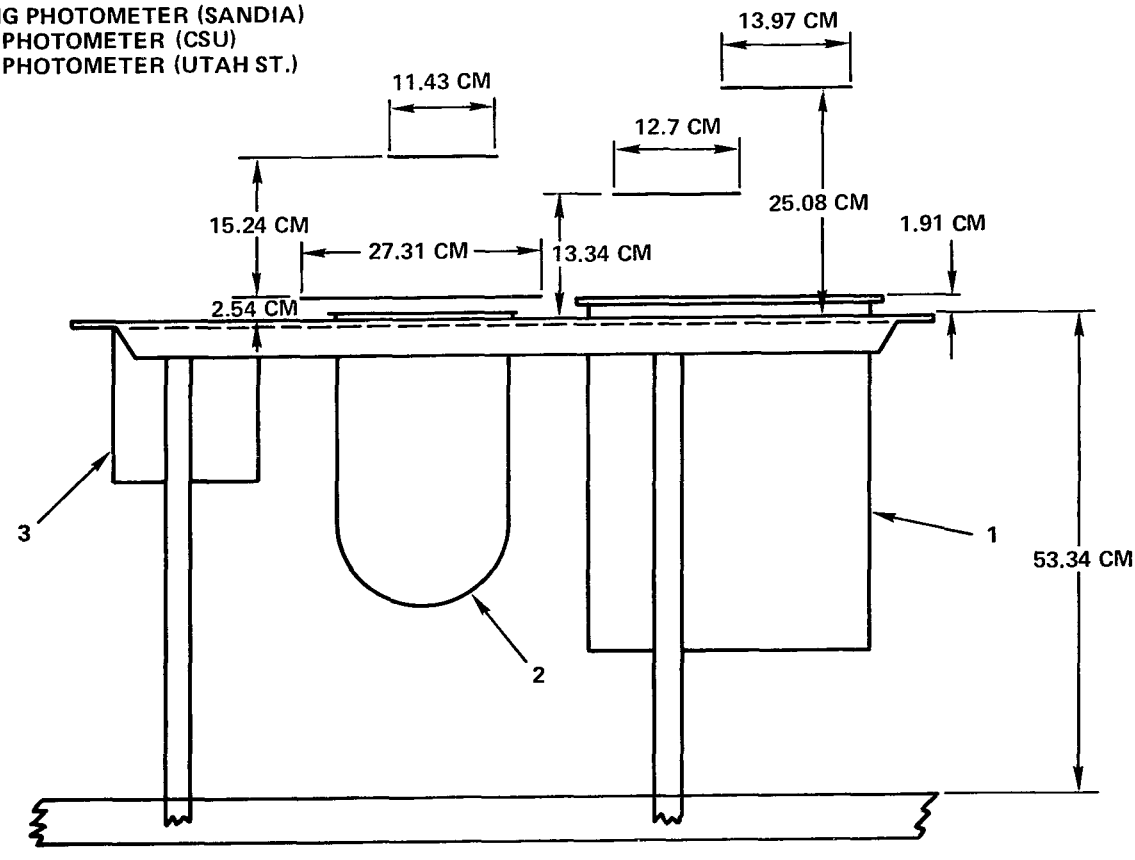

Figure 6. Location of the UV instruments and their sheilds.

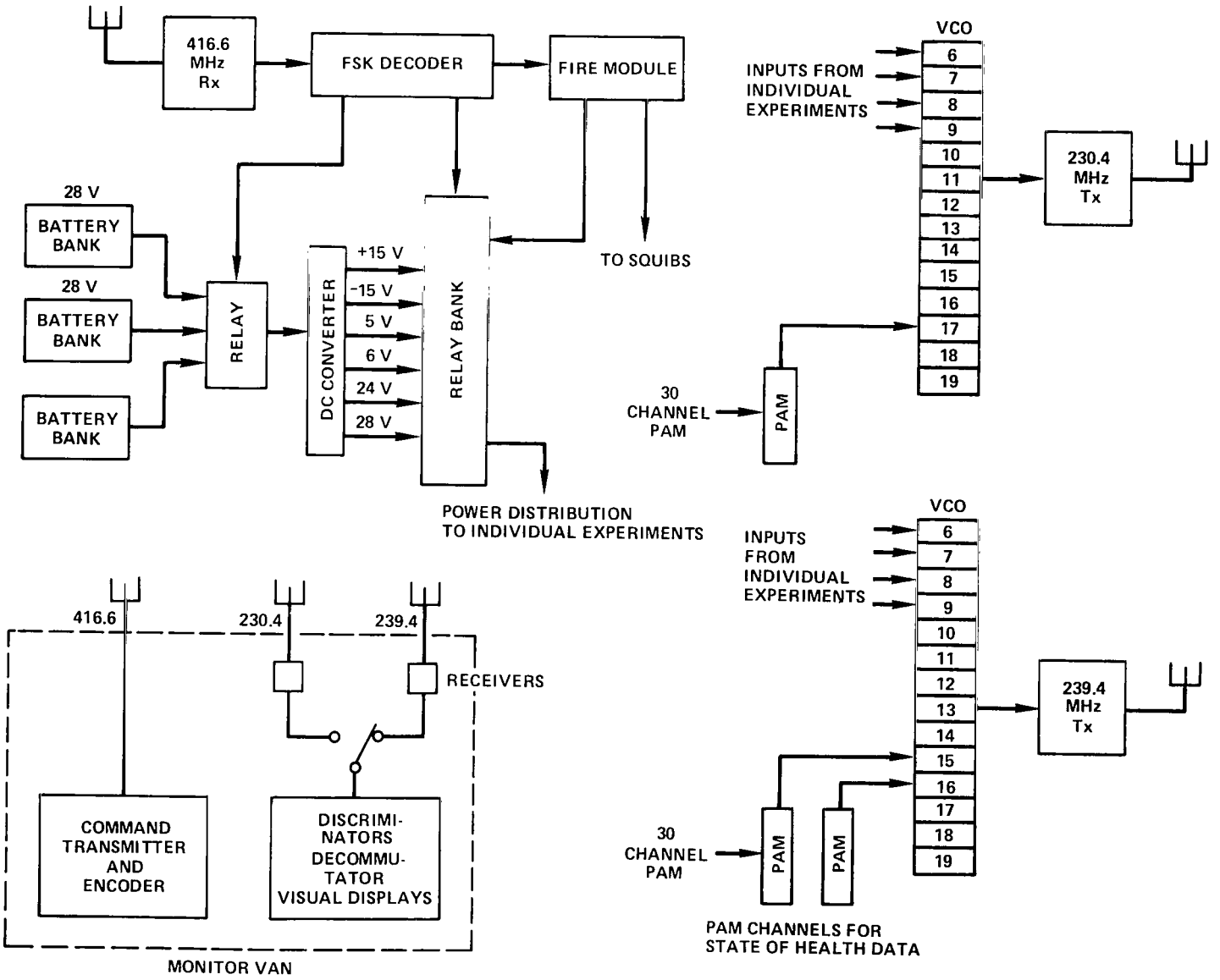

Figure 7. Outline of the power, control and telemetry systems for the main payload of Balloon VIII-A.

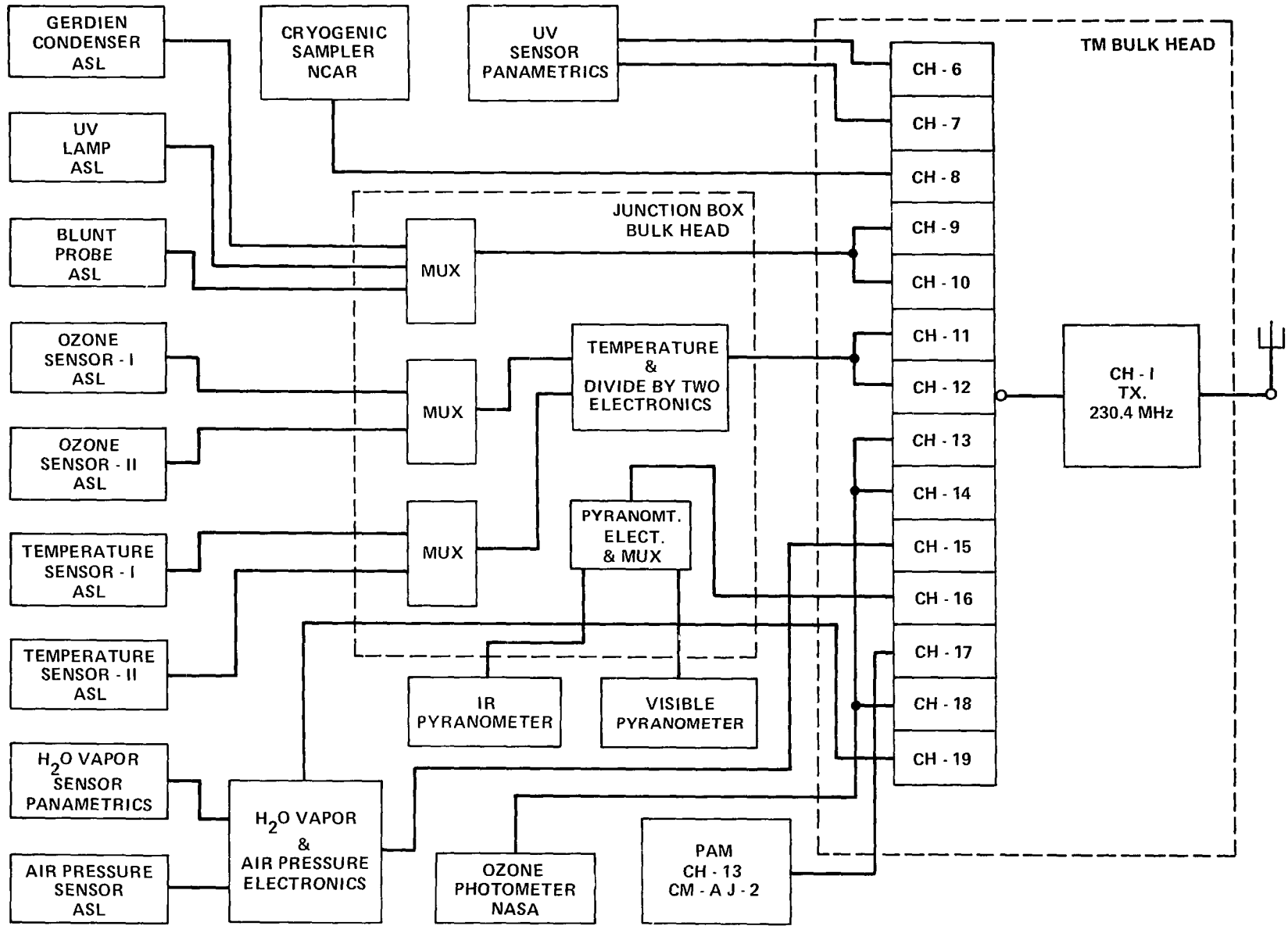

Figure 8. Distribution of channels for the 230.4 MHz telemetry link.

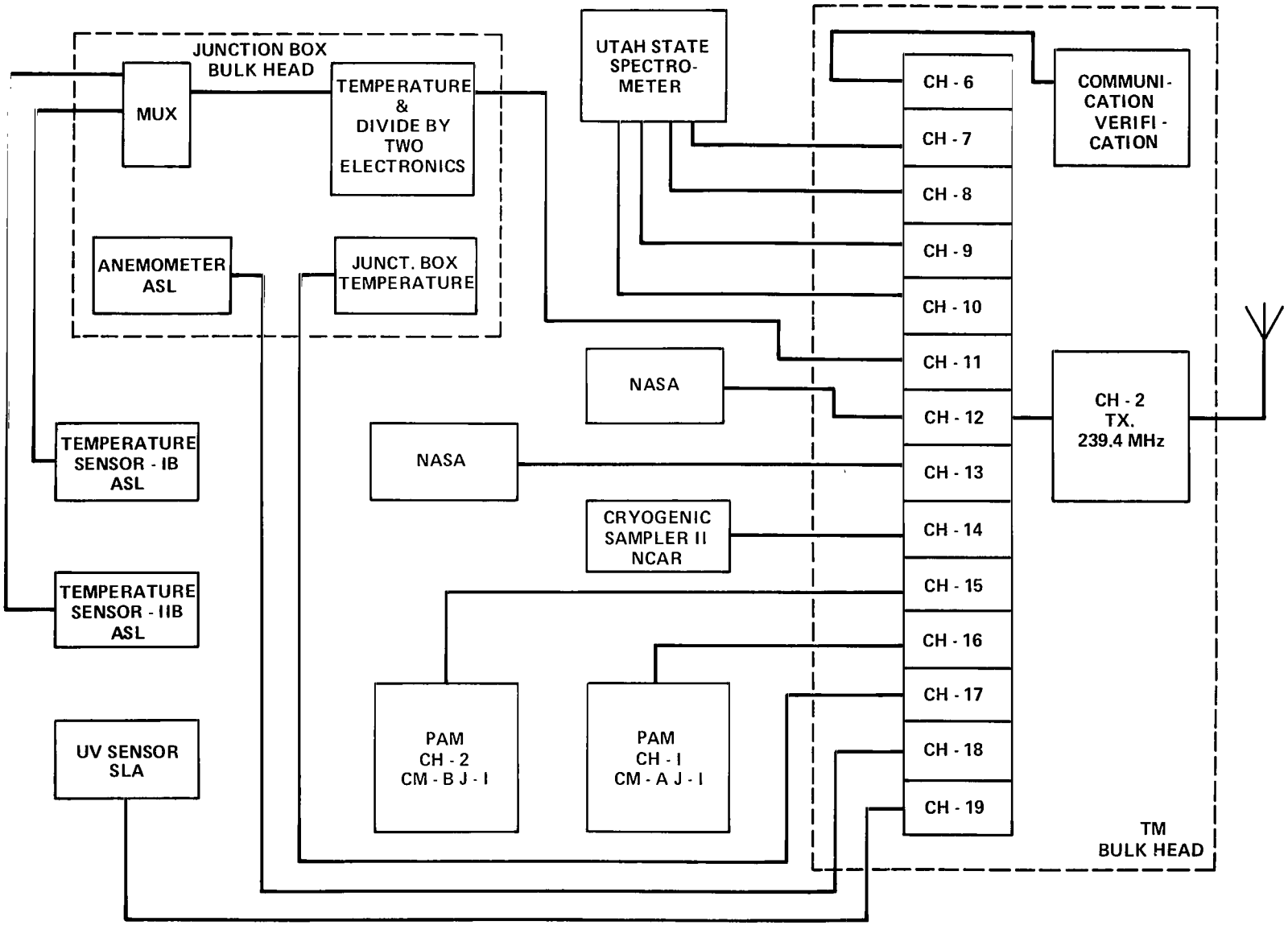

Figure 9. Distribution of channels for the 239.4 MHz telemetry link.

A portable monitor van was used during integration, preflight checks and flight operations to monitor the various telemetry channels and to send commands to the main payload. In the van were two P-bank receivers with yagi antennas, one bank of IRIG channel discriminators, and one PAM decommutator. The command system in the van included a 416.6-MHz transmitter with either 50- or 100-W power capability and an end fire helix antenna. The transmitter was modulated by an FSK encoder with 60 commands.

Further details on the electronic systems prepared by the University of Texas at El Paso may be found in their report on this flight (Reference 1).

The Stratcom VIII-B Payload

The payload prepared by D. G. Murcray and his colleagues at the University of Denver supported several types of infrared measurements. A view of this payload during launch preparations is shown in Figure 10. The gondola was constructed of brazed conduit and configured to keep the center of gravity low. The floor of the gondola was reinforced with aluminum I-beams. The rectangular design makes mounting the various components into the gondola much easier and helps keep the unit upright on impact. This type of construction has been used successfully on a number of past programs. The gondola is suspended from the corners by aircraft cables. Crash pads of crushable paper honeycomb reduce the accelerations on the instruments during impact after the flight.

The prime instrument is a 1-1/4 m Czerny-Turner IR grating spectrometer with an azimuth pointing control (at the top of its four-line suspension) and a mirror arrangement so as to observe the setting Sun. The two horizon-pointing radiometers on the left portion of the payload were for observations of the 4.3 μm and the 15 μm CO_2 thermal emission bands. Another view of this same payload, shortly before release, is shown in Figure 11. The small package extending to the side of the payload is a standard meteorological sonde.

OPERATIONS

The Stratcom VIII operation was conducted by Harold Ballard of the Atmospheric Sciences Laboratory, assisted by the staff and facilities of Holloman Air Force Base and the White Sands Missile Range. The large balloon launches were conducted by the Balloon Branch of the Air Force Geophysics Laboratory. The following section provides data concerning the balloon train, flight paths, and summaries of the related small balloon and rocket operations.

The Stratcom VIII-B Balloon

The Stratcom VIII-B Balloon, prepared by D. G. Murcray and his colleagues at the University of Denver, was the first of the large balloons to be flown, being launched from Holloman Air Force Base at 1251 MST, September 28, 1977. Range availability and weather considerations led to the

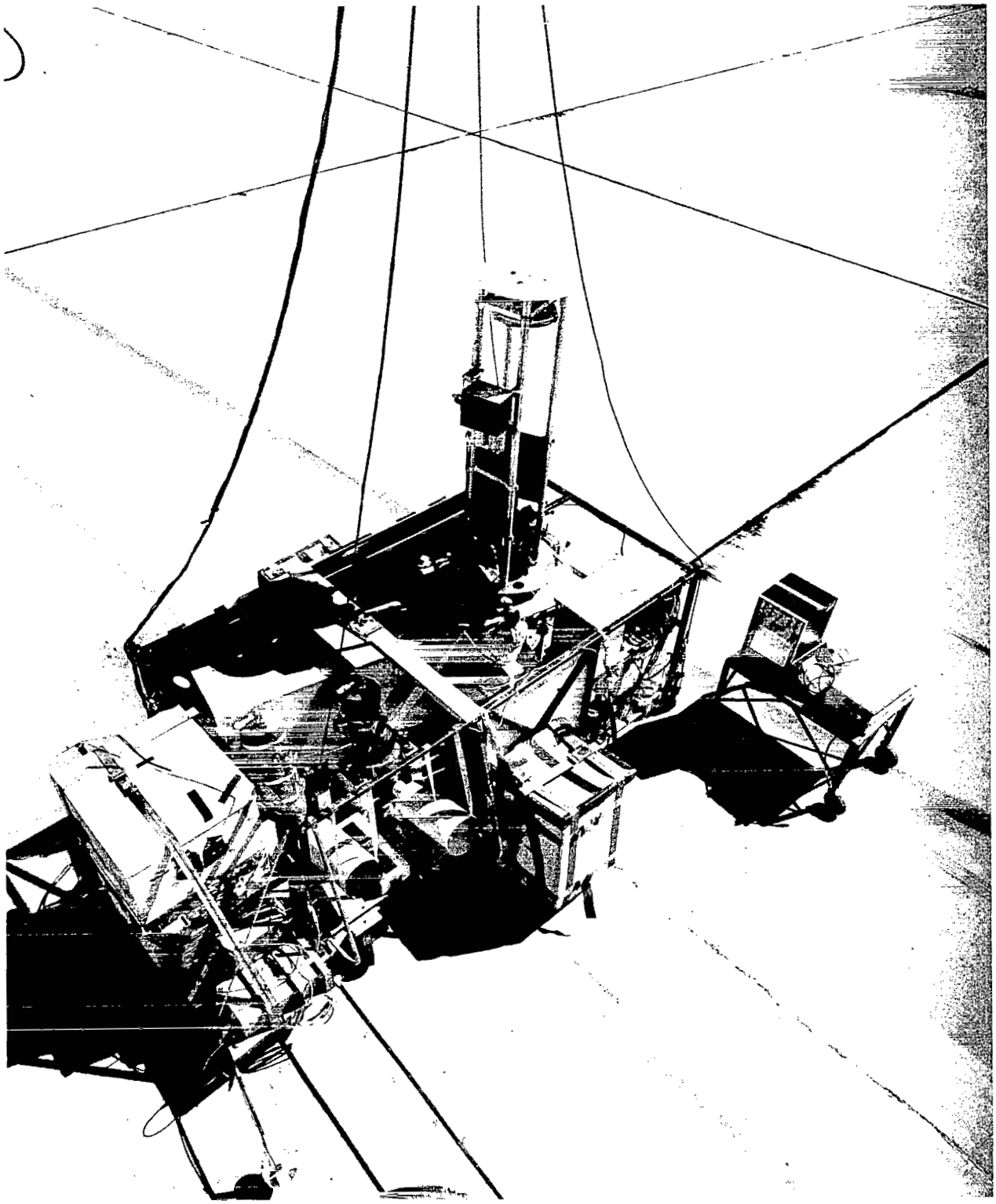

Figure 10. The Stratcom VIII-B payload during preparation at the launch site.

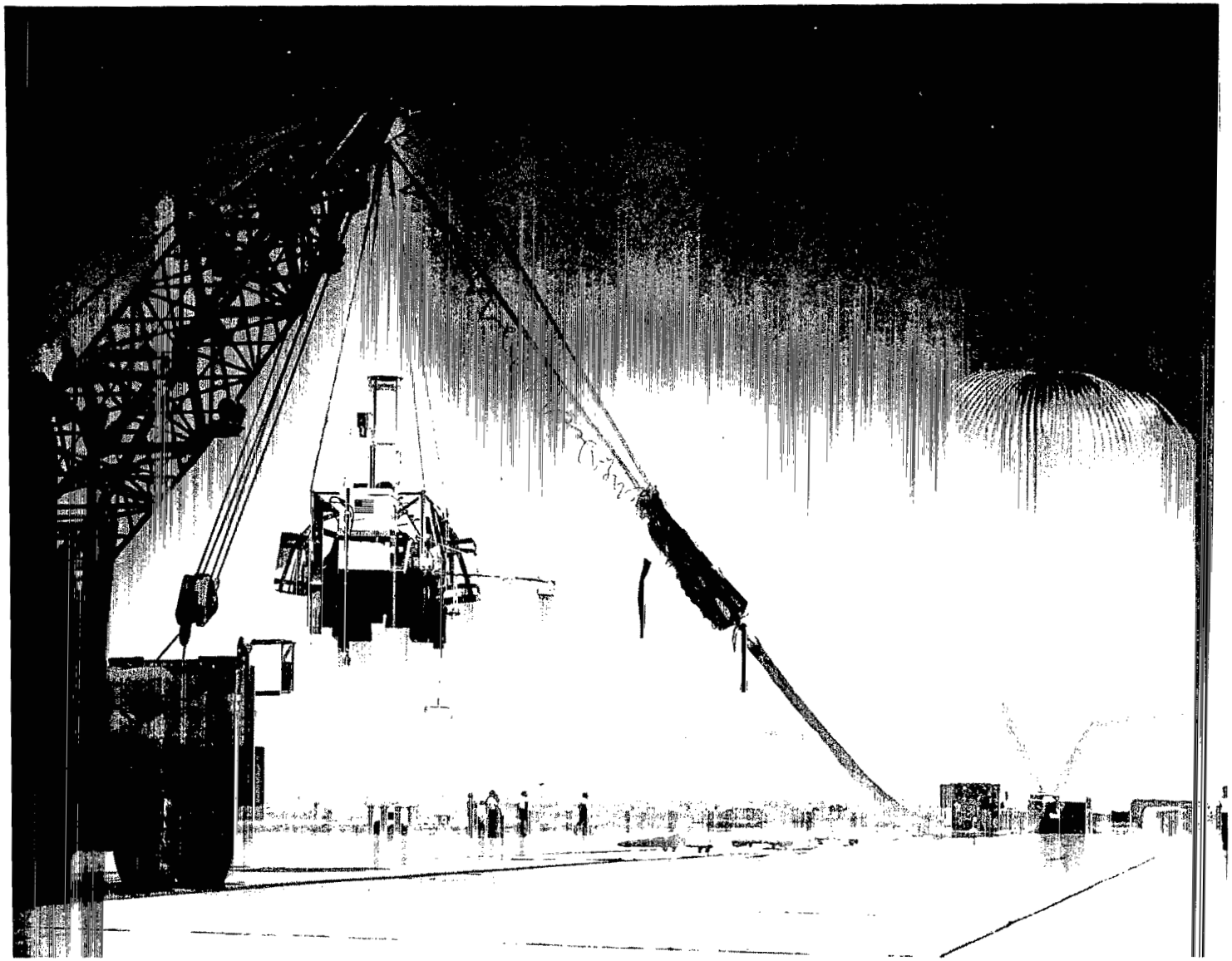

Figure 11. The Stratcom VIII-B payload prior to release.

launching of the VIII-B Balloon on the afternoon prior to the launch of the VIII-A Balloon, instead of afterwards, as originally planned.

Engineering data for the VIII-B Balloon and its payload are given in Table 3. The data system included on-board digital tape recorders, and, for the first time in the long history of this payload, a telemetry system. The latter proved to be invaluable; for the parachute system failed and the payload, including the digital tapes, burned upon impact.

Table 3
Engineering Data for Balloon VIII-B and Its Payload

Balloon:		Payload:	590 kg (1300 lb)
Material:	Stratofilm, 0.5 mil; 0.9 mil cap		
Manufacturer:	Wizen	Parachute:	
Diameter:	97.3 m (319 ft)	Quantity:	2
Volume:	3.29×10^5 m^3 (11.6×10^6 ft^3)	Type:	flat, circular
Length:	130.5 m (428 ft)	Diameter:	19.5 m (64 ft)
Weight:	568 kg (1252 lb)	Length:	27.4 m (90 ft)
		Weight:	38 kg (83.5 lb)
Ballast:	90.7 kg (200 lb)		

The VIII-B balloon followed a vertical trajectory as shown in Figure 12 and a horizontal path as shown in Figure 13. The balloon remained near its float altitude of 39 km from about 1521 MST through sunset (1822 MST) until termination at 1914 MST. The U-2 aircraft, Flight No. 77-157, flew from Moffett Field, California, to the vicinity of the VIII-B Balloon. The aircraft altitude as a function of time is shown in Figure 12, and its horizontal flight path in Figures 13 and 14.

The Stratcom VIII-A Balloon

The Stratcom VIII-A Balloon included experiments from a number of organizations, as indicated in the previous sections. Engineering data for this balloon and its payload are given in Table 4.

The Stratcom VIII-A Balloon was launched at 0607 MST, September 19, 1977, about 11 hours after the termination of the VIII-B Balloon. Figure 15 shows the vertical flight path of the VIII-A Balloon, release times for the three dropsondes, and launch times for the small balloons and rockets associated with this effort. Since the control system for the helium valves at the top of Balloon VIII-A and for ballast release became inoperable, it was not possible to descend as had been planned (see Figure 1). The variations in the altitude of the balloon that did occur are due to the changes of temperature (and density) of the helium in the balloon.

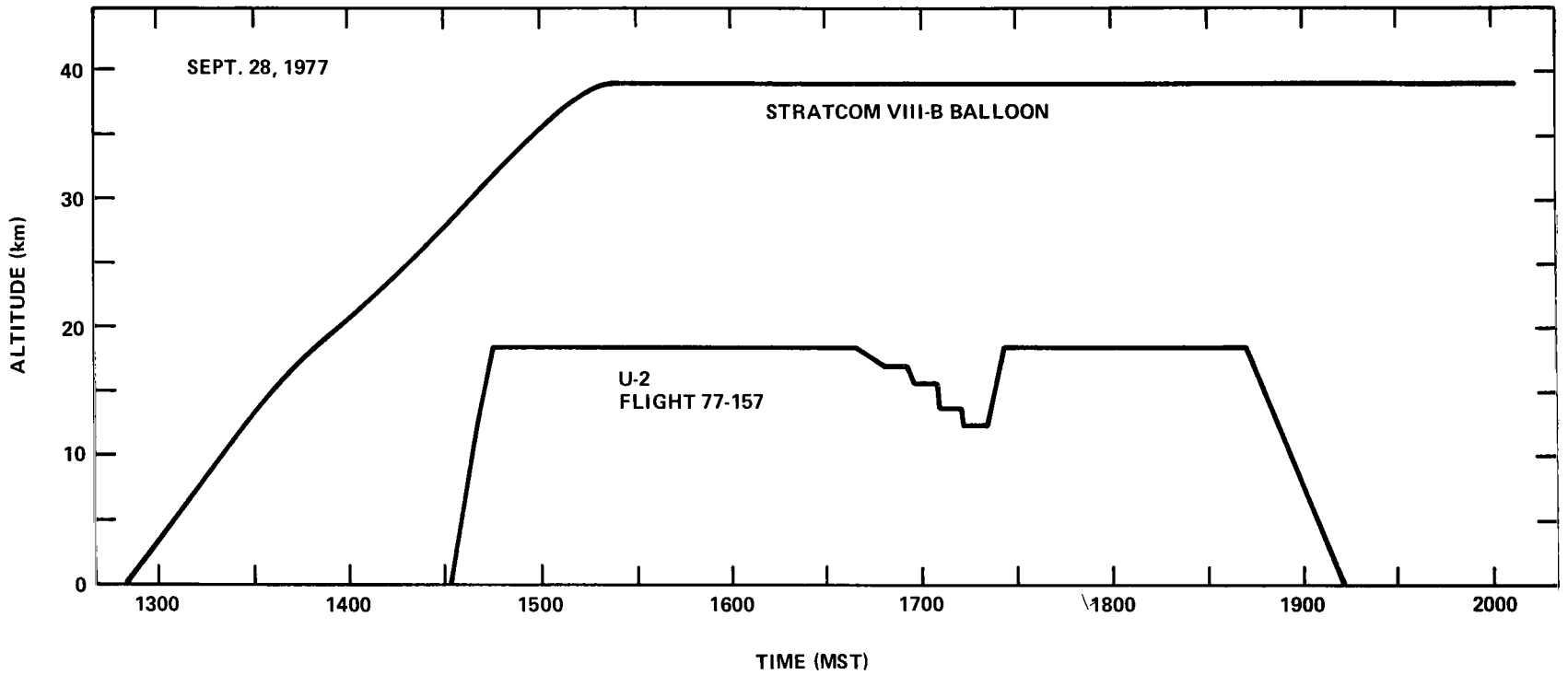

Figure 12. Vertical flight paths of Balloon VIII-B and the U-2 aircraft.

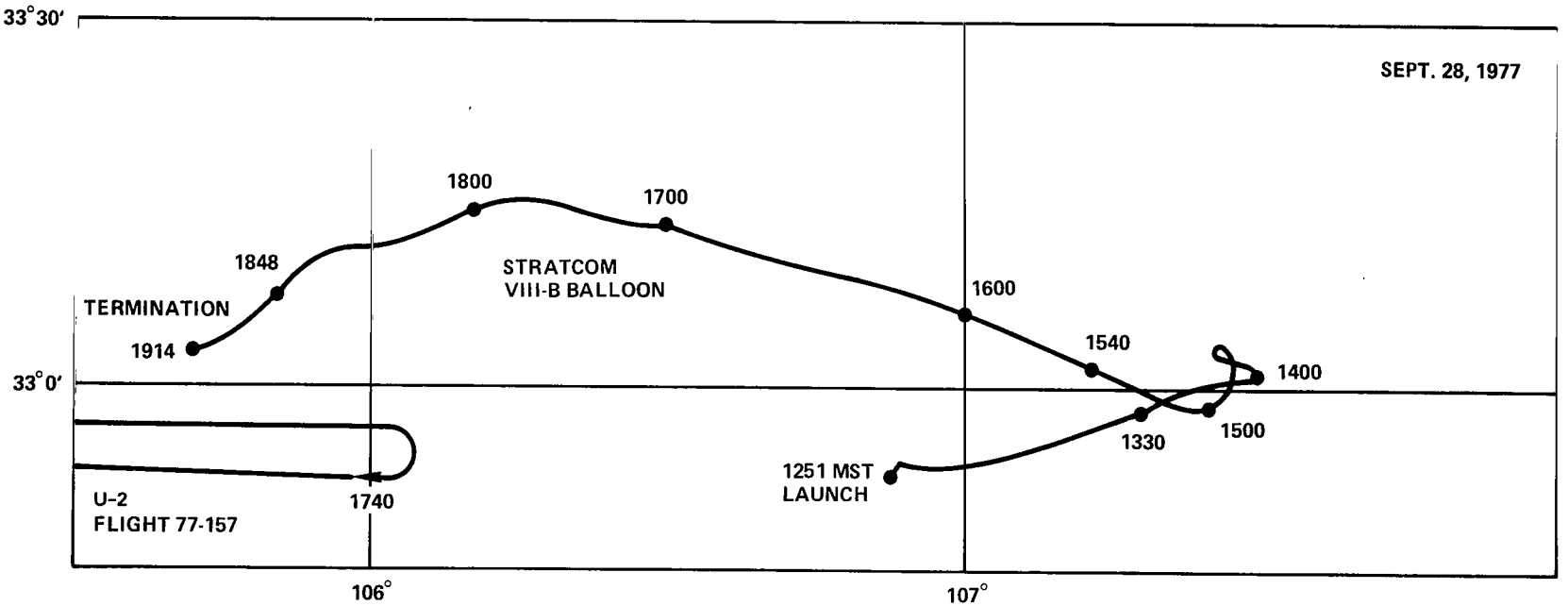

Figure 13. Horizontal flight path of Balloon VIII-B and the U-2 aircraft.

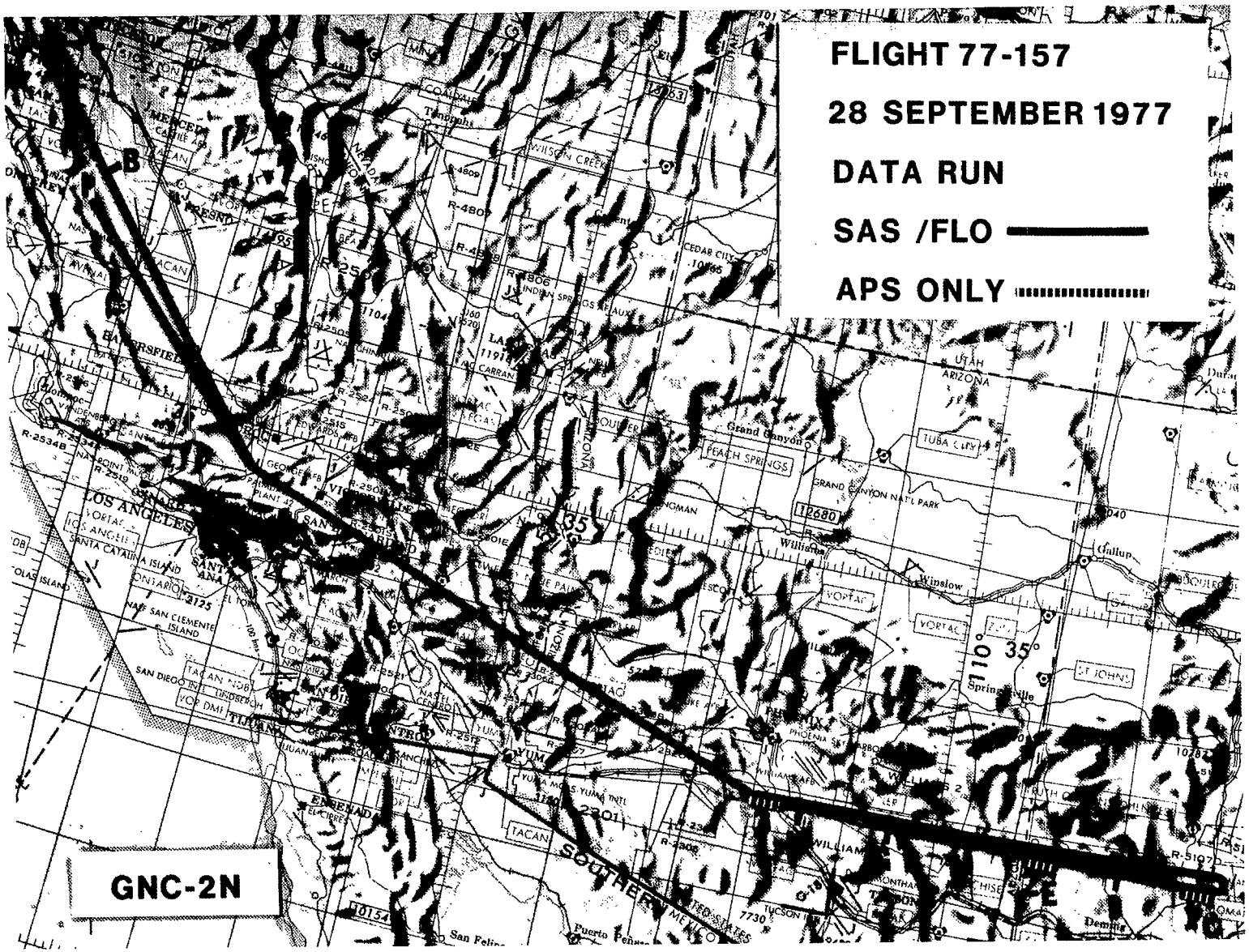

Figure 14. Flight path for U-2 flight 77-157.

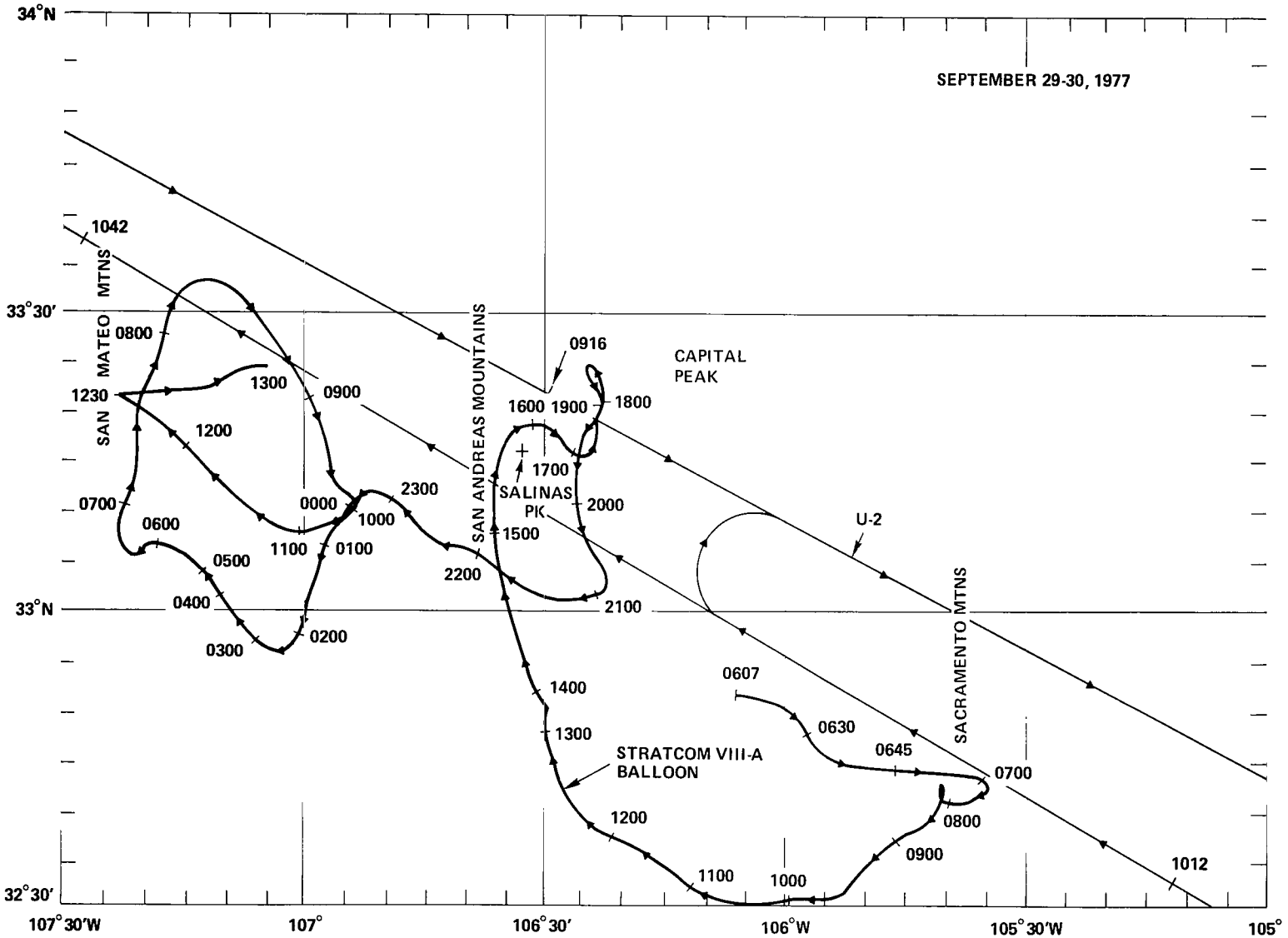

Figure 6. Horizontal flight path of Balloon VIII-A and the U-2 aircraft.

BIBLIOGRAPHY

Ballard, H. N., N. J. Beyers, B. T. Miers, M. Izquierdo, and J. Whitacre, "Atmospheric Tidal Measurements at 50 km from a Constant-Altitude Balloon," *J. Appl. Meteor.*, 11, 1138–1149, 1972.

Beyers, N. J., and B. T. Miers, "Diurnal Temperature Change in the Atmosphere between 30 and 60 km over White Sands Missile Range," *J. Atmos. Sci.*, 22, 262–266, 1965.

Beyers, N. J., B. T. Miers, and R. J. Reed, "Diurnal Tidal Motions near the Stratopause during 48 hours at White Sands Missile Range," *J. Atmos. Sci.*, 23, 325–333, 1966.

Miers, B. T., "Wind Oscillations between 30 and 60 km over White Sands Missile Range, New Mexico," *J. Atmos. Sci.*, 22, 382–387, 1965.

Taubensee, R. E., "Weather and Circulation of September 1977," *Mon. Wea. Rev.*, 105, 1619–1625, 1977.

STRATOSPHERIC TEMPERATURES FROM METEOROLOGICAL SONDES

Edith I. Reed
NASA, Goddard Space Flight Center
Greenbelt, Maryland 20771

In support of the Stratcom VIII effort, 25 balloon sondes and 12 rocket sondes were flown from September 21 to 30, 1977, to provide meteorological data. Some of the sondes were flown from the Holloman Air Force Base and others from the White Sands Missile Range about 55 km away. Details of time, location, and peak altitude are given in "The Stratcom VIII Effort" (Reed) of this document.

Air temperature data in the stratosphere for 19 of the sondes are plotted in Figure 1, showing air temperature at selected pressure levels as a function of time from September 26 to 30, 1977. Detailed vertical temperature profiles representative of conditions during the Stratcom VIII-A Balloon flight are shown in Figure 2. Data up to 24 km from 6 rawinsonde stations in the Texas-Mexico-Arizona area for September 28 are given in "Carbon Dioxide Radiant Temperature Measurements" (Murcray et al.) of this document.

Appreciation is expressed to S. Kubinski of the Atmospheric Sciences Laboratory for coordinating the flight of these many sondes in support of the Stratcom-VIII effort and for the forwarding of these data.

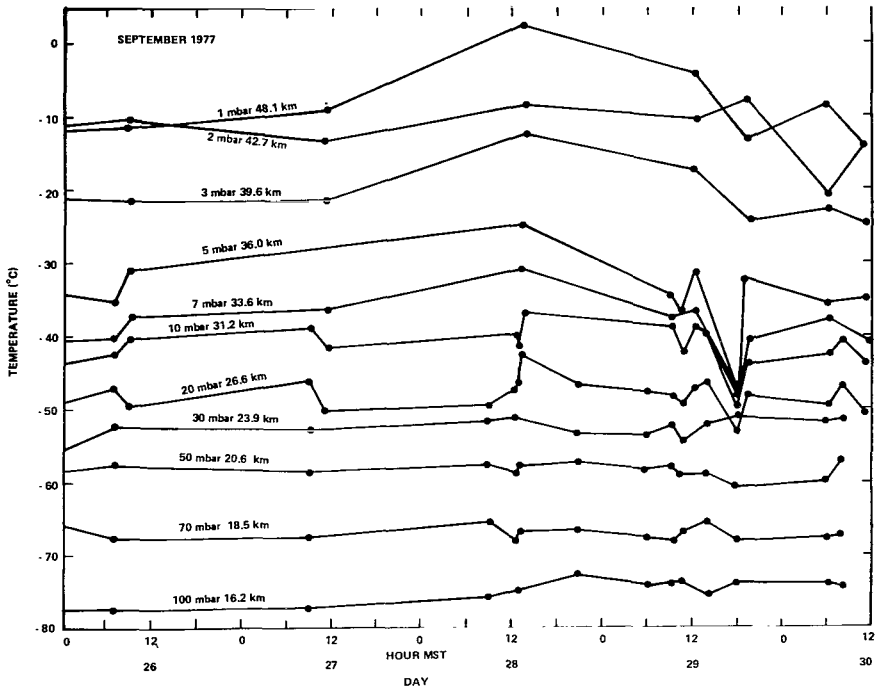

Figure 1. Air temperatures at selected pressure levels during the Stratcom VIII effort.

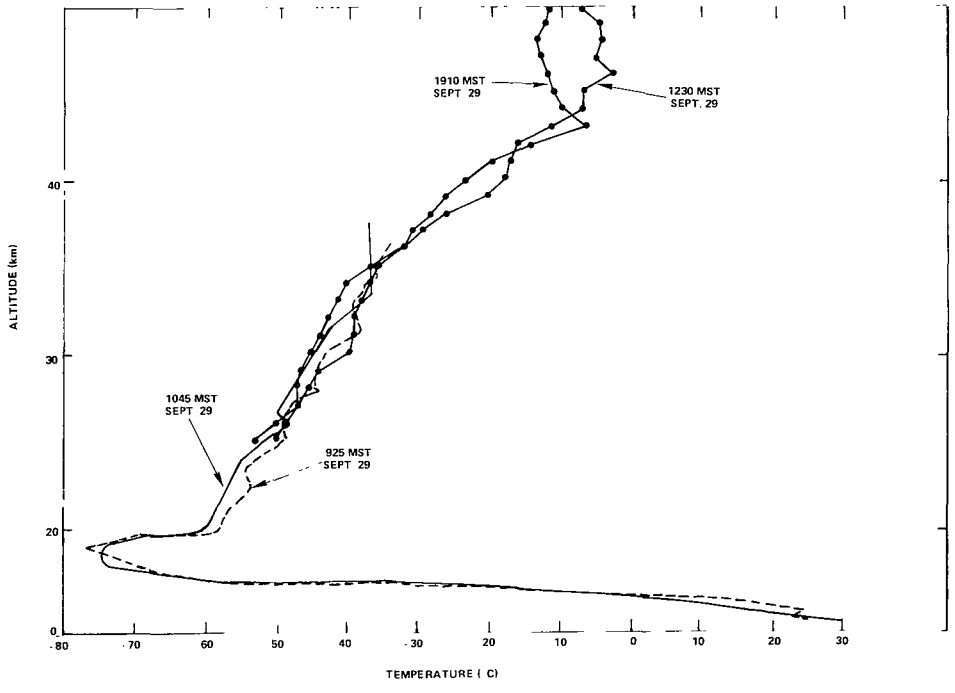

Figure 2. Vertical temperature profile on the morning of the Stratcom VIII-A Balloon flight.

AIR TEMPERATURE MEASUREMENTS WITH FILM-MOUNTED THERMISTORS

Harold N. Ballard
Atmospheric Sciences Laboratory
White Sands Missile Range
New Mexico 88002

ABSTRACT

Air temperatures in the vicinity of the main payload of the Stratcom VIII-A Balloon launched September 29, 1977, from Holloman Air Force Base, New Mexico, were measured by pairs of film-mounted bead thermistors. Above 25 km, daytime air temperatures were 10 to 15°C higher than those measured by meteorological sondes flown the same day.

INTRODUCTION

Air temperature sensors were included on the two large Stratcom VIII balloon flights in order to:

1. Measure the detailed temporal and spatial variation of air temperature at times of darkness, sunrise, and daylight; the daylight variations are to be related to the measured ultraviolet solar flux. Implicit in this objective is the determination of the diurnal tidal temperature variations at altitudes above 30 km.

2. Serve as a tool for obtaining detailed information concerning the balloon and payload behavior.

3. Provide background data for temperature-dependent experiments.

The temperature sensors are similar to those used on past Stratcom balloon flights. The results of the previous flights as well as details of sensor construction and theory are discussed in References 1 and 2.

INSTRUMENTATION

Each air temperature sensor consists of a pair of film-mounted spherical bead thermistors. The two films are arranged perpendicular to each other so that, as the payload rotates, each film-mounted bead is alternatively parallel to or fully illuminated by the Sun's rays. The maximum difference in the temperature of the sensors during a period of rotation gives an experimental determination of

the maximum solar irradiation correction. Magnetometers are used to confirm the inferred orientation. During the times when the film is parallel to the Sun's rays, shaded by other parts of the payload, or at night, no correction need be applied to the recorded temperatures. Thus accurate (±1°C) measurements of air temperatures can be made throughout the flight.

RESULTS

Sensors were placed in three locations: on the Top Package at the apex of the VIII-A Balloon; slightly below the VIII-A main payload, which was located about 200 m below the balloon; and slightly below the gondola of the VIII-B Balloon. Of the three, the sensor on the Top Package broke during launch operations and an electrical problem interferred with the temperature data on the VIII-B payload. The data reported here are from the VIII-A main payload.

Data for the entire flight are shown in Figure 1 together with radar data as a function of time. It is to be noted that the film-mounted thermistors were entirely shaded from direct solar radiation by the gondola from about 0800 MST until about 1600 MST. Data during the ascent are plotted as a function of altitude in Figure 2 along with the air temperature according to the U.S. Standard Atmosphere, 1976. In Figure 3 are added other temperature measurements: the Dasibi inlet air temperatures which also was on the VIII-A main payload, and air temperatures from the ECC sonde launched on the same day. In Figure 2 of "Ozone Measurements by a Dasibi Ozone Monitor" (Ainsworth and Hagemeyer) the observed temperatures from the film-mounted thermistors and from the Dasibi inlet thermistor are plotted as a function of time.

The temperatures in the vicinity of the main payload, while at float, are consistently 10 to 15° higher in the daytime than are air temperatures inferred from meteorological sondes. The fluctuations in the vicinity of the VIII-A payload appear to be real. As noted in the discussion by Rubio et al. ("Measurement of Radiation Energy Transfer"), there is no clear correlation of air temperature with the measured upwelling long-wave irradiance.

The data reported from the earlier flights (Stratcom II, III, VI, and VII) were from similar sensors, similarly located, i.e. 200 to 300 m beneath the balloon. These data, associated with vertical velocities of greater than 0.5 m/s, represent true air temperatures. Similarly, the data during the ascent (4.4 m/s) of Stratcom VIII represent true air temperatures. However, data during float and the subsequent slow descent (0900 to 1800 MST when vertical velocities were less than 0.5 m/s) are representative of the temperature of the thermal envelope surrounding the large balloon and its payload.

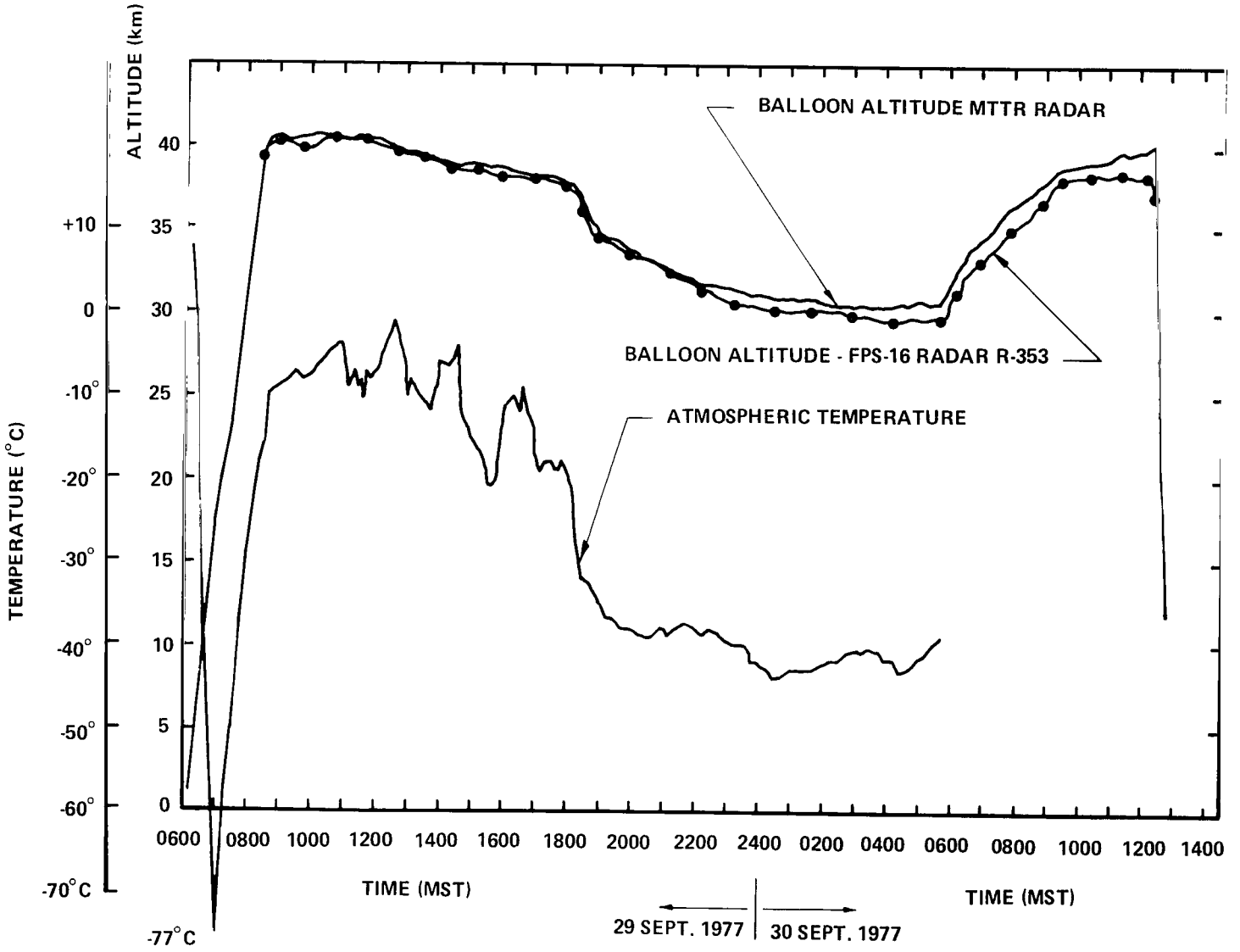

Figure 1. Temperatures measured from the Stratcom VIII-A Balloon.

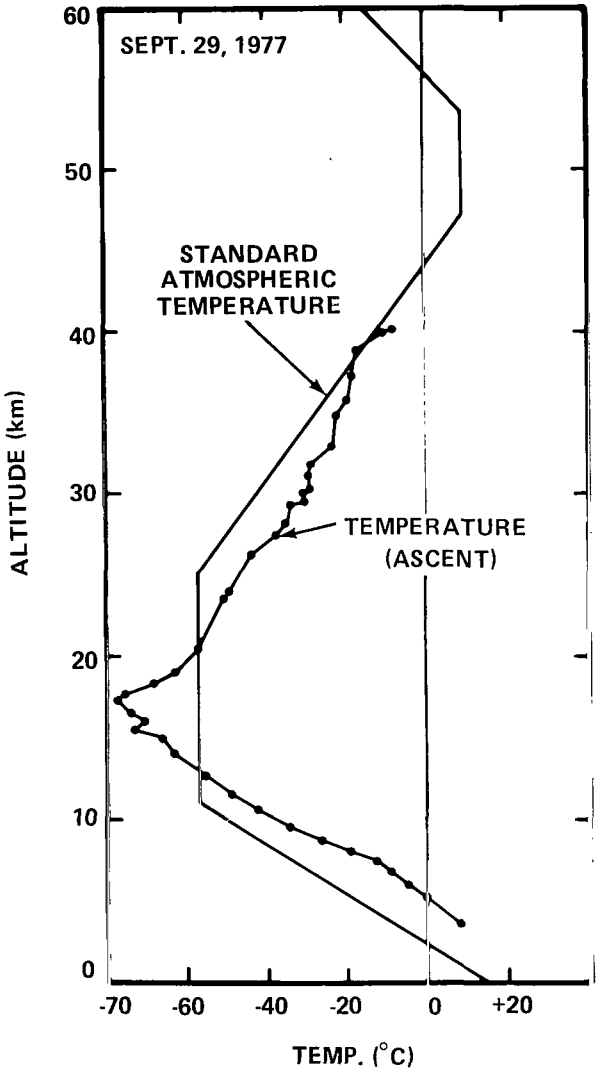

Figure 2. Film-mounted thermistor temperature profile.

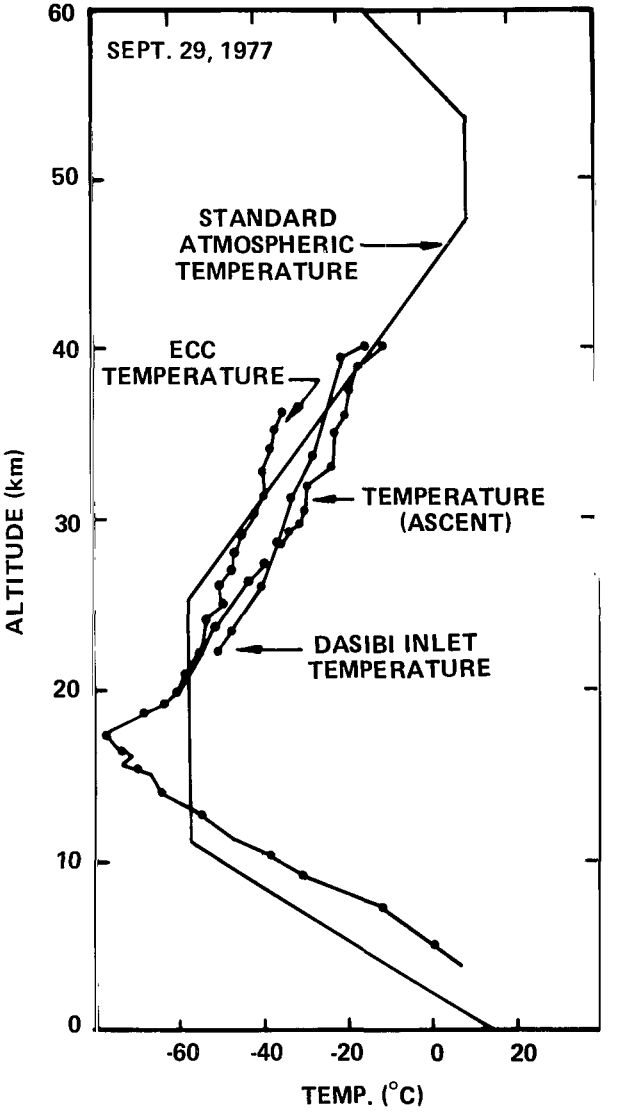

Figure 3. Temperature profile on the morning of September 29.

REFERENCES

1. Ballard, H. N., M. Izquierdo, C. McDonald, and J. Whitacre, "Atmospheric Temperatures Measured Near 48 Kilometers by Balloon-Borne Thermistors," Proceedings, Eighth AFCRL Scientific Balloon Symposium, Sept. 30 to Oct. 3, 1974, AFCRL-TR-74-0393, A. S. Carten, Jr., Editor, pp. 401-416.

2. Ballard, H. N., M. Izquierdo, C. McDonald, and J. Whitacre, "Temperature Measurements in the Stratosphere from Balloon-Borne Instrument Platforms, 1968-1975," ECOM-5808, Dec. 1976. U.S. Army Electronics Command, Fort Monmouth, New Jersey 07703, 45 pp.

AIR PRESSURE MEASUREMENT

Harold N. Ballard
Atmospheric Sciences Laboratory
U.S. Army Electronics Command
White Sands Missile Range
New Mexico 88002

A sensor to measure atmospheric pressure was included on the Stratcom VIII-A balloon flown September 29, 1977 from Holloman Air Force Base, New Mexico. The Rosemount Model 830J sensor uses a capacitive diaphragm, has a range of 0 to 133 millibars, and a response time of 0.25 second. It is temperature compensated over the range of -55° to +70°C, and has an accuracy of 2.5 percent. The resolution, as limited by the external systems, is 0.06 mb. For this flight, the sensor was turned on during ascent at an altitude of 20 km. The observed pressures as a function of time and altitude are shown in Figures 1 and 2. For reference purposes, the pressure values given by the U.S. Standard Atmosphere 1976 are also included in Figure 2. Selected data values are given in Table 1.

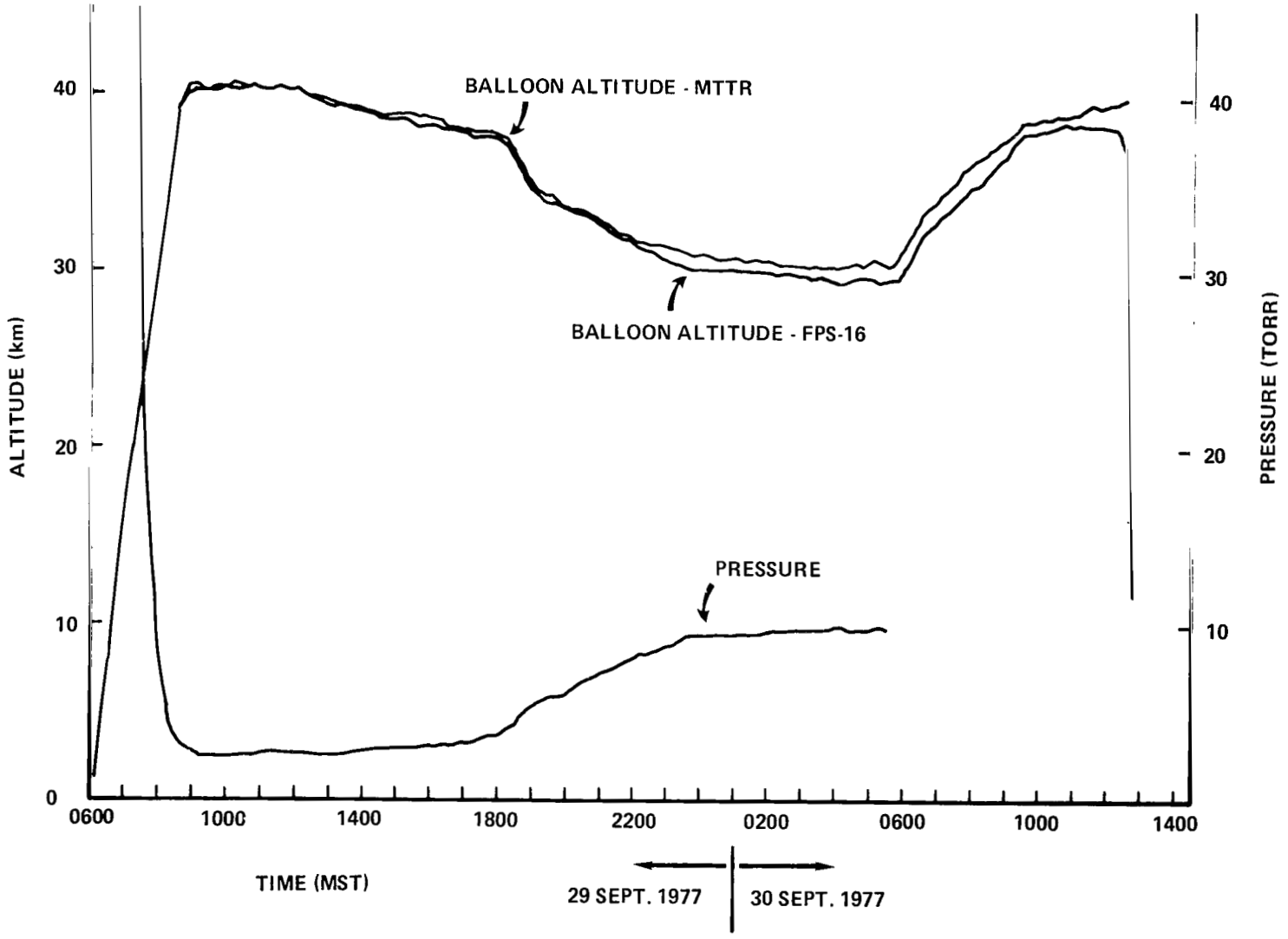

Figure 1. Atmospheric pressure and Balloon VIII-A altitude as a function of local time.

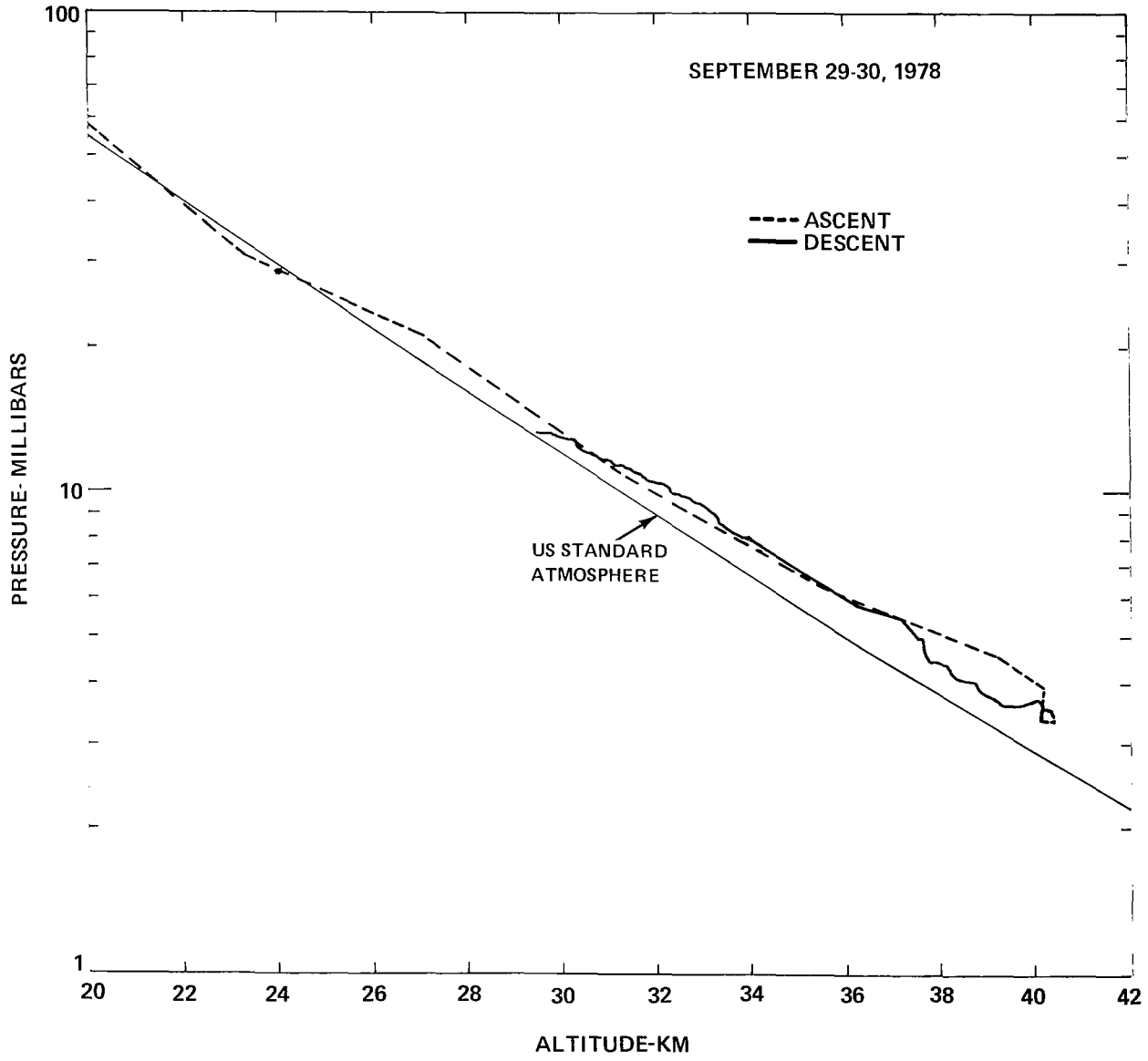

Figure 2. Atmospheric pressure as measured on the VIII-A Balloon gondola as a function of altitude. Also included are pressures from the U.S. Standard Atmosphere.

Table 1
Atmospheric Pressure, Altitude, and Time

MST Time	Alt. km	Press. mbar	MST Time	Alt. km	Press. mbar
0715	20.051	57.13	1931	33.963	8.0
0730	23.385	30.8	1946	33.795	8.0
0745	27.113	20.1	1958	33.601	8.27
0801	31.282	10.8	2014	33.398	8.53
0816	35.444	6.33	2030	33.215	9.09
0830	39.305	4.53	2045	32.971	9.47
0847	40.200	3.93	2100	32.753	9.80
0908	40.194	3.33	2115	32.328	9.87
0920	40.223	3.33	2130	32.136	10.20
0942	40.35	3.33	2144	31.955	10.40
1000	40.424	3.33	2200	31.617	10.8
1013	40.399	3.33	2215	31.322	11.27
1028	40.363	3.5	2230	31.217	11.27
1049	40.250	3.5	2245	30.948	11.57
1107	40.237	3.67	2300	30.725	11.80
1123	40.392	3.67	2317	30.533	12.0
1138	40.380	3.63	2330	30.373	12.3
1211	40.136	3.67	2345	30.224	12.7
1244	39.653	3.6	0000	30.238	12.7
1250	39.600	3.6	0015	30.216	12.7
1318	39.321	3.6	0030	30.222	12.7
1337	39.259	3.67	0045	30.306	12.7
1353	39.114	3.73	0100	30.306	12.7
1413	38.862	3.87	0115	30.176	12.77
1433	38.790	4.00	0132	30.214	12.67
1452	38.629	4.00	0146	30.070	12.67
1508	38.514	4.00	0200	30.046	12.93
1536	38.284	4.1	0215	29.946	12.93
1551	38.218	4.29	0230	29.930	12.93
1617	38.159	4.27	0245	29.856	13.00
1632	38.054	4.33	0300	29.832	13.13
1649	38.057	4.40	0315	29.791	13.13
1708	37.769	4.40	0330	29.681	13.13
1724	37.670	4.67	0345	29.658	13.13
1739	37.660	5.00	0400	29.576	13.33
1801	37.528	5.00	0416	29.560	13.13
1814	37.169	5.47	0430	29.697	13.00
1830	36.263	5.80	0445	29.649	13.00
1845	35.142	6.73	0500	29.627	13.00
1903	34.381	740	0515	29.558	13.33
1916	34.195	7.67	0530	29.581	13.00

WATER VAPOR MEASUREMENTS WITH ALUMINUM OXIDE SENSORS

Philip Goodman*
Panametrics, Inc.
221 Crescent Street
Waltham, Massachusetts 02154

ABSTRACT

Four Aquamax aluminum oxide water vapor sensors were flown on the Stratcom VIII-A Balloon on September 29, 1977, from the Holloman Air Force Base, New Mexico. Two sensors were in the vicinity of the main payload, one was on the apex plate at the top of the balloon, and one was on a dropsonde released from the main payload near an altitude of 40 km. The first two sensors were primarily for observation of the environment in the vicinity of the payload, and showed water vapor densities appreciably higher than ambient. The data from the sensor on the apex plate during ascent through the stratosphere and the data from the dropsonde indicated that the water vapor profile in the stratosphere was layered and had an average of about 2 ppm_w.

INTRODUCTION

Water vapor is an important constituent in the stratosphere since it participates in the photochemistry of ozone, is involved in the energy balance in the stratosphere, and is useful as a tracer in the study of transport processes. Furthermore, a knowledge of the water vapor content in the immediate vicinity of the balloon payload is often needed for a proper interpretation of data from other instruments.

Water vapor measurements were made aboard the Stratcom VIII-A Balloon (launched from Holloman Air Force Base, New Mexico, at 0607 MST on September 29, 1977) by means of aluminum oxide sensors. This flight was the fourth in a series of such measurements. Measurements during the Stratcom V (Reference 1) and Stratcom VI-A (Reference 2) efforts used foil type Al_2O_3 water vapor sensors. For the Stratcom VII-A flight, a new integrated-circuit Aquamax sensor was used for the first time (Aquamax is a registered trademark of Panametrics, Inc.). This new sensor is described in greater detail in Reference 3, which discusses the results obtained during the Stratcom VII-A flight. The same type sensor was used for the Stratcom VIII-A observations.

*Current address: Office of Science and Technology, Department of Commerce, Washington, D.C. 20230.

The Stratcom VIII-A water vapor experiment was designed to measure both the ambient densities of water vapor, and also the water vapor content associated with the main instrument package during flight. To accomplish this, water vapor was measured at the apex of the Stratcom VIII-A Balloon and at two locations on the main gondola, thus permitting an estimate of the gradient. In addition, a fourth sensor was installed on a dropsonde to measure the ambient water vapor profile during descent from maximum altitude.

INSTRUMENTS

The sensors for the Stratcom VIII-A effort were identical to the Aquamax sensors that were used in the Stratcom VII effort. These sensors, their thin film construction by means of semiconductor fabrication techniques, their performance characteristics, and their calibration (including temperature dependence) are described in detail in Reference 3. The only significant difference between the sensors for the Stratcom VIII-A effort and those used earlier is a minor change in the sensor system so that the impedance is more nearly a linear function of frost point. This results in greater sensitivity, particularly in the low frost-point region.

The sensors aboard the Stratcom VIII-A Balloon were positioned the same as those on the Stratcom VII-A Balloon. One sensor was part of the top package on the balloon apex plate. Two sensors were part of the instrument package and were deliberately placed at different distances from the frame. One of these sensors was suspended about 90 cm below one of the two chemiluminescent ozone instruments which was itself positioned about 120 cm to the side of the frame. The second sensor was suspended 90 cm below the frame of the instrument package. One sensor was incorporated into a small (3-kg) parachute-supported dropsonde for release after achieving peak altitude. This sensor, suspended below the entire dropsonde train and, hence, sampling unperturbed air, was designed to measure the ambient water vapor concentration as the sonde descended from peak altitude through the stratosphere until it entered the top layers of the troposphere.

RESULTS

Ambient water vapor values are obtained from the dropsonde (parachute drop no. 3) released from the Stratcom VIII-A Balloon at 0945 MST, shortly after achieving peak altitude. These data in terms of frost point are shown in Figure 1. The points on the curve are at 1-minute intervals. Temperature corrections were made assuming the temperature profile shown in Figure 1 from ECC sonde data. The dashed line is an extrapolation of the ECC sonde data; the points above 35 km are air temperatures from three rocket meteorological sondes, one on September 27 and two on September 30. The accuracy of the frost point data in the stratosphere is estimated to be ±3°C. The initial value from the dropsonde is relatively high, as would be expected within the boundary layer of the main payload. However, the values drop rapidly, consistent with a time constant of less than 1 minute to values of less than -100°C, indicating a very dry and presumably ambient atmosphere with less than 1 ppm_w water vapor. A layering is evident in the altitude profile; these layers are superimposed

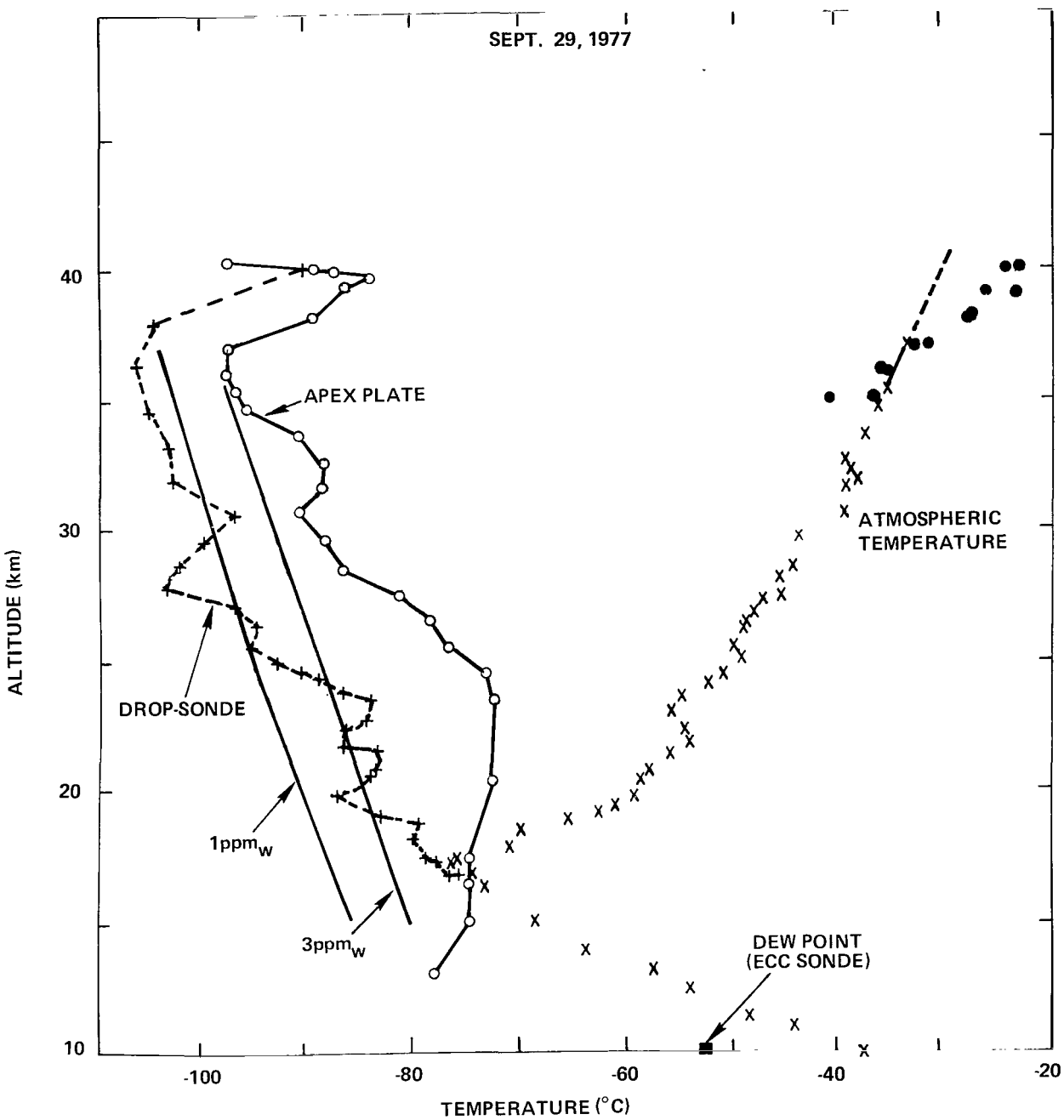

Figure 1. Water vapor data. Crosses are frost points at 1-minute intervals from dropsonde No. 3 during its descent. Circles are frost points at the apex of the Stratcom VIII-A Balloon during its ascent. The X's represent air temperature measured by the ECC sonde flown the same morning. The dots above 35 km are air temperatures from rocket sondes. The square at 10 km is the dew point from the ECC sonde.

upon an increase, below 25 km, to a saturated value at the tropopause near 17 km. The telemetry recorders were turned off at that time, precluding data from the dropsonde at lower altitudes. The ECC sonde indicated a relatively dry troposphere, with a relative humidity of less than 20 percent from 4 km to at least 10 km.

At the top of the balloon, water vapor values in the stratosphere are influenced by the presence of the balloon. Data from the sensor on the apex plate during ascent are shown in Figure 1, where they can be compared to the dropsonde data. The apex data were temperature corrected using the ECC sonde air temperature. Data from the apex sensor start at 13 km and indicate a dry troposphere. This is in contrast to the experience on Stratcom VII where ice, deposited on this sensor while in the troposphere, remained on the sensor for much of the ascent. The apex sensor, in close agreement with the dropsonde sensor, indicates a saturated condition at the tropopause near 17 km. In the stratosphere, the warming balloon continues to evolve water vapor, keeping frost points at the apex plate as much as 30°C above ambient, although the trend follows that of the dropsonde with some evidence of layering.

During the ascent, near 35 km, dropsonde no. 1, weighing about 70 kg was released. This, no doubt, was accompanied by a brief "shudder" of the entire balloon as the change in tension propagated upward. This may have released bits of frost that had accumulated on the balloon during its passage through the troposphere, resulting in the marked increase in water vapor as monitored at the apex plate. Shortly after reaching peak altitude, telemetry from the Top Package ceased.

The close agreement between the Apex sensor and the dropsonde sensor at the saturated tropopause indicates a precision, and probably an accuracy as well of ±1°C.

Water vapor values in the vicinity of the main payload were obtained from two sensors from about 1030 to 1745 MST. The reasons for the absence of data before and after this period are not known. The available data from the two sensors, shown in Figure 2 and Table 1, are in reasonably good agreement. Also shown is the air temperature near the main payload as measured by the film temperature sensors (see Ballard, this document) and which were used in correcting the data from the water vapor sensors. The data in Figure 2 start about 1-1/2 hours after the balloon reached its float altitude. Between 1030 and 1745 MST the balloon descended slowly to 35 km, as is also shown in Figure 2. In this portion of the flight, as in preceding flights, a relatively rapid outgassing of the balloon and instrument package is taking place. During this flight the two sensors showed divergences from one another during certain portions of the flight but were frequently in good agreement with each other. The sensor suspended below the instrument package showed somewhat lower water vapor concentrations than the sensor located in the horizontal plane of the package, as would be expected. Slightly higher values measured during this flight as compared with ambient concentrations in the instrument package vicinity during the Stratcom VII-A flight are consistent with the temperatures measured in the envelope surrounding the instrument package which were considerably higher than free ambient temperatures. Such envelope temperatures would be expected to induce greater desorption from the instrument package surfaces and interior structures. A correlation between the air temperature (as influenced by the temperature of the payload) and the water vapor content is evident.

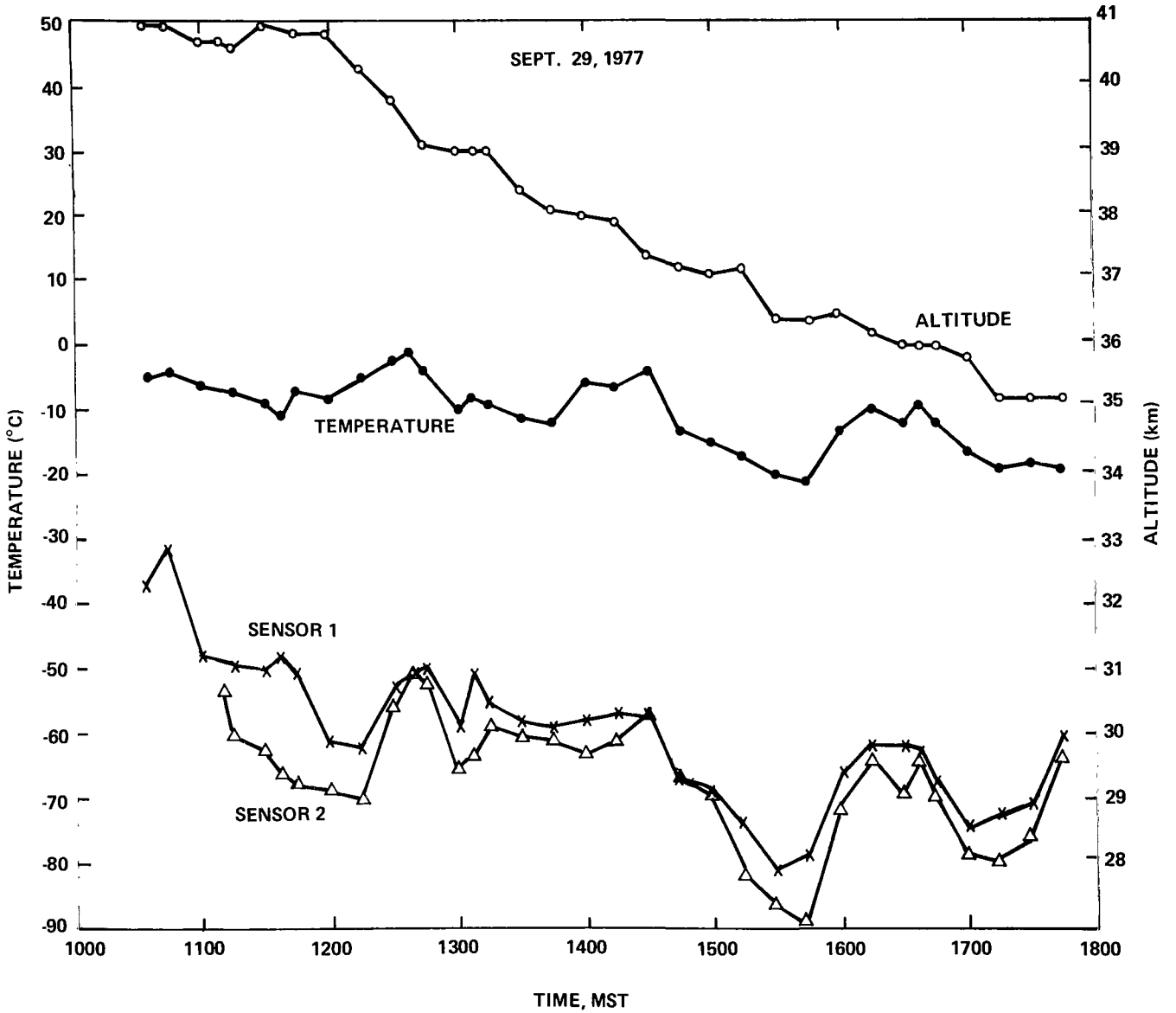

Figure 2. Payload environment for Stratcom VIII-A. Shown are altitude, temperature near the main payload, and frost points from the two water vapor sensors on the payload.

Table 1
Water Vapor Measurements–Frost Point and Mixing Ratio Data from Stratcom VIII-A Gondola-Mounted Sensors

Time (MST)	Altitude (km)	Frost Point, °C		$PPM_W(H_2O) \times 10^{-2}$	
		Sensor 1	Sensor 2	Sensor 1	Sensor 2
1100	40.7	-47.5	-	127	-
1200	40.8	-61.5	-69.0	21.2	7.3
1300	39.0	-58.5	-65.5	25.0	9.5
1400	38.0	-58.0	-63.0	23.2	11.8
1500	37.1	-59.0	-59.5	18.0	16.8
1530	36.4	-81.0	-87.0	0.61	0.22
1600	36.5	-66.0	-72.0	5.8	2.6
1700	35.8	-75.0	-78.5	1.5	0.85
1745	35.2	-60.0	-64.0	12.0	6.9

CONCLUSIONS

Once again, as in the Stratcom VII series, the Aquamax sensors have provided useful and informative data with regard to the water vapor concentrations at different locations in the Stratcom VIII-A environment. All sensors performed satisfactorily and provided generally internally consistent data which, at the apparently saturated tropopause, were also in excellent agreement with ambient temperature data. The rapid sensor response time permitted much detail of the altitude and temporal variation to be detected.

Unperturbed ambient concentrations, as determined from dropsonde data, average approximately 2 ppm_W but much structure and wide variations, ranging from a low of 0.3 ppm_W to a high of 5.7 ppm_W, were observed in the stratosphere. It is to be noted that an accuracy estimate of ±3°C in these frost point data would, if appropriately applied, reduce, but not eliminate, the magnitude of the variation. Nevertheless, the data obtained could, for this particular stratosphere, be interpreted to indicate a mixing ratio which slowly decreases with altitude above the tropopause. Superimposed upon the decrease is a layered structure. More data of this type are required to ascertain whether this is an isolated or a more general phenomenon.

A relatively dry upper tropopause permitted the sensor located on the apex plate to provide data during most of the ascent. Such data indicated a similar layering structure in the stratosphere as was observed by the dropsonde despite the evident contamination arising from the balloon and surrounding structure. Previous Stratcom flights has provided usable data only at much higher altitudes

during the ascent because of ice film formation on the sensor surface in wet tropospheres. The sensor now under development, for which the substrate is heated well above the ambient, should obviate the problem even if wet tropospheres are encountered in future flights.

The two sensors positioned in the vicinity of the instrument package provided data in general accord with previous experience as modified by a temperature at this location which was significantly higher than the unperturbed ambient. Outgassing rates and local concentrations were higher with the result that concentration gradients were smaller.

Water vapor data from previous Stratcom flights have provided supporting evidence for circulatory features detected by other instruments and have suggested other such features as a result of the water vapor data themselves. Preliminary attempts at such correlations for this flight indicate that such correlative features are once again present but more detailed examination and analysis is required.

REFERENCES

1. Goodman, P., "Water Vapor Measurements During a 48-km Balloon Flight, in Stratospheric Composition Balloon-Borne Experiment 18 September 1972," ECOM Report 5554, compiled by H. N. Ballard and F. P. Hudson, U.S. Army Electronics Command, Fort Monmouth, New Jersey, January 1975.

2. Goodman, P., "Measurement of Water Vapor Concentrations During Stratcom VI-A Experiment," Final Report on Contact DAAD 07-75-C-0080, White Sands Missile Range, New Mexico, July 1976; and published in "Stratospheric Composition Balloon-Borne Experiment, 23-26 September 1975," ECOM Report 5830, compiled by H. N. Ballard and F. P. Hudson, U.S. Army Electronics Command, Fort Monmouth, New Jersey, October 1977, pp. 87-97.

3. Goodman, P., "Stratcom VII-A Water Vapor Environment and Stratospheric Profile," Final Report on Contract DAEA 18-76-C-0177, White Sands Missile Range, New Mexico, August 1977.

TOTAL OZONE FROM THE DOBSON SPECTROPHOTOMETER

Jagir Randhawa
U.S. Army Electronics Command
Atmospheric Sciences Laboratory
White Sands Missile Range
New Mexico 88002

A Dobson spectrophotometer, Serial No. 86 located at the Atmospheric Sciences Laboratory, is routinely used to make observations of the total column content of ozone each day near noon. This instrument was last calibrated against the U.S. standard (No. 83) in Boulder, Colorado, in 1975, and continues to perform as expected.

During the Stratcom VIII effort, the data obtained were:

September 28, 1977	0.291 atm-cm
September 29, 1977	0.279 atm-cm
September 30, 1977	0.282 atm-cm

TOTAL OZONE FROM AN ULTRAVIOLET FILTER PHOTOMETER

Peter G. Simeth
SenTran Company
2705 de la Vina St.
Santa Barbara, California 93105

An ultraviolet filter photometer was operated at Holloman Air Force Base simultaneously with the Dobson spectrophotometer at the Atmospheric Sciences Laboratory (White Sands Missile Range) on September 29, 1977, in order to assess the ability of the filter photometer to measure total column content of ozone.

INSTRUMENT

The SenTran filter photometer is a four-channel instrument similar in construction to the Rocoz photometer widely used on sounding rockets for ozone profile measurements (Reference 1). The filters were chosen to correspond to the A and C pairs used by the Dobson spectrophotometer, that is, with center wavelengths of 325.5 nm/305.5 nm and 332.5 nm/311.5 nm. The field of view was set at 2.3° by replacing the flat plate diffuser with a lens system. The instrument was manually pointed to the Sun.

RESULTS

For the Dobson spectrophotometer, total ozone values were derived from the A and D pair; for the filter photometer, total ozone was calculated from the 332.5-nm and 311.5-nm data, corresponding to the Dobson C pair. The results are as follows:

Local Time	0858	1000	1102	1301	1401	1500	Average
Dobson (atm-cm)	0.278	0.278	0.284	0.285	0.282	0.278	0.281
SenTran (atm-cm)	0.279	0.284	0.289	0.283	0.277	0.280	0.282

DISCUSSION

Ozone values derived from the C pair UV filter photometer readings agreed very well with those from the Dobson spectrophotometer, but values from the A pair readings were approximately 15 percent low. Investigation showed that calibration of the A pair filters was not adequate. A subsequent comparison test was made with the Dobson spectrophotometer at Wallops Flight Center (June 26

through June 29, 1978) using the same photometer with a set of recently calibrated filters. This time, ozone values derived from both the A pair and the C pair were within 3 percent of the Dobson ozone values during the entire 4-day period.

REFERENCE

1. Krueger, A. J., P. G. Simeth, B. C. Ellison, W. R. McBride, M. Hill, C. A. Flanagan, W. Gammill, and S. G. Park, 1978: "Design of an Optical Ozonesonde for the Super Loki-Dart Rocket," *NASA Technical Report*, in preparation, 1979.

OZONE PROFILE FROM THE ECC OZONESONDE

Charles Manion
NASA, Wallops Flight Center
Wallops Island, Virginia 23337

ABSTRACT

An Electrochemical Concentration Cell (ECC) ozonesonde was flown from a small balloon to an altitude of 36 km at the White Sands Missile Range on September 29, 1977, as part of the Stratcom VIII effort. It was included primarily for the purpose of comparing the ECC in situ ozone data with that from other sensors, both in situ and remote. The ECC sonde provided an ozone profile to an altitude of 36 km with a maximum ozone density of 4.30×10^{18} molecules/m^3 at 25 km and an integrated total ozone value of 0.280 atm-cm.

INSTRUMENT

The Electrochemical Concentration Cell (ECC) balloon ozonesonde is a lightweight, compact, and relatively inexpensive instrument developed for measuring the vertical distribution of atmospheric ozone. It was developed by W. D. Komhyr and T. B. Harris for the Department of the Navy (References 1 and 2). The balloon-launched instrument is physically and electronically coupled to a standard NOAA radiosonde and collects and transmits data from the surface to approximately 35 kilometers.

The sensor is based on an iodine/iodide redox cell in which ozone is consumed in the oxidation of iodide ions to molecular iodine. The latter is quickly converted back to the iodide form in a reaction driven by the iodide concentration differential that exists between the cell anode and cathode. The electrical current produced is proportional to the mass flow rate of ozone into the cell and is detected and transmitted via telemetry back to a ground-based receiver. The ozone cell is made of two bright platinum electrodes immersed in potassium iodide solutions of different concentrations contained in separate cathode and anode chambers. The chambers are linked together with an ion bridge that serves as an ion pathway and retards mixing of the cathode and anode electrolytes, thereby, preserving their concentrations. The ECC sensor does not require application of an external emf for operation. Driving emf for the cell is derived from a difference of potassium iodide concentrations present in the two half cells caused by bubbling air containing ozone through the cathode electrolyte. The current flowing in the cell external circuit is directly related to the rate of conversion of iodine to iodide, or iodide to iodine. The air pump used within the sonde is of unique design that permits pump operation without the use of ozone-destroying lubricants. All pump components that come in contact with sampled air are fabricated from Teflon reinforced with 15 percent glass fibers, materials that are inert to ozone.

The minute current (0 to 6 μA) emitted by the electrochemical concentration cell during the measurement of ozone is impressed upon a simple two-transistor coupler, the resistance of which varies with the magnitude of the impressed current. Data telemetry is accomplished by periodic connection of the coupler, by means of a mechanical sequencing switch, to a 1680-MHz radiosonde. The sequencing switch used is of the "stepper" type, the duration of each "step" being about 3½ seconds. One complete revolution of the switch takes 2 minutes. Telemetry data signals are atmospheric pressure, temperature, humidity, ozone, sonde box temperature, "ozone zero", and "ozone calibrate". The last two signals provide for in-flight calibration of the telemetry systems.

As part of an on-going evaluation of the ECC sonde, total ozone column content inferred from flights of ECC sondes has been compared to total ozone as simultaneously observed by the Dobson spectrophotometer (References 3 and 4). In this set of data, the total ozone from the ECC profiles was less than that from the Dobson by 5.7 percent with an uncertainty in the comparison of ±8.5 percent.

RESULTS

An ECC sonde was launched at 0925 MST, September 29, 1977, from the White Sands Missile Range. Prior to flight the ECC sonde had been calibrated in an absolute sense at Wallops Flight Center by comparison with a Dasibi ozone monitor. The performance of the system was satisfactory in every way. Ozone and temperature data are plotted in Figure 1 and listed in Table 1.

Explanation of the Column Headings in Table 1

TIM MIN	Minutes after launch
ALT GP MT	Altitude above sea level, geopotential, meters
OZONE MICMB	Ozone pressure, micromillibars
TOTOZ ATMCM	Ozone column content beneath sonde, atmosphere-cm
OZDEN GAMMA	Ozone density, micrograms/meter^3
OZMXR MICGG	Ozone mixing ratio, micrograms/gram
PRESS MB	Atmospheric pressure, millibars
LOG PRESS	Logarithm of atmospheric pressure, base 10
TEMP DEG K	Atmospheric temperature, kelvin
PTEMP DEG K	Potential temperature, kelvin
VTEMP DEG K	Virtual temperature, kelvin
HUMTY PRCNT	Relative humidity, percent
DEWPT DEG K	Dew point, kelvin
SPECIFIC HUMTY	Specific humidity
SPD MPS	Wind speed, meters/second
DIR DEG	Wind direction, degrees
NS MPS	Wind, north-south component, meters/second
EW MPS	Wind, east-west component, meters/second

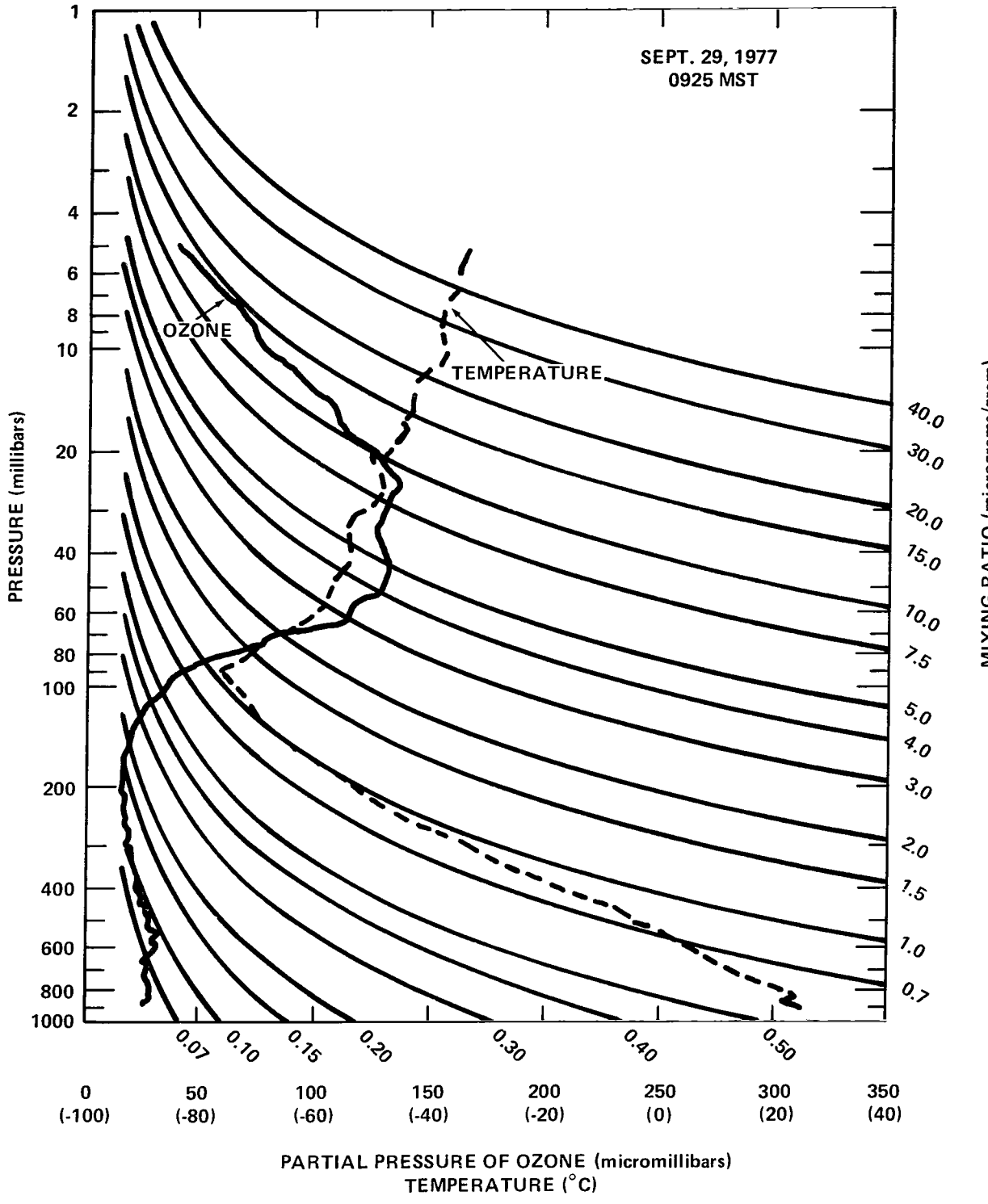

Figure 1. Partial pressure of ozone (solid line) and temperature (dashed line).

Table 1
Electrochemical Concentration Cell Ozonesonde

STATION WHITE SAND LAUNCH DATE 92977 LAUNCH ZULU 1625 ECC SONDE SA=205X

SURFACE CONDITIONS PRESS 878,5 MB TEMP 299,4 DEG K HUMIDITY 45,0 PRCNT

TB CAL 30,0 DEG C AT 74,2 ORD 003= 37,4 OIZ= 86,3 PZC= 64,5 IO=0,198 PS= 27,6

BASELINE CAL TEMP 30,0 DEG C AT 74,0 DIV HUMIDITY 62,2 PRCNT AT 46,0 ORD

AQ= 0. A1= 1,000

TIME MIN	ALT GP MT	OZONE MICMB	TOTOZ ATMCM	OZDEN GAMMA	OZMXR MICGS	PRESS MB	LOG PRESS	TEMP DEG K	PTEMP DEG K	VTEMP DEG K	HUMTY PRCNT	DEWPT DEG K	SPECIF HUMTY	SPD MPS	DIR DEG	NS MPS	EW MPS
0.	1219	24.9	0.	48,3	0,05	878,5	2,9447	297,5	308,7	299,91	62,3	289,8	0,0135	2,0	60,0	-1,0	-1,7
1.0	1445	26.2	0,00052	51,4	0,05	856,0	2,9325	294,2	307,6	295,93	52,3	284,1	0,0095	0,4	143,5	0,3	=0,2
1.2	1506	26.2	0,00067	51,4	0,05	850,0	2,9294	295,0	309,0	296,80	52,0	284,7	0,0104	0,5	233,9	0,3	0,4
2.0	1703	26.4	0,00114	51,2	0,05	831,0	2,9196	297,5	313,6	299,59	51,2	286,7	0,0117	2,4	265,0	0,2	2,4
3.0	1980	27.7	0,00182	54,2	0,06	805,0	2,9058	295,4	314,2	297,31	52,2	285,1	0,0108	4,8	266,3	0,3	4,8
3.2	2033	27.5	0,00195	53,8	0,06	800,0	2,9031	294,8	314,3	296,79	56,3	284,9	0,0107	5,2	264,8	0,5	5,2
4.0	2264	26.5	0,00252	52,2	0,06	779,0	2,8915	292,7	314,3	294,56	58,0	284,2	0,0106	6,9	260,4	1,2	6,8
5.0	2544	25.8	0,00319	51,3	0,06	754,0	2,8774	290,1	314,5	291,85	61,8	282,7	0,0099	9,4	253,6	2,6	9,0
6.0	2842	24.4	0,00389	48,9	0,06	728,0	2,8621	288,0	315,4	289,52	57,9	279,8	0,0084	10,7	253,2	3,1	10,2
7.0	3124	24.7	0,00453	49,9	0,06	704,0	2,8476	285,7	315,8	286,72	47,6	274,8	0,0061	12,2	257,6	2,6	11,9
7.2	3174	25.2	0,00465	51,0	0,06	700,0	2,8451	285,5	316,1	286,50	45,1	273,8	0,0055	12,3	258,8	2,4	12,1
8.0	3402	27.8	0,00522	56,3	0,07	681,0	2,8331	284,7	317,7	285,41	35,2	269,1	0,0041	13,0	264,1	1,3	12,9
9.0	3687	23.4	0,00592	48,0	0,06	658,0	2,8182	281,9	317,7	282,52	35,0	267,3	0,0037	12,9	269,5	0,1	12,9
10.0	3967	25.1	0,00657	51,6	0,07	636,0	2,8065	280,8	319,5	281,14	20,2	259,4	0,0021	12,2	271,7	=0,4	12,2
11.0	4256	33.4	0,00738	68,8	0,09	614,0	2,7882	280,2	322,2	280,25				8,6	276,2	=0,9	8,6
11.7	4444	31.8	0,00796	65,7	0,09	600,0	2,7782	279,0	322,8	278,96				7,0	277,9	=1,0	6,9
12.0	4543	30.9	0,00826	64,2	0,09	593,0	2,7731	278,3	323,1	278,31				6,2	279,2	=1,0	6,1
13.0	4847	27.0	0,00913	56,1	0,08	571,0	2,7586	277,8	326,0	277,79				5,9	287,9	=1,8	5,6
14.0	5164	30.8	0,01002	64,8	0,09	549,0	2,7396	274,7	326,1	274,74				6,4	306,3	=3,8	5,2
15.0	5493	25.8	0,01094	54,8	0,08	527,0	2,7218	272,1	326,8	272,19				8,4	318,2	=6,3	5,6
16.0	5829	26.8	0,01182	57,3	0,09	505,0	2,7063	269,8	327,9	269,81				9,1	324,7	=7,4	5,3
16.2	5907	26.4	0,01202	56,5	0,09	500,0	2,6990	269,2	328,1	269,20				9,2	324,8	=7,5	5,3
17.0	6146	25.1	0,01265	54,3	0,09	485,0	2,6857	267,3	328,7	267,35				9,5	324,9	=7,8	5,5
18.0	6475	24.7	0,01348	53,6	0,09	465,0	2,6675	266,3	331,4	266,30				11,1	320,0	=8,5	7,1
19.0	6783	22.6	0,01421	49,4	0,08	447,0	2,6503	263,9	332,2	263,98				8,2	291,7	=3,0	7,6
20.0	7064	22.5	0,01486	49,6	0,09	431,0	2,6345	261,5	332,5	261,50				8,7	332,3	=7,7	4,1
21.0	7385	21.3	0,01561	47,7	0,09	413,0	2,6160	258,6	333,0	258,68				13,7	352,3	=13,6	1,8
21.8	7625	20.4	0,01612	46,2	0,08	400,0	2,6021	255,6	332,1	255,68				11,8	342,0	=11,2	3,7

Table 1 (Continued)

STATION WHITE SAND LAUNCH DATE 92977 LAUNCH ZULU 1625 ECC SONDE SA&20&X

22.8	7682	25.2	0.01625	45.8	0.06	397.0	2,5988	254.9	331.9	254.97	11.4	339.1	=10.7	4.1
24.8	8027	21.0	0.01700	47.9	0.09	379.0	2,5786	252.8	333.5	252.81	14.8	331.8	=13.0	7.0
24.8	8364	21.0	0.01776	48.6	0.10	362.0	2,5587	249.7	333.8	249.74	17.6	326.7	=14.7	9.7
24.7	8653	19.6	0.01829	45.8	0.09	350.0	2,5441	247.4	333.9	247.38	20.3	321.2	=15.8	12.7
25.8	8734	18.9	0.01857	44.3	0.09	344.0	2,5366	246.1	333.9	246.18	21.7	318.8	=16.3	14.3
26.8	9119	19.3	0.01937	45.7	0.10	326.0	2,5162	243.4	335.3	243.43	25.5	315.7	=18.3	17.8
27.8	9498	18.2	0.02017	43.6	0.10	309.0	2,4900	240.5	336.4	240.54	26.1	312.6	=17.7	19.2
27.8	9755	17.0	0.02057	41.0	0.09	300.0	2,4771	239.6	338.0	239.61	23.5	308.3	=14.6	18.4
28.8	9847	16.2	0.02084	39.2	0.09	294.0	2,4683	238.9	339.0	238.97	21.8	304.8	=12.5	17.9
29.8	10186	16.9	0.02152	40.3	0.11	280.0	2,4472	235.9	339.4	235.96	18.3	303.7	=10.2	15.2
30.8	10538	16.5	0.02223	40.9	0.10	266.0	2,4249	232.7	339.7	232.70	15.4	311.4	=10.2	11.5
31.8	10877	15.9	0.02287	39.8	0.10	253.0	2,4061	230.1	340.8	230.12	17.8	312.2	=11.9	13.1
31.2	10956	15.7	0.02302	39.5	0.10	250.0	2,3979	229.5	341.0	229.50	18.2	311.1	=12.0	13.7
32.8	11202	15.2	0.02347	38.6	0.10	241.0	2,3820	227.6	341.8	227.62	19.8	308.1	=12.2	15.6
33.8	11514	15.8	0.02404	40.6	0.11	230.0	2,3617	225.1	342.5	225.06	17.2	294.4	=7.1	15.7
34.8	11832	15.9	0.02465	41.1	0.12	219.0	2,3404	223.0	344.2	223.02	22.8	283.0	=5.1	22.3
35.8	12166	14.0	0.02526	36.6	0.11	208.0	2,3191	220.6	345.5	220.62	27.5	284.5	=6.9	26.6
35.8	12418	14.4	0.02570	37.8	0.12	200.0	2,3010	219.4	347.5	219.40	26.3	284.7	=6.7	25.4
36.8	12483	14.5	0.02581	38.2	0.12	198.0	2,2987	219.1	348.0	219.08	26.0	284.7	=6.6	25.1
37.8	12814	14.3	0.02640	37.9	0.13	188.0	2,2782	217.5	350.6	217.51	20.5	276.2	=2.2	20.3
38.8	13124	14.8	0.02696	39.8	0.14	179.0	2,2529	215.2	351.9	215.23	23.5	269.5	0.2	23.5
39.8	13447	15.3	0.02758	41.5	0.15	170.0	2,2304	213.0	353.4	213.05	28.9	272.3	=1.1	28.8
40.8	13784	15.9	0.02825	43.7	0.16	161.0	2,2088	210.7	355.1	210.73	25.6	271.7	=0.7	25.6
41.8	14097	17.5	0.02892	48.3	0.19	153.0	2,1887	209.4	358.1	209.45	28.2	278.8	=4.3	27.9
41.8	14217	17.6	0.02922	48.6	0.19	150.0	2,1781	208.9	359.2	208.89	28.1	278.6	=4.2	27.8
42.8	14467	17.7	0.02976	49.2	0.20	144.0	2,1584	207.7	361.4	207.75	27.7	278.1	=3.9	27.5
43.8	14768	18.8	0.03048	52.7	0.23	137.0	2,1357	206.0	363.5	205.97	20.7	265.4	1.7	20.6
44.8	15129	24.0	0.03143	59.2	0.27	129.0	2,1106	204.5	367.2	204.54	18.5	269.7	0.1	18.5
44.8	15316	21.9	0.03197	62.3	0.29	125.0	2,0989	203.9	368.5	203.46	19.4	278.0	=2.7	19.2
45.8	15461	22.7	0.03235	64.6	0.31	122.0	2,0864	202.6	369.6	202.62	20.4	283.8	=4.9	19.8
46.8	15862	26.4	0.03317	75.6	0.38	114.0	2,0569	202.0	375.6	201.96	18.6	286.6	=5.3	17.8
47.8	16235	30.8	0.03513	88.4	0.48	107.0	2,0294	200.8	380.3	200.85	3.2	245.4	1.3	2.9
48.8	16515	33.4	0.03634	96.5	0.54	102.0	2,0086	199.7	383.3	199.66	4.4	211.2	3.8	2.3
48.3	16631	34.0	0.03688	98.6	0.56	100.0	2,0000	199.2	384.6	199.19	5.1	229.6	3.3	3.9
49.8	16868	35.4	0.03799	103.0	0.61	96.0	1,9823	198.2	387.2	198.21	7.7	251.5	2.4	7.3
50.8	17245	40.8	0.03993	119.9	0.75	90.0	1,9542	196.4	390.8	196.43	2.5	235.5	1.4	2.0
51.8	17502	46.2	0.04149	135.2	0.89	86.0	1,9365	197.2	397.5	197.20	0.7	198.5	0.7	0.2
52.8	17854	59.7	0.04399	170.8	1.22	81.0	1,9065	201.7	413.7	201.73	11.2	288.6	=3.6	10.7
52.2	17924	63.0	0.04464	180.1	1.31	80.0	1,9031	202.0	415.7	202.00	13.0	294.8	=5.5	11.8
53.8	18154	73.3	0.04664	208.5	1.58	77.0	1,8865	202.8	422.0	202.84	19.2	306.1	=11.3	15.9

Table 1 (Continued)

STATION WHITE SAND LAUNCH DATE 92977 LAUNCH ZULU 1625 ECC SONDE SA=205X

54.0	18553	75.7	0.05059	215.2	1.74	72.0	1.8573	203.1	430.6	203.05	8.8	325.4	-7.2	5.0
54.5	18719	85.8	0.05250	241.3	2.04	70.0	1.8491	205.2	438.7	205.18	3.2	23.5	-3.0	-1.3
55.0	18893	96.3	0.05447	268.1	2.35	68.0	1.8325	207.4	447.0	207.36	7.9	100.4	1.4	-7.8
56.0	19169	109.3	0.05813	300.1	2.79	65.0	1.8129	210.4	459.4	210.37	17.1	107.2	5.0	-16.4
57.0	19462	110.4	0.06222	300.7	2.95	62.0	1.7924	212.0	469.2	211.98	1.7	95.1	0.2	-1.7
57.5	19665	111.6	0.06511	302.7	3.08	60.0	1.7782	212.8	475.5	212.83	4.7	273.7	-0.3	4.7
58.0	19876	112.8	0.06813	304.7	3.22	58.0	1.7664	213.7	482.1	213.72	11.2	273.9	-0.8	11.2
59.0	20209	119.4	0.07296	321.3	3.60	55.0	1.7404	214.6	491.4	214.56	8.1	217.5	6.4	4.9
60.0	20442	124.3	0.07652	333.8	3.88	53.0	1.7283	214.9	497.4	214.90	7.4	246.3	3.0	6.8
61.0	20777	126.9	0.08171	340.5	4.18	50.3	1.7016	215.2	505.7	215.23	7.8	294.0	-3.2	7.1
61.1	20807	126.9	0.08267	340.4	4.21	50.0	1.6990	215.3	506.7	215.29	7.5	299.1	-3.6	6.5
62.0	21104	127.0	0.08702	340.0	4.41	47.7	1.6785	215.7	514.6	215.75	7.6	344.7	-7.3	2.0
63.0	21432	128.6	0.09223	342.1	4.70	45.3	1.6591	217.0	525.4	217.05	7.0	30.7	-6.0	-3.6
64.0	21763	129.2	0.09753	342.1	4.98	43.0	1.6395	218.1	536.0	218.14	7.3	89.2	-0.1	-7.3
65.0	22083	128.0	0.10281	337.7	5.18	40.9	1.6217	218.8	545.3	218.77	5.2	96.7	0.6	-5.1
65.4	22225	127.1	0.10484	335.7	5.27	40.0	1.6021	218.6	548.4	218.63	4.3	94.4	0.3	-4.3
66.0	22404	126.1	0.10764	333.2	5.37	38.9	1.5879	218.5	552.4	218.46	3.2	89.8	-0.0	-3.2
67.0	22742	123.7	0.11284	327.9	5.56	36.9	1.5670	217.8	559.2	217.83	5.1	118.6	2.4	-4.5
68.0	23078	121.8	0.11796	323.3	5.77	35.0	1.5441	217.5	566.8	217.51	6.9	144.0	5.6	-4.0
69.0	23453	123.4	0.12365	326.3	6.20	33.0	1.5185	218.3	575.5	218.30	8.2	261.9	1.2	8.1
70.0	23813	126.1	0.12917	332.3	6.70	31.2	1.4982	219.1	590.0	219.08	11.6	291.9	-4.3	10.8
70.7	24064	127.7	0.13311	333.6	7.06	30.0	1.4771	221.0	601.9	221.01	3.8	41.7	-2.9	-2.6
71.0	24173	128.4	0.13485	334.1	7.21	29.5	1.4678	221.8	607.0	221.83	8.6	74.8	-2.2	-8.3
72.0	24535	128.4	0.14045	333.3	7.63	27.9	1.4496	222.4	618.4	222.43	4.0	73.0	-1.2	-3.8
73.0	24921	133.1	0.14654	342.6	8.39	26.3	1.4300	224.3	634.4	224.34	4.6	299.5	-2.3	4.0
73.5	25252	133.4	0.15187	344.0	8.84	25.0	1.4179	223.9	642.3	223.87	3.3	12.2	-3.2	-0.7
74.0	25332	133.4	0.15314	344.3	8.95	24.7	1.4127	223.8	644.2	223.76	3.9	27.7	-3.4	-1.8
75.0	25777	128.3	0.16006	332.0	9.21	23.1	1.4036	223.2	654.9	223.17	5.4	344.8	-3.3	0.9
76.0	26089	125.6	0.16495	324.5	9.46	22.0	1.3924	223.5	665.3	223.46	9.7	348.1	-9.5	2.0
77.0	26425	123.7	0.16999	318.6	9.81	20.9	1.3801	224.2	677.0	224.19	4.3	326.9	-3.6	2.4
77.5	26714	121.6	0.17424	312.2	10.07	20.0	1.3710	224.8	687.4	224.78	14.4	137.1	10.6	-9.8
78.0	26787	121.1	0.17521	310.8	10.13	19.8	1.3697	224.9	689.7	224.92	18.7	137.6	13.8	-12.6
79.0	27157	114.8	0.16053	293.3	10.18	18.7	1.3718	226.1	704.7	226.06	19.7	119.6	9.7	-17.1
80.0	27447	108.4	0.18466	274.6	10.03	17.9	1.3529	227.9	719.3	227.90	6.7	87.1	-0.3	-6.7
80.5	27597	107.6	0.18636	272.0	10.19	17.5	1.3460	228.4	725.5	228.38	7.5	72.5	-2.3	-7.2
81.0	27752	106.7	0.18826	269.2	10.34	17.1	1.3360	228.9	731.9	228.88	8.8	61.1	-4.2	-7.7
82.0	28113	103.3	0.19274	262.2	10.57	16.2	1.3095	227.5	738.8	227.48	8.0	62.2	-3.8	-7.1
83.0	28494	104.5	0.19743	263.6	11.32	15.3	1.1847	228.9	755.5	228.88	3.9	83.3	-0.5	-3.9
83.3	28626	103.6	0.19904	261.3	11.44	15.0	1.1761	228.9	759.9	228.88	3.7	79.8	-0.6	-3.6
84.0	28947	101.3	0.20292	255.7	11.74	14.3	1.1553	228.9	770.3	228.88	3.1	68.9	-1.1	-2.9

Table 1 (Continued)

STATION WHITE SAND LAUNCH DATE 92977 LAUNCH ZULU 1625 ECC SONDE SA=20DX

85.6	29382	92.6	0.20789	233.5	11.45	13.4	1.1271	229.0	785.2	229.01	3.3	64.0	≈1.4	≈3.0
85.9	29848	88.3	0.21284	222.3	11.71	12.5	1.0909	229.4	802.3	229.39	3.9	56.0	≈2.2	≈3.2
86.0	29962	87.8	0.21342	221.1	11.74	12.4	1.0954	229.4	804.2	229.43	4.0	55.3	≈2.3	≈3.3
87.0	30352	84.4	0.21795	210.6	12.06	11.6	1.0685	231.5	827.1	231.48	3.3	62.2	≈1.5	≈2.9
88.0	30776	78.6	0.22195	194.0	11.94	10.9	1.0374	233.8	850.2	233.78	1.7	124.2	1.0	≈1.4
89.0	31234	79.9	0.22587	174.5	11.52	10.2	1.0086	234.6	869.5	234.58	3.9	124.7	2.2	≈3.2
89.3	31366	79.3	0.22696	173.2	11.65	10.0	1.0000	234.4	873.8	234.39	4.6	124.6	2.6	≈3.8
90.0	31718	68.8	0.22976	169.8	12.00	9.5	0.9777	233.9	884.8	233.91	6.3	124.4	3.6	≈5.2
91.0	32242	68.2	0.23392	168.4	12.83	8.8	0.9485	233.6	903.3	233.64	0.9	114.8	0.4	≈0.8
92.0	32895	62.4	0.23883	153.7	12.92	8.0	0.9061	234.3	930.9	234.31	1.3	233.7	0.8	1.1
93.0	33463	59.7	0.24256	146.8	13.37	7.4	0.8692	234.8	954.1	234.85	8.7	144.2	7.1	≈5.1
94.0	33819	55.0	0.24513	134.7	13.02	7.0	0.8491	235.8	973.2	235.78	8.3	154.5	7.5	≈3.6
95.0	34219	51.9	0.24758	126.6	13.03	6.6	0.8195	236.7	993.6	236.71	6.6	158.8	6.1	≈2.4
96.0	34652	47.8	0.25004	116.4	12.77	6.2	0.7924	237.0	1012.6	236.97	9.9	148.6	8.5	≈5.2
96.5	34879	46.5	0.25124	113.3	12.84	6.0	0.7782	237.0	1022.5	237.04	8.8	143.1	7.0	≈5.3
97.0	35115	45.2	0.25249	110.1	12.91	5.8	0.7634	237.1	1032.7	237.10	7.7	135.6	5.5	≈5.4
98.0	35612	40.5	0.25495	98.2	12.43	5.4	0.7324	238.2	1058.7	238.16	3.6	123.9	2.0	≈3.0
99.0	36149	35.7	0.25722	86.3	11.82	5.0	0.6990	238.7	1084.6	238.68	999.9	999.9	999.9	999.9

*** RECORDER INSTRUMENT HUMIDITIES ***
*** LESS THAN 20 PRCNT NOT LISTED ***

INTEGRAL 0.25722
RESIDUAL 0.02252

INTEGRATED
TOTAL OZONE 0.27973

DOBSON
TOTAL OZONE 0.

REFERENCES

1. Komhyr, W. D., "A Carbon–Iodine Sensor for Atmospheric Soundings," (Proc. Ozone Symposium, WMO, Albuquerque, NM), 1964.

2. Komhyr, W. D., and T. B. Harris, "Development of an ECC Ozonesonde," NOAA Technical Report ERL–APCL 18, Boulder, Colorado, 1971.

3. Torres, A. L., and A. R. Bandy, *Performance Evaluation of Electrochemical Concentration Cell Ozonesondes*, Final Report, NASA/WFC Grant No. NSG–6007, 1977.

4. Tores, A. L., and A. R. Bandy, "Performance Characteristics of the Electrochemical Concentration Cell Ozonesonde," *J. Geophys. Res.*, 83, pp. 5501–5504, 1978.

OZONE PROFILE FROM THE MAST OZONESONDE

Jagir Randhawa
Atmospheric Sciences Laboratory
White Sands Missile Range
New Mexico 88002

As part of the Stratcom VIII effort, the Mast* ozonesonde (a commercial version of the Brewer ozone sensor) was flown at 0700 MST, September 30, 1977 on a meteorological balloon from the Small Missile Range.

INSTRUMENTATION

Mast Ozonesondes employ a bubbler sensor conceived and patented by Dr. A. W. Brewer of the University of Toronto and licensed to the Mast Development Company for development and sale. The sensor is based on the electrochemical reaction which takes place when air containing ozone is bubbled into a potassium-iodide sensing solution. The resulting exchange of electrons is directly proportional to the quantity of ozone introduced through continuous air sampling. The current is amplified and conditioned for transmittal through the standard balloon radiosonde system. Two milliliters of potassium-iodide sensing solution added just prior to launch is sufficient for the entire flight. The air sample is supplied to the sensor by a constant volume reciprocating piston pump at a rate of 200 ml/min (calibrated at factory). Power is supplied by self-contained batteries.

A balloon is used to carry the ozonesonde/radiosonde to approximately 30 km at a speed of 300 m per minute. After the balloon ruptures, the sonde descends at a rate of between 600 and 1200 m/min by parachute. To allow for variations in time aloft, the Model 730 is built to operate for 4 hours. The bubbler solution is self-degassing so that internal pressure is always equal to that of the surrounding atmosphere. Temperature control for this unit is essential because the reagent in the ozone sensor has approximately the same freezing and boiling point as water. The internal temperature is maintained between 2° and 7°C by means of a specially molded flight case of expanded polystyrene beads.

RESULTS

Data from the Mast ozonesonde are shown in Figure 1.

*Mast Development Company, 2212 E. 12 St., Davenport, Iowa, 52803 based on U.S. Patent No. 3,329,599.

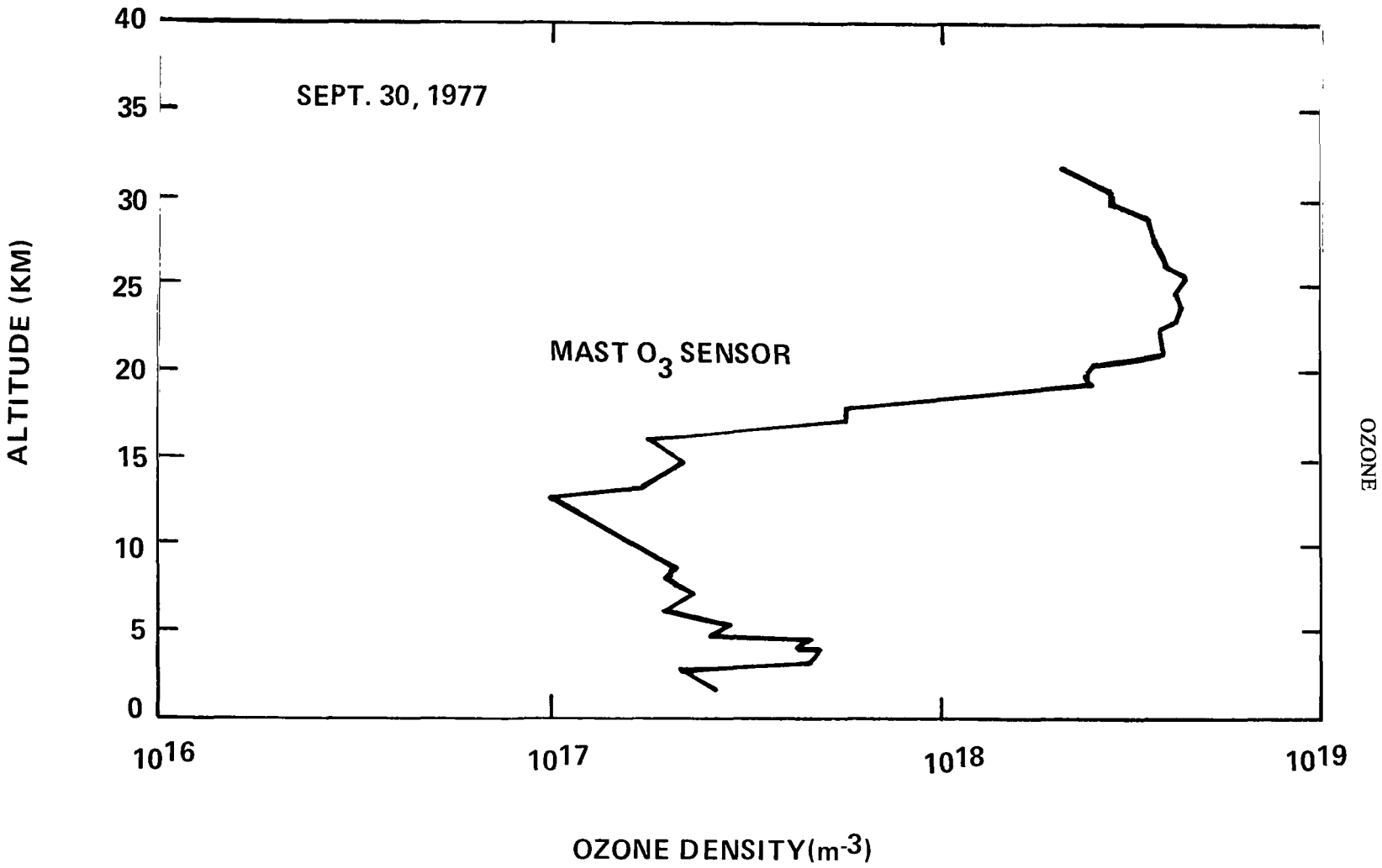

Figure 1. Data from the Mast ozonesonde.

OZONE MEASUREMENTS BY CHEMILUMINESCENT SONDES

Jagir Randhawa
Atmospheric Sciences Laboratory
White Sands Missile Range
New Mexico 88002

ABSTRACT

A chemiluminescent (Rhodamine-B) ozonesonde was flown on an Arcas rocket, September 29, 1977, during the Stratcom VIII effort near Holloman Air Force Base, New Mexico, providing an altitude profile from 15 to 60 km. On the same day, two similar instruments on the Stratcom VIII-A Balloon provided an altitude profile up to 40 km and data during a 20-hour period of float.

INTRODUCTION

Two chemiluminescent ozonesondes were flown on the Stratcom VIII-A Balloon from Holloman Air Force Base on September 29, 1977. A similar instrument was deployed from an Arcas rocket to measure the ozone profile from 60 to 15 km. Objectives of this experiment were: the determination of ozone concentration in the tropopause and stratosphere; the measurement of diurnal variation of the ozone density in the stratosphere and its importance to ozone photochemistry; and comparison of ozone concentrations measured by other techniques on the same balloon.

INSTRUMENTS

The chemiluminescent ozonesonde (Figure 1) for the Stratcom Balloon flight consists of two main parts:

a. A constant-volume sampling pump made from Teflon is used for the intake of the air sample. Sample is drawn at a rate of 200 ml/min.

b. Ozone is detected by the chemiluminescent process (Rhodamine-B). Ozone molecules in the air sample flow over the detector, and the photons produced by the destruction of ozone molecules on the chemiluminescent material are monitored by the photomultiplier tube, the output signal from which is transmitted to the ground receiver.

The instrument is calibrated under simulated flight conditions in the laboratory and is capable of measuring ozone concentration with an uncertainty of ±10 percent of the actual concentration.

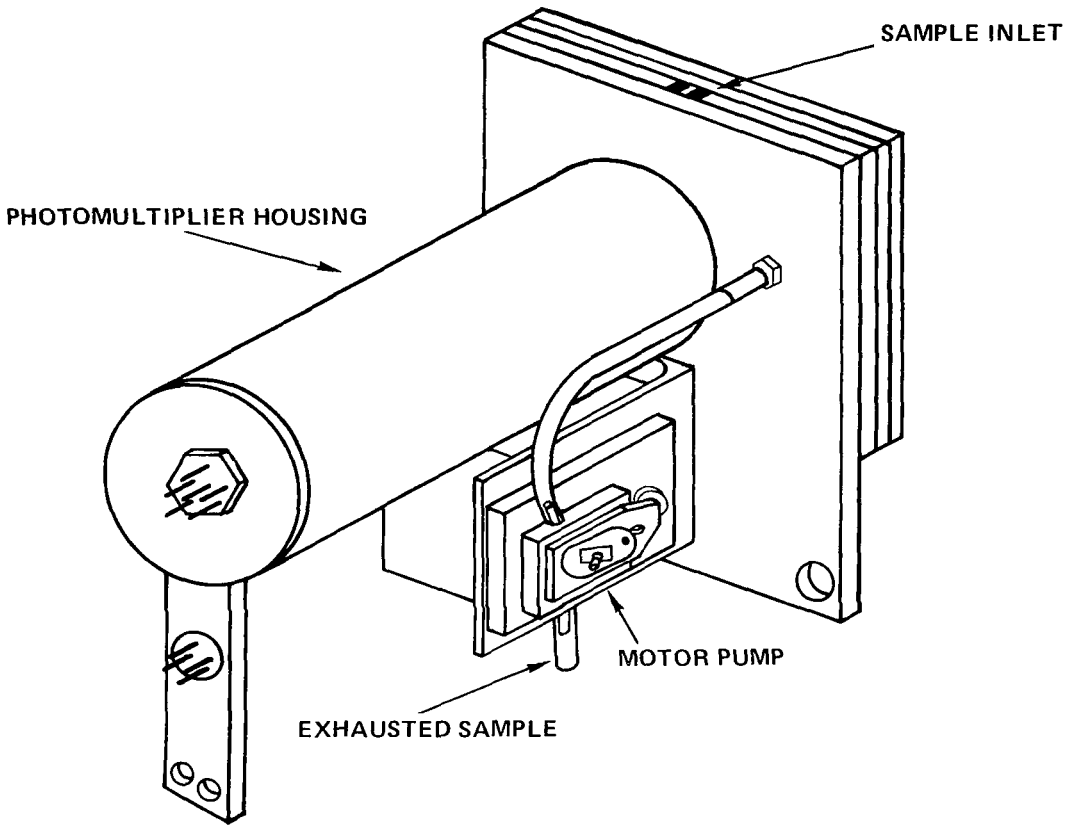

Figure 1. Balloon version of the chemiluminescent ozone sonde.

RESULTS

Ozone data from one of the chemiluminescent sondes on the main payload of the Stratcom VIII-A Balloon are shown in Figure 2 as a function of time and in Figure 3 as a function of altitude. No data were available from the second sonde on this payload.

Data from the sonde deployed from the Arcas rocket launched from the Small Missile Range at 1520 MST, September 29, are shown in Figure 4, along with a reference ozone profile (U.S. Standard Atmosphere 1976). It is noted that above 40 km the measured ozone values become increasingly larger than the reference profile. Laboratory studies are under way to determine whether the sensitivity of the chemiluminescent surface is dependent on total pressure.

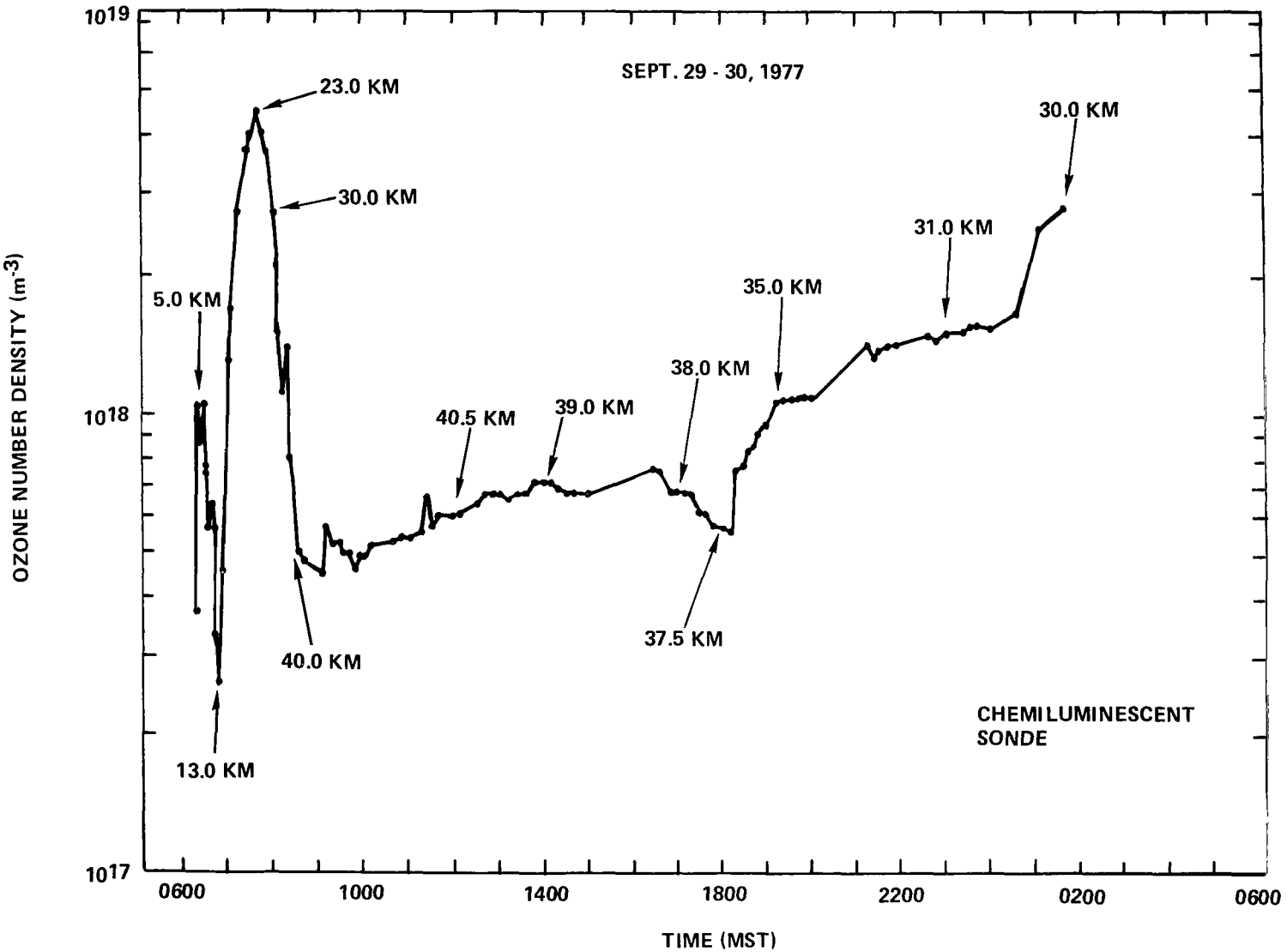

Figure 2. Ozone densities measured by the chemiluminescent ozone sonde on the Stratcom VIII-A main payload.

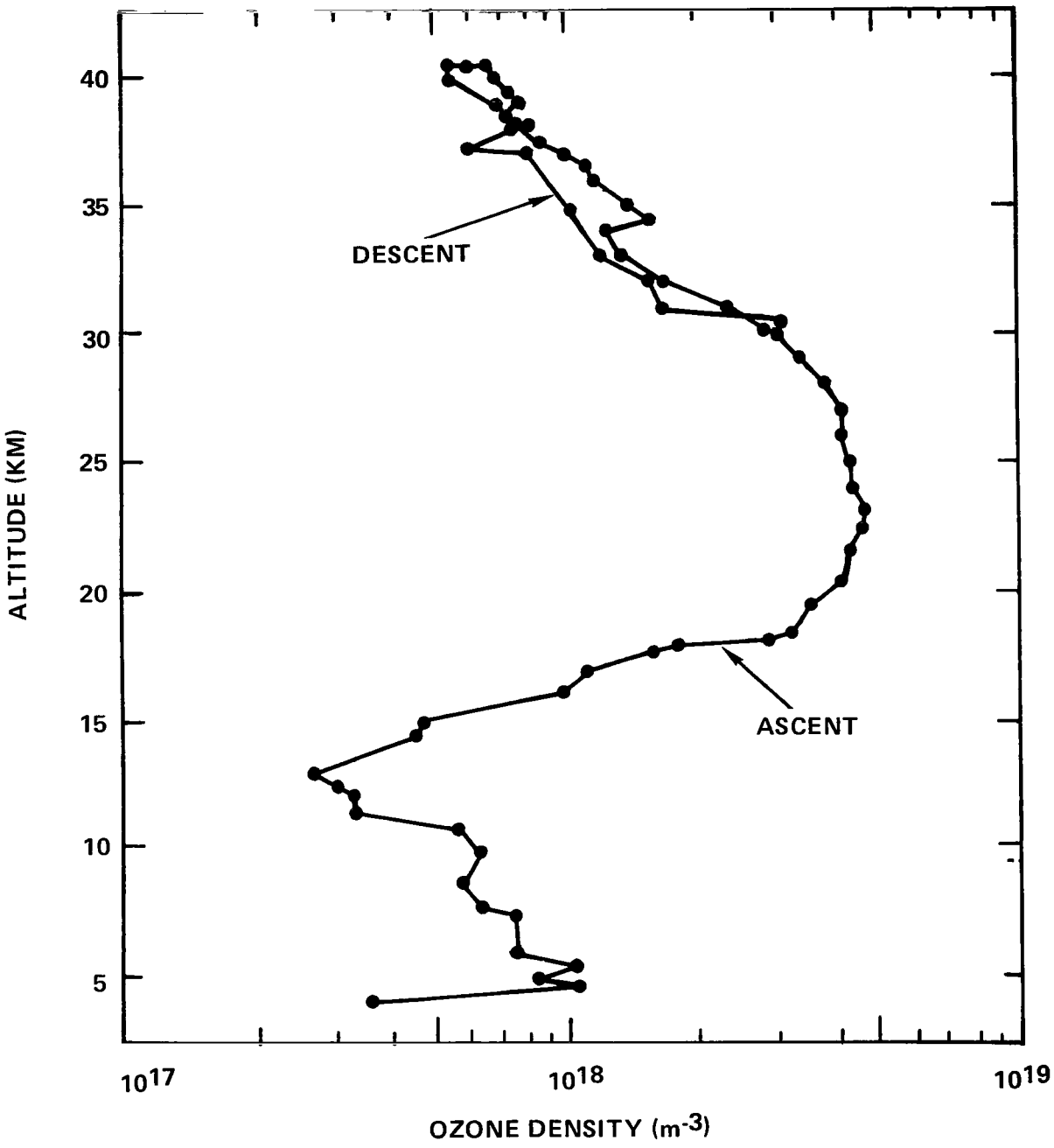

Figure 3. Ozone densities from the Stratcom VIII-A chemiluminescent sonde as a function of altitude, September 29, 1977.

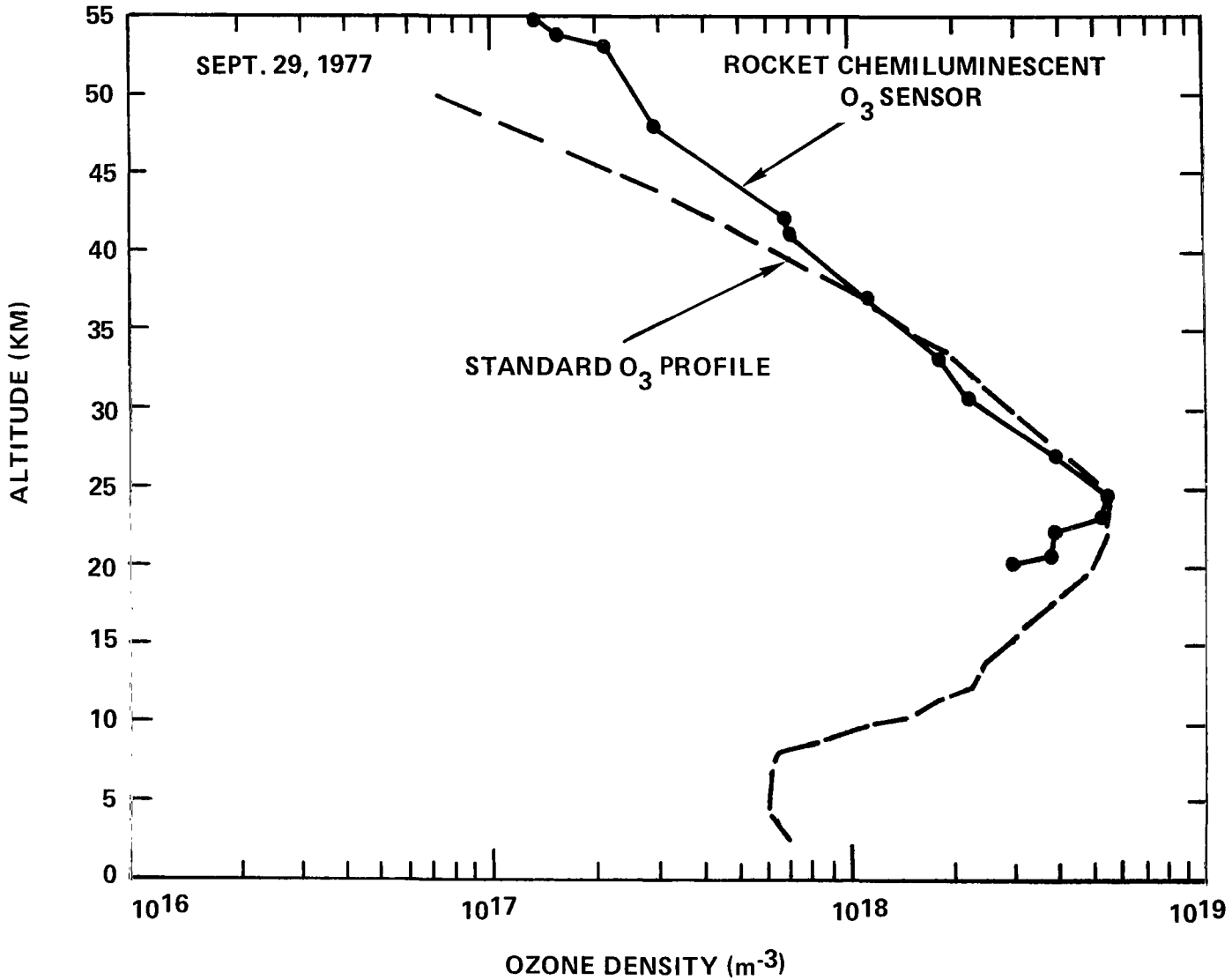

Figure 4. Ozone data from the chemiluminescent ozone sonde developed from an Arcas rocket September 29, 1977, with U.S. Standard Atmosphere 1976 reference ozone profile.

MEASUREMENT OF OZONE BY A DASIBI OZONE MONITOR

John E. Ainsworth and James R. Hagemeyer
NASA, Goddard Space Flight Center
Greenbelt, Maryland 20771

ABSTRACT

A modified Dasibi ozone monitor was flown on the Stratcom VIII-A Balloon launched September 29, 1977, from the Holloman Air Force Base, New Mexico. Ozone densities were measured from 2 to 8 km altitude and for 5 hours near 40 km. Air temperature measurements were made at the same time by means of a bead thermistor mounted at the entrance of the air inlet tube of the ozone monitor.

INTRODUCTION

A Dasibi ozone monitor, modified for flight use, and an associated bead thermistor for the measurement of ambient air temperature were flown as part of the main payload of the Stratcom VIII-A Balloon. Our objectives were to compare the ozone densities measured by the Dasibi with those measured by other ozone sensing systems and to assess the error in the measurement of ambient temperatures using a particular mounting configuration for the bead thermistor.

INSTRUMENT

The Dasibi ozone monitor is a commercially available instrument which we have modified extensively for balloon use. It contains an absorption chamber, 0.71 m in length, irradiated by the 253.7 nm line from a mercury lamp. The absorption chamber is first filled with a sample of the ambient atmosphere from which the ozone has been removed by means of a catalytic scrubber. The scrubbed sample is then replaced with a sample of the ambient atmosphere. To obtain the ambient ozone density, the instrument compares the absorption of the 253.7 nm line by the scrubbed-atmosphere sample with that of the ambient atmosphere sample. Important features of the instrument are its insensitivity to changes in the rate of air flow through the absorption chamber and its ability to ensure that the total photon flux is the same for both the scrubbed and ambient air samples. The commercial instrument was modified to obtain greater resolution and accuracy in the measurement of ozone by using the instrument at its maximum sensitivity and by noting the zero reference associated with each ozone measurement. The instrument was placed in a pressurized container to prevent arcing of its high voltage components at the low atmospheric pressures encountered during the balloon flight.

To measure ambient air temperature, a 0.25 mm diameter bead thermistor was placed 2 cm inside the open end of the Dasibi air inlet tube (1 cm I.D.). The thermistor was shielded from direct sunlight by the teflon inlet tube and was bathed by ambient air pumped continuously through the Dasibi inlet tube at a speed of 1 m/s.

RESULTS

Ambient ozone densities are shown in Figures 1 and 2. Because of an intermittent failure in the monitor's air pump, measurements of ozone were limited to the periods from 0607 to 0630 MST (2 to 8 km) and from 1117 to 1623 MST (40.5 to 38 km). The ozone monitor was calibrated at the National Bureau of Standards at roughly 1000 mb and 300 K by comparison with their secondary standard (a Dasibi monitor). The ozone density data set was corrected to account for the fact that the temperature and pressure of air in the absorption chamber differed from the temperature and pressure of the ambient atmosphere. The error estimates shown in Figures 1 and 2 include an estimated ±2 percent error due to the uncertainty in our knowledge of the value of the coefficient for the absorption of the 253.7 nm line by ozone and an additional 1 percent due to the error associated with the use of a secondary standard. Altitudes were determined by ground based radar with an estimated error of ±0.5 percent.

The fluctuations in the ozone in Figures 1 and 2 have several different causes. The frequent small-scale fluctuations represent the usual noise level of the instrument. Large, single-point spikes (e.g., at 1152 MST) and bursts that appear in both the ozone signal and the zero reference signal (at 1230, 1356, 1421, 1516, and 1550 MST) are also considered instrument noise. At low altitudes (up to 8 km) noise associated with the transition from turbulent to laminar flow within the absorption chamber also appears. Short term variations in the ozone signal extending over a number of data points and not accompanied by changes in the zero reference signal (such as the decrease at 1255 MST, the increase at 1522 MST, and the decrease at 1600 MST) are considered to represent changes in ozone content.

Ozone densities were also measured by other instruments on the same gondola and on other vehicles. In the troposphere, densities disagreed by a factor of 5; at float altitudes, the disagreement was as much as a factor of 2. A further comparison of the ozone results is given in "Highlights of the Stratcom VIII Results" (Reed) in this document.

Figure 3 presents the ambient air temperature profile obtained from the measurements made with the bead thermistor mounted in the Dasibi air inlet tube. The error in the air temperatures measured from 0607 to 0630 MST (2 to 8 km) when the Dasibi air pump was operating is believed to be less than ±1.5 K. Extrapolation of the temperature profile at 0630 MST shows that, immediately after the air flow past the thermistor ceased, the thermistor temperature rose 6 K above the ambient air temperature.

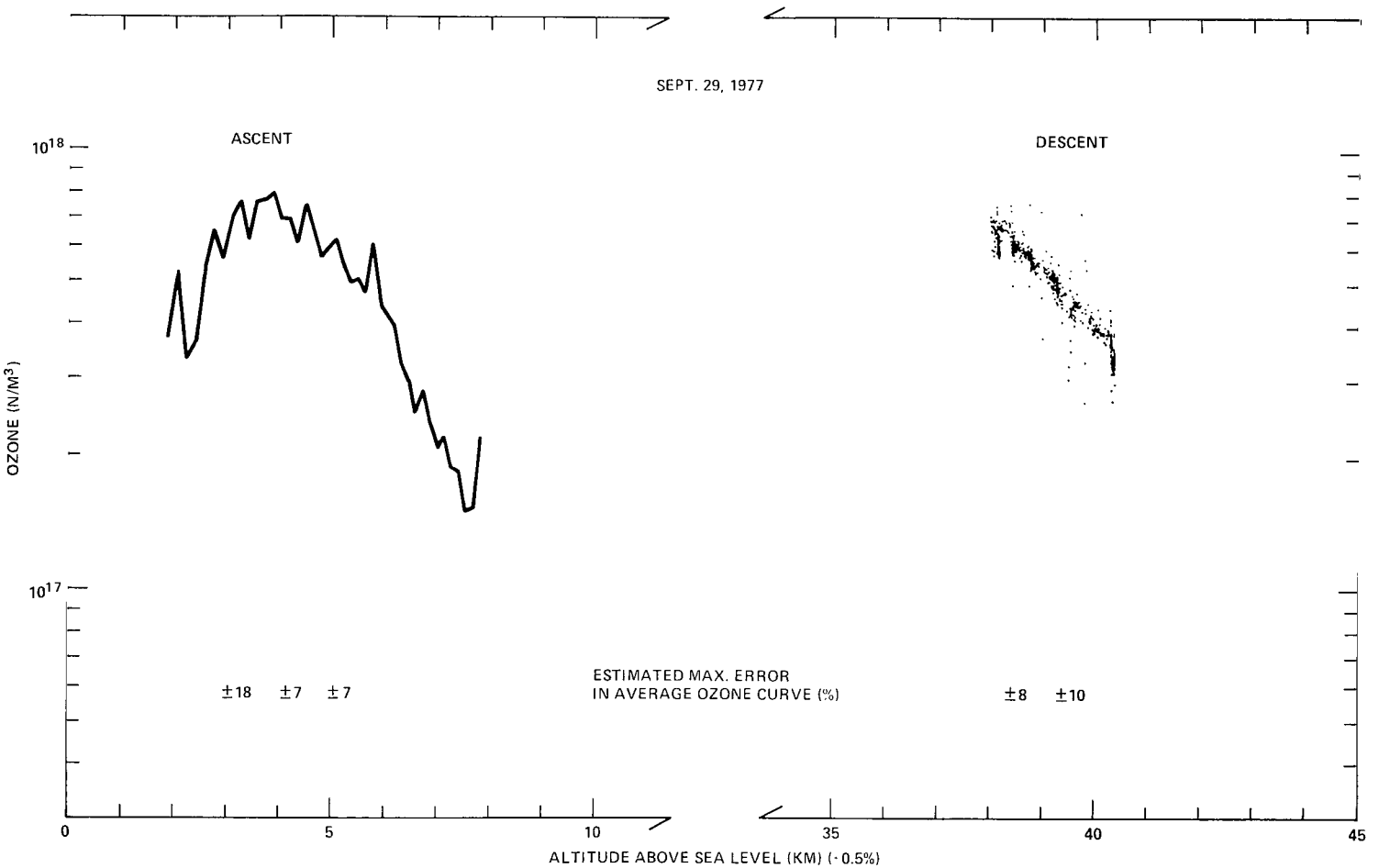

Figure 1. Dasibi ambient ozone measurements. The measurements at 40.5 to 38 km are replotted versus time in Figure 2.

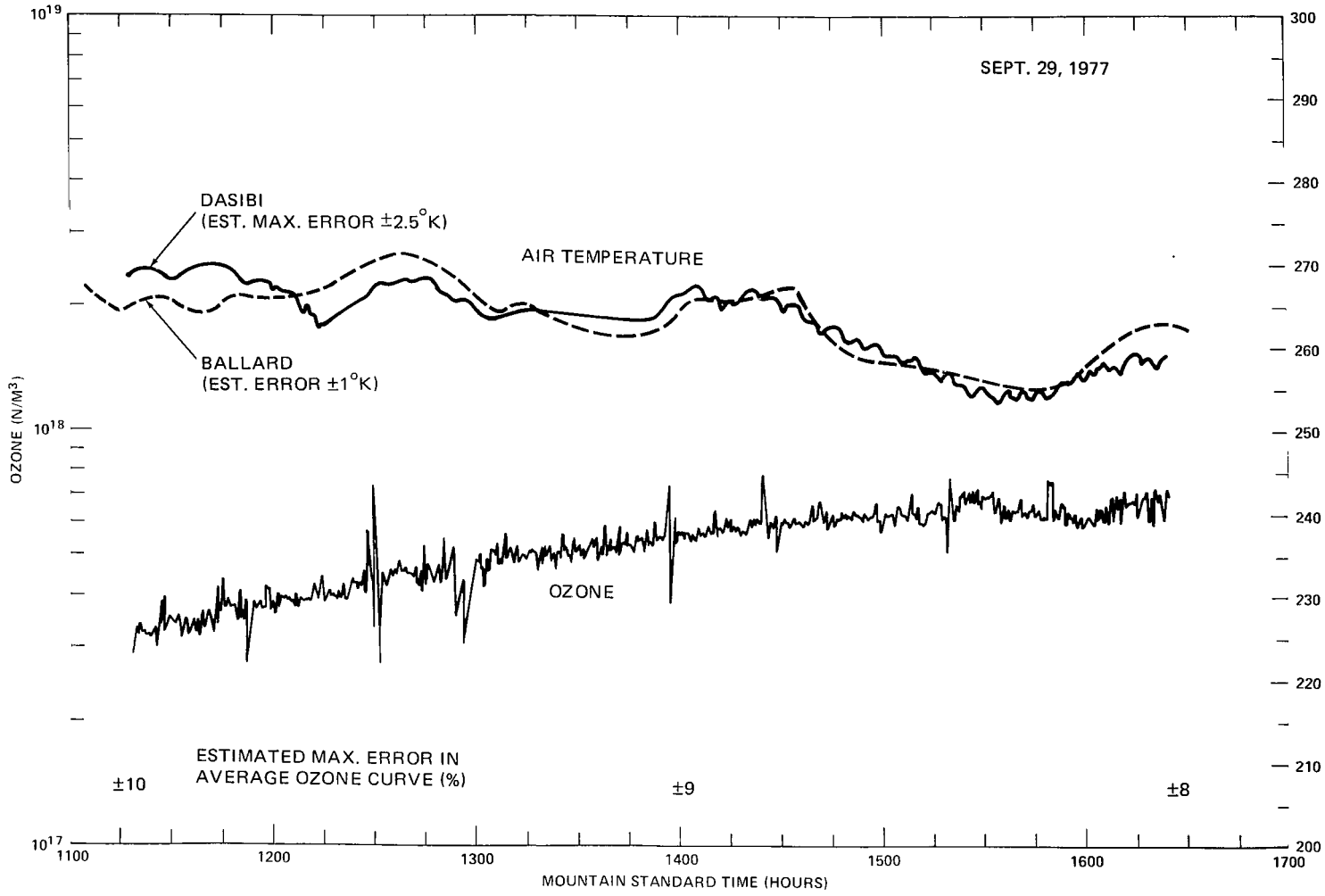

Figure 2. The lower curve presents the Dasibi ambient ozone measurements during descent from 40.5 to 38.0 km. Shown also is a comparison of the temperatures measured using the Dasibi air-inlet-tube bead thermistor (solid line) and using the film-mounted bead thermistor (dashed line).

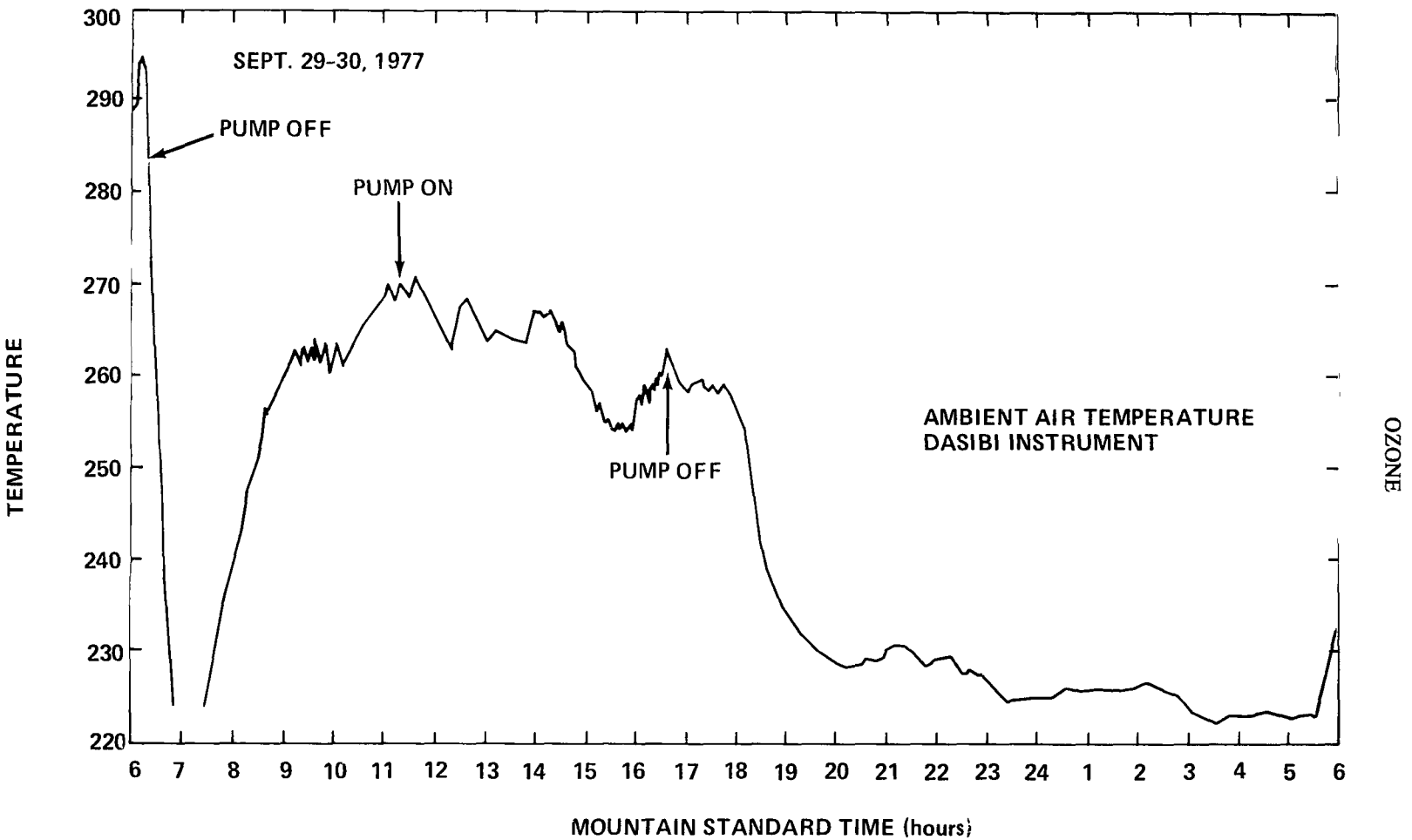

Figure 3. Ambient air temperature profile obtained from the Dasibi air-inlet-tube bead thermistor. Measurement error was least during the two intervals when the pump was operating.

From 1115 to 1630 MST the Dasibi air pump was again in operation and the error in the air temperature measurement is believed to be ±2.5 K or less after correction for self-heating. Despite the absence of forced convection cooling of the thermistor, due to the low air density at these altitudes, conduction to the continuously flowing air in the inlet tube is apparently sufficient to maintain low measurement error.

In Figure 2, we compare the Dasibi air temperature measurements with those of Ballard's film mounted thermistor measurements ("Air Temperature Measurements with Film-Mounted Thermistors") from 1115 to 1630 MST. Despite a difference of as much as 5.5 K between the two curves, there is general agreement in their shapes and the average temperature difference over the interval from 1100 to 1630 MST is approximately 0.2 K.

ACKNOWLEDGMENT

We wish to express our appreciation to R. Dennis Endres for his assistance in preparing the Dasibi monitor for flight, to Arthur F. Reid for the computer processing of the data, and especially to Edith I. Reed for many discussions of the problems of ozone measurement and for extensive assistance in preparing this article.

A DROPSONDE FOR NITRIC OXIDE AND OZONE

Alan Shaw
Center for Atmospheric and Space Sciences
Utah State University
Logan, Utah 84322

The first of three parachute dropsondes released from the Stratcom VIII-A Balloon on September 29, 1977, carried instruments to measure nitric oxide, ozone, solar flux and the earth albedo; the dropsonde is shown in Figure 1. The NO detector was based on chemiluminescence resulting from the addition of ozone and was built at Utah State University. The ozone detector was similar to the chemiluminescent instrument using Rhodamine-B (see "Ozone Measurements by Chemiluminescent Sondes"). The solar flux for the measurement of ozone overburden and the flux for the determination of underlying albedo were measured by small filter photometers (see "Filter Photometer Measurements of Solar Flux and Underlying Albedo").

This first flight of the dropsonde was not successful because an electrical failure precluded the operation of the data recording system. The sonde was recovered in good condition and the tape recorder was replaced with a more reliable unit. The sonde was then flown successfully on December 2, 1977 from Palestine, Texas.

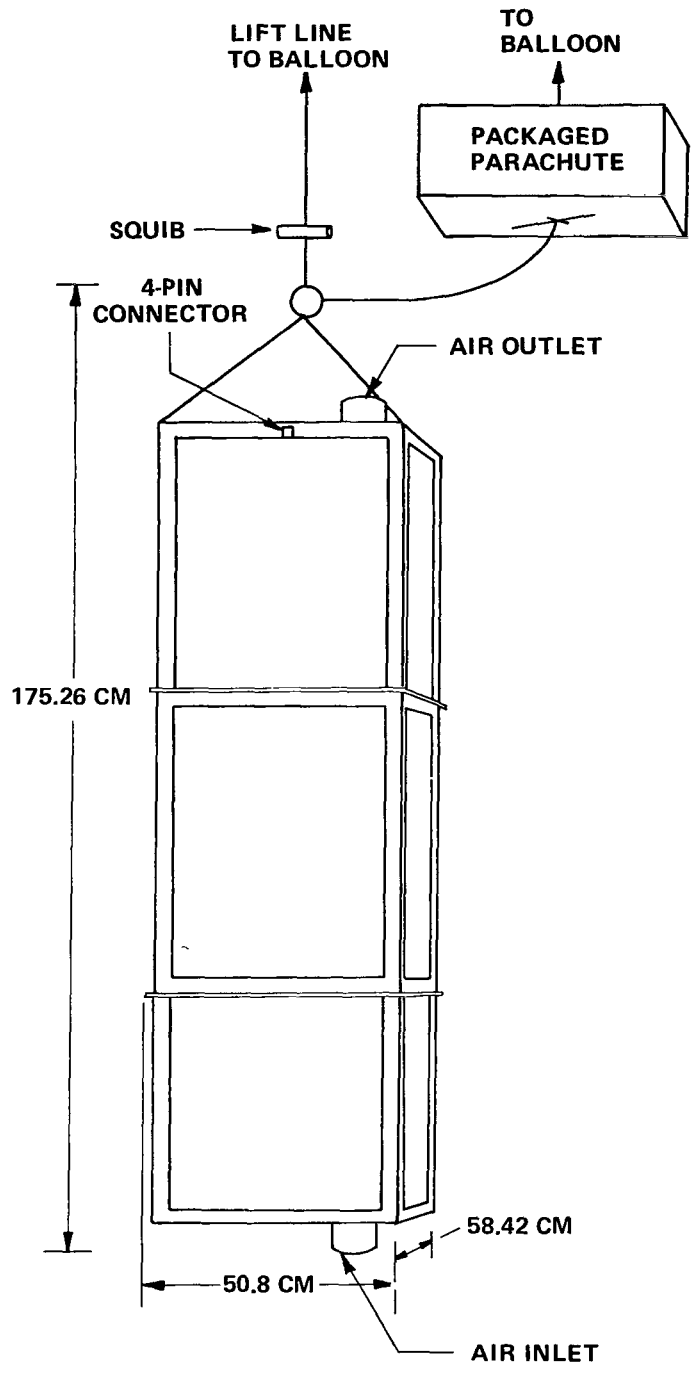

Figure 1. Chemiluminescent nitric oxide dropsonde.

OZONE AND NITRIC OXIDE DATA FROM THE SAS-II INSTRUMENT

Max Loewenstein, Walter L. Starr and Roger A. Craig
National Aeronautics and Space Administration
Ames Research Center
Moffett Field, California 94035

ABSTRACT

The Ames SAS-II air sampler for the in situ measurement of NO and O_3 was used aboard the Ames U-2 aircraft during two flights in the vicinity of Holloman Air Force Base, New Mexico, September 29, 1977, as part of the Stratcom VIII effort. The instrument is based on the chemiluminescent reaction between NO and O_3. An electronic problem degraded the performance of the NO measurement system, precluding analysis of the data at this time. The ozone instrument performed satisfactorily and the results are presented as a vertical ozone profile between 13 and 21 km.

INTRODUCTION

One of the objectives of the Ames in situ stratospheric measurements program is to determine concentrations of odd nitrogen species and ozone in the lower stratosphere. Measurements are made in situ at U-2 flight altitudes up to 21 km. As part of this program, and in cooperation with the Stratcom VIII effort, two U-2 aircraft flights were made from Moffett Field, California, to the vicinity of Holloman Air Force Base, New Mexico, and return. The first flight on the afternoon of September 28, 1977, was timed to underfly the Stratcom VIII-B Balloon during local sunset. The second flight, the next morning, coincided with the flight of the Stratcom VIII-A Balloon. The purpose of these flights was to compare data from the U-2 sensors along a long horizontal path with the sunset solar absorption data from the VIII-B Balloon and with the various ozone and nitric oxide sensors planned for the VIII-A Balloon. In addition, the U-2 data will be used to test predictions of atmospheric models that are in use or under development at Ames Research Center and elsewhere.

INSTRUMENT

The Ames in situ stratospheric air sampler, SAS II, collects real-time data on NO and O_3 as part of an overall NASA Program for stratospheric studies. System details and measurement results have been presented previously (References 1 to 3). Capability for measuring NO_2 is being developed.

The air sampler system weighs 230 kg and is specially designed to be mounted in the instrument bay of the U-2 high-altitude research aircraft. Each instrument consists of an NO/O_3 chemiluminescence sensor: to measure ozone, NO is added to the sample; to measure nitric oxide, O_3 is added. Light from the chemiluminescent reaction is detected by cooled photomultipliers operated in pulse-counting mode. The chemiluminescence signals, along with a variety of pressure, temperature, and system diagnostic measurements, are recorded on magnetic tape for later analysis.

A cylinder of NO-in-N_2 calibration gas is carried on flights to allow periodic calibration of the NO sensor. The O_3 sensor is calibrated in the laboratory both before and after a flight operation.

The sampler has two modes of operation:

1. Automatic – In this mode, 3 minutes each are provided for measurement, calibration, and null (zeroing) for each constituent channel. The system is fully automatic in this mode.

2. Manual – In this mode, after 3 minutes of calibration and 3 minutes of null, a measurement period of arbitrary length can be selected by the pilot. At the end of the measurement period the calibration and null are repeated.

The system can be switched from one mode to the other at any time during the flight.

A Rosemount total air temperature probe is mounted on the U-2 aircraft, providing continuous temperature data during the in situ sampling flights. Mach number information from the air data system is used to convert total to static air temperature.

FLIGHT RESULTS

In situ measurements of NO and O_3 were carried out in conjunction with the Stratcom VIII-A and -B Balloon flights: The U-2 flight paths are shown in Figures 14 through 17 of "The Stratcom VIII Effort" in this document.

The O_3 and air temperature data acquired during the two flights are presented in Figures 1 and 2 as altitude profiles. The data have been averaged over 6-minute intervals corresponding to 72 km of flight path. The data of the first flight were taken at UT 0000 to 0145 between 107°W and 112°W; on the second flight, data were taken at 1540 to 1815 UT between 105°W and 109°W. For comparison, ozone and air temperature data from an EEC sonde flown from White Sands Missile Range (23.3°N 106.5°W) at 1625 UT, September 29, have also been included.

The dots in Figure 1 represent the average values of ozone observed at each altitude; the bars indicate the range of values observed. These fluctuations are due primarily to variations in the atmospheric

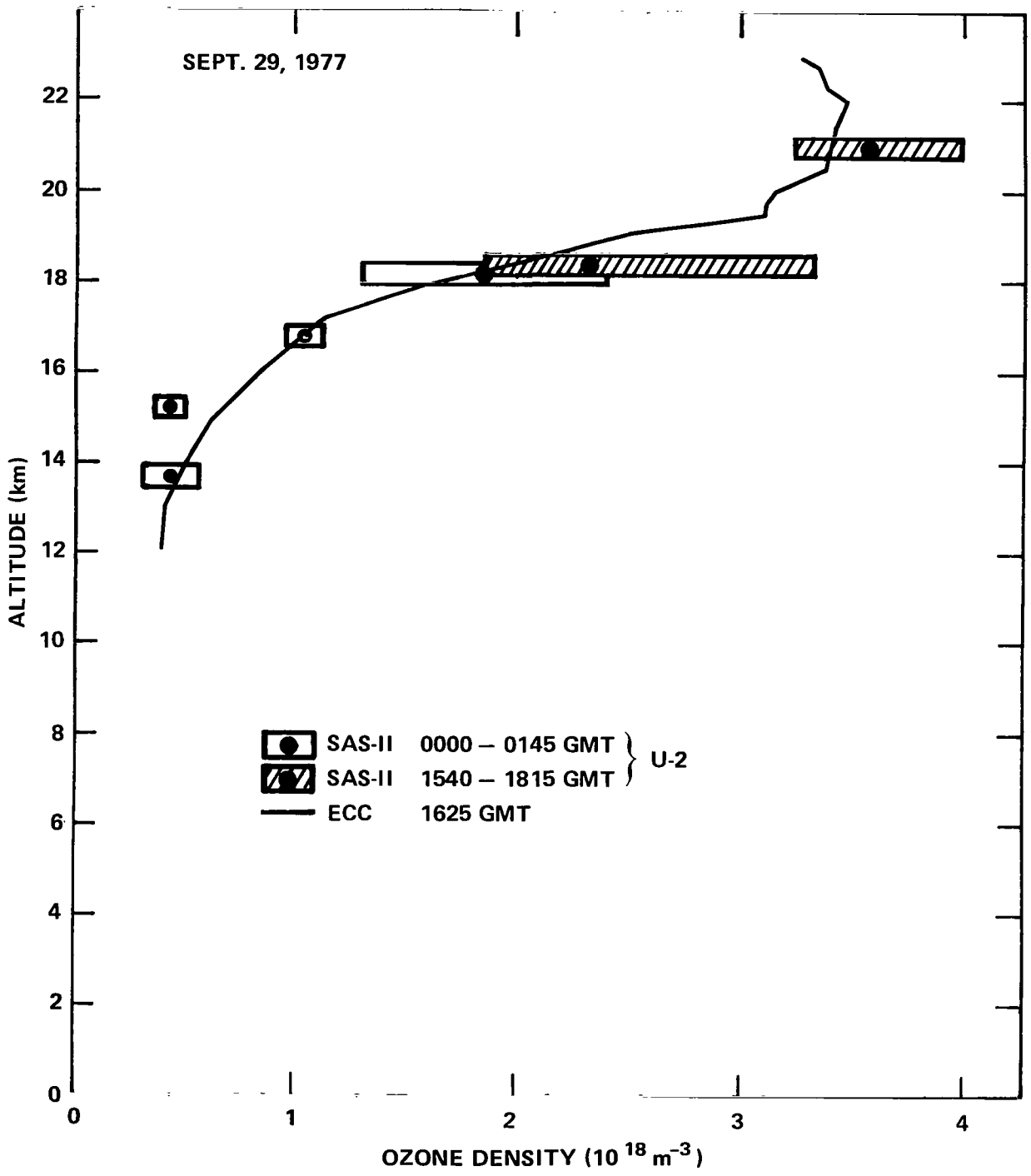

Figure 1. Ozone data obtained with the Ames in situ sampler on the U-2 aircraft. Points represent the observed average ozone and the horizontal bars show the total spread of the observed ozone. The line represents ozone data from the ECC ozonesonde flown from White Sands Missile Range at 1625 GMT.

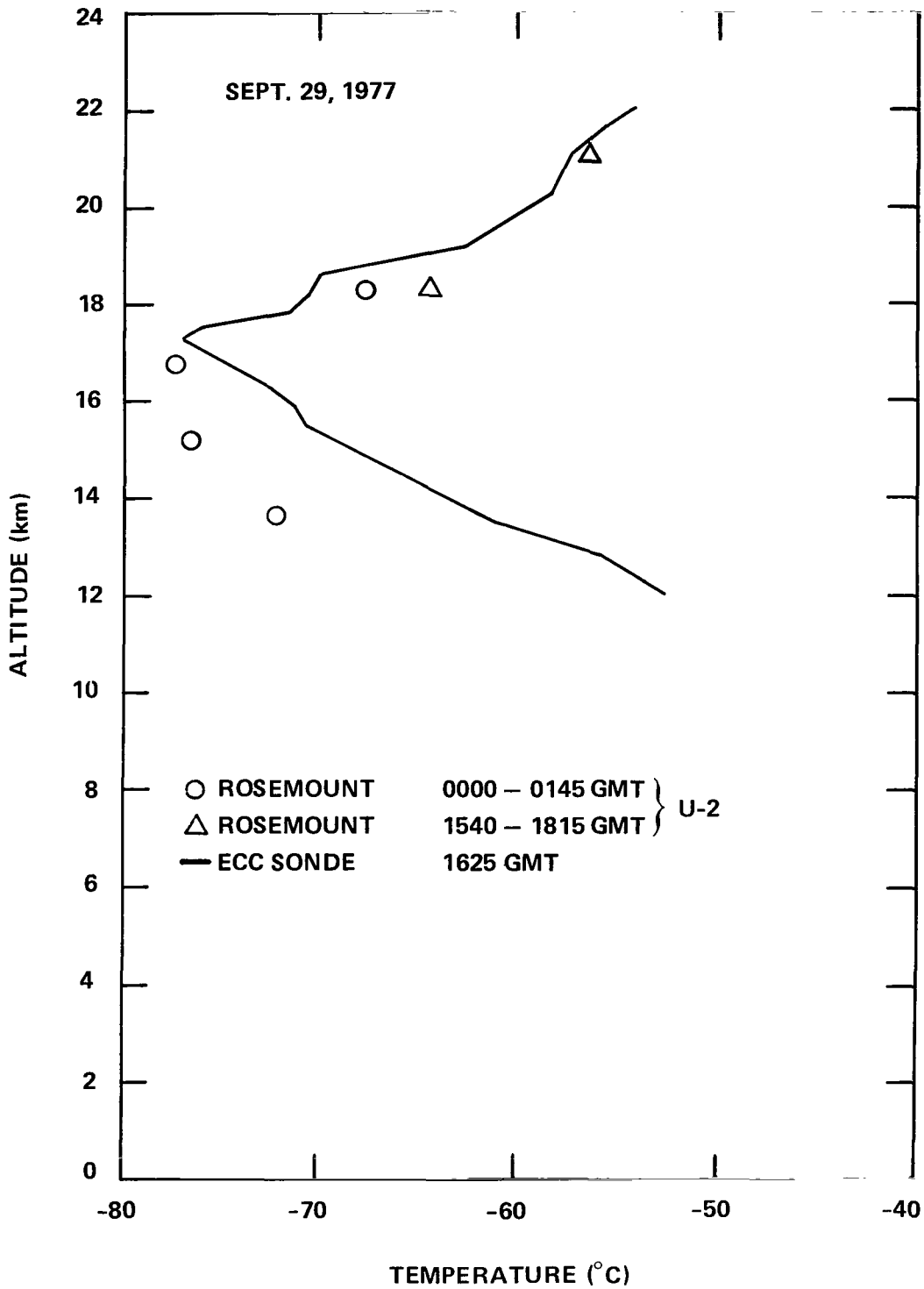

Figure 2. Temperature data obtained with the Rosemount total air temperature probe on the U-2 aircraft. Also shown is the air temperature profile from the ECC sonde flown from the White Sands Missile Range at 1625 GMT.

densities of ozone and are much larger than the variations attributable to short-term instrument stability or to variation in aircraft altitude. The fluctuations at times suggest a wavelike structure; this phenomenon is undergoing study using a more extensive data base and is intended to be the topic of a later report.

REFERENCES

1. Loewenstein, M., W. L. Starr, and D. G. Murcray, "Stratospheric NO and HNO_3 Observations in the Northern Hemisphere," *Geophys. Res. Lett.*, **5**, 1978, pp. 531–534.

2. Loewenstein, M., W. J. Borucki, H. F. Savage, J. G. Borucki, and R. C. Whitten, "Geographical Variations of NO and O_3 in the Lower Stratosphere," *J. Geophys. Res.*, **83**, 1978, pp. 1875–1882.

3. Loewenstein, M., H. F. Savage, and J. G. Borucki, "Geographical Variations of NO and O_3 in the Lower Stratosphere," Proceedings of the International Conference on Problems Related to the Stratosphere, Utah State University, Logan, Utah, September 15–17, 1976, JPL Publication 77-12, 1977, pp. 230–233.

OZONE PROFILE TO 60 KM FROM THE ROCOZ INSTRUMENT

Arlin J. Krueger and David U. Wright
NASA, Goddard Space Flight Center
Greenbelt, Maryland 20771

Peter Simeth
SenTran Company
2705 de la Vina St.
Santa Barbara, California 93102

Staff
NASA, Wallops Flight Center
Wallops Island, Virginia 23337

ABSTRACT

A rocket carrying an optical ozonesonde was launched at 1822 GMT on September 29, 1977, from White Sands Missile Range, New Mexico, as part of the Stratcom VIII-A effort. The integral ozone amount above the balloon ceiling altitude of 40 km was measured as 0.0117 atm-cm with an uncertainty less than ±7 percent. The ozone density at 40 km was 6.77×10^{17} mol/m^3. Ozone densities in molecules/m^3 at higher altitudes were 2.28×10^{17} at 45 km, 6.72×10^{16} at 50 km, 2.20×10^{16} at 55 km, and 7.26×10^{15} at 60 km. In addition, the ozone distribution was measured at lower altitudes from the tropopause at 17 to 40 km. A similar instrument was placed on the main gondola of the Stratcom VIII-A balloon; however, interfering objects in the field of view did not permit interpretation of the balloon data in terms of an ozone profile.

INTRODUCTION

Several Stratcom VIII experiments require a determination of the amount of ozone remaining above the balloon's ceiling altitude for interpretation of results which depend on the incident solar flux in the middle ultraviolet. The present experiment determined that parameter with an optical ozone sensor carried aloft with a Super Loki-Dart rocket, launched from White Sands Missile Range on September 29, 1977, 1122 MST, while the Stratcom VIII-A Balloon was near its ceiling altitude of 40 km.

INSTRUMENTATION

The Rocoz optical ozonesonde measures the attenuation of ultraviolet sunlight in atmospheric layers. The ozone density is directly computed from the attenuation per kilometer height interval, given the ozone absorption coefficient for the wavelength band in use. The instrument used for this rocket observation is the standard unit in use for the past 2 years at Wallops Flight Center and Churchill Research Range. A description of the instrument may be found in Reference 1.

The ozonesonde determines the vertical ozone profile from measurements of the height gradient of relative solar irradiance in three narrow UV bands of about 3 to 4 nm width. The center wavelengths of these bands are selected for optimum sensitivity to ozone in adjacent height regions over the height range of 20 to 60 km. A fourth narrow band at a wavelength with a low ozone absorption coefficient is also included to monitor extraneous sources of signal change, such as aerosol scattering.

The Rocoz ozonesonde operates over solar zenith angles from 0 to 84°. A flat plate diffuser with approximately Lambertian angular response is used as the first optical element such that acceptable signal levels are obtained at the detector over this range of angles. This diffuser was selected because light from the horizon is minimized and because such measurements are directly amenable to radiative transfer calculations. The light from the diffuser plate passes through a beamsplitter and then through narrow-band interference filters mounted in a filter wheel. Visible and infrared light transmitted by the interference filter are removed with a broadband UV-filter. A quartz lens focuses light from the diffuser plate on a UV enhanced silicon photodetector. The lens also limits rays passing through the interference filter to 8.5° from the normal.

An amplitude modulation of the optical signals, caused by changes of the angle of incidence of sunlight on the diffuser, is removed in the following manner: A small percentage of the light from the diffuser plate is redirected by a 45° beamsplitter to a second photometer similar in construction to the primary UV photometer, but sensitive to a fixed band near 375 nm. The output of this photometer feeds into the X input (denominator) of the dividing circuit. The output of the UV photometer connects to the Z input (numerator). Changes in light input level (pendulation, rotation, or partial shading of the diffuser plate) affect both divider input signals equally and, therefore, are cancelled in the dividing circuit. In the rocket instrument the output of the dividing circuit is commutated into four sample and hold circuits which are updated when their corresponding narrow-band filter is lined up with the UV optical assembly. Each sample and hold circuit provides a 0- to 5-V output signal to the telemetry system.

The compensation signal which is proportional to the input light level is also transmitted to the ground to provide information about pendulation and rotation of the sonde. A sixth output signal is derived from the thermistor which monitors the temperature of the UV optical assembly. A Super Loki-Dart vehicle is used to deliver the ozonesonde to an altitude of 65 to 70 km. The actual measurements are made while the instrument package is descending on a parachute (a 7-ft starute). The measured data are sampled at a rate of 110 per second and transmitted to a ground station via a PCM telemetry system operating at 1680 MHz.

Balloon Borne Instrument

For balloon use, a Rocoz optical ozone sonde was modified by replacing the filters in channels 3 and 4 with ones at wavelengths useful below 40 km, and modifying the electrical characteristics of the output so as to be compatible with the Stratcom VIII telemetry system. The photometer was mounted on the top level of the main payload for the Stratcom VIII-A balloon, adjacent to several other solar UV sensors. See Figures 3, 4, 5, and 6 of "The Stratcom VIII Effort". Immediately above the gondola were a packed parachute and a control package with reflective surfaces.

CALIBRATION

The ozonesonde is designed such that the calibration is dependent only on effective ozone absorption coefficients for the UV filters. These coefficients are computed using detailed measurements of the filter transmission characteristics. The particular instruments flown had characteristics as given in Table 1.

Table 1
Optical Characteristics of Rocoz Photometers

Filter No.	Center Wavelength (nm)	Half-width (nm)	$\alpha(\tau = 0)$ (cm^{-1})	Altitude Region (km)
Ser. No. 250; rocket flight No. 174				
0	319.43	3.87	0.674	Reference
1	304.18	4.00	5.297	17–38
2	283.60	3.84	76.83	38–49
3	258.40	7.11	294.33	44–64
Ser. No. 276; Stratcom VIII-A balloon				
0	319.8	3.32	0.678	Reference
1	305.0	3.82	4.762	25–34
2	299.8	3.50	9.64	29–38
3	287.8	3.36	49.16	35–40

The half-width, given in column 3, is the wavelength interval between the points where the filter transmission is 50 percent of the peak transmission. The parameter in column 4 is the ozone

absorption coefficient in cm^{-1} for an ozone optical depth of zero. A slight dependence of the absorption coefficient on ozone optical depth is included in the data reduction. The correction is generally less than 1 percent at unit optical depth. The temperature dependence of the ozone absorption spectrum is approximately accounted for by assuming that 44°C coefficients apply to wavelengths longer than 290 nm (used for ozone measurements in the lower stratosphere) and +18°C coefficients for wavelengths shorter than 290 nm (used in the upper stratosphere and mesosphere). This assumption is justified by the higher air temperatures near the stratopause and the lower temperature coefficients at the shorter wavelengths in the Hartley bands.

Filter No. 0 is a reference channel, while the other filters are used at overlapping altitude intervals, as indicated in column 5.

RESULTS

The rocket data Rocoz sonde was flown on a Super Loki rocket launched at 1822 GMT (1122 MST), September 29, 1977, from the Small Missile Range (WSMR, New Mexico) to an altitude of 65 km. The flight data were processed in the manner established for the Rocoz sondes regularly used in the Meteorological Rocket Network soundings.

The ozone profile from the three active filters in this instrument is shown in Figure 1, and the composite data from merging the results in overlap regions are given in Table 2. The results from Filter No. 3 average 1 percent higher than the Filter No. 2 ozone densities from 44 to 49 km. In the single overlapping height between Filters No. 1 and 2, the Filter No. 2 results are 4 percent higher. (This value changes to −1 percent if the Filter No. 1 data are extended 5 km upwards beyond the limit of optimum accuracy.) The ozone profile exhibits only minor structural deviations from a constant scale height (11 = 4.3 km) profile above 38 km. Below this the local scale height increases until the ozone density maximum of 5.2×10^{18} m^{-3} near 25 km is reached.

The ozone mixture ratio profile is shown in Figure 2. This exhibits a peak of 18.4 μg/g (11 ppm) near 33 km and a rather featureless decay above and below, becoming less than 10 μg/g at 25 and 44 km, and less than 5 μg/g at 21.5 and 50 km.

The probable errors in the results are generally less than 10 percent between 21 and 50 km. Above 50 km, the errors grow due to parachute pendulation and lower attenuation per unit height. Below 21 km, the errors grow rapidly due to a small signal level. The relationships between the Rocoz data and that from other ozone sensors during this effort is indicated in "Highlights of the Stratcom VIII Effort", and, in terms of column content, in Table 3.

An initial inspection of the rocket data has shown that a completely unreasonable telemetry zero offset would be required to bring the rocket profile into agreement with the ECC data. Likewise, a filter temperature coefficient 10 times larger than the manufacturer's specification would be required. The discrepancy could be accounted for by postulating interference in the 304.2 nm band by another

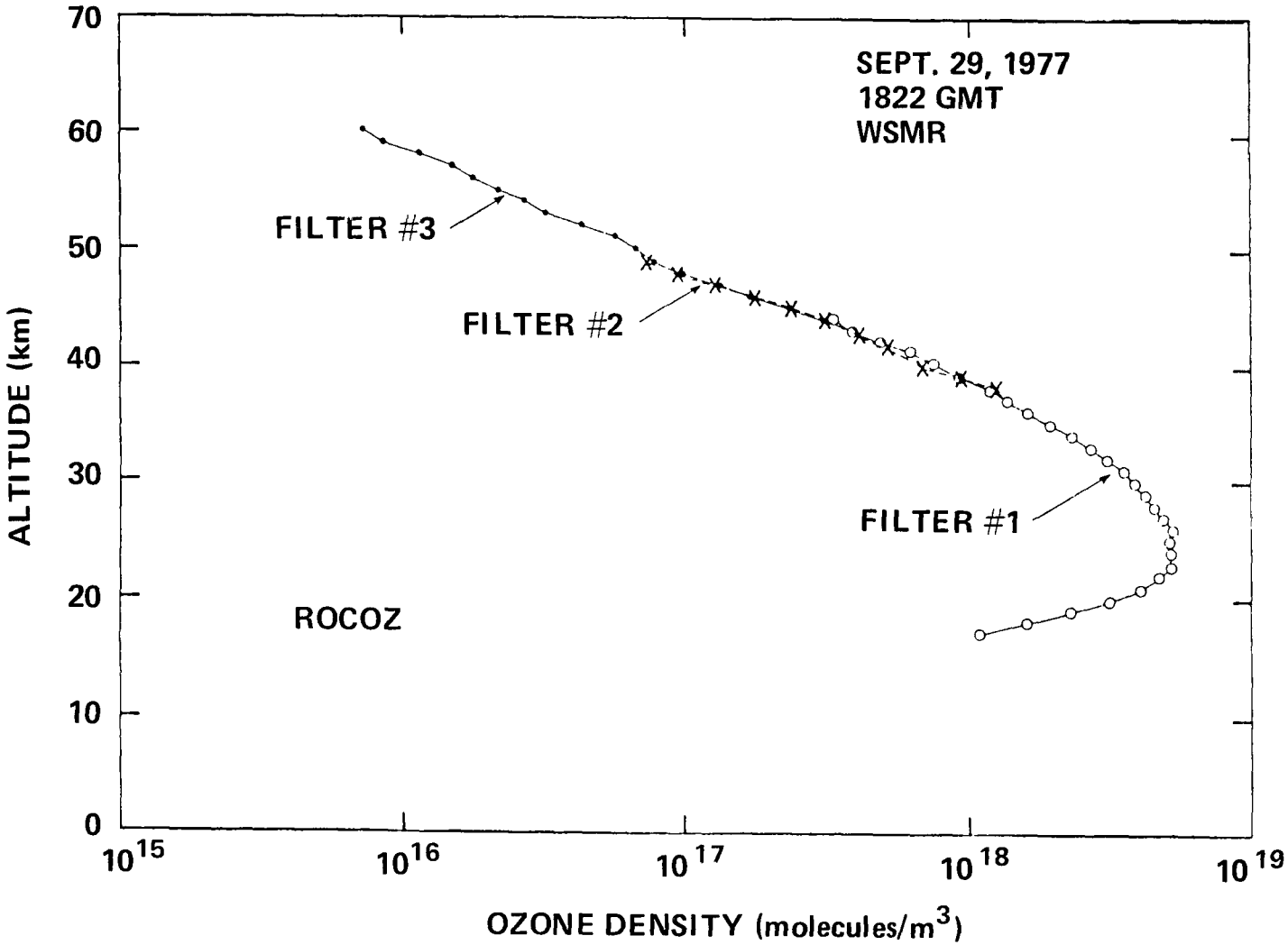

Figure 1. Ozone density profile observed with Rocoz system.

Table 2
Data Report for Rocoz Flight Number 174
(White Sands, New Mexico, 1822 GMT, Sept. 29, 1977)

Height, km	O_3 Density mol/cm^3	Mix Ratio Mass	Mix Ratio Volume	Air Density, g/cm^3	Air Temp. °C
60	7.254E + 09	1.85	1.12	0.31	-14.6
59	8.598E + 09	1.91	1.15	0.36	-16.8
58	1.182E + 10	2.29	1.38	0.41	-18.0
57	1.505E + 10	2.59	1.56	0.46	-15.3
56	1.746E + 10	2.68	1.62	0.52	-11.2
55	2.203E + 10	3.02	1.82	0.58	- 8.0
54	2.687E + 10	3.20	1.93	0.67	-11.5
53	3.224E + 10	3.43	2.07	0.75	- 7.0
52	4.299E + 10	3.98	2.40	0.86	-10.6
51	5.642E + 10	4.61	2.78	0.97	- 9.6
50	6.717E + 10	4.88	2.95	1.10	- 7.0
49	7.792E + 10	5.04	3.04	1.23	- 4.5
48	9.941E + 10	5.67	3.42	1.40	- 4.0
47	1.290E + 11	6.49	3.92	1.58	- 4.6
46	1.693E + 11	7.60	4.58	1.78	- 2.3
45	2.284E + 11	8.87	5.35	2.05	- 6.5
44	3.063E + 11	10.49	6.33	2.33	- 6.5
43	3.896E + 11	11.57	6.98	2.68	-10.8
42	4.890E + 11	12.51	7.55	3.11	-15.8
41	5.723E + 11	12.82	7.73	3.56	-16.6
40	6.771E + 11	13.24	7.99	4.08	-17.5
39	9.162E + 11	15.55	9.39	4.69	-20.0
38	1.201E + 12	17.41	10.50	5.50	-26.0
37	1.354E + 12	16.88	10.18	6.40	-29.0
36	1.574E + 12	16.87	10.18	7.44	-31.9
35	1.913E + 12	17.57	10.60	8.68	-35.4
34	2.300E + 12	18.22	11.00	10.06	-36.5
33	2.679E + 12	18.31	11.05	11.66	-37.6
32	3.063E + 12	18.05	10.89	13.53	-38.7
31	3.466E + 12	17.65	10.67	15.62	-38.9
30	3.842E + 12	16.97	10.24	18.05	-39.5
29	4.191E + 12	15.59	9.41	21.43	-43.8
28	4.487E + 12	14.34	8.65	24.95	-45.4
27	4.890E + 12	13.39	8.08	29.12	-46.9
26	5.239E + 12	12.24	7.39	34.12	-48.4
25	5.186E + 12	10.34	6.24	39.99	-50.0
24	5.212E + 12	8.78	5.30	47.33	-52.2
23	5.186E + 12	7.37	4.45	56.10	-55.7
22	4.756E + 12	5.82	3.51	65.17	-54.4
21	4.030E + 12	4.17	2.51	77.10	-57.5
20	3.144E + 12	2.65	1.60	94.62	-59.5
19	2.297E + 12	1.60	0.97	114.31	-65.8
18	1.588E + 12	0.92	0.55	138.08	-71.2
17	1.094E + 12	0.52	0.31	168.88	-75.0

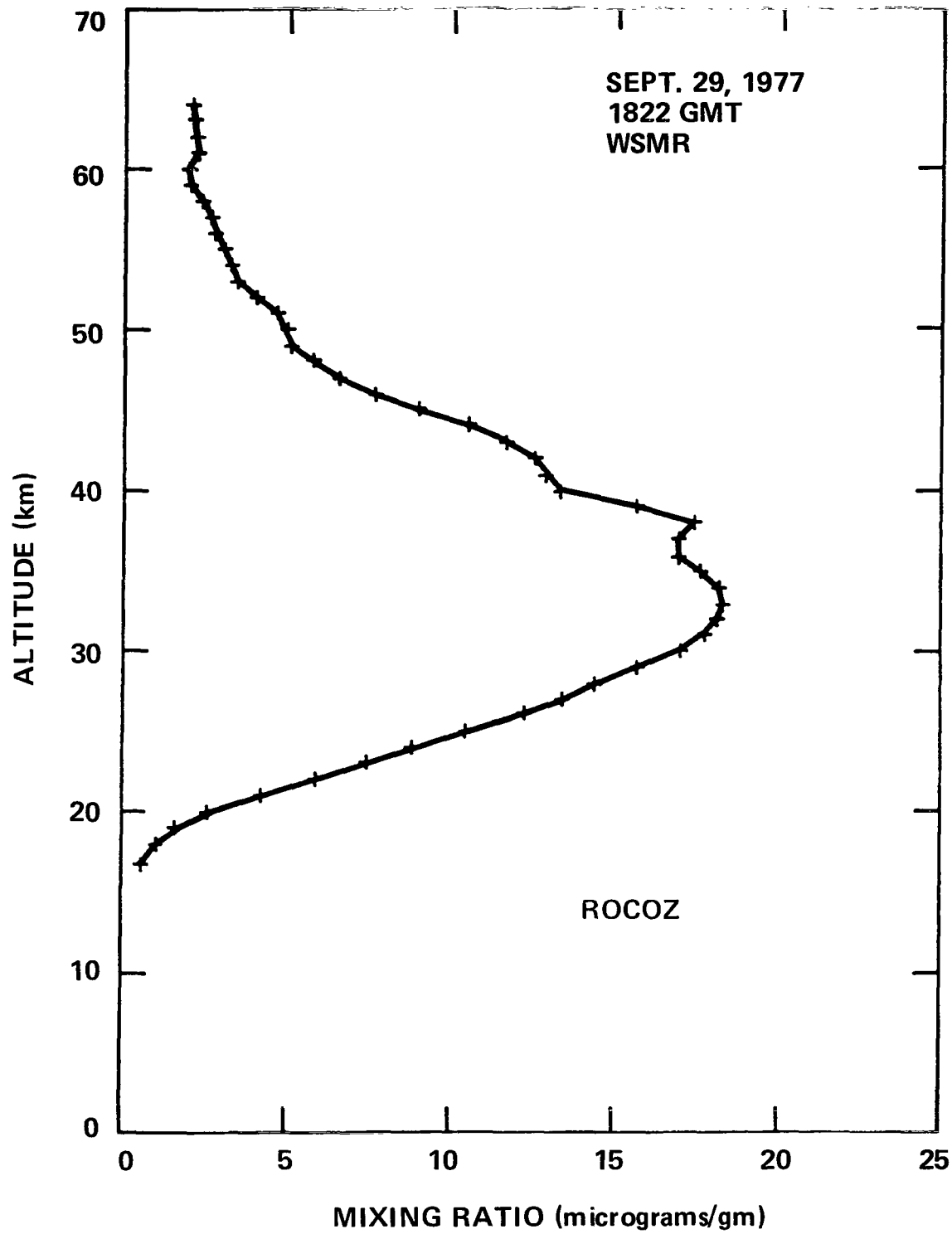

Figure 2. Ozone mixing ratio profile from Rocoz data.

Table 3
Ozone Column Content (atm-cm)

Instrument	0-21.5 km	Above 21.5 km	Total
ECC sonde	0.093		
MAST sonde	0.045		
Dasibi	0.06 (est.)		
Rocoz		0.242	
Dobson (1100 MST)			0.284
SenTran (1100 MST)			0.289

(unidentified) atmospheric constituent. This is, of course, highly speculative because the absorption would have to be comparable (30 percent) to the ozone attenuation per unit height between 25 and 35 km.

The ozone overburden for observations from the Stratcom VIII-A ceiling altitude of 40 km can be computed from the rocket profile. A value of 0.012 atm-cm with an uncertainty on the order of ±7 percent is obtained. The error is estimated from the errors in the ozone density just above 40 km. It should be pointed out that the optical ozone data for heights above 38 km are internally consistent and that the usual test for validity of data, namely, close correspondence in the regions of redundant data, is completely satisfied.

Balloon Data

Data were obtained from the balloon borne photometer throughout the daylight hours of September 29. Particular attention was given to the analysis of the ascent data in terms of ozone content. The reference channel showed three superimposed repetitive patterns:

(1) A 30-second periodicity, probably due to a rocking motion of the payload about its suspension point. The design of the photometer readily permitted compensation for these changes in apparent solar elevation.

(2) A periodicity of about 80 seconds, associated with the rotation of the gondola (see the magnetometer data in "Main Payload Monitors for Stratcom VIII-A") and corresponding to shadowing of the entrance optics by suspension cables and portions of the adjacent instruments. This is an intensity modulation and can be properly compensated in the data reduction.

(3) A long period modulation of 700 to 1200 seconds which is probably due to the rotation of the parachute–control package relative to the gondola immediately below. This results in a change of the spectral content of the light falling on the photometer. Since the spectral reflectivity of the upper package is unknown, compensation for the long period modulation cannot be made.

The long period modulation continued throughout the float period of the balloon flight, and prevented a meaningful data analysis in terms of ozone density distribution or in terms of changes of ozone overburden during float.

ACKNOWLEDGMENTS

We sincerely appreciate the efforts of the Physical Sciences Laboratory, Las Cruces, New Mexico, for telemetry fabrication; the Naval Weapons Center, China Lake, California, and P&P Industries, College Park, Maryland, for payload calibrations; National Weather Service personnel at Wallops Flight Center and the White Sands Missile Range personnel for flight operations; and Miss Carol Fry of P&P Industries for data processing.

REFERENCE

1. Krueger, A. J., P. G. Simeth, B. C. Ellison, W. R. McBride, M. Hill, C. A. Flanagan, W. Gammill, and S. G. Park, 1978: "Design of an Optical Ozonesonde for the Super Loki-Dart Rocket," *NASA Technical Report*, 1979.

OZONE PROFILE AND SOLAR FLUXES FROM A GRATING SPECTROMETER

James E. Mentall and Jay R. Herman
NASA, Goddard Space Flight Center
Greenbelt, Maryland 20771

Bernard Zak
Sandia Laboratories
Albuquerque, New Mexico 87185

ABSTRACT

Solar ultraviolet flux measurements were obtained by means of an 1/8 m Fastie-Ebert grating spectrometer flown on the Stratcom VIII-A Balloon, September 29, 1977. Spectra covered the wavelength range from 197.9 to 287.9 nm, at altitudes from about 25 to nearly 41 km, and over a wide range of solar zenith angles. Good agreement is obtained between the observed spectra and synthetic spectra calculated using a two stream radiative transfer model. Ozone densities were derived from the spectra during the ascent from 32 to 40 km and ozone overburdens from the spectra during the day long float.

INTRODUCTION

Considerable attention has been focused on the stratosphere over the past few years. This concern has been the result of realizing that the ozone layer is fragile and that the depletion of this protecting layer would have serious consequences for humanity. These facts are reflected by the number of experiments in the Stratcom VIII effort which were concerned with the measurement of ozone directly or through measuring the attenuation of the solar radiation by the ozone layer.

For the study of the stratosphere, the wavelength region of interest is from about 175 to 320 nm. At wavelengths shorter than 175 nm solar radiation does not penetrate to the stratosphere due to strong absorption by O_2. Above 320 nm, the atmosphere is essentially transparent. The 175- to 320-nm region can be divided into three regions of interest determined by the dominant absorption process. From 175 to 200 nm, absorption is predominantly via the O_2 Schumann-Runge bands. Between 200 and 220 nm absorption results from the weak O_2 Herzberg continuum, which allows UV radiation to penetrate to the lower stratosphere. The 220- to 300-nm region is dominated by the strong O_3 absorption.

Since it was impossible for the flight spectrometer to cover the entire wavelength range of interest, the grating drive was set to cover as much of the 200- to 300-nm interval as possible. Although the

instrument was on at liftoff, the sensitivity of the instrument was such that no useful data were obtained below 25 km. Effectively, solar spectra were obtained as a function of altitude and a low solar zenith angle (~60°) on the ascent portion of the flight and at a constant float altitude (~40 km) as a function of solar zenith angle. The data are compared with a theoretical model and are used to obtain an ozone profile and ozone overburdens.

INSTRUMENT

The ultraviolet scanning spectrometer is an 1/8-m Fastie-Ebert instrument manufactured by Ray Lee Instruments. Equipped with a 3600-line/mm holographic ruled grating, it has a measured resolution of 1.1 nm. The grating is driven by means of a cam, and scans from about 190 to 290 nm in 3.6 sec. The dispersed photons are detected with an EMR 510F solar blind (CsTe photocathode) photomultiplier which has a nominal long wavelength cutoff of 320 nm. Although scattered light in the instrument is less than 1 part in 10^{-4}, it was necessary to place an interference filter in front of the entrance slit to obtain solar spectra down to about 30 km. This reduces the scattered light at 250 nm by more than 2 orders of magnitude while reducing the signal by a factor of 10. The efficiency at 240 nm (zero solar zenith angle) is 4.5×10^{-8} counts per photon.

The flight spectrometer was mounted in a hermetically sealed container with a blackened shield above the entrance aperture to block reflections from the balloon overhead. A conical diffuser allowed the solar spectra to be obtained from near zenith to about 90°. The instrument sensitivity drops rapidly as the solar zenith angle increases from 15 to 30°. In the Stratcom VIII flight, the solar zenith angle at local noon is about 35°. At this angle, the sensitivity of the system is about 20 percent of that for an overhead Sun. At sunrise and sunset the efficiency is about 3 percent of maximum.

The entire system was calibrated using a standard lamp at wavelengths above 250 nm and using a double monochromator technique to extend the calibration to below 200 nm. A relative accuracy of ±5 percent in the calibration was obtained with an additional ±10 percent error in the absolute flux. However, the presence of the conical diffuser markedly decreased the accuracy of the measurements under flight conditions. It was found that the sensitivity of the instrument varied not only with solar zenith angle but with changes in azimuth as well. This can be qualitatively understood by realizing that the diffuser would not be uniformly illuminated unless the sun were directly overhead. These angular dependencies are probably amplified by the fact that the spectrometer has curved slits. During the ascent of the balloon, the gondola rotated at a rate of about once-per-minute. During float, the gondola continued to rotate but at a much slower rate. Although it was possible to correct for the motion of the gondola, it is felt that the absolute accuracy of the solar flux measurements is not better than ±50 percent. It is noted that the problems associated with the conical diffuser and the motion of the gondola could have been circumvented by extending the wavelength scan to 320 nm. At this wavelength the atmosphere is essentially transparent and all spectral scans could have been normalized to the value of the unattenuated solar flux at this wavelength. Mechanical considerations would have necessitated replacing the 3600 line/mm grating used in this flight with a 2400 line/mm one; the resulting decrease in resolution (from 1.2 nm to 1.8 nm) would have been barely discernable in the data.

EXPERIMENTAL RESULTS

Solar flux measurements as a function of time are presented in Figure 1. Measurements at 200 and 285 nm were selected for presentation because they are close to the end points of each spectral scan. Measurements are also given at 220 nm where radiation penetrates to the base of the stratosphere, and at 255 nm where the absorption due to ozone is at a maximum. It is emphasized that the absolute accuracy of these measurements of solar flux is ±50 percent while the relative accuracy is ±5 percent.

Float altitude was reached at approximately 0830 MST and remained nearly constant at 40 km until noon. After 1200, the balloon began a very slow descent, reaching an altitude of 38.2 km at 1648. At wavelengths where the attenuation due to O_2 and O_3 is small, the solar flux is nearly constant. The intensity at 255 nm, however, is strongly influenced by both changes in solar zenith angle and small changes in altitude.

The spectrum near local noon is shown in Figure 2. A theoretical profile is also given in this figure for comparison. The solar flux entering the spectrometer, $\phi_\lambda(h)$, is calculated from Beer's law

$$\phi_\lambda(h) = \phi_\lambda(\text{sun}) \exp\left[-\sum_k \sigma_{\lambda k}\, \text{Ch}(\chi) \int_h^\infty n_k\,(h')\, dh'\right]$$

where $\phi_\lambda(\text{sun})$ is the solar flux above the atmosphere, $\sigma_{\lambda k}$ are the absorption cross sections, $\text{Ch}(\chi)$ is the Chapman function for the solar zenith angle χ, n_k are the absorbing species densities, and h is the altitude. At 40 km scattering can be neglected compared to the direct solar flux over the wavelength range of interest. Solar fluxes are obtained from Broadfoot (Reference 1), except below 230 nm where they are obtained from Ackerman (Reference 2). Cross sections are obtained from Ackerman for O_3 and O_2 except for the Schumann-Runge band interval where the computations of Park (Reference 3) are used. Ozone and molecular oxygen profiles are obtained from stratospheric modelling calculations (Reference 4) appropriate for the latitude and date of the balloon flight.

In Figure 2, the calculated and measured curves have nearly identical shapes demonstrating that the overhead ozone column density calculated by the model is correct. This is a particularly good test of the model because at 40 km the ratio of the intensity at 255 nm to that at 220 nm is very sensitive to the ozone overburden; a 20 percent change in column density results in a 50 percent change in this ratio. That the calculated spectrum is a factor of two above the measured one appears to be a consequence of not accurately correcting for the orientation of the spectrometer with respect to the Sun.

During the ascent of the balloon, the gondola was rotating rapidly. Averaging the spectra over 50-minute intervals results in an average of the data over all orientations of the spectrometer. Ozone densities were determined by using the relation

$$N(h) = (\sigma_\lambda \sec\chi)^{-1}\, \ln[I\,(h+\Delta h)/I(h)]$$

since it is not necessary to know the absolute magnitude of the solar flux. The ozone density profile

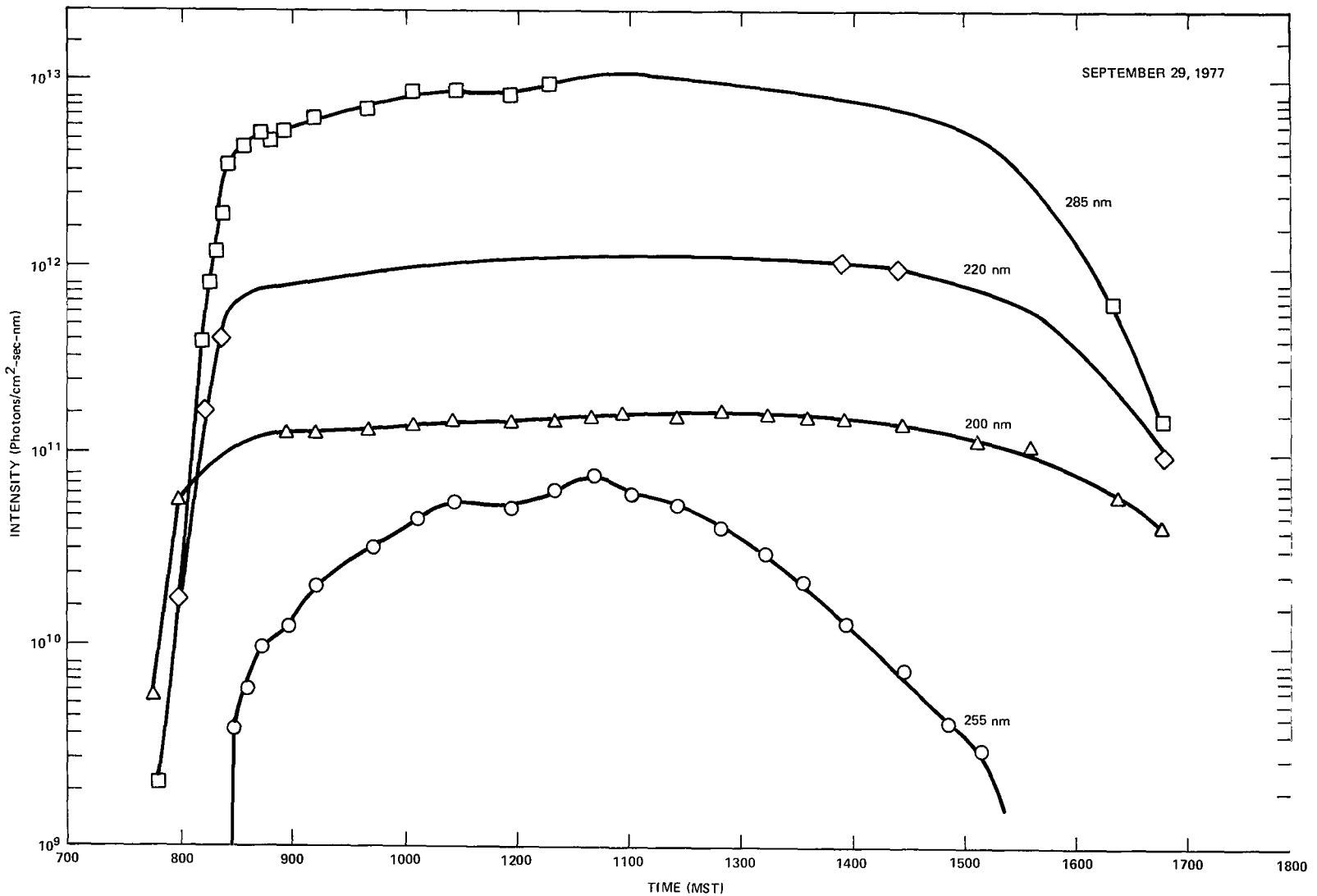

Figure 1. Variation of solar flux with time at four selected wavelengths.

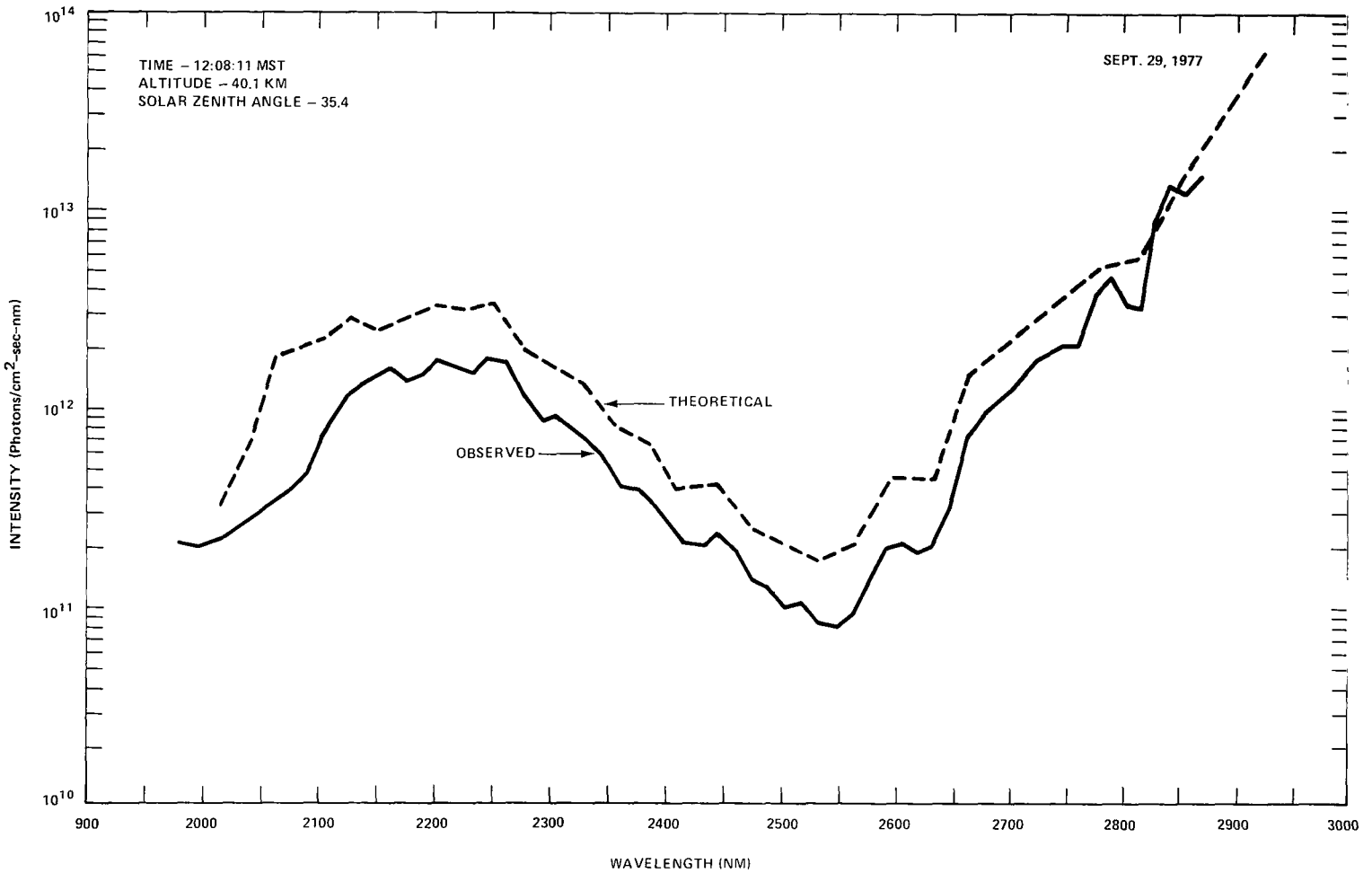

Figure 2. Typical solar spectrum at a float altitude.

between 33 and 40 km during ascent is presented in Figure 3. Below 33 km the signal was too small to obtain a reliable measurement while above 40 km the change in altitude with time was too slow. The dashed line in Figure 3 is the mid-latitude standard ozone profile (U.S. Standard Atmosphere 1976). The measurements lie about 7 percent below the standard profile and are consistent with most of the other ozone measurements made during the Stratcom VIII effort.

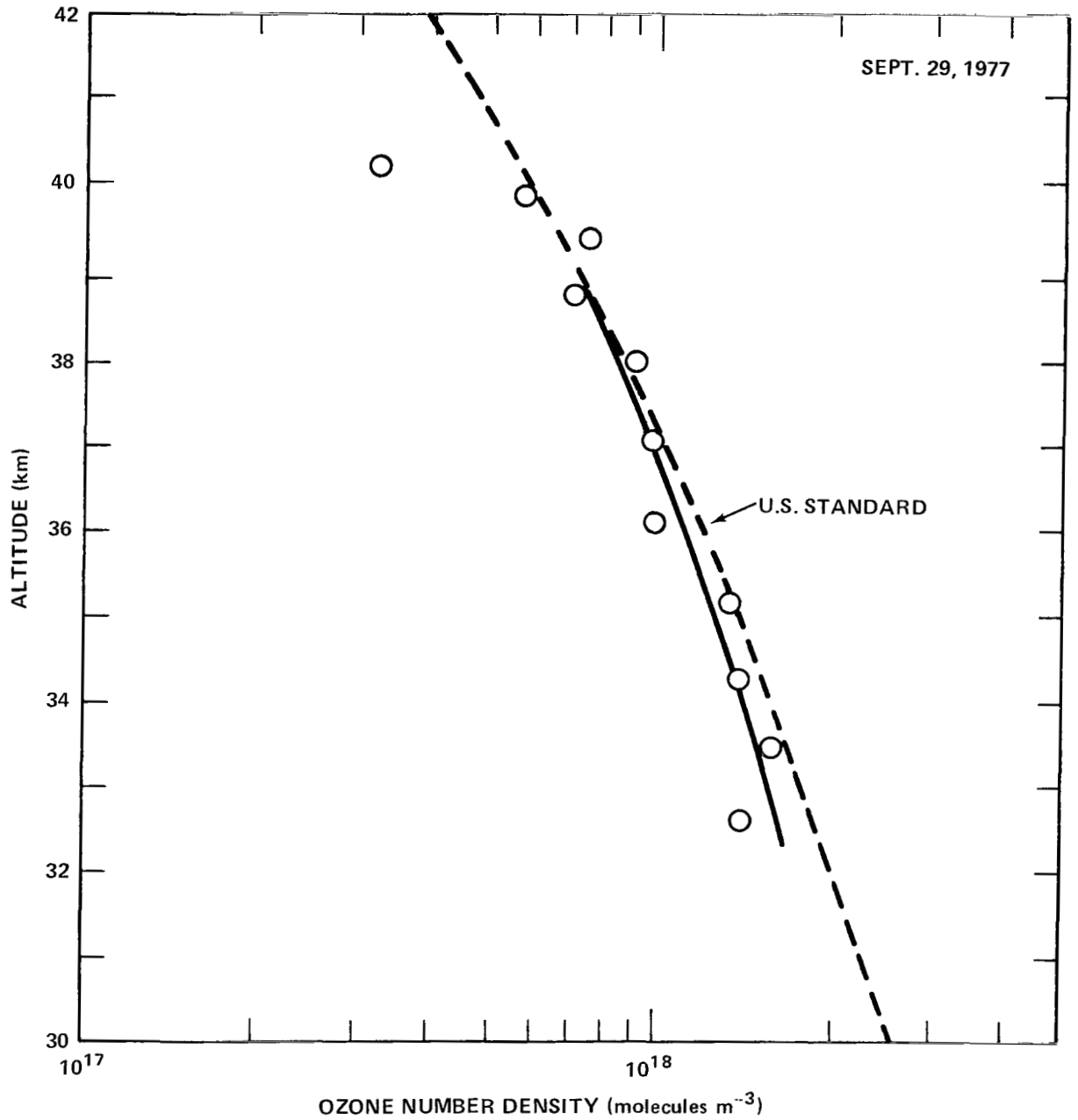

Figure 3. Ozone profile during the balloon ascent.

During float, ozone overburdens can be calculated by taking advantage of the fact that the period of rotation of the spectrometer is long (tens of minutes) compared to the 3.6-second scan time of the spectrometer. The relative accuracy within each spectrum is thus preserved although the absolute error may be large. Ozone overburdens are calculated by taking the ratio of the flux at a wavelength where the absorption due to ozone is large (255.0 nm) to the flux where the absorption is small (213.6 nm). Then,

$$\int_N^\infty N(h)\,dh = \frac{R + \tau(O_2)\sec\chi - \ln\,[I(255.0)/I(213.6)]}{\Delta\sigma\cos\chi}$$

where R is the ratio of the unattenuated solar flux at the two wavelengths, $\tau(O_2)$ is the optical depth due to absorption by O_2, and $\Delta\sigma$ ($\sigma(255.0) - \sigma(213.6)$) is the difference in the O_3 absorption cross section at these wavelengths. Results are presented in Figure 4. Here the data has been adjusted to a constant altitude of 40 km assuming that the change in ozone column density is that given in the U.S. Standard Atmosphere 1976. This adjustment is less than 10 percent and introduces negligible error into the results. All the data fall within 7 percent of a straight line and it is difficult to determine whether the apparent systematic deviations from a constant overburden are real.

REFERENCES

1. Broadfoot, L., "The Solar Spectrum 2100 – 3200 A", *Ap. J.*, **173**, 681-689, 1972.

2. Ackerman, M., "Ultraviolet Solar Radiation related to Mesospheric Processes", Mesospheric Models and Related Experiments, edited by G. Fiocco, Springer-Verlag, New York, 1971, pp. 149-159.

3. Park, J. H., "The Equivalent Mean Absorption Cross Sections for the O_2 Schumann-Runge Bands: Application to the H_2O and NO Photodissociation Rates", *J. Atmos. Sci.*, **31**, 1893-1897, 1974.

4. Herman, J. R., "The response of stratospheric constituents to a solar eclipse, sunrise, and sunset", *J. Geophys. Res.*, **84**, 3701-3710, 1979.

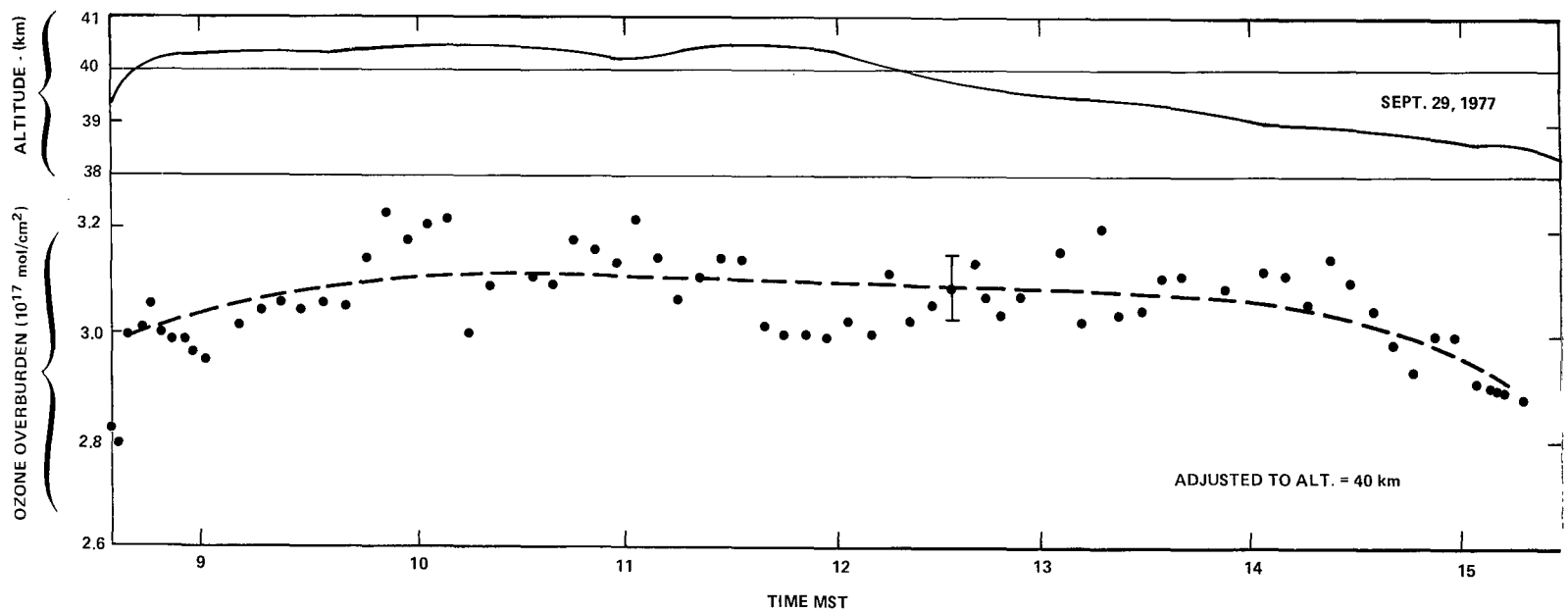

Figure 4. The ozone overburden adjusted to an altitude of 40 km plotted as a function of local time. Also shown is the actual altitude of the balloon.

OZONE PROFILE AND SOLAR FLUXES FROM THE ULTRAVIOLET SPECTROIRRADIOMETER

Bach Sellers, Frederick A. Hanser, and Jean L. Hunerwadel
Panametrics, Inc.
221 Crescent Street
Waltham, Massachusetts 02154

ABSTRACT

A filter wheel UV spectroirradiometer was used to measure solar UV fluxes in 10 wavelength regions in the 200- to 400-nm region at altitudes up to 40 km on the Stratcom VIII-A Balloon, September 29-30, 1978, near Holloman Air Force Base, New Mexico. Ozone layer thicknesses were derived from balloon ascent measurements and an ozone density profile obtained, with a peak density of 5.6×10^{18} molecules/m^3 at an altitude of 24 km. Measurements at the 39- to 40-km float altitude before and after local noon gave a solar flux in the 220 ±5 nm $O_2 - O_3$ transmission window of 4.53×10^{-6} W/(cm^2-nm).

INTRODUCTION

The ultraviolet spectroirradiometer (UVS) flown on the Stratcom VIII-A Balloon payload was originally developed to measure high altitude solar UV fluxes from aircraft as part of the Climatic Impact Assessment Program (CIAP) (Reference 1). The UVS was previously flown on Stratcom VI-A in September 1975 (References 2 and 3), and on VII-A in September 1976 (Reference 4). On both of these balloon flights the UVS gave measurements of the solar flux in the 200- to 400-nm region at altitudes up to 40 km. Much tabular and graphical data are contained in the referenced reports, giving the variation of UV flux with altitude and solar zenith angle. Reference 4 provides more detail than that given here for the Stratcom VIII-A results.

Data on the altitude profile of the solar ultraviolet flux are needed for the following studies:

1. Photochemical calculations of the reaction rates related to the various stratospheric species measured as part of the chemical modeling efforts.

2. Verification and development of radiation transport models.

3. Determination of ozone overburden as a function of altitude for comparison with similar data from other instruments. In addition, the measured variations of the overburden can be used to calculate local ozone densities for comparison with in situ measurements.

4. Indication of the variability of the ultraviolet solar flux near 220 nm and its relationship to the daily sunspot number (Rz), its 27-day average, and/or solar flares.

INSTRUMENT

The UVS is a filter wheel irradiometer. The instrument uses a special UV diffuser to scatter the light incident on the diffuser at an angle, θ_{sd}, to the diffuser axis. The scattered light passes through one of 10 filter sets, located on a rotating wheel, and then into a ruggedized EMR photomultiplier. Additional positions on the wheel are provided for calibration purposes. A cross-sectional drawing of the cylindrical housing is shown in Figure 1, with detection details in Figure 2. For the Stratcom VIII-A Balloon flight the UVS had a cone diffuser and quartz shield to allow vertical mounting with no Sun-pointing requirement.

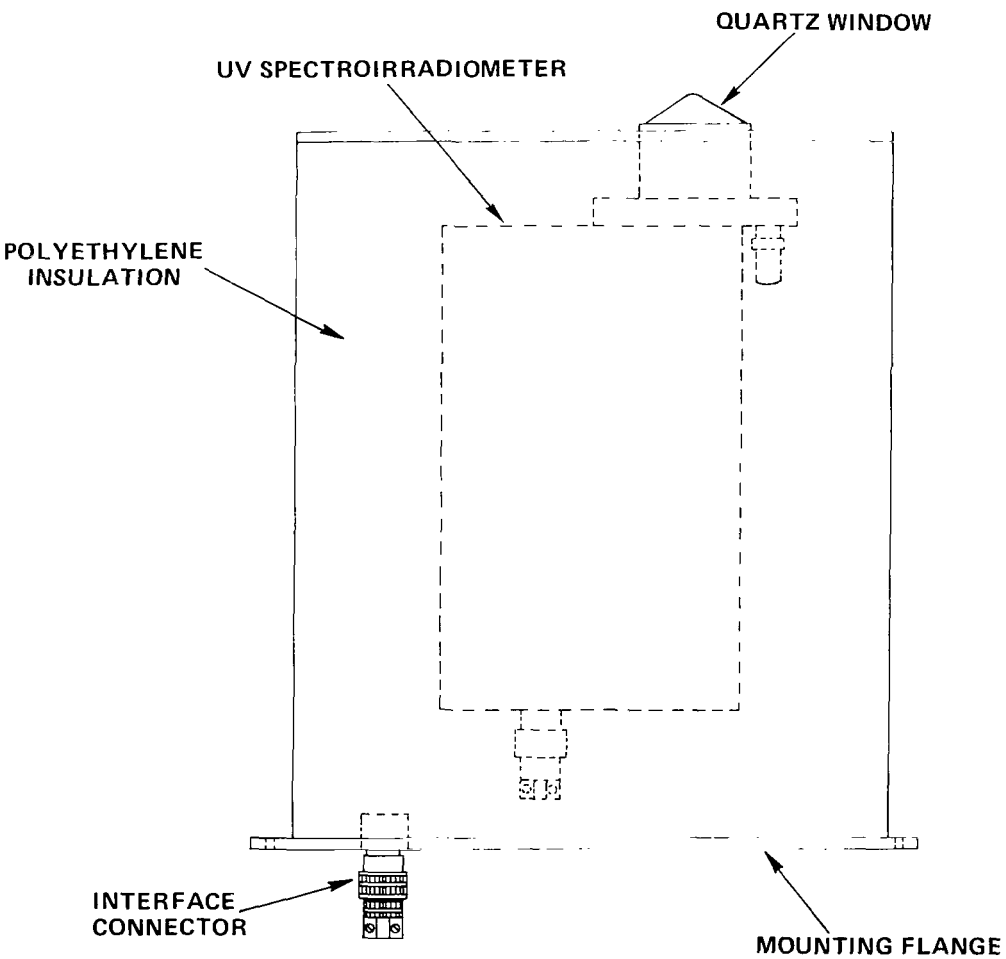

Figure 1. Cross-sectional drawing of the cylindrical housing of the UV spectroirradiometer.

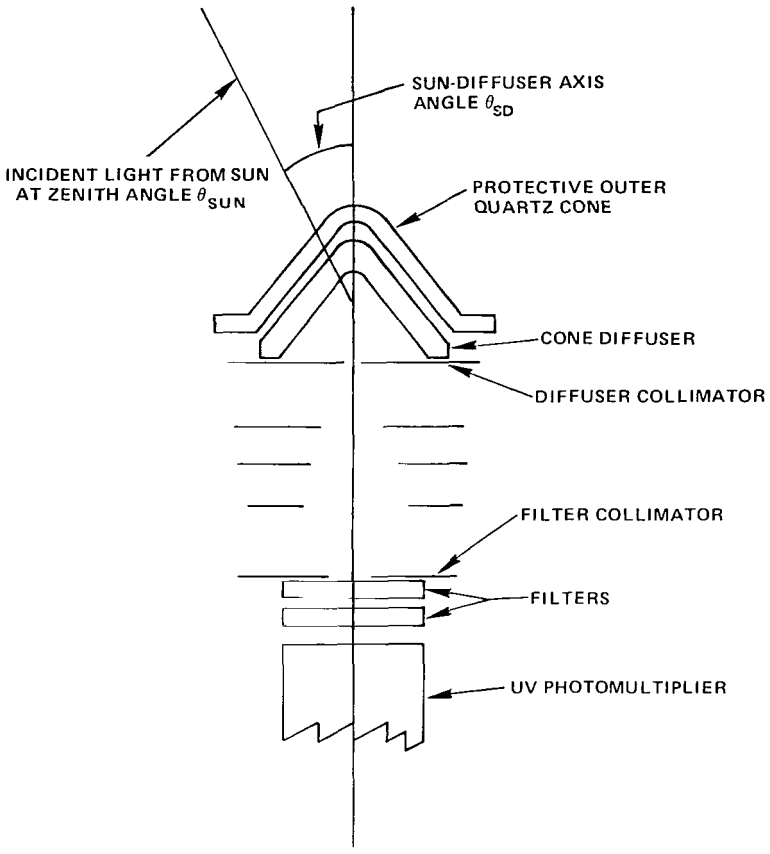

Figure 2. Detection details of UV spectroirradiometer.

Light is received from all azimuths and from a zenith angle of 20° to more than 90° (light scattered from the overhead balloon is blocked by a shield). The precise position of the optical axis is deduced by use of data from the pendulum and magnetometers (See "Main Payload Monitors for Stratcom VIII-A"). The solar zenith angles needed for data analysis are calculated as a function of location (radar data) and time. Intensity is measured up to four orders of magnitude down from the unattenuated solar flux. The 12 positions of the filter wheel are sampled at 1 second each during ascent of the balloon and during parachute descent following cut-down, and at 10 seconds each during float. The filters are shown in Table 1. In order to reduce "leakage flux" problems, each filter set is formed of two or more individual filters used in tandem. The calibration is from a 200-W quartz-iodine Standard of Spectral Irradiance (traceable to NBS), converted to solar spectral shape.

The UVS was located at the top level of the gondola as were the other solar UV instruments on this payload; see Figure 3 which was taken during launch preparations. The UVS, at the extreme left, has a black disc large enough to obscure the balloon itself, but small enough to permit the noon sun to enter the instrument.

Table 1
UVS Calibration Sensitivities
for the Stratcom VIII-A Balloon Flight

Filter Set Average Wavelength (nm)	Filter Set Bandwidth (nm)	Solar Calibration Sensitivity A/[W/(cm^2 -nm)]
220	10	5.034×10^{-1}
289.3	2	1.217×10^{-2}
291.8	2	7.213×10^{-2}
297.4	2	7.923×10^{-2}
302.0	2	2.253×10^{-2}
306.8	2	1.791×10^{-2}
311.7	2	1.144×10^{-2}
329.7	2	6.691×10^{-3}
371.6	28	3.574×10^{-3}
401.9	26	1.369×10^{-3}

RESULTS

The Stratcom VIII-A Balloon was launched at 0607 MST on September 29, 1977; reached its peak altitude, near 40 km, at about 0830, and descended slowly, reaching about 30 km near midnight.

The UVS provided good solar UV flux data from sunrise through sunset (Reference 5). Ozone layer thicknesses may be derived from these data except near sunrise and sunset. A vertical profile of ozone density was obtained from the data during the ascent of the balloon. The 220-nm filter data at float altitude gave a good measure of the solar UV flux at this wavelength. From the viewpoint of photochemistry the high resolution measurements near 300 nm [dissociation of O_3 to produce $O(^1D)$] and coverage up to 400 nm [dissociation of NO_2 to produce $O(^3P)$ – see Reference 6)] are of principal importance. The application of UVS measurements to determination of $O(^1D)$ photoproduction in the troposphere (measurements made from an aircraft platform) is discussed in Reference 7.

DATA ANALYSIS PROCEDURE

The UVS signals are converted to downward-going flux as described in References 1, 2, and 3. For the Stratcom balloon flights the fluxes are also divided by $\cos \theta_{sun}$, θ_{sun} being the solar zenith angle,

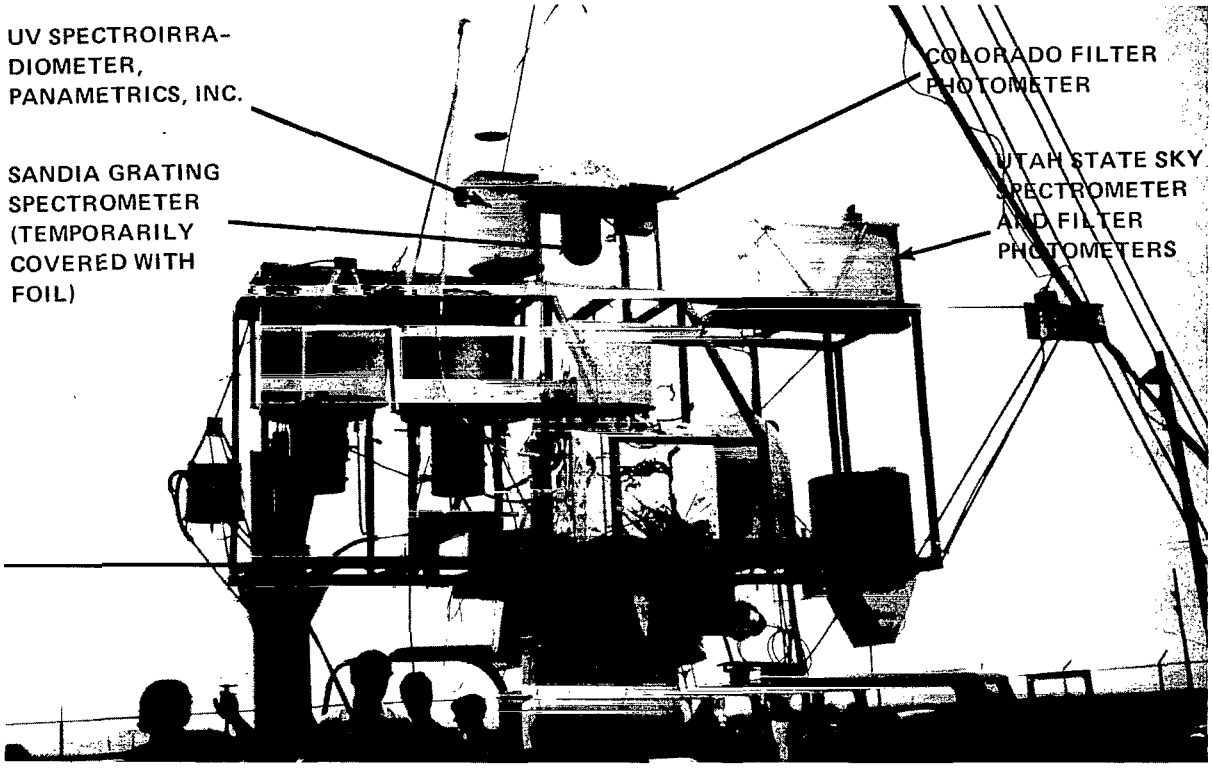

Figure 3. Stratcom VIII-A payload during launch preparation.

so that the high altitude response is the direct solar flux attenuated only by O_3 and O_2. The ratios of the UV fluxes at several wavelengths are used to calculate the vertical overburden of the ozone layer above the balloon altitude. Differences of ozone overburden (Reference 8) calculated for different altitudes allow the vertical ozone density profile to be obtained.

At the highest altitudes the 220 nm filter results are used to obtain the unattenuated solar flux at (220 ±5) nm. This is done by plotting the logarithm of the measured flux against the pressure (at the UVS altitude)/cos θ_{sun}, which latter is proportional to the attenuation path length. The extrapolation of the straight line portion (high altitude, small θ_{sun}) of the data to zero pressure gives the solar flux unattenuated by O_3 and O_2.

OBSERVATIONS

The Stratcom VIII-A fluxes derived by the above procedure were placed in tabular form (similar to those in References 1, 2, 3, and 4) for purposes of further analysis. Some of the results are given in Figure 4 where the measured UV fluxes at four wavelengths are shown as a function of altitude. The solar zenith angle is also decreasing during ascent, so the solar fluxes increase partly because of the decreasing slant path through the ozone layer above the balloon. The major influence on the shorter wavelengths (292 and 307 nm) is the decrease in ozone attenuation as the balloon rises through the stratospheric ozone layer.

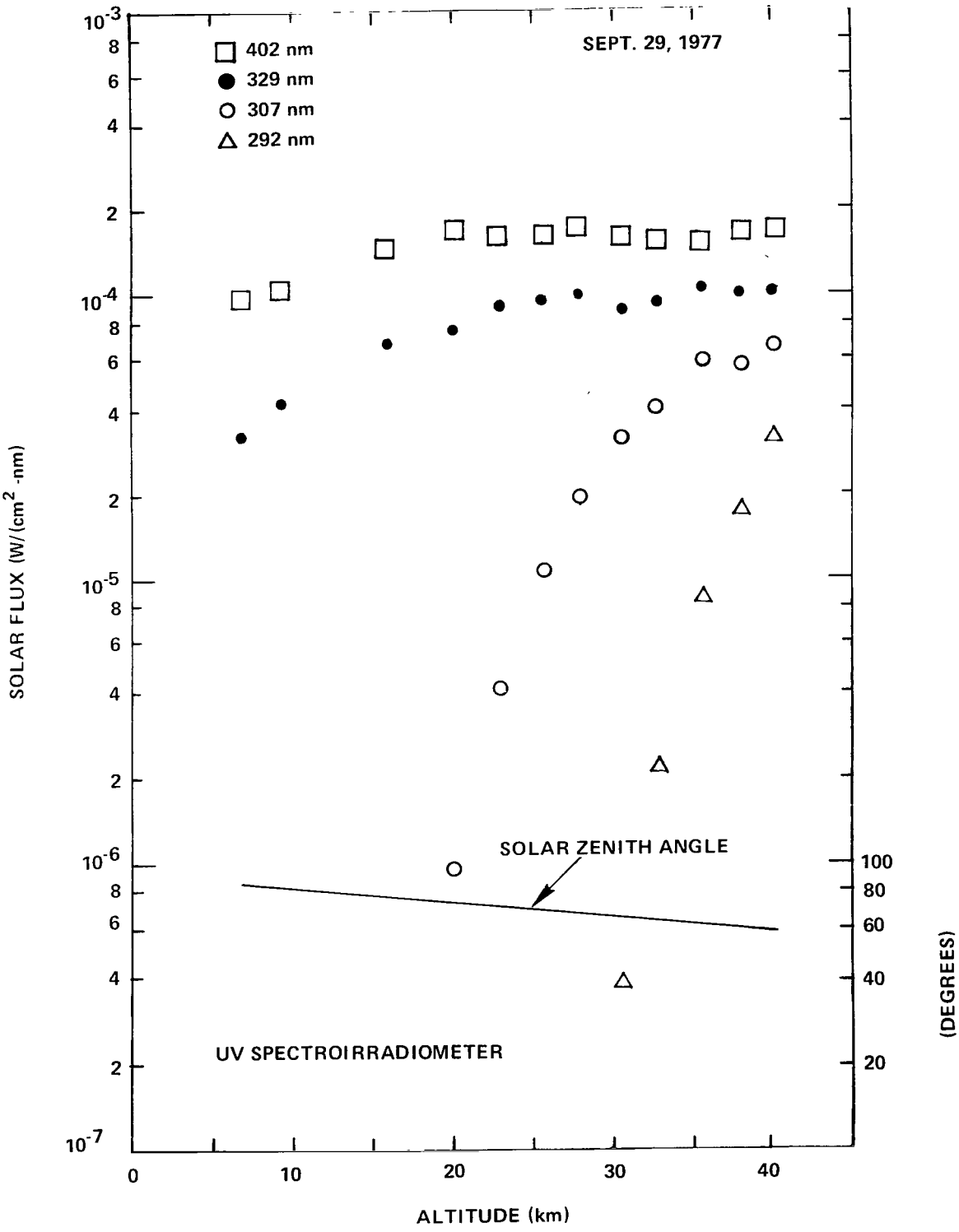

Figure 4. Measured UVS solar fluxes during ascent of Stratcom VIII-A.

The ozone thickness calculated from the measured UV fluxes have been used to calculate the vertical ozone density profile plotted in Figure 5. The altitude bars show the altitude limits used for each density calculation, the ozone density is an effective average over that altitude range. The density values are estimated to be accurate to about ±10 percent.

The 220-nm solar flux measurements are shown in Figure 6. Here the measurements at float altitude are plotted against pressure/cos θ_{sun} on a semilog scale. The straight line fit for pressure/cos θ_{sun} < 10 mb gives 4.53 x 10^{-6} W/(cm^2-nm), with the ascent-sunrise data and the sunset data both giving about the same result. In Table 2, this result is compared with other observations made during the last 10 years. Also shown in this table are the solar activity as measured by the Zurich sunspot number and 2800 MHz flux measured at Ottawa – both obtained from Reference 9.

The 220-nm solar flux data in Table 2 shows a positive correlation with sunspot number and with 2800-MHz flux. The one high point from Ackerman et al. (Reference 11) is slightly anomalous, as the shorter wavelength part of their measurement does not show as large a deviation from other measurements. This strong deviation at 220 nm for the Reference 10 data is especially noticeable in comparisons (e.g., Figure 9 in Reference 13). The trend shown in Table 2 suggests an approximate doubling of the 220-nm solar flux as the sunspot number rises from 0 to 200, or the 280-MHz flux goes from about 70 to 250 [10^{-22} W/(cm^2-Hz)]. This trend is also suggested by the data plots of Simon (Reference 13), although he believes that such a conclusion is somewhat ambiguous. Evidence for about 50 percent variability near 200 nm during the solar cycle has also been presented by Heath and Thekaekara (References 14 and 15).

Because the data come from several different instruments used by different investigators, cross-calibration errors to some extent mask the solar flux variability. Thus the UVS data become quite important, as the same instrument is used each time, being calibrated before each measurement. Thus far the UVS data are for low to moderate solar activity. Measurements with the UVS during the coming years at high solar activity (sunspot maximum) would thus be extremely valuable for determining solar flux variability at 220 nm.

CONCLUSIONS

There are now three sets of UVS-measured data on the atmospheric transmission of the UV fluxes at the wavelengths in Table 1 (Stratcom VI-A, References 2 and 3; Stratcom VII-A, Reference 4; Stratcom VIII-A, Reference 5). At the time of Stratcom VI-A (1975) only three other vertical profiles of UV flux had been made in the stratosphere (of which we are aware): Brewer and Wilson (Reference 16), Simon (Reference 10), and Ackerman et al. (Reference 11). Those measurements emphasized, principally, the 200 nm region. It was our opinion that much useful information on the objectives listed above could be obtained by more detailed measurements. The UVS results now available provide far more coverage in wavelength, altitude, and solar zenith angle than any of the previous work. Discussion of the application of these results to some of the objectives has been presented in our reports (References 1 to 5). We note that the UVS is now a *proven* stratospheric UV flux measurement instrument.

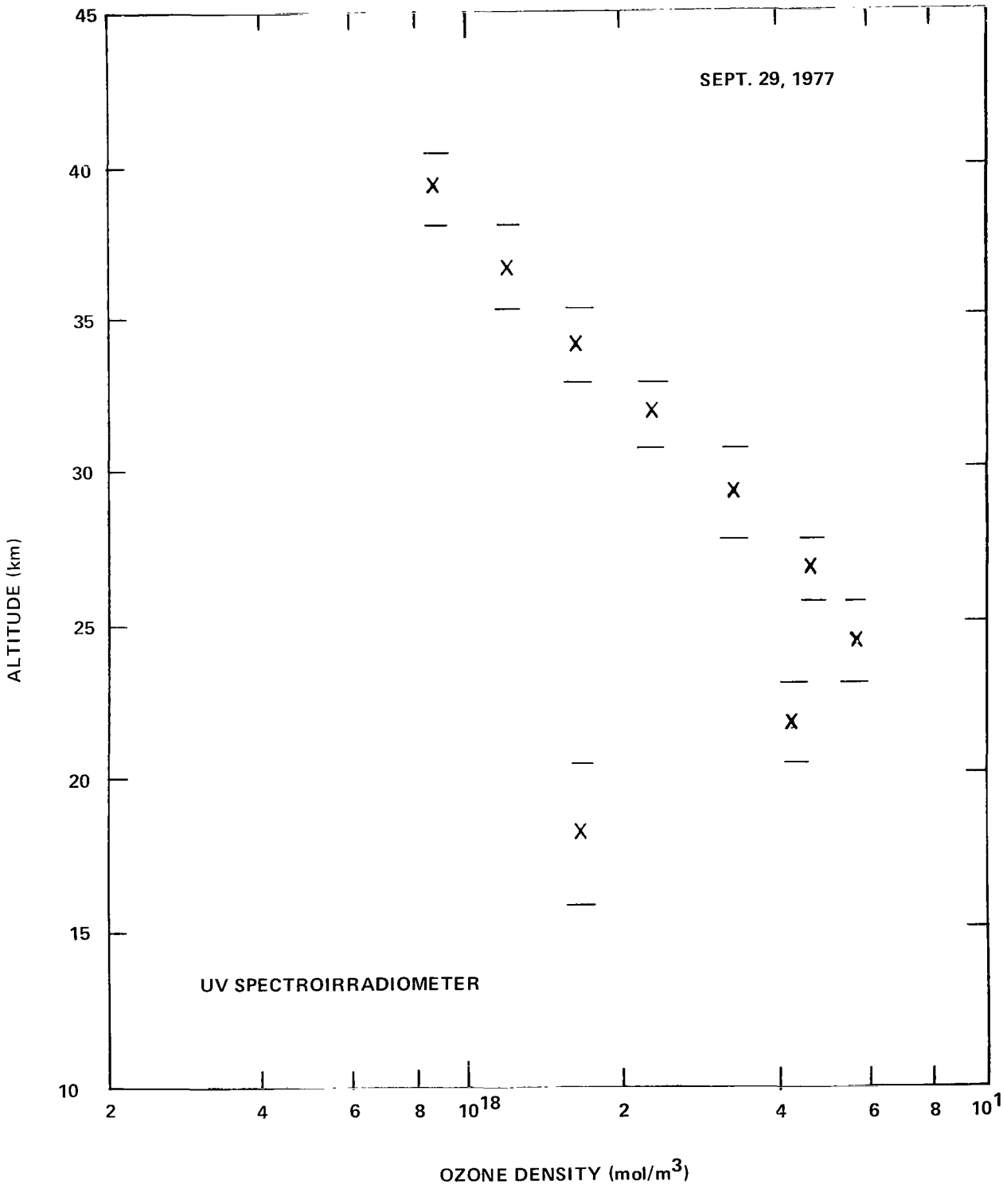

Figure 5. Vertical ozone density profile from UVS data for Stratcom VIII-A ascent.

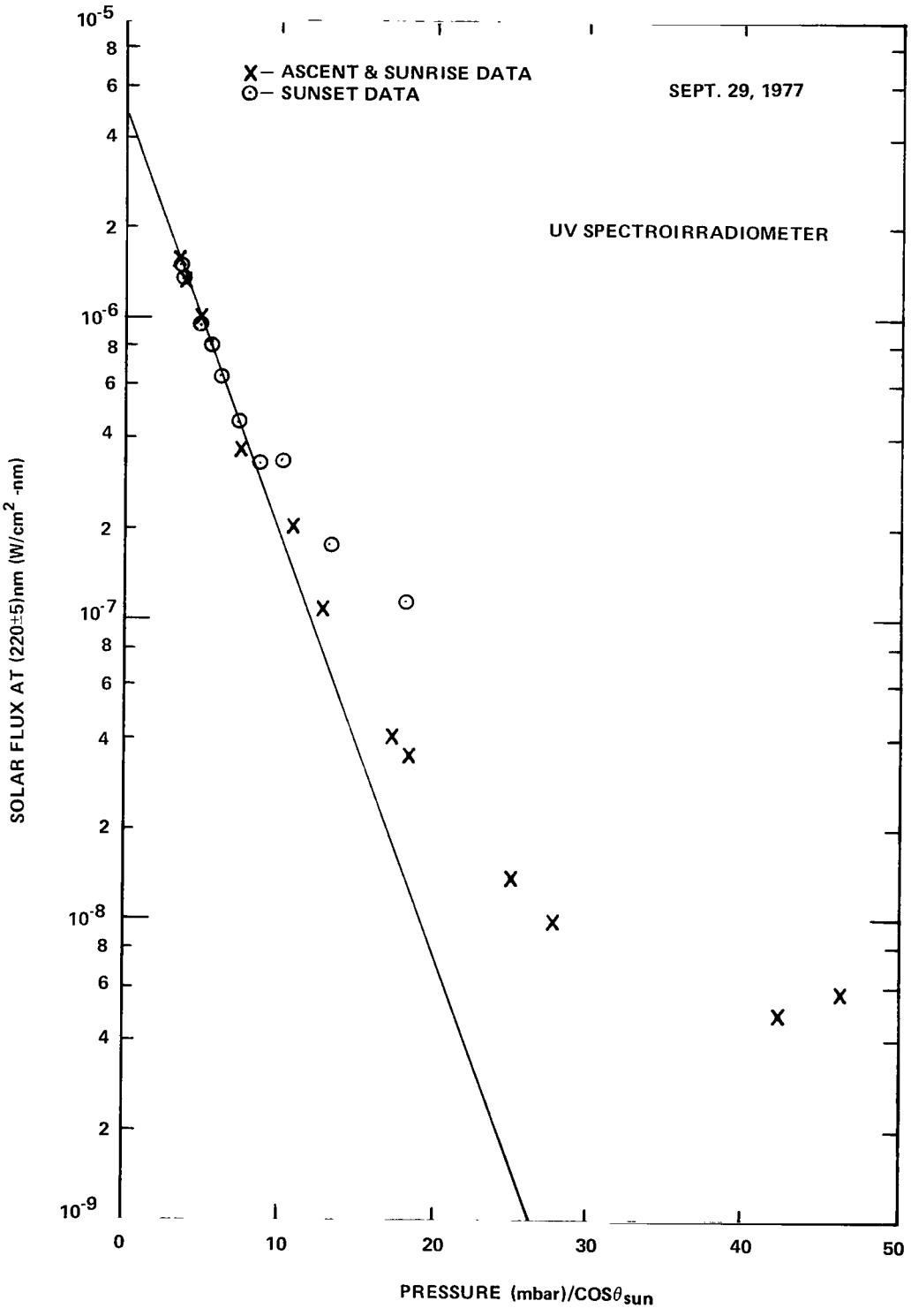

Figure 6. Plot of UVS measured 220-nm solar flux versus attenuation path length in atmosphere.

Table 2
Solar Flux at 220 nm vs. Solar Activity

Solar Flux at 220 nm (±5 nm) [W/(cm^2 - nm)]	Zurich Sunspot Number	Ottawa 2800 MHz Solar Flux [10^{-22}W/(m^2 - Hz)]	Date of measurement MM/DD/YY	Data Source and Comments
4.19 X 10^{-6}	0	76.8	9/(24-25)/75	Previous Stratcom UVS results,
3.27 X 10^{-6}	18	73.6	9/28/76	Ref. 2
4.39 X 10^{-6}	33	89.5	5/16/73	Avg. for date, Ref. 10
4.53 X 10^{-6}	63	99.4	9/29/77	Stratcom VIII-A
4.91 X 10^{-6}	65	125.2	9/23/72	Avg. for date, Ref. 10
9.16 X 10^{-6}	115	139.5	5/10/68 4/19/69 10/3/69	Data for all dates averaged together, Ref. 11
5.78 X 10^{-6}	168	209.2	6/15/70	Ref. 12

REFERENCES

1. Hanser, F. A., B. Sellers, And J. L. Hunerwadel, Design, Fabrication, and Flight of a UV Spectrophotometer Aboard a WB57F High Altitude Aircraft for the CIAP Flight Series – Summary Report, PANA-UVS-7, Panametrics, Inc., Waltham, Mass., December 1975. (Available as ADA019745 from NTIS, Springfield, Virginia.)

2. Hanser, F. A., B. Sellers, and J. L. Hunerwadel, "Measurement of 200-400 nm Solar UV Fluxes at Altitudes up to 40 km," in Stratospheric Composition Balloon-Borne Experiment 23-26 September 1975, Compiled by H. N. Ballard and F. P. Hudson, ECOM-5830 (October 1977). ADA049030.

3. Sellers, B., F. A. Hanser, and J. L. Hunerwadel, Stratcom VI-A UV Flux and 30-65 km Low Background Betasonde Air Density Measurements, PANA-AIR-1, Panametrics, Inc., Waltham, Mass., July 1976. ADA055772.

4. Hanser, F. A., B. Sellers, and J. L. Hunerwadel, Measurement of 200-400 nm Solar UV Fluxes at Altitudes up to 39 km on the stratcom 7A Balloon Flight, PANA-AIR-3, Panametrics, Inc., Waltham, Mass., September 1977. ADA055774.

5. Sellers, B., F. A. Hanser, and J. L. Hunerwadel, UV Spectroirradiometer Measurements of Solar UV Fluxes on the Stratcom VIII-A Balloon Flight, PANA-AIR-4, Panametrics, Inc., Waltham, Mass., June 1978. ADA055775.

6. Johnston, H. S., and R. Graham, "Photochemistry of NO_x and HNO_x Compounds," *Can. J. Chem.*, **52**, 1974, pp. 1415-1424.

7. Sellers, B., and F. A. Hanser, "Measurement of Tropospheric 300 nm Solar Ultraviolet Flux for Determination of $O(^1D)$ Photoproduction Rates," *J. Atm. Sci.*, **35**, 1978, pp. 912-918.

8. Hanser, F. A., B. Sellers and D. C. Briehl, "UV Spectrophotometer for Measuring Columnar Atmospheric Ozone from Aircraft," *Appl. Optics*, **17**, 1978, pp. 1649-1656.

9. Solar-Geophysical Data, issued monthly by U.S. Department of Commerce, NOAA, Environmental Data Service, Boulder, Colorado.

10. Simon, P., "Balloon Measurements of Solar Fluxes between 1960 Å and 2300 Å," in Proceedings of the Third Conference on the Climatic Impact Assessment Program, A. J. Broderick and T. M. Hard, Editors, DOT-TSC-OST-74-15, November 1974, p. 137.

11. Ackerman, M., D. Frimount, and R. Pastiels, "New Ultraviolet Solar Flux Measurements at 2000 A using a Balloon Borne Instrument," in New Techniques in Space Astronomy, Labuhn and Lust, Eds., Reidel, Dordrecht, Holland, 1971, p. 251.

12. Broadfoot, A. L., "The Solar Spectrum 2100-3200 Å," *Astrophys. J.*, **173**, 1972, pp. 681-689.

13. Simon, P. C., "Irradiation Solar Flux Measurements between 120 and 400 nm. Current Position and Future Needs," *Planet. Space Sci.*, **26**, 1978, pp. 355-365.

14. Heath, D. F. and M. P. Thekaekara, "The Solar Spectrum Between 1200 and 3000 Å," in The Solar Output and Its Variation, O. R. White, Ed., Colorado Associated University Press, Boulder, Colorado, pp. 193-212, 1977.

15. Hudson, R. D., Editor, "Chlorofluoromethanes and the Stratosphere," NASA Reference Publication 1010, August 1977.

16. Brewer, A. W., and A. W. Wilson, "Measurements of Solar Ultraviolet Radiation in the Stratosphere," *Quart. J. Roy. Meteor. Soc.*, **91**, 1965, pp. 452-461.

FILTER PHOTOMETER FOR SOLAR FLUX AND UNDERLYING ALBEDO

Rex Megill
Center for Atmospheric and Space Sciences
Utah State University
Logan, Utah 84322

Two pairs of photometers were included in the Stratcom VIII-A payload flown from Holloman Air Force Base, New Mexico, September 29, 1977. One pair of photometers was mounted in the main gondola of Balloon VIII-A, and the other pair was in parachute dropsonde no. 1. These measurements of direct solar flux and of underlying albedo are to be used in the computation of J-values and to determine the usefulness of these simple filter techniques for the determination of ozone overburdens.

INSTRUMENT

The four-channel photometers have filters at nominal values of 292.5 nm, 297.5 nm, and 300.0 nm for the measurement of the direct solar flux, and values of 300.0 nm, 350.0 nm, 400.0 nm, and 450.0 nm for the measurement of the underlying albedo. Each has a flat plate diffuser to provide a wide field of view. The solar flux photometer points to the zenith; the photometer for underlying albedo points in the nadir direction.

RESULTS

Data are available for the pair of photometers that was mounted on the gondola of the Stratcom VIII-A balloon. Since data were not recorded by the dropsonde no. 1 system, nothing will be available from the pair that was on that package. Analysis of the gondola photometer data is underway.

ULTRAVIOLET SPECTROMETER FOR SCATTERED LIGHT

Kay D. Baker and Larry Jensen
Center for Atmospheric and Space Sciences
Utah State University
Logan, Utah 84322

An ultraviolet spectrometer observed scattered light in the 200-nm to 310-nm range, scanning between zenith and horizon. The observations were made on September 29, 1977, from the Stratcom VIII-A Balloon near Holloman Air Force Base, New Mexico.

INSTRUMENT

The instrument package with its associated Sun sensor is shown in Figure 1. The spectrometer measures the light scattered from the atmosphere in the wavelength region from 200 nm to 310 nm with a resolution of about 0.3 nm. The mirror at the entrance to the spectrometer scans the sky from zenith to horizon and back, at an azimuth fixed with respect to the payload structure. The Sun sensor is used to determine the location of the spectrometer's field of view relative to the Sun.

RESULTS

The instrument observed the sky throughout the day. For about 2 hours during the float portion of the flight, the wavelength range of the spectrometer shifted (inadvertently) to longer wavelengths, limited to about 400 nm by the response of the detector, making possible a determination of the scattered light component over the entire 200-nm to 400-nm region. Analysis of the data is underway.

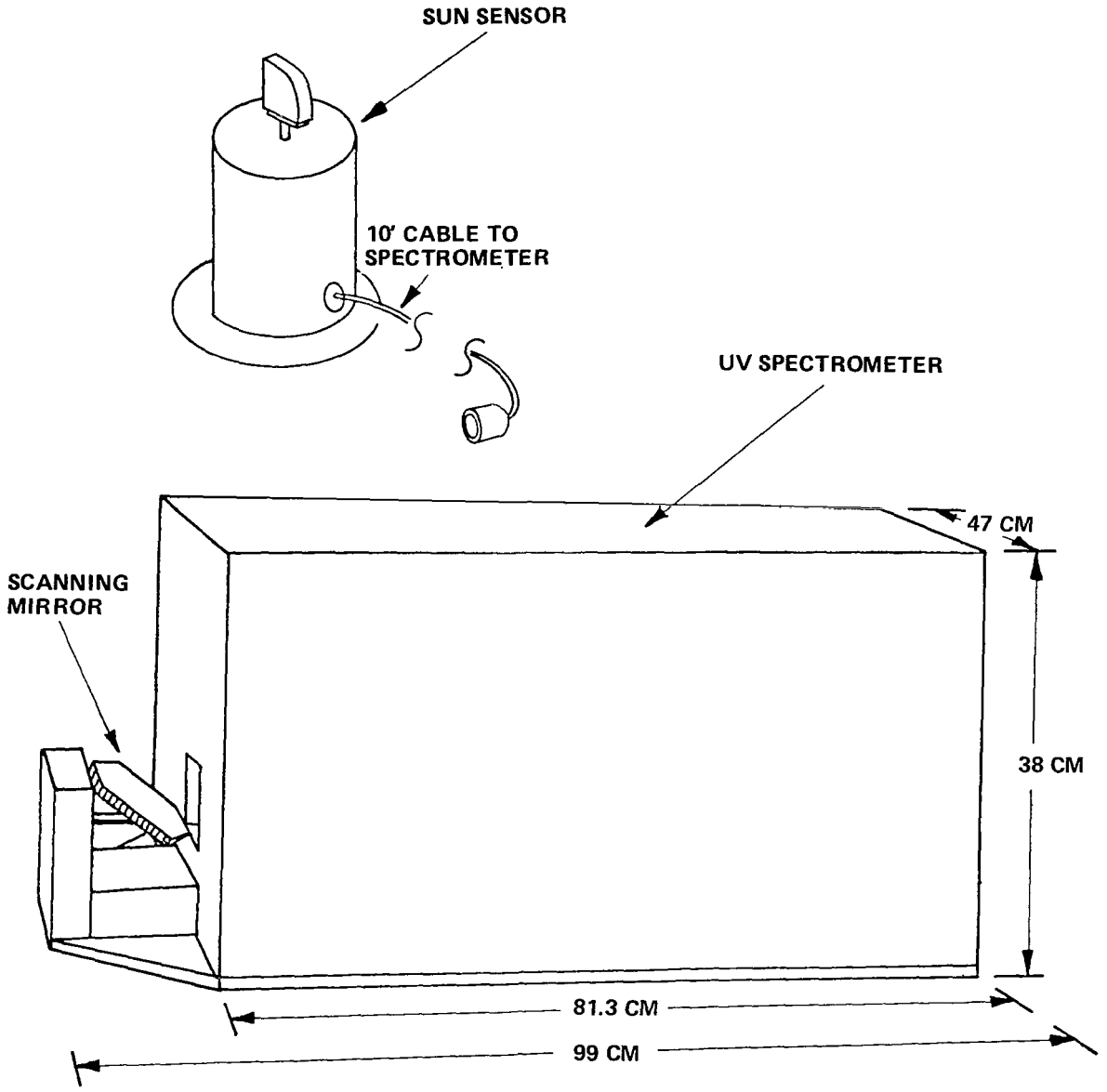

Figure 1. Spectrometer package for scattered solar ultraviolet radiation.

INFRARED SOLAR ABSORPTION MEASUREMENTS

David G. Murcray, Frank H. Murcray, John J. Kosters,
Aaron Goldman and W. John Williams
Department of Physics
University of Denver
Denver, Colorado 80208

INTRODUCTION

Solar absorption spectra in the 4.9- to 6.2-μm and 6.5- to 8.3-μm regions were measured during sunset from the Stratcom VIII-B Balloon, at an altitude of 39 km, September 28, 1977, near the Holloman Air Force Base, New Mexico. The wavelength regions were chosen to include useful absorption lines related to the oxides of nitrogen. Sunset absorption spectra in these regions should provide altitude profiles of NO, N_2O, HNO_3, O_3, H_2O, CH_4, and possibly on CF_2Cl_2, and $ClONO_2$.

INSTRUMENT

The two-channel 1¼-m Czerny-Turner infrared grating spectrometer with a solar pointing system was used. The payload included digital tape recorders as well as a telemetry system for backup recording of the data at a ground station.

RESULTS

The balloon, launched at 1251 MST, ascended at an average rate of approximately 250 m/min and arrived at a float altitude near 39 km at 1531 MST. The balloon remained at this altitude through sunset and the flight was terminated an hour later.

Solar absorption spectra in the 4.9- to 8.2-μm region were obtained continuously during ascent and through sunset on the balloon. The spectral resolution of these data should be between 0.1 and 0.15 cm^{-1}. Spectral scans were obtained once every 3 minutes during sunset until the tangent path was well into the troposphere. The balloon position at this time was 106°55′ longitude, 33°12′ latitude and the solar azimuth was approximately 270°.

The recovery of the Stratcom VIII-B payload was not successful. Therefore, it has been necessary to use the PCM telemetry for data reduction. Several minor difficulties with this process have delayed the reduction of the spectral data. Preliminary reduction of the sunset data indicate slightly higher noise than anticipated but all the spectral data are intact. Emphasis will continue on the sunset data and altitude profiles from 20 to 39 km will be calculated for HNO_3, N_2O, CH_4, H_2O, O_3, and probably NO_2. Due to the noise problem, NO and $ClONO_2$ will probably be evaluated as upper limits.

INFRARED EMISSION MEASUREMENTS OF NITRIC ACID AND OTHER CONSTITUENTS

David G. Murcray and D. Boyd Barker
Department of Physics
University of Denver
Denver, Colorado 80208

The Denver University Infrared Spectrometer (DUIRS) was mounted in the right wing pod of the U-2 aircraft that underflew Stratcom VIII-A and VIII-B Balloons on September 28 and 29, 1977, near Holloman Air Force Base, New Mexico. The spectrometer measured molecular radiation (thermal emission) from the atmosphere. The objective was to use the data in determining the overburden of various constituents (HNO_3, CH_4, O_3, N_2O, $CFCl_3$ (F-11), CF_2Cl_2 (F-12), etc.). These calculations involve recorded signal strengths, blackbody calibrations and molecular parameters.

A simultaneous flight of instruments on the Stratcom VIII-B Balloon would provide correlated measurements of certain spectral regions. The U-2 and Balloon VIII-B data analysis should make possible an improvement in the interpretation of the thermal emission spectral data.

INSTRUMENTATION

The liquid-helium-cooled spectral radiometer is mounted in the right wing pod of the U-2 looking at right angles to the flight path and 13 degrees above the horizon with a field of view of 1° vertical and 4° horizontal. Radiation enters through a zinc selenide window, is scanned by a grating spectrometer, and imaged through a beam splitter onto two copper-doped germanium detectors covering the 3- to 7-μm and 6- to 14-μm spectral regions. Scans, 42 seconds in length, with a resolution of 2 cm^{-1} are taken continuously during each flight with all data recorded on a digital tape recorder for subsequent analysis. The U-2 with this instrument underflew the Stratcom VIII-B Balloon on the afternoon of September 28, 1977, and the Stratcom VIII-A Balloon on the morning of September 29. No data were obtained on the September 28 flight, because of a malfunctioning helium vent line which depleted the supply of liquid helium about an hour after the U-2 departed from Moffett Field, California.

Significant data were recorded throughout the Stratcom VIII-A flight on September 29. The HNO_3 data are shown in Figure 1 together with data from other flights of this instrument over a wide range of latitude. The average column number density of HNO_3 measured when the aircraft flew near the vicinity of the VIII-A Balloon was

$$9.63\ (10^{19})\ \text{molecules/m}^2 \text{ at } 18.3\ \text{km}$$

$6.05\ (10^{19})$ molecules/m^2 at 21.3 km

The more difficult data reduction for CH_4, O_3, and N_2O is in progress and will be reported on at a later date.

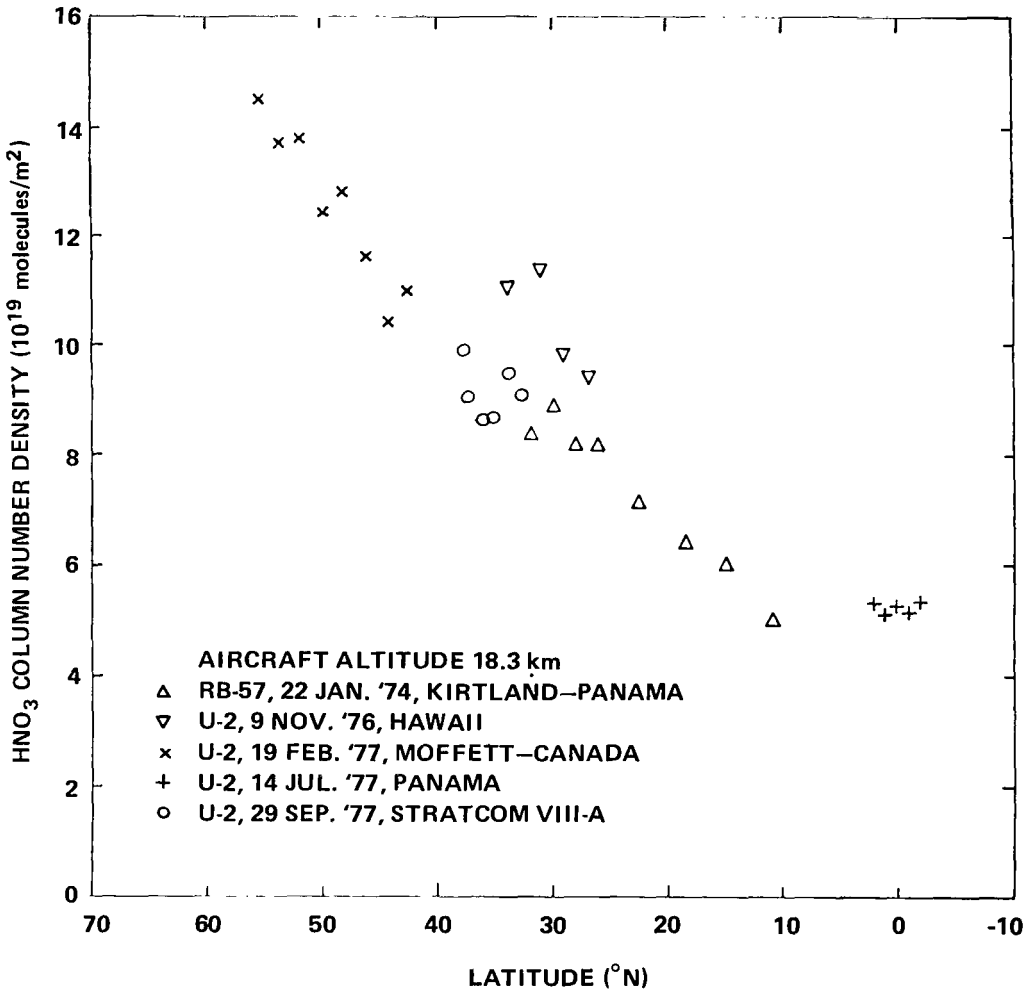

Figure 1. HNO_3 column number density versus latitude.

CARBON DIOXIDE RADIANT TEMPERATURE MEASUREMENTS

Frank H. Murcray and David G. Murcray
Department of Physics
University of Denver
Denver, Colorado 80208

Don Snider
Atmospheric Sciences Laboratory
U.S. Army Electronics Command
White Sands Missile Range
New Mexico 88002

Robert McClatchey
Air Force Geophysics Laboratory
Hanscom Air Force Base
Massachusetts 01731

ABSTRACT

A pair of infrared radiometers pointing near the horizon were flown to aid in the development of suitable algorithms for the interpretation of CO_2 infrared radiance data in the stratosphere. They were included on the Stratcom VIII-B Balloon flown September 28, 1977, near Holloman Air Force Base, New Mexico. The radiances from the 15 μm instrument are compared to those inferred from air temperatures measured by several rawinsondes flown during the same period.

INTRODUCTION

Observations of the spectral distribution of the radiances in the infrared CO_2 bands have been used for a number of years for remote measurements of air temperatures in the troposphere and stratosphere. The observational and inversion techniques are reasonably well established for tropospheric altitudes, but become increasingly uncertain above the tropopause. To obtain further insight into this problem, a pair of infrared radiometers were included on the Stratcom VIII-B Balloon payload, flown September 28, 1977, from Holloman Air Force Base, New Mexico, to an altitude of 39 km. Radiance data from these instruments are compared with the air temperature profiles obtained from rawinsondes and rocketsondes.

To make the interpretation of the data as unambiguous as possible, the spectral regions of the two radiometers were chosen to correspond to the "blackest" part of the 4.3-μm and the 15-μm CO_2

bands. Since the horizontal temperature gradients are much smaller than the vertical temperature gradients, the radiometers were pointed toward the horizon rather than in the vertical or nadir. Thus the radiation entering the radiometers was from a layer that is more nearly uniform in temperature, and would require a less complex inversion algorithm to infer an atmospheric temperature profile. In its simplest form, the radiance measured by the filter radiometers is related directly to the atmospheric local thermodynamic equilibrium temperature through the Planck blackbody function.

Information pertaining to the flight of these radiometers is reported in Reference 1; the remainder of this chapter is based on that report.

FLIGHT DATA

For the Stratcom VIII-B payload, the 4.3 μm radiometer was equipped with a filter centered at 2362 cm^{-1} with a 16 cm^{-1} bandwidth. The 15 μm radiometer used a 3.5 cm^{-1} filter centered at 682.3 cm^{-1}. Launch of the instrumentation was at 1257 MST on September 28, 1977 from Holloman Air Force Base, New Mexico, and the unit reached its float altitude of 39 km by 1500 MST. Unfortunately, the payload was destroyed in a free-fall because of a parachute malfunction. Primary data recording was to have been by means of an on-board digital magnetic tape recording system, backed up by a PCM telemetry system. Since the payload was destroyed, data reduction had to be accomplished using the telemetered data. The 15 μm unit functioned well throughout the flight. The 4.3 μm unit apparently malfunctioned shortly after launch. Data from the 15 μm unit was recorded from about the 400 mb level through float altitude. The high gain data did not come on scale until the 300 mb pressure level was reached. Samples of the low gain data are available from the telemetry data; however, since primary interest is on the higher altitude data, reduction of the low gain data has been postponed.

The telemetry data was transmitted in 10-bit PCM format. The data channels were decoded and converted to analog outputs and fed to a chart recorder for real-time viewing. It was necessary, however, to computer-process a tape recording of the original PCM in order to maintain the original 10-bit accuracy of the telemetry. Once this was done, radiance values were generated by converting the 10-bit words to the equivalent voltages and then multiplying the voltages by a factor derived from averaging the slope dN/dV of the four calibration plots.

Experience has shown that temperatures measured by rawinsondes attached to payloads of large polyethylene balloons are usually in error, with the errors amounting to several degrees. Presumably this error is due to the fact that the lower ascent rates and large envelopes of these balloons do not provide proper convective flow.

The Atmospheric Sciences Laboratory at White Sands Missile Range has developed a technique for measuring local atmospheric temperatures from large balloon payloads that overcomes most of the problems encountered with the conventional rawinsonde. This type of apparatus was flown as part of the payload for this flight. However, the data output from this ASL sensor was not entirely

compatible with the PCM telemetry, so a considerable amount of effort was required to reconstruct the instrument output from the PCM data. In addition, the ASL sensors depend on rotation of the gondola to provide a correction for solar input. Since the gondola during this flight was azimuth-stabilized, the usefulness of the ASL data is not clear at this time.

Rawinsonde temperatures for comparison with radiance data were, therefore, obtained from standard rawinsonde ascents made in conjunction with the flight. In addition, rawinsonde runs from several sites surrounding the Holloman Air Force Base area have been collected. The major advantage of an on-board rawinsonde would have been a more exact altitude registration for comparison of the profiles. Since this was not available, the radiance values were plotted as a function of pressure as measured by on-board pressure transducers and are shown in Figures 1 and 2. Blackbody radiance values for measured rawinsonde temperatures were plotted on the same scale as a function of pressure. These curves are shown in Figures 3 and 4, which represent the radiance inferred from a rawinsonde released at 0900 MST from Holloman Air Force Base. Similarly, Figures 5 and 6 show rawinsonde data from Holloman Air Force Base at 1300 MST and 2100 MST, and from White Sands Missile Range at 1250 MST. Figures 7 and 8 present the 1750 MST significant level rawinsonde data from several sites in the southwest.

DATA ANALYSIS

In comparing the radiance values at a given pressure, one must keep in mind the sensitivity of the 15 μm radiance to temperature in the range represented by these plots. At 240 K a temperature change of 1 degree represents a change 5.1 $\mu w\ cm^{-2}\ sr^{-1}\ \mu m^{-1}$ in the 15 μm radiance of a blackbody.

Comparison of the radiometer data, Figures 1 and 2, with the HAFB rawinsonde released at 0900 MST, Figures 3 and 4, shows excellent agreement in the 300-200 mb range. In fact, on the average, the agreement is within the 0.1 degree to which the rawinsonde temperatures are given. Although there are fine structure differences of several tenths of a degree, it is tempting to cite the good agreement and consider both sets of data validated. However, through this same altitude region, a WSMR rawinsonde launched at 1250 MST shows considerable (1 to 2 degrees) departure from the 0900 MST HAFB rawinsonde and, to a lesser extent, from the HAFB rawinsonde launched at 1300 MST less than 15 miles away, Figures 5 and 6. On the other hand, a rawinsonde launched at 2100 MST from HAFB shows excellent agreement with both the 0900 MST and the radiometric data.

The data from the three HAFB runs tends to converge in the 200-120 mb region where the temperature spread is considerably less than 1 degree. The radiometer data lies within the spread of these three runs. All the runs show large divergence through the 120-80 mb regions, even discounting the large "lump" in the 2100 MST run. Unfortunately, the radiometer data through this region may show the influence of increased atmospheric transmission within the filter bandpass. Some fraction of the radiation emitted from higher, warmer layers may be reaching the altitude of the balloon payload (the radiometer unit was looking up at a 20° angle). By 60 mb the atmospheric path has obviously become partially transparent, even for the total remaining path, since the radiance level begins to decrease with altitude although the temperature continues to increase.

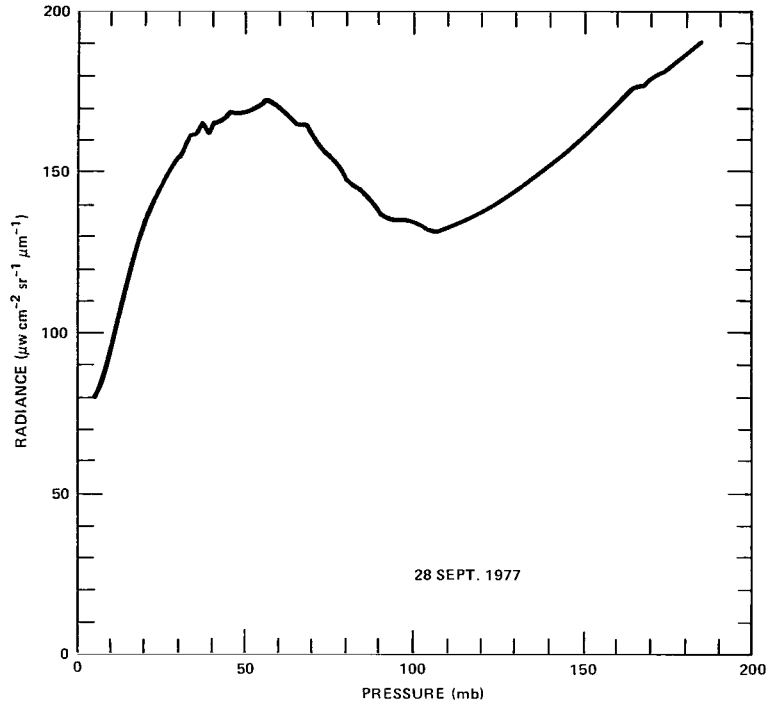

Figure 1. Radiance vs pressure as measured by on-board pressure transducers during the September 28, 1977 flight from Holloman AFB, New Mexico.

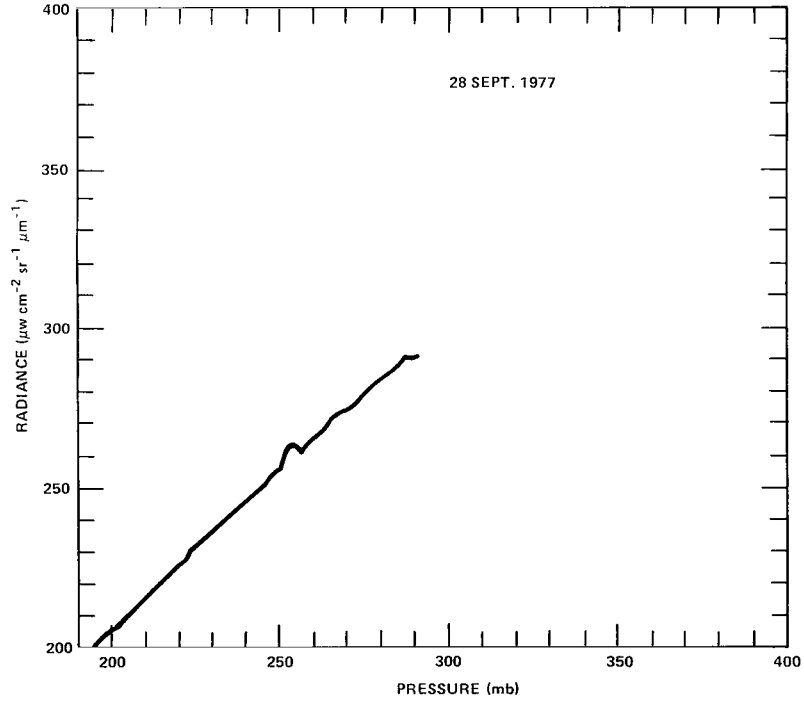

Figure 2. Radiance vs pressure as measured by on-board pressure transducers during the September 28, 1977 flight from Holloman AFB, New Mexico.

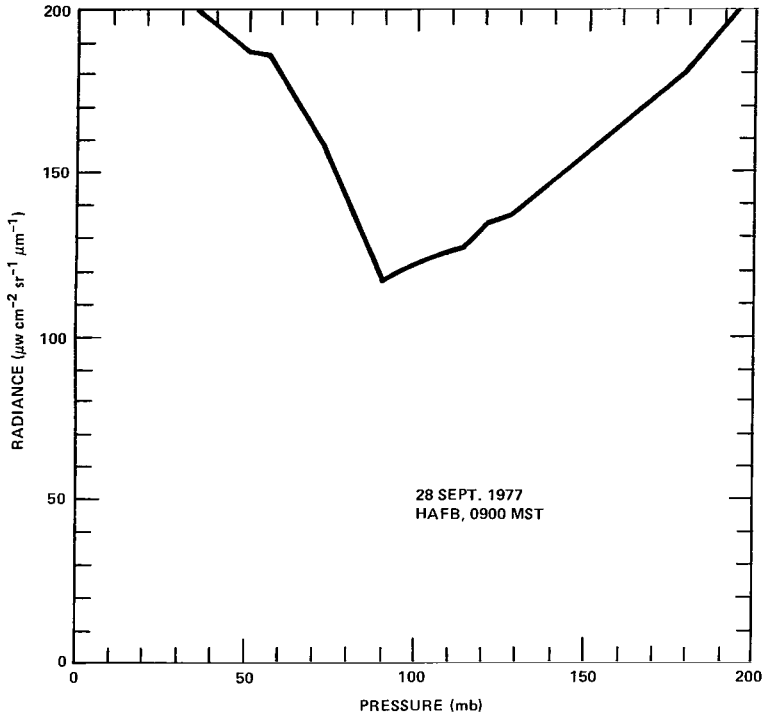

Figure 3. Blackbody radiance values for temperatures measured by Holloman AFB rawinsonde vs pressure obtained by on-board pressure transducers.

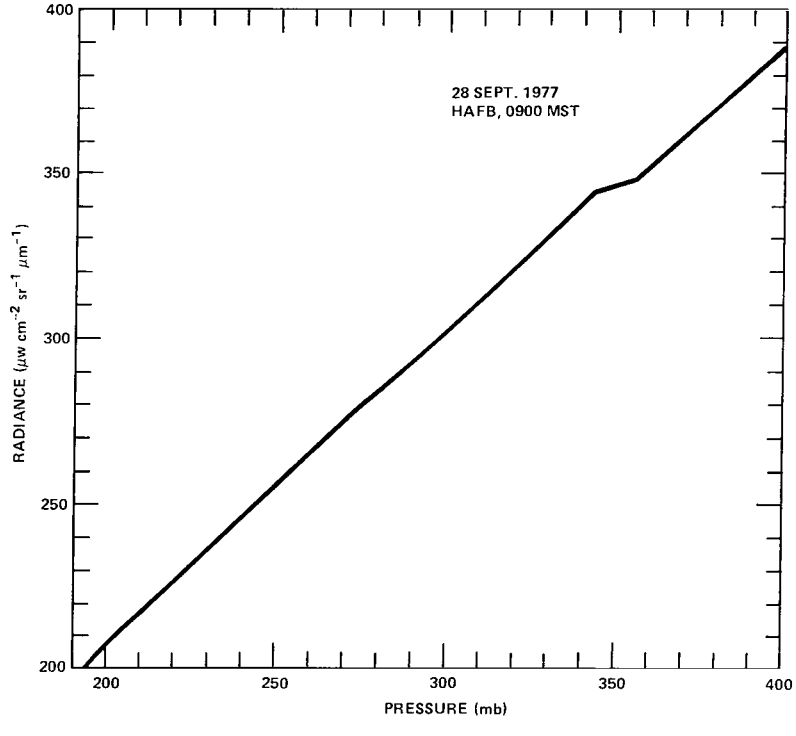

Figure 4. Blackbody radiance values for temperatures measured by Holloman AFB rawinsonde vs pressure obtained by on-board pressure transducers.

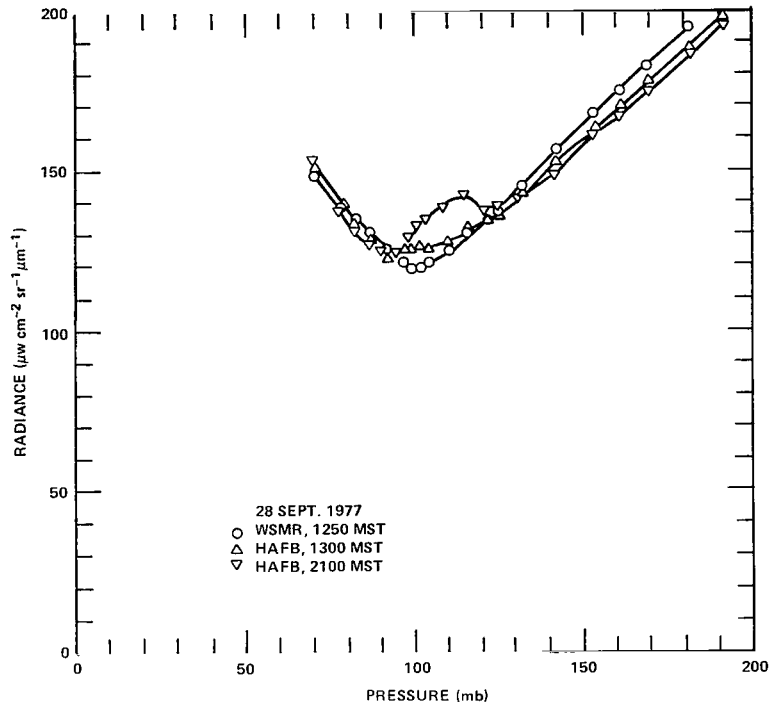

Figure 5. Rawinsonde data for September 28, 1977, from Holloman AFB and White Sands Missile Range.

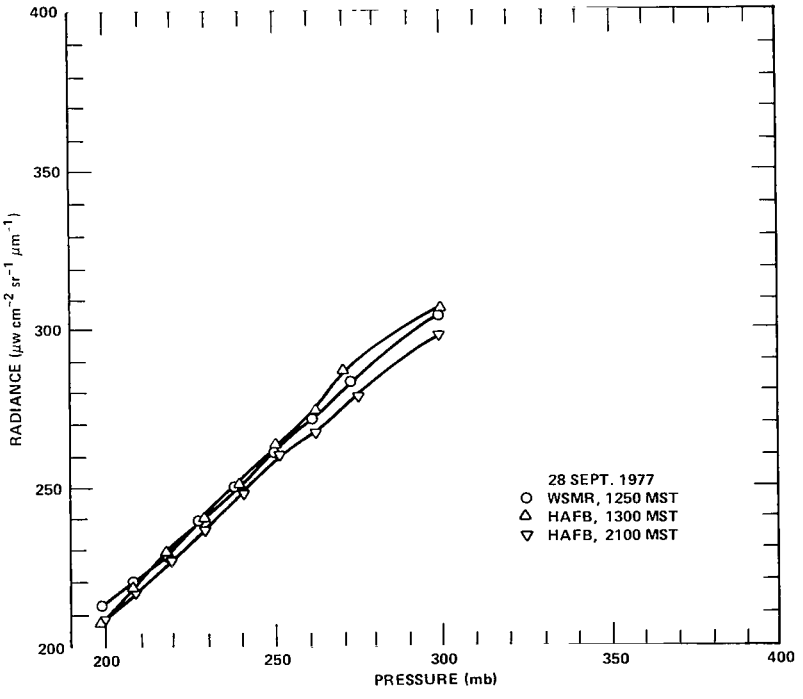

Figure 6. Rawinsonde data for September 28, 1977, from Holloman AFB and White Sands Missile Range.

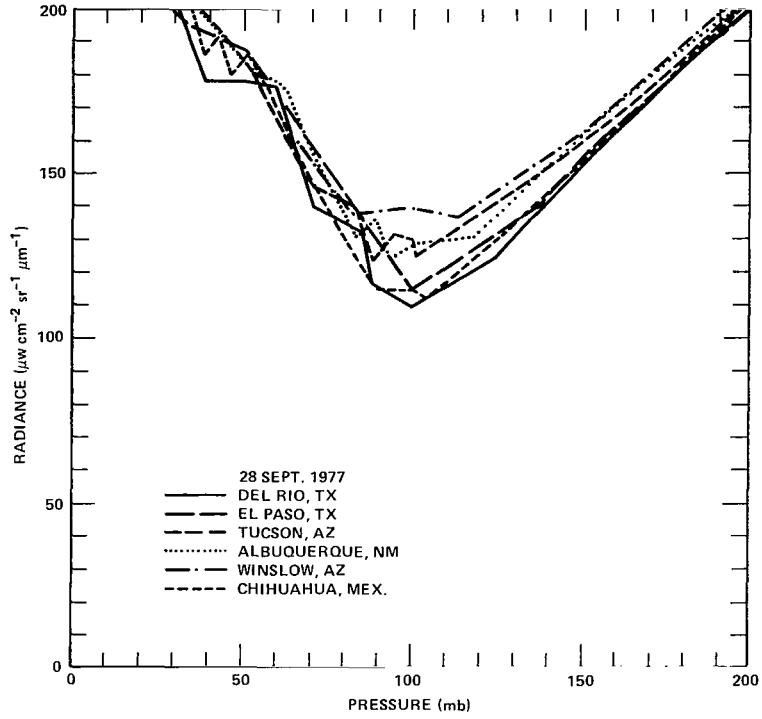

Figure 7. Rawinsonde data for September 28, 1977, at 1750 MST from various sites in the southwest.

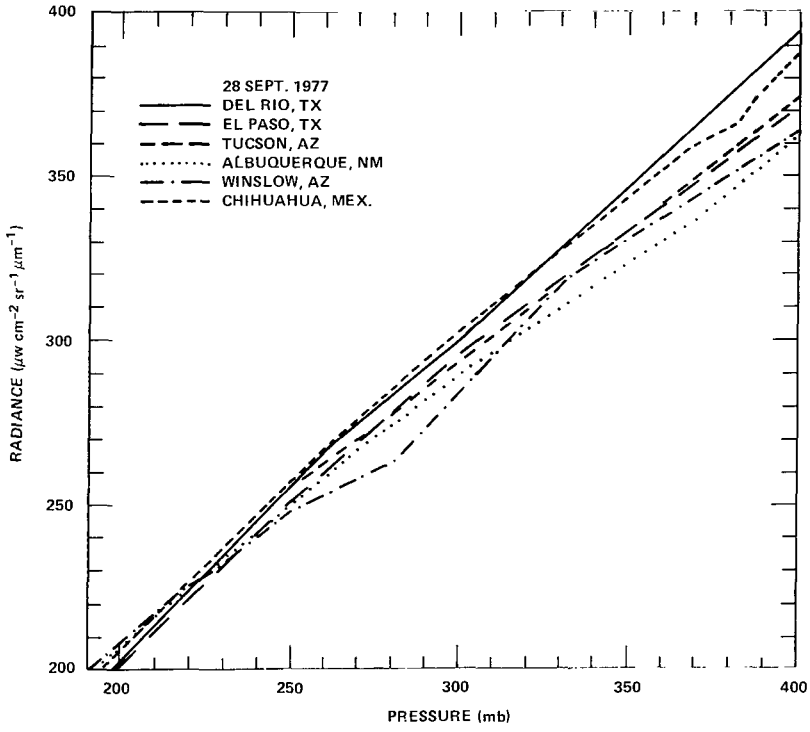

Figure 8. Rawinsonde data for September 28, 1977, at 1750 MST from various sites in the southwest.

The temperature structure above the 100 mb region is still calculable, but the calculation becomes less precise and changes from a simple operation with a hand calculator to a complex problem requiring large computer capacity. These computations are to be performed, but are not completed at this time.

The altitude for which the simple Planck function calculation would be sufficient could be extended by working in a wavelength region where the CO_2 absorbs more strongly, or by using a more nearly horizontal field-of-view for the instrument. The first of these was intended with the 4.3 μm radiometer, but was negated by the instrument failure. The second was not practical for this flight because the upward look-angle is necessary for the prevention of window frost at the lower altitudes. Future flights will include a mechanism for rotating the look-angle towards the horizon at the high altitudes.

ERROR ANALYSIS

The random noise level of the radiometer signal was below the least count of the PCM A to D converter, and therefore, the quantization noise of the PCM encoder ($\pm$ 1/1023) dominates the random component of the error in the radiometer signal. The pressures for the radiometric data were taken from three on-board pressure transducers covering the range from 1000-0 mb. A partial check on the validity of the indicated pressures was made by comparing the outputs in the short ranges where the transducer useful ranges overlap. Agreement within $\pm$1 mb was found. Since the authors are not familiar with the accuracy of the standard rawinsonde pressure readings, they have been used exactly as reported.

The accuracy of the radiometric data is primarily a question of the accuracy of the calibration. Errors in the calibration procedure can be produced by blackbody emissivity too far from unity, errors in the measurement of blackbody temperature, and temperature gradients within the blackbody. The calibration procedure used was designed to minimize these effects or, at least, to reveal their presence at a significant level. For each calibration run, the blackbody was cooled until the copper rod from which it was machined was immersed in liquid nitrogran and the temperature sensor checked against the boiling point of liquid nitrogen for the ambient pressure. For the CO_2 experiment the radiance level at this temperature was too low to produce a measurable output. With the blackbody emission at this low level an appreciable deviation of the source from unit emissivity would be revealed by a residual signal, due to reflectance of radiation from the comparatively warm baffles. A reflectivity of 0.003 or less would show up under these conditions.

After the liquid nitrogen evaporates and the cavity begins to warm, voltages are obtained at about 5 K intervals over the temperature range, resulting in approximately 40 output voltage vs. radiance points per run. Plots of these points exhibit excellent linearity. Typically, the maximum departures of individual points from the best straight line do not exceed 2 percent of the reading. The slope of the best straight line is computed and used as the calibration coefficient for reduction of the data. The calibration coefficient utilized for reduction of the flight data was actually the average of the slopes of four runs, none of which deviated from the mean by more than $\pm$0.5 percent.

The linearity of the output with radiance over a signal range approaching three orders of magnitude provides good evidence as to the lack of gradient effects on temperature measurement errors, since neither of these is likely to remain constant over the wide temperature range of the calibration. In short, the systematic error in the radiance measurements should not be as large as 1 percent.

SUMMARY AND CONCLUSIONS

The radiometer data agree (to better than 0.5 K) over fairly extensive altitude ranges with each of three rawinsondes launched from Holloman Air Force Base at 0900, 1300 and 2100 MST. However, the agreement with each one does not hold throughout the 300–120 mb range.

Since the major possible source of error in the radiometric data is in the calibration constant, one would expect consistent differences with the rawinsonde runs. The agreement with portions of the various rawinsondes, particularly where two or more agree strongly, suggests that the radiometric data is valid throughout the 300–120 mb, but that an individual rawinsonde sounding may be in error by as much as 2 K or more for portions or all of the ascent.

REFERENCE

1. Murcray, D. G., F. H. Murcray, F. J. Murcray, and W. J. Williams, "Infrared Background Measurements", *Quarterly Progress Report*, University of Denver, AFGL Contract F19628-77-C-0016, April 1978. AFGL-TR-78-0249.

MEASUREMENT OF RADIATION ENERGY TRANSFER

Robert Rubio
Atmospheric Sciences Laboratory
U.S. Army Electronics Command
White Sands Missile Range
New Mexico 88002

Carlos McDonald and Miguel Izquierdo
Department of Electrical Engineering
University of Texas at El Paso
El Paso, Texas 79968

ABSTRACT

Pyranometers were used to measure solar shortwave and terrestrial infrared irradiance from the Stratcom VIII-A Balloon, and to measure solar shortwave irradiance from ground level. These data are needed for study of the transformation of radiative energy within the Earth's atmosphere as a function of other atmospheric parameters. The data were taken in the vicinity of the Holloman Air Force Base, New Mexico, on September 29-30, 1977.

INTRODUCTION

The ultimate objective of this experiment is to measure the amount of radiative energy transformed within the Earth's atmosphere's heat budget as a function of other atmospheric parameters such as O_3, H_2O, CO_2, and air density. A secondary objective is to simultaneously determine Earth albedo at balloon altitudes and near the Earth's surface. By measuring the impinging solar shortwave irradiance, the corresponding shortwave irradiance reflected by the Earth and atmosphere, and the longwave infrared irradiance escaping towards space on two successive cloudless days, the above objectives may be accomplished. Although two complete sets of irradiance data satisfying all the aforementioned requirements have not yet been obtained, progress toward that goal has been made and is the subject of this report.

METHOD

To determine the Earth's atmosphere's heat budget, two 0.28- to 2.8-μm pyranometers and one 4- to 50-μm Epply pyranometer were included in the Stratcom VIII-A payloads. Two additional shortwave pyranometers were operated at ground level. The experimental arrangement of the five pyranometers is depicted in Figure 1 in juxtaposition with a mean annual heat budget for the whole

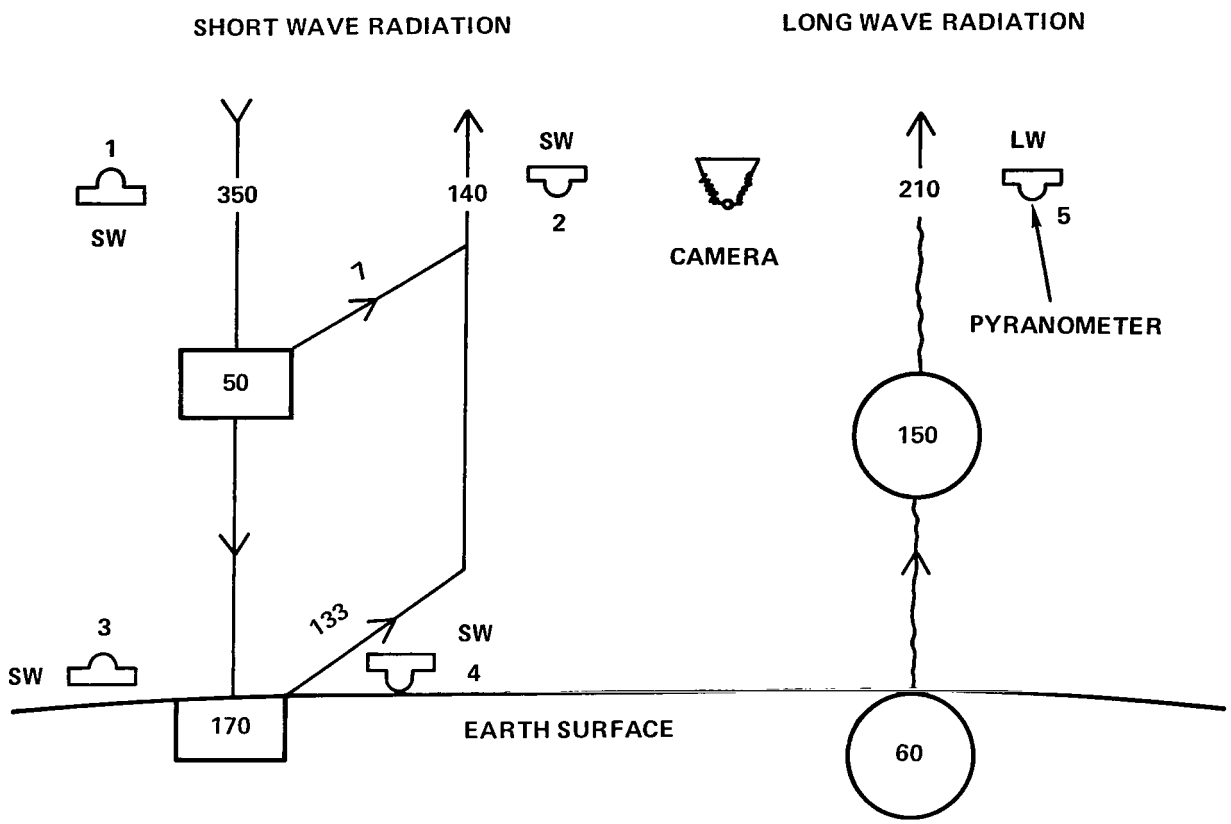

Figure 1. Arrangement of the pyranometers with estimates of the corresponding components of the mean annual heat budget (Wm^{-2}).

Earth as depicted by G. D. Robinson (Reference 1). Pyranometer 1 was mounted on the balloon's top plate and used to measure incoming solar flux while pyranometers 2 and 5 were located on the main instrumentation platform facing downward. Sensors 2 and 5, respectively, measured the total shortwave irradiance escaping into space and the total outgoing longwave irradiance. Pyranometers 3 and 4 were unobstructively located 1.52 m above the desert floor and used to measure the shortwave irradiance impinging on the ground and the amount of ground reflected radiation. As is illustrated in Figure 1, this arrangement of pyranometers will provide a measurement of those energy magnitudes entered in Robinson's diagram. For example, the radiation energy difference recorded with pyranometers 1 and 3 provide a measure of the amount of incoming radiation attenuated by the intervening atmosphere, while pyranometers 2 and 4 yield the same information about outgoing shortwave energy. These energy differences may be examined for quantitative dependence on atmospheric density, H_2O, CO_2, and O_3, provided the sky is devoid of clouds. Consequently, a Nikon camera, also illustrated in Figure 1, was attached to the main payload facing downward in order to detect the presence of clouds and photograph the terrain's reflective features. The combinations of pyranometers 1–2 and 3–4 should yield a measure of the Earth's albedo at balloon altitudes and at ground level.

INSTRUMENTATION

The shortwave radiometers are Epply Precision Spectral Pyranometers (Epply Laboratory, Inc., 12 Sheffield Ave., Newport RI), Model PSP, each with two concentric dome light filters which provide a 180° field of view and a wavelength transparency of 0.28 to 2.8 μm. The actual sensor comprises a circular multifunction thermopile with a sensitivity in the order of 11 μv/(W m^{-2}) and a 1-second time response. The expected performance accuracy of 8.5 percent for the zenith viewing PSP pyranometer is based on manufacturer specifications, payload calibration, and accounts for solar zenith angle variations caused by Top Package (balloon) wobble during the flight. The nadir viewing PSP instrument performance accuracy was calculated to be 2.5 percent. An Epply Precision Infrared Radiometer (Pyrgeometer) with a 180° field of view and a wavelength transparency of 4 to 50 μm was the longwave radiation sensor. This pyranometer also has a thermopile detector, but its sensitivity is approximately 7.2 μV/(W m^{-2}) and its time response is 2 seconds. An overall expected performance accuracy of 3 percent was computed for this instrument and its associated electronics. The camera is a Nikon, model F2AS, with a DS-1 automatic aperture control. The lens was a Nikor 16-mm full frame fisheye providing a 170° viewing angle. Photographs were synchronized for exposure to occur at the beginning of each pyranometer data sample and was keyed to the telemetry clock such that the time between exposures was about 5 minutes.

ANALYSIS

Incoming shortwave radiation data at balloon altitudes was obtained for a period of approximately 3-1/2 hours on the morning of September 29, 1977, from the pyranometer on the Top Package on the apex of the balloon. These data, plotted in Figure 2, show that irradiance magnitudes varied from 35.0 W m^{-2} at 0615 to 983 W m^{-2} at 0950 MST. After 0950, the telemetry signal from the balloon's Top Package transmitter diminished and no additional data were collected. The nadir viewing infrared pyranometer, mounted on the balloon's main gondola, provided considerably more data. Upwelling longwave irradiance values were recorded from 0615 MST, September 28, to 0530 MST, September 29. These values are shown in Figure 2 and on an expanded power density ordinate scale in Figure 3. Also included in Figure 3 is a plot of absolute temperatures at balloon altitudes as a function of time. Examination of the infrared irradiance and temperature plots in Figure 3, reveals that this pyranometer sensed primarily the radiation of the atmosphere in the proximity of the radiometer. Longwave irradiance values recorded ranged from 118 to 237 W m^{-2}. Upwelling shortwave irradiance data at balloon altitudes was not acquired because of a payload malfunction throughout the flight.

Nadir viewing photographs, which are not included here, displayed a general absence of clouds throughout the flight except for a very few tenuous cirrus that occurred on the morning of September 29. The terrain features varied from forested terrain when above the Sacramento Mountains to desert-type terrain when above the basin regions.

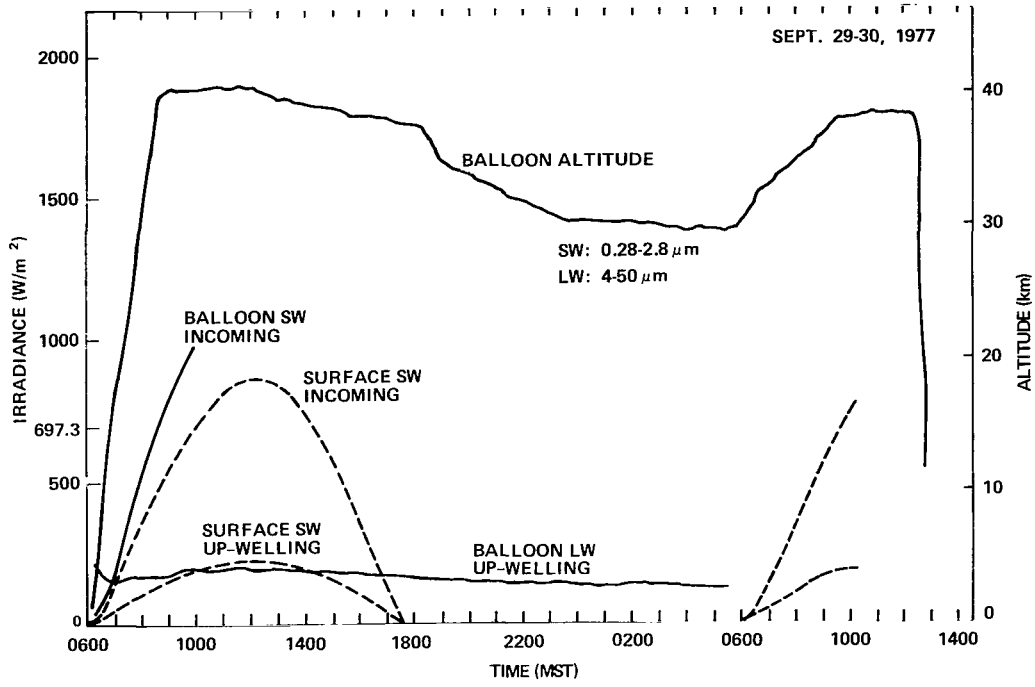

Figure 2. Irradiance data from the four pyranometers. Also shown is the altitude of the two balloon-borne pyranometers.

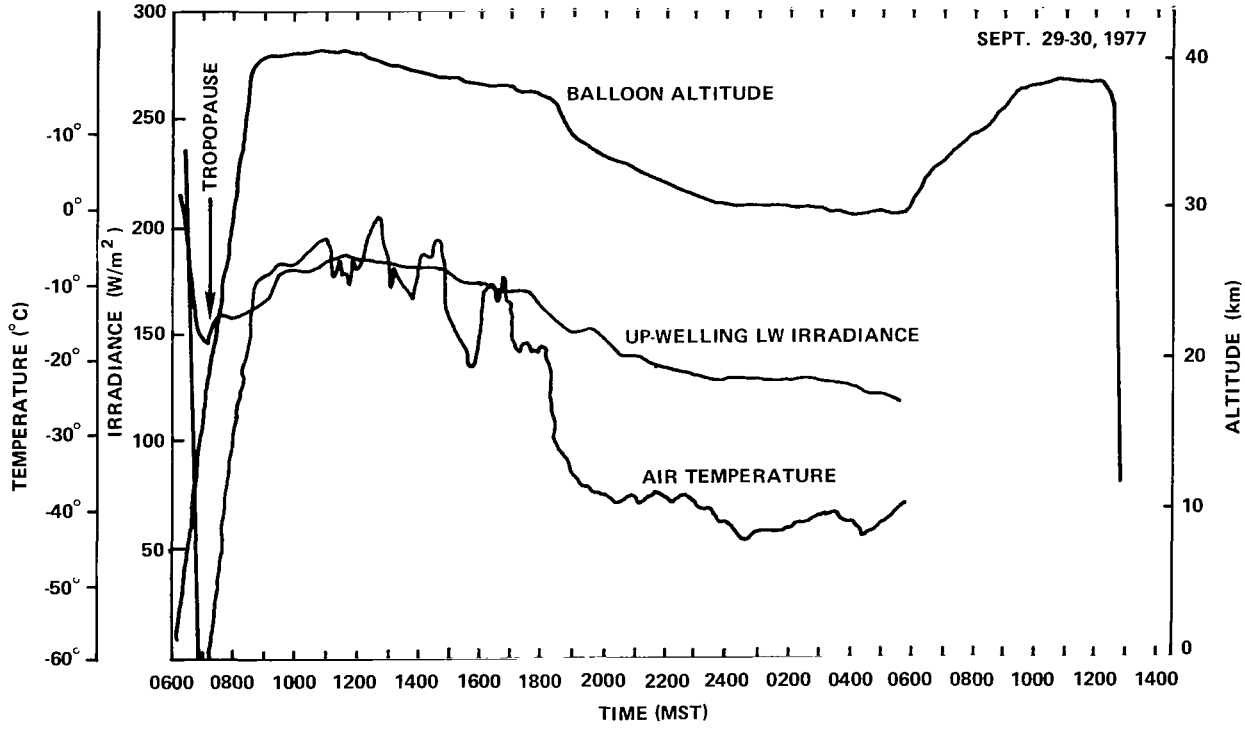

Figure 3. Data from the nadir-pointed pyranometer on the VIII-A Balloon. Also shown are the altitude of the balloon and the air temperature in the vicinity of the gondola.

Surface measurements of both the incoming and the Earth-reflected irradiances were successfully obtained for all daylight hours during which the balloon was aloft. Plots of these surface measurements are also given in Figure 2. The maximum shortwave irradiance impinging upon the Earth was found to be 858 W m^{-2} while the magnitude of the maximum reflected irradiance was 223 W m^{-2}. These magnitudes yield an Earth surface albedo of 0.26 for desert-type terrain. Figure 2 illustrates the shortwave radiation absorbed and reflected by the atmosphere between the balloon altitude and the Earth's surface. For instance, at 0900 MST and an approximate solar zenith angle of 55°, about 265 W m^{-2} were absorbed within the intervening atmosphere. The lack of upwelling shortwave irradiance data precluded calculating Earth's albedo at balloon altitudes and construction of an Earth-atmosphere heat distribution diagram for September 29, 1977 in a fashion similar to Figure 1.

REFERENCE

1. Robinson, G. D., "Some Meteorological Aspects of Radiation and Radiation Measurement," *Advances in Geophysics,* Vol. 14, Academic Press, N. Y., 1970, pp. 285-306.

PHOTOGRAPHS OF EARTH TERRAIN AND CLOUD COVER

Robert Rubio and Claude Tate
U.S. Army Electronics Command
Atmospheric Sciences Laboratory
White Sands Missile Range
New Mexico 88002

A Nikon camera was included in the main payload of the Stratcom VIII-A Balloon launched from Holloman Air Force Base, New Mexico, on September 29, 1977. The camera was used to aid in the interpretation of data from the nadir-viewing pyranometers, by detecting the presence of clouds and photographing the terrain's reflective features and to confirm the orientation as indicated by the magnetometers.

INSTRUMENT

The instrument was a Nikon Model F2AS camera with DS-1 automatic aperture control and a motor-driven film transport MD-11, set at M-1. The lens was a Nikor 16-mm full-frame fisheye, 170° viewing angle pointed at nadir, with speed set 1/125 second. The film used was Kodak Ektachrome MS-64, 250-frame pack, with a frame size of 35 mm square. Exposures were made every 6 minutes and were synchronized with the telemetry sampling of the pyranometers.

An insulated package was designed to house the Nikon camera. The package was insulated with 1 inch of Styrofoam and heated to maintain a minimum temperature of O°C. The package was designed to allow easy installation of the camera at the launch site. A four-bar linkage and a 12-bolt, 1-rpm gear motor were used to position a protective cover over the lens prior to impact. The package configuration and the protective system are shown in Figure 1.

RESULTS

Nadir-viewing photographs displayed a general absence of clouds throughout the flight except for a very few tenuous cirrus clouds that occurred on the morning of September 29. The terrain features varied from the forested areas of the Sacramento Mountains to desert terrain of the basin regions.

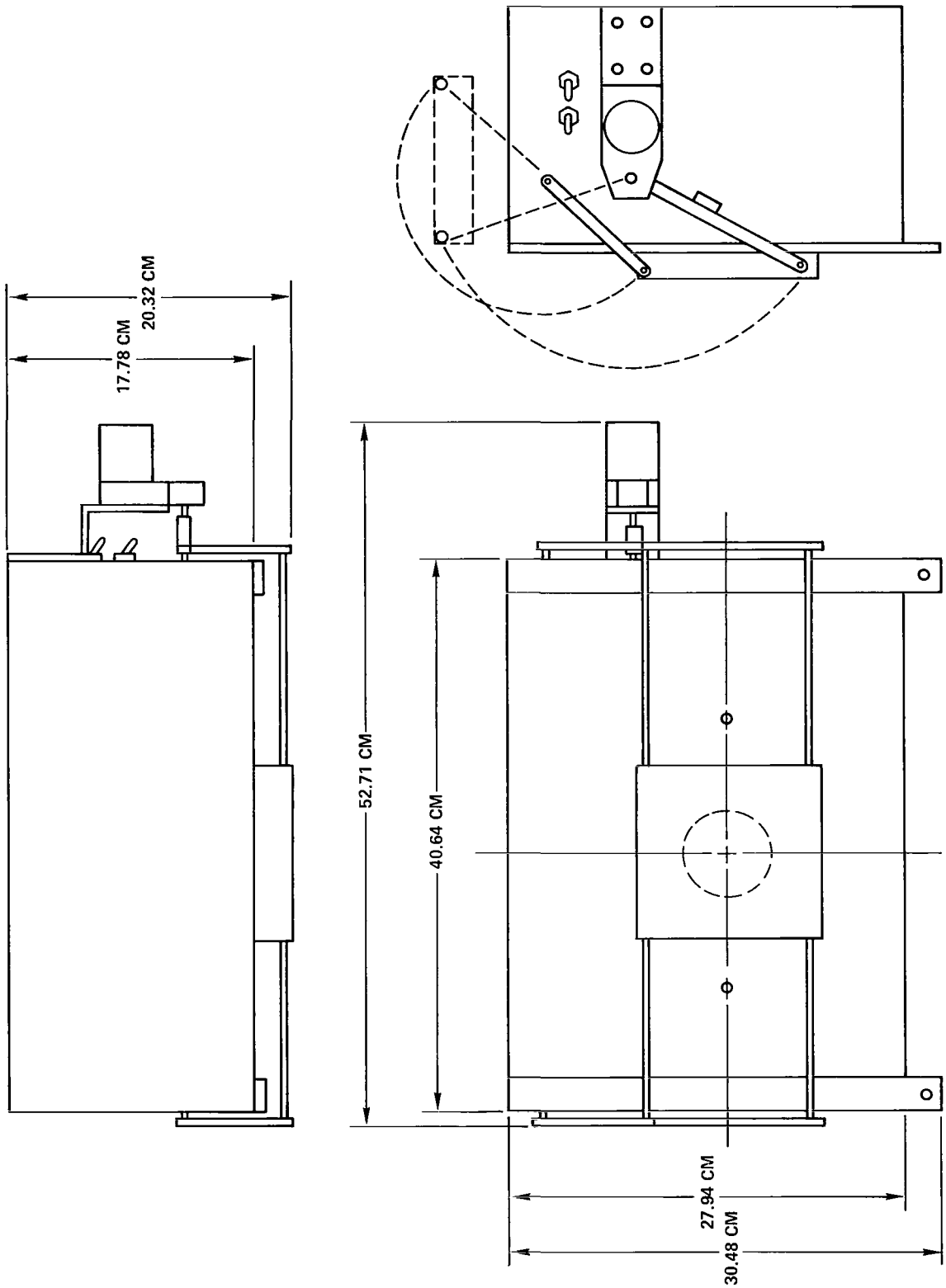

Figure 1. Nikon camera package.

ELECTRICAL CONDUCTIVITY MEASUREMENTS FROM STRATCOM VIII

John D. Mitchell and K. John Ho
Electrical Engineering Department
The University of Texas at El Paso
El Paso, Texas 79968

Leslie C. Hale and Charles L. Croskey
Ionosphere Research Laboratory
The Pennsylvania State University
University Park, Pennsylvania 16802

Robert O. Olsen
Atmospheric Sciences Laboratory
U.S. Army Electronics Command
White Sands Missile Range
New Mexico 88002

ABSTRACT

A blunt probe experiment for measuring electrical conductivity was flown with the Stratcom VIII-A instrument package on September 29-30, 1977. Data were obtained by the instrument throughout the entire measurement period (approximately 23 hours). An analysis of the data indicates an enhancement in conductivity associated with the krypton discharge ionization lamp (123.6 nm), particularly in negative conductivity. The conductivity values and their altitude dependence are consistent with previous balloon and rocket results.

INTRODUCTION

A blunt probe, a Gerdien condenser, and a krypton lamp were a part of the instrumentation suspended from the Stratcom VIII-A Balloon flown from Holloman Air Force Base, New Mexico, September 29-30, 1977. The purpose of this experiment was to study electrical conductivity in the atmosphere in an unperturbed condition and as modified by the ionizing radiations of the krypton lamp. A similar experiment was also flown on a parachute drop from the VIII-A gondola. The dropsonde results are discussed separately (see Hale and Croskey, "Electrical Structure and Ionizable Constituent Measurements"). In addition, a rocket-launched, parachute-borne blunt probe experiment for measuring electrical conductivity was conducted from nearby White Sands Missile Range, New Mexico, during the balloon flight.

INSTRUMENTATION

The balloon electrical conductivity experiments included a blunt probe and a Gerdien condenser mounted parallel to each other with their collectors directed vertically downward. The collection voltage waveform was common to both instruments. Positioned between the two instruments was a krypton discharge ionization lamp (123.6 nm) which was cycled on and off such that the probes could measure the enhancements in conductivity associated with the lamp's radiation.

The blunt probe is a two-electrode instrument for measuring the polar electrical conductivity of the atmosphere (References 1, 2, and 3). Under suitable flow conditions, the Gerdien condenser measures ion mobility and charge number density as well as electrical conductivity (References 4, 5, and 6). When flown with other experiments as on this balloon system, it is desirable to place the probes as far as possible from the rest of the package to reduce possible effects other instruments might have on the collection of charged particles. For the Stratcom VIII-A gondola, the instruments were extended horizontally on an arm approximately one meter from the main instrument package. Pictures of the probe configuration are given in Figures 1 and 2.

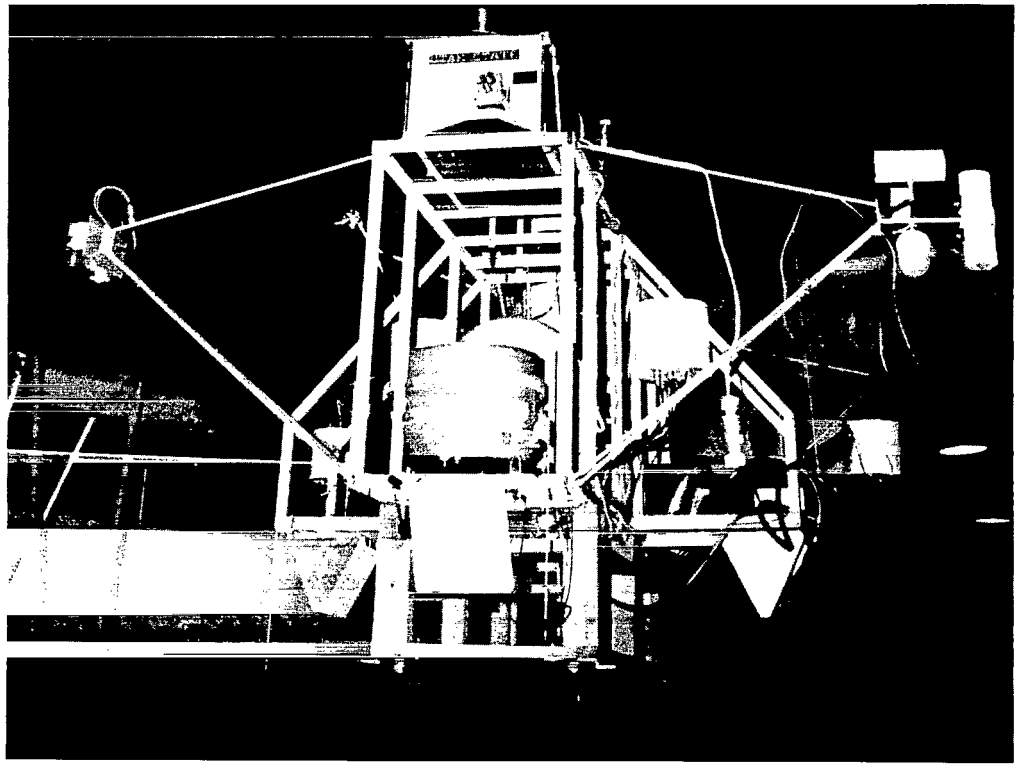

Figure 1. Stratcom VIII-A overall payload showing the location of the electrical conductivity instruments on the boom at the left.

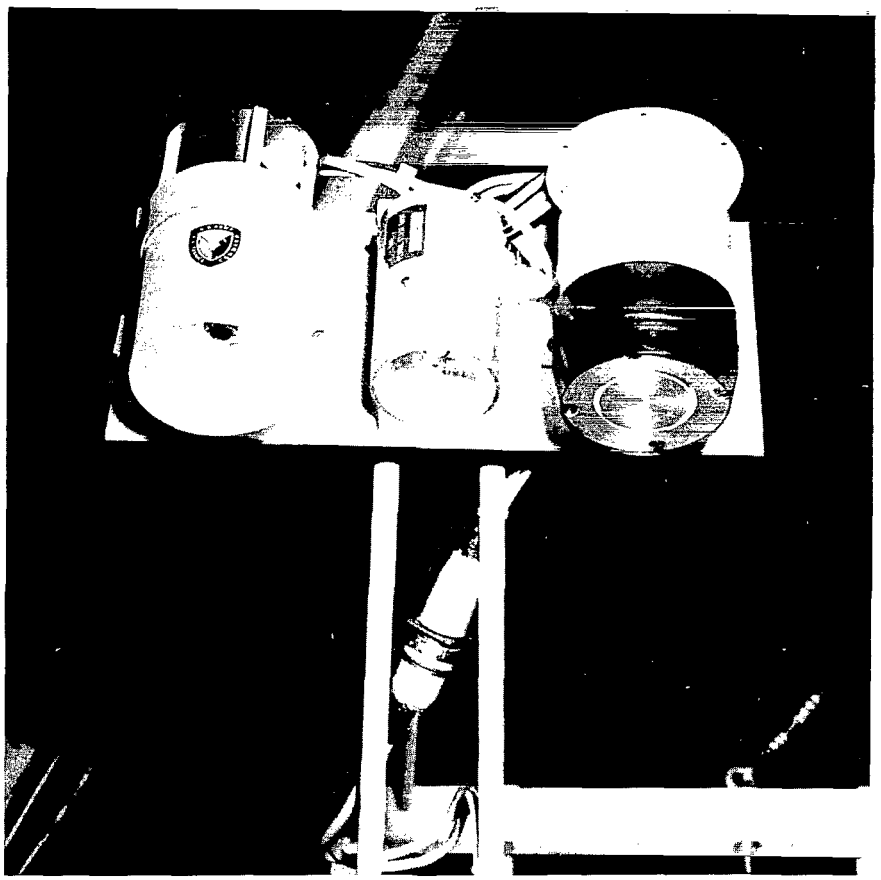

Figure 2. A close-up view of the Gerdien condenser (left), krypton lamp (center) and blunt probe (right) during preparation for flight.

RESULTS

Balloon Experiment—Ionization Lamp Off

Ten-minute, time-averaged values of electrical conductivity obtained with the krypton discharge lamp off are shown versus local time in Figure 3. The plus and minus signs represent positive and negative conductivity values, respectively, and the dots represent time intervals during which no distinct differences were observed between the positive and negative conductivity measurements. The upper curve in the figure shows the balloon's altitude as a function of local time.

The conductivity values measured on this balloon flight are in good agreement with previous balloon (References 7 and 8) and rocket (Reference 9) flights. In general, the differences observed between the positive and negative conductivity values for the same altitude are relatively small, and are thought to be associated with differences in the respective ion mobility values.

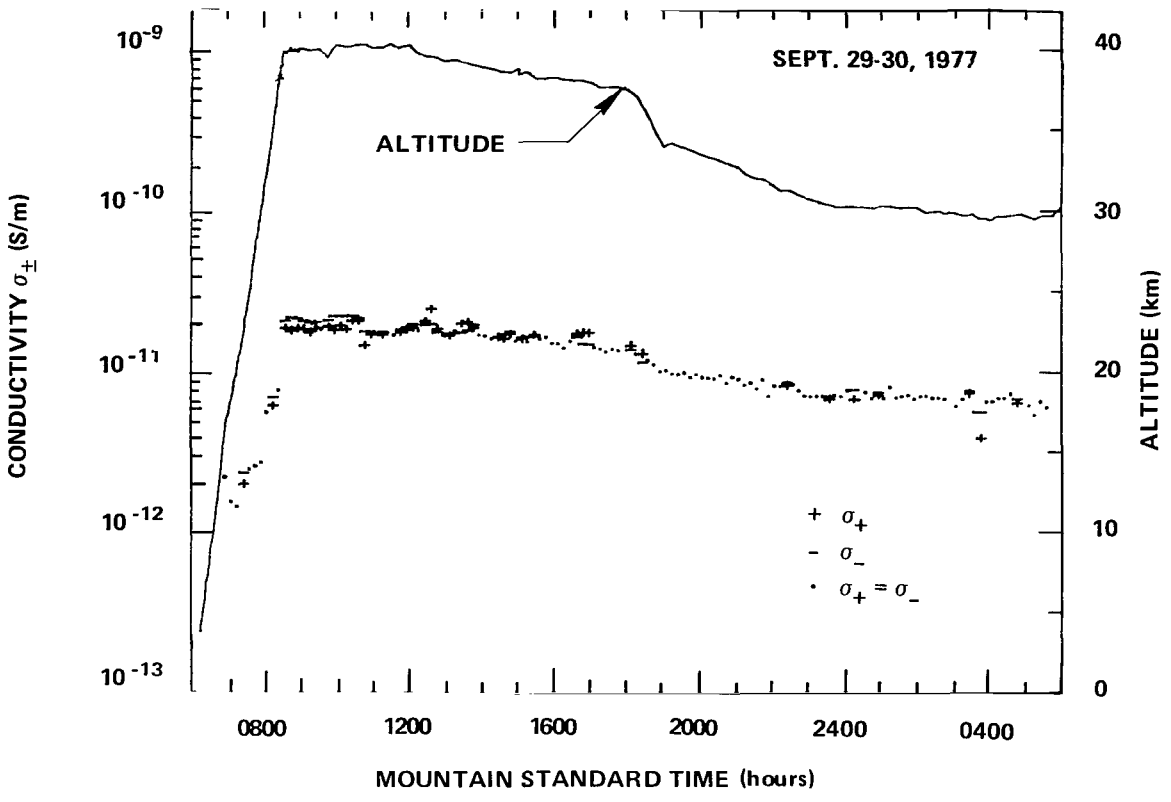

Figure 3. Time-averaged electrical conductivity values (lamp off) (1 siemens (S) = 1 mho).

A noticeable altitude dependence for electrical conductivity was observed during the complete measurement period of the flight. The altitude dependence in this region typically is inversely proportional to that for neutral number density (Reference 10). This is better demonstrated in Figure 4 where electrical conductivity values for the descent phase of the flight (1200 MST on September 29 to 0400 MST on September 30) are plotted for the balloon's altitude. The notation for the conductivity values in this figure is consistent with Figure 3.

Balloon Experiment—Ionization Lamp On

As discussed previously, a krypton discharge lamp was used as an ionization source with the blunt probe during designated periods of the flight. The enhanced positive and negative conductivity values (averaged over 10-minute intervals) are represented by the x's in Figures 5 and 6, respectively. In addition, the plus signs in Figure 5 and the minus signs in Figure 6 represent the respective positive and negative conductivity values for the lamp off as shown in Figure 3.

The enhanced positive conductivity values are typically a factor of 1.5 to 2.0 larger than the respective conductivity values measured with the lamp off. In contrast, the Gerdien condenser dropsonde

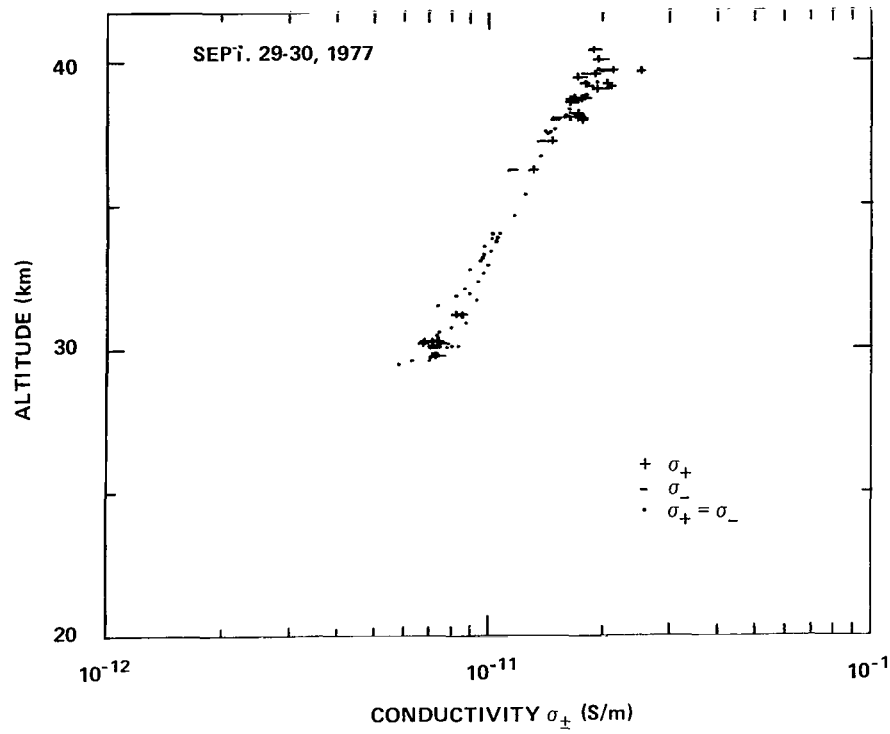

Figure 4. Altitude dependence of electrical conductivity during descent (lamp off).

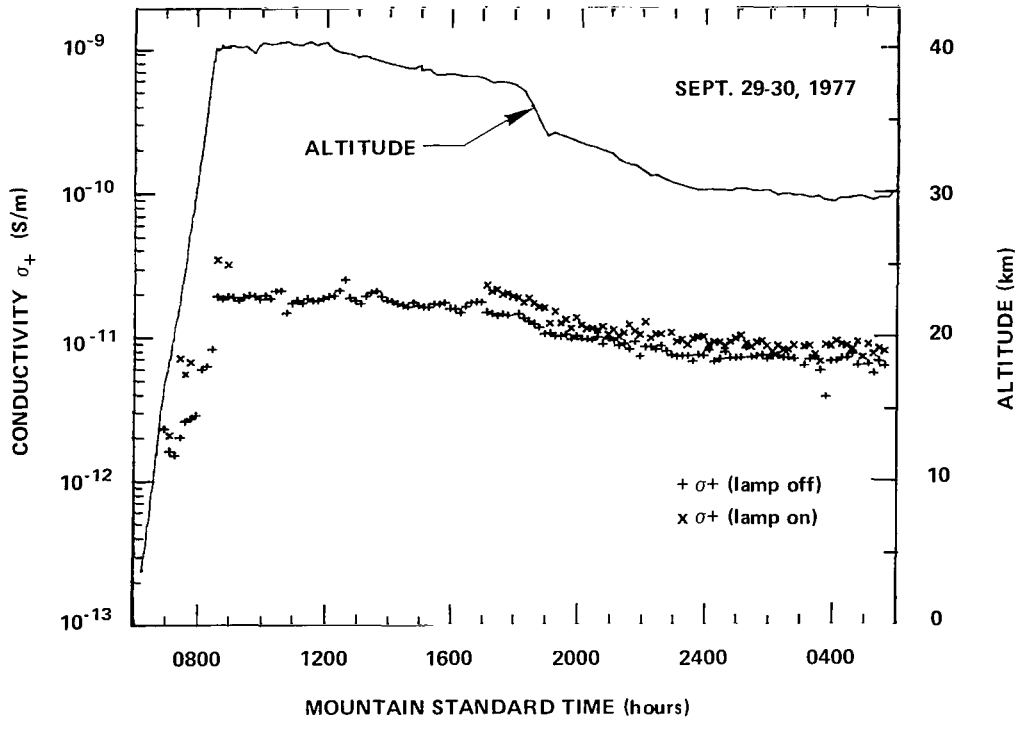

Figure 5. Time-averaged positive electrical conductivity values.

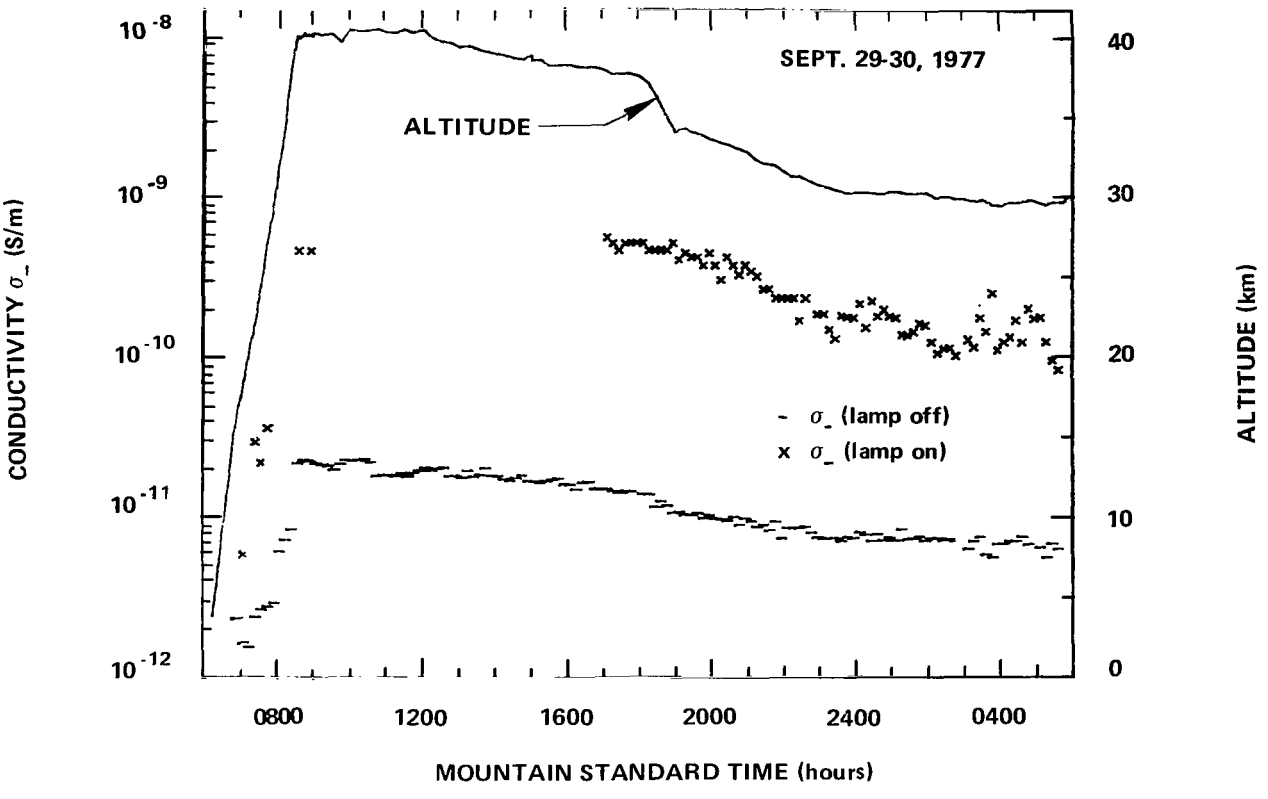

Figure 6. Time-averaged negative electrical conductivity values.

(with an ionization lamp) measured considerably larger positive conductivity enhancements during its relatively faster descent (see Hale and Croskey, "Electrical Structure and Ionizable Constituent Measurements"). The smaller positive conductivity enhancements measured by the balloon instrument would indicate a flow dependence for the collection of positive ions associated with the lamp.

Excluding the initial ascent, the enhancements in the blunt probe negative conductivity measurements for the lamp on are at least an order of magnitude larger than the respective values with the lamp off. This would suggest that the negatively charged species associated with the krypton lamp are generally more mobile than the positive ions.

Rocket Experiment

The electrical conductivity measurements from the rocket-launched, parachute-borne blunt probe experiment conducted at White Sands Missile Range, New Mexico, are shown in Figure 7. The plus and minus signs represent measured positive and negative conductivity values, respectively, while the dots indicate altitudes at which the two conductivity values are comparable. The launch time for this experiment (1345 MST) corresponds to when the VIII-A Balloon was at an altitude of approximately 38 km.

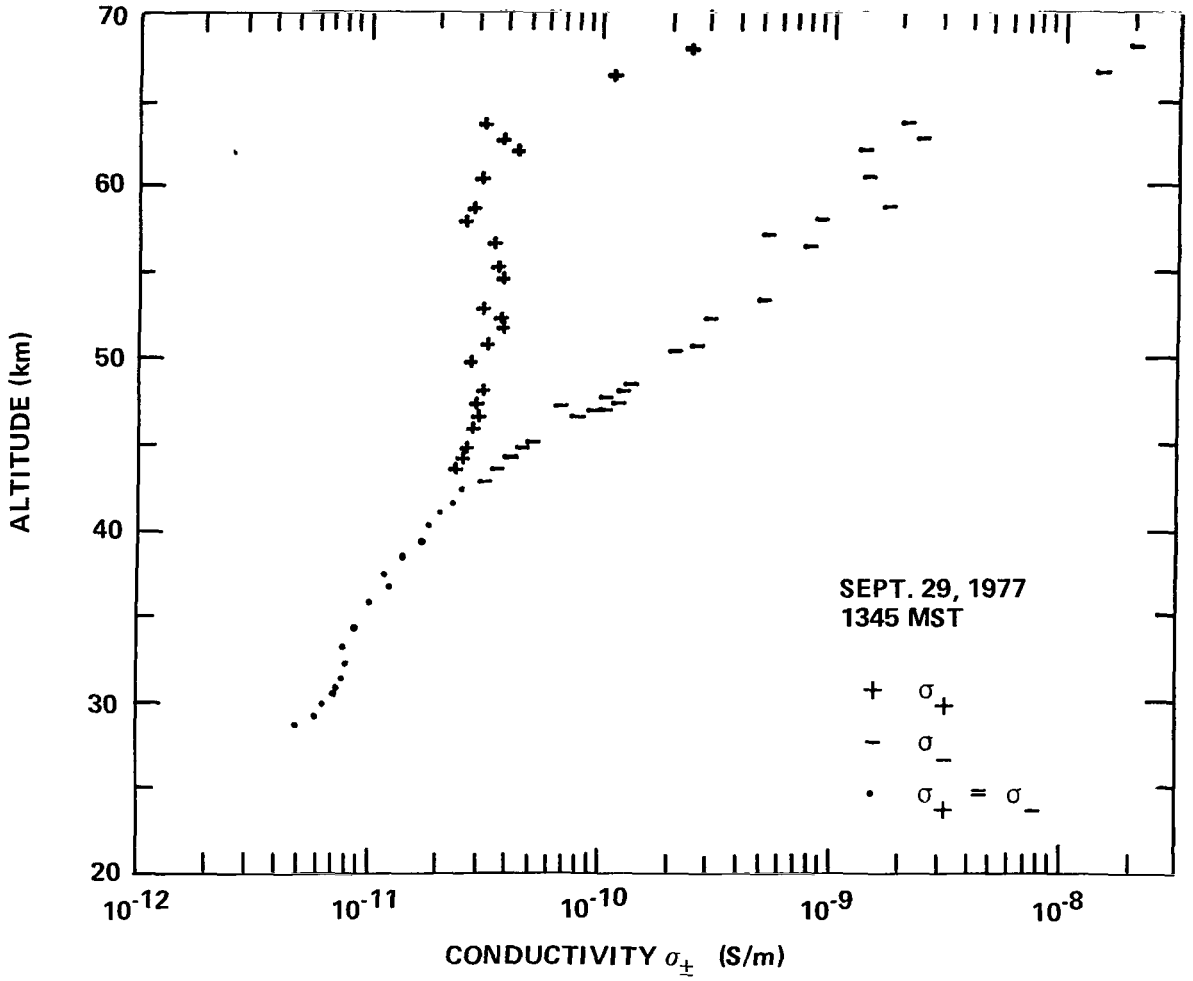

Figure 7. Rocket-launched, parachute-borne blunt probe electrical conductivity measurements.

Above 45 km, the negative conductivity values are larger than the corresponding positive conductivity values, resulting from the generally larger ion mobility values for the negatively charged species. Below 40 km, which corresponds to the measurement region for the balloon instrument, the positive and negative conductivity values for the same altitude are comparable. The generally good agreement between the rocket measurements and the corresponding balloon data (see Figure 4) demonstrates the measure consistency between the two experimental techniques.

CONCLUSIONS

A preliminary analysis of the blunt probe electrical conductivity data indicates that the balloon instrument operated successfully throughout the entire measurement period of the flight. Positive and negative conductivity measurements for the same altitude and with the lamp off are generally comparable, and are observed to be in good agreement with corresponding rocket data. Enhancements in

both positive and negative conductivity were observed during the times when the krypton discharge lamp was operating. The relatively smaller positive conductivity enhancements would indicate a flow dependence for the collection of positive ions associated with the ionization lamp.

REFERENCES

1. Hale, L. C., *Space Research VII,* North-Holland, Amsterdam, 1967, pp. 140–151.

2. Hale, L. C., D. P. Hoult, and D. C. Baker, *Space Research VIII*, North-Holland, Amsterdam, 1968, pp. 320–331.

3. Mitchell, J. D., Ionosphere Research Laboratory *Scientific Report No. 416,* The Pennsylvania State University, 1973.

4. Croskey, C., Ionosphere Research Laboratory *Scientific Report No. 442,* The Pennsylvania State University, 1976.

5. Pedersen, A., *FOA 3 Report A 607*, Research Institute of National Defense, Stockholm, 1964.

6. Rose, G. and H. U. Widdel, *Radio Sci. 7,* 1972, pp. 81–87.

7. Mitchell, J. D., L. C. Hale, and C. L. Croskey, *Space Research XVIII*, ed. by M. J. Rycroft and A. C. Steckland, Pergamon Press, 1978, pp. 143–146.

8. Mitchell, J. D. and L. C. Hale, *Air Force Geophysics Laboratory Report No. AFGL-TR-76-0306*, 1976, pp. 425–439.

9. Cipriano, J. P., L. C. Hale, J. D. Mitchell, *J. Geophys. Res.*, **79**, 1974, pp. 2260–2264.

10. Mitchell, J. D. and L. C. Hale, *Space Research XIII*, Akademie-Verlag, Berlin, 1973, pp. 471–476.

ELECTRICAL STRUCTURE AND IONIZABLE CONSTITUENT MEASUREMENTS

Leslie C. Hale and Charles L. Croskey
Ionosphere Research Laboratory
Pennsylvania State University
University Park, Pennsylvania 16802

ABSTRACT

To study the conductivities in the stratosphere, a sonde containing a Gerdien condenser with a krypton lamp was dropped from the Stratcom VIII-A Balloon on September 29, 1977, near Holloman Air Force Base, New Mexico. In situ stratospheric ions showed typical characteristics. The krypton lamp created large numbers of additional ions of remarkably high mobility with a product of number density and ionization cross section of the ionizable constituent(s) ($N\sigma$) greater than 10^{-9} cm^{-1}.

INTRODUCTION

For the study of conductivities, dropsonde no. 2, carrying a Gerdian condenser with a krypton lamp, was released from the Stratcom VIII-A Balloon on September 29, 1977. The objectives were: the determination of NO densities from the change in positive electrical conductivity produced by the lamp; measurements of an additional enhancement in negative conductivity produced by photodetachment of electrons from aerosol particles; and species differentiation from an analysis of charged particle mobilities. Related instruments were included on the gondola of the VIII-A Balloon and on two rockets (see Mitchell et al.,"Electrical Conductivity Measurements from Stratcom VIII" of this document).

The accuracy of the NO determination by this method has not yet been thoroughly evaluated, and the Stratcom-VIII flight was to allow comparison with the more generally accepted chemiluminescent technique. The potential of the photo-ionization technique is seen as a relatively simple means for determining variability over a wide altitude range.

INSTRUMENTATION

The parachute-borne dropsonde included a Gerdien condenser for measuring the electrical properties of the atmosphere including polar conductivities, ion mobility, and number densities. The dropsonde, 61 cm long, 30 cm in diameter, and 4.5 kg in weight, also included a lamp with a MgF_2 window to ionize low ionization-potential species such as NO and to produce electrons by photodetachment from aerosols. The total lamp output was about 4×10^{13} photons/second in a 38° beam (see Reference 1).

RESULTS

The sonde was dropped from the Stratcom VIII-A Balloon at 0832 MST on September 29 from an altitude of 39 km. The observed conductivities are shown in Figure 1, both with and without the lamp on. The conductivities in the stratosphere are similar to those observed previously with rocket deployed payloads, but, of course, do not show the unusual variability observed above 42 km between 18 January 1976 (an "anomalous" winter day) and January 23, 1976 (a "normal" winter day), at Wallops Flight Center. The stratospheric in situ conductivities show the normal exponential altitude dependence. The enhancement produced by the lamp in the positive conductivities below 40 km is quite large, much greater than expected. (The negative lamp-on data are very much more difficult to analyze because of the creation of large numbers of free electrons by the lamp and are not included here.)

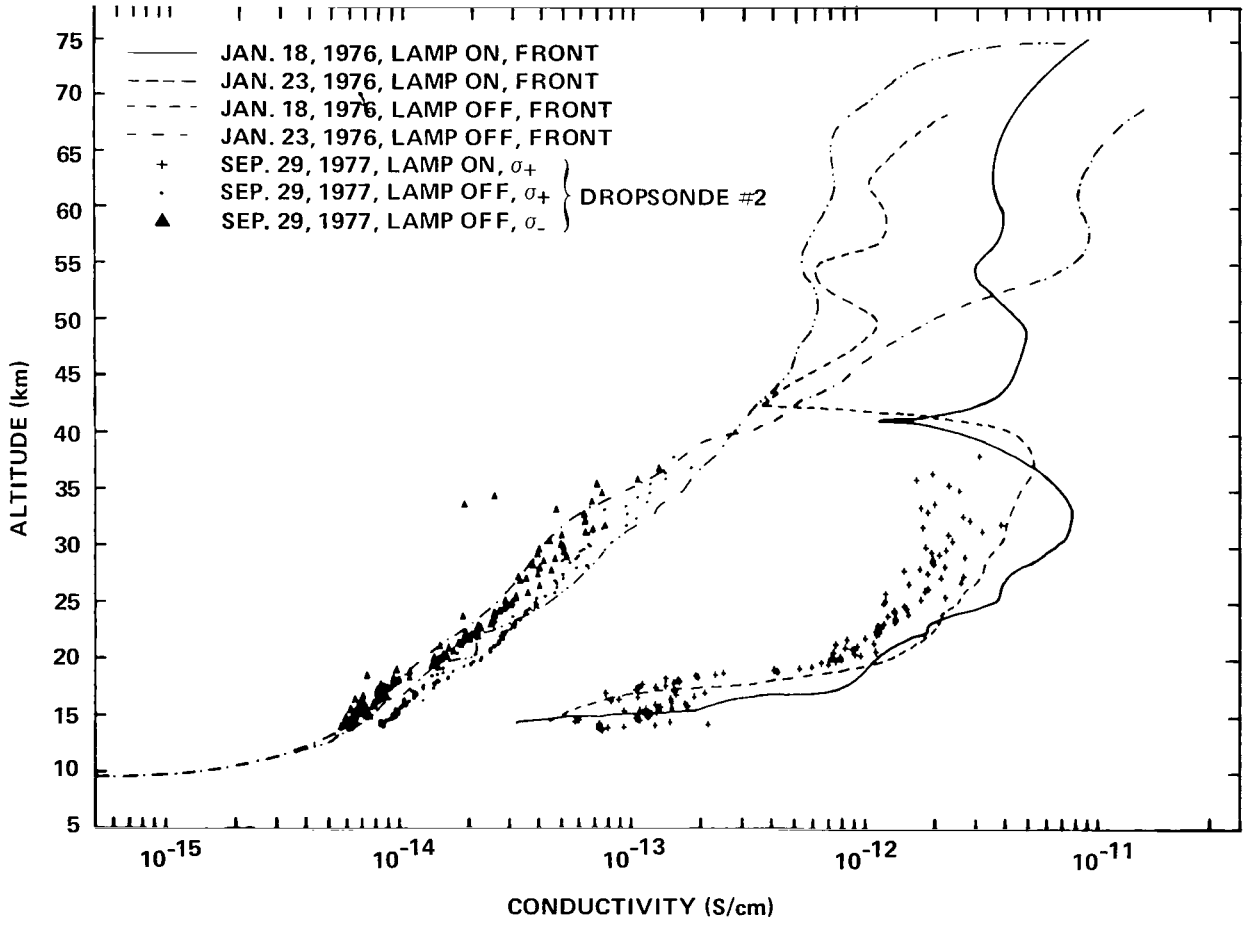

Figure 1. Conductivity [1 siemens (S) = 1 mho] as a function of altitude with and without ultraviolet irradiation from the kryptone lamp.

Wind tunnel tests of this type of instrument conducted at the von Karman Institute for Fluid Dynamics showed a positive conductivity increase due to NO and not to other tunnel air constituents or photoelectron effects. The dropsonde data indicate that the product of ionizable constituent density and ionization cross section is on the order of 2×10^{-9} cm^{-1}. If interpreted as NO density, this yields 10^9 cm^{-3}, which is probably too high. From this (and the mobility data, see below) we conclude that large quantities of a low ionization potential constituent exist in the stratosphere that do not occur in (fairly dirty) tropospheric air. This constituent is unknown, but tentative possibilities are addressed below.

The data on the in situ ions are not remarkable (see Figures 2, 3, and 4), except perhaps that the principal negative and positive ions seem to have precisely the same mobility over the entire stratosphere. A narrow layer of higher mobility positive and negative ions appears below 20 km. An analysis of the number densities and mobilities of ions created by the lamp shows that the ions created by the lamp are of very much higher mobility than the in situ ions. Apparently, three groups are formed, all with mobilities at least one order of magnitude greater than the in situ ions and approximately in the ratio of 2/3:1:3/2. The mobilities are so high that we are forced to consider the following possibilities:

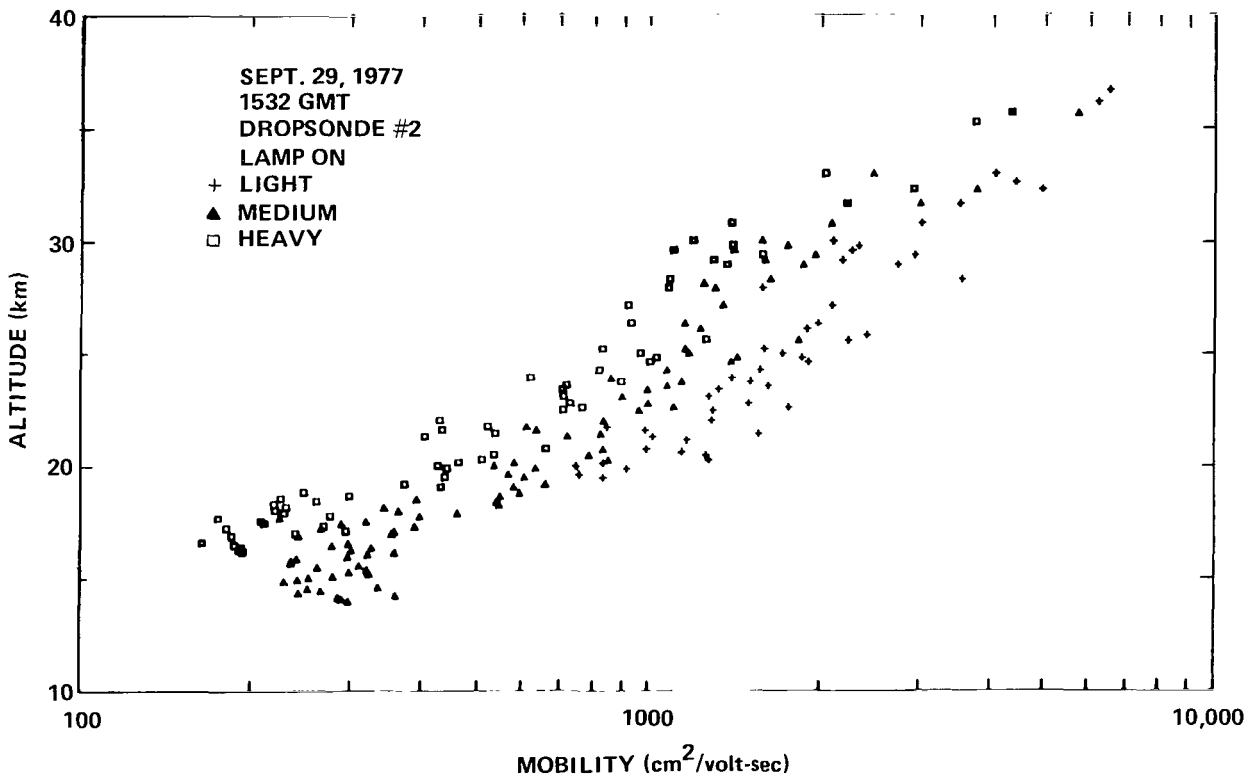

Figure 2. Mobility of positive ions present with the lamp on.

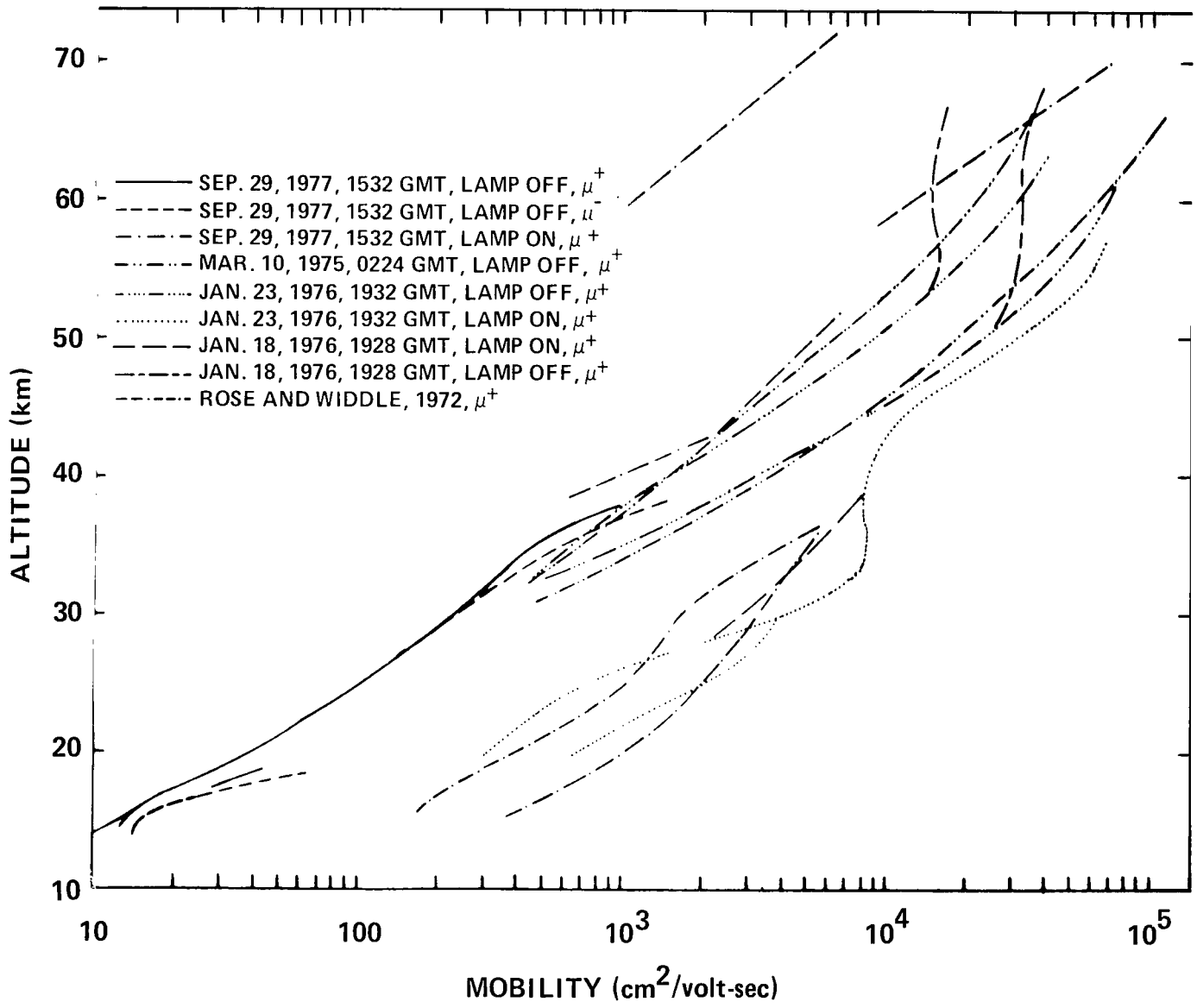

Figure 3. Mobility of ions observed from the Stratcom-VIII dropsonde compared to earlier observations.

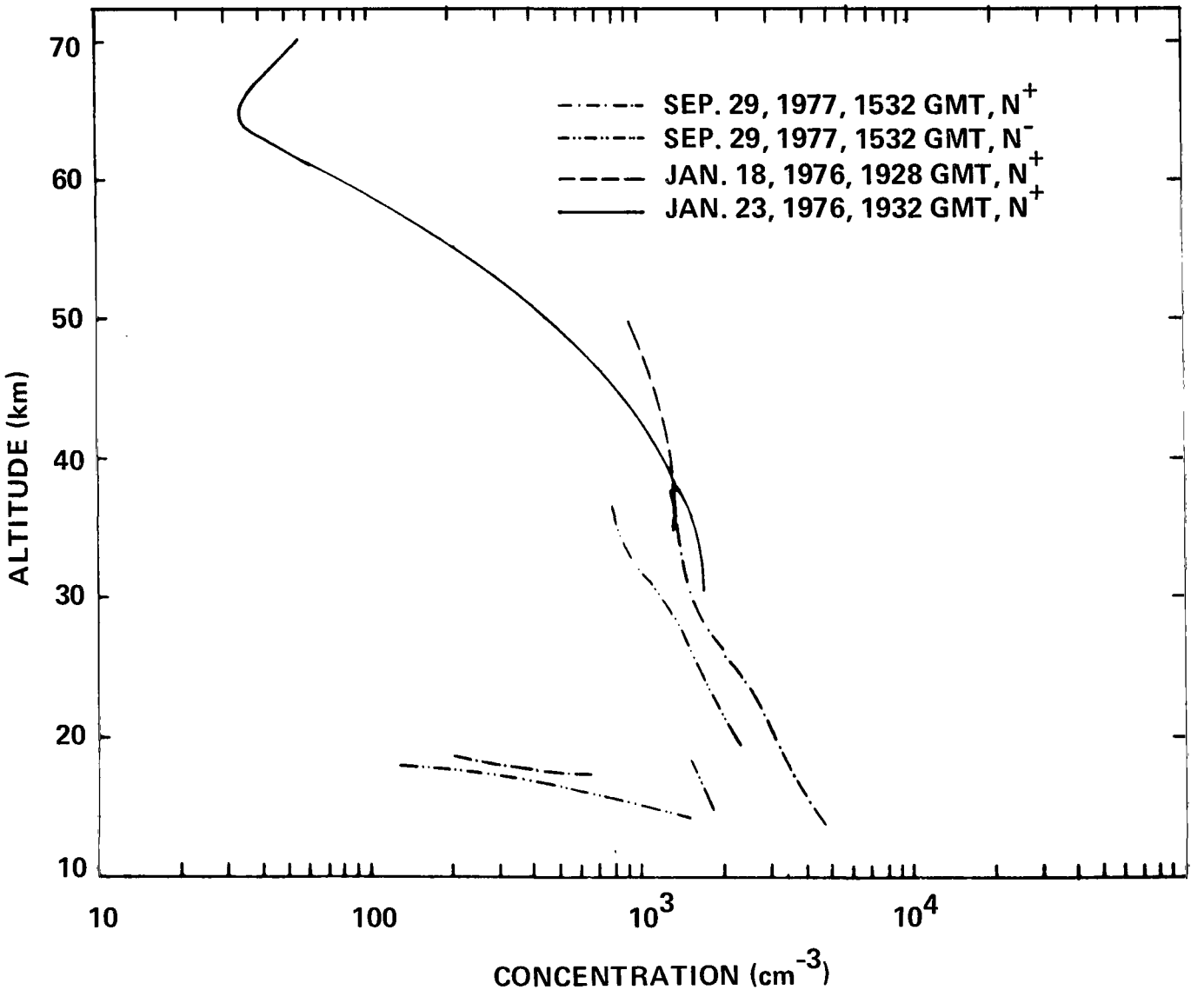

Figure 4. Number of densities of positive and negative ions compared to other observations.

1. The particles are effectively much smaller than ordinary molecules.

2. They are multiply charged.

Alternative (1) requires the presence of three groups of positive particles with mobilities greater than protons and hence, not ordinary chemical constituents.

Alternative (2) requires that many electronic charge units be emitted in a single photon interaction, which is perhaps possible with a tenuous particulate which is demolished by the interaction, leaving a multiply charged nucleus.

Alternative (2) is consistent with the existence in the stratosphere of a very much higher density of small (less than 10 nm) particles than is generally recognized (Reference 2), which dominate ionization processes above 40 km, where hard ultraviolet radiation penetrates. The UV krypton lamp extends this response to lower altitudes, and is similar to the "sunrise" response observed above 40 km (Reference 3).

REFERENCES

1. PSU-IRL Scientific Report No. 442, 1976.

2. Hale, L. C., Particulate transport through the mesosphere and stratosphere, *Nature,* **268**, pp. 710-711, 1977.

3. Mitchell, J. D., R. S. Sagar, and R. O. Olsen, "Positive Ions in the Middle Atmosphere During Sunrise Conditions," *Space Research XVII*, M. J. Rycroft and A. C. Stickland, ed., Pergamon Press, 1977, pp. 199-204.

D-REGION ELECTRON DENSITY MEASUREMENTS BY PARTIAL REFLECTION SOUNDER

Robert O. Olsen
Atmospheric Sciences Laboratory
U. S. Army Electronics Command
White Sands Missile Range
New Mexico 88002

D. L. Mott and Billy G. Gammill
Physical Science Laboratory
New Mexico State University
Las Cruces, New Mexico 88001

ABSTRACT

Measurements of electron density in the lower ionosphere were made at White Sands Missile Range throughout the Stratcom VIII-A launch day, September 29, 1977, using a partial-reflection sounder. In addition, information regarding the sounder's antenna pattern was gained from the passage of the balloon over the array.

INTRODUCTION

The Atmospheric Sciences Laboratory (ASL), White Sands Missile Range (WSMR), currently operates a partial-reflection sounder at the Range. The sounder provides measurements of free-electron density in the D-region of the ionosphere (below 100 km). Measurements were made throughout the day on September 29, 1977, the launch day for Stratcom VIII-A, and results are included herein.

APPARATUS

The ASL sounder is a monostatic radar operating at 2.24 MHz with a pulse width of 20 μsec and a pulse repetition rate of 17 per second. Pulses are transmitted vertically, and the received echoes, partially reflected from the lower ionosphere, are digitally recorded. Reflections from altitudes between 56 and 114 km are recorded at 2-km increments. The antenna array, used for both transmitting and receiving, consists of five pairs of crossed dipoles, strung between wooden poles. Four of the pairs are located at the corners of a square area of dimension 134-m per side, and the fifth pair is located at the center of the square.

Pulses are transmitted and received in circular polarization, alternating between left and right hand polarization. This provides signals in the ordinary and extraordinary modes – terms that are associated with differing indices of refraction in the ionosphere. As is well known (see, for example, Reference 1), the ratio of echo amplitudes for the two modes provides a determination of electron density as a function of altitude.

ANALYSIS

In our data-processing procedure, the amplitude ratio is used only to provide a system-calibration constant. This constant, along with corrections for the echo altitude and for signal attenuation below the altitude of interest, is then used to transform the ordinary-mode echo profile into an electron-density profile. Details of the data-processing procedure will be published at a later date.

Fourteen runs were recorded on September 29. Within each run, data were collected for approximately 10 minutes. Figures 1, 2, and 3 show results for three of the runs. The starting time of the run is noted in each figure. The average density over the run plotted in terms of altitude in kilometers (relative to the radar which is at 1.25 km above sea level) and electron density in free-electrons per cubic centimeter.

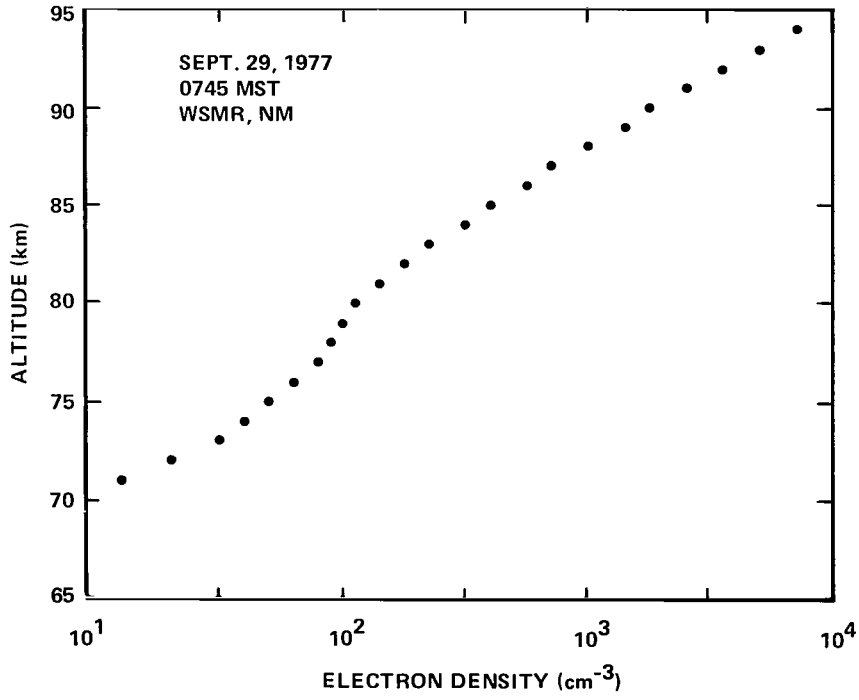

Figure 1. Electron density from the partial reflection sounder – 0745 MST.

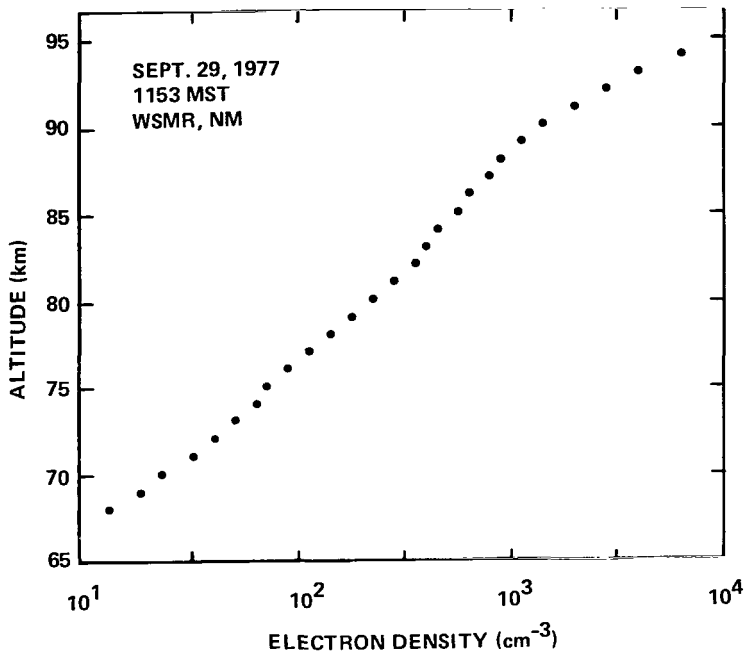

Figure 2. Electron density from the partial reflection sounder – 1153 MST.

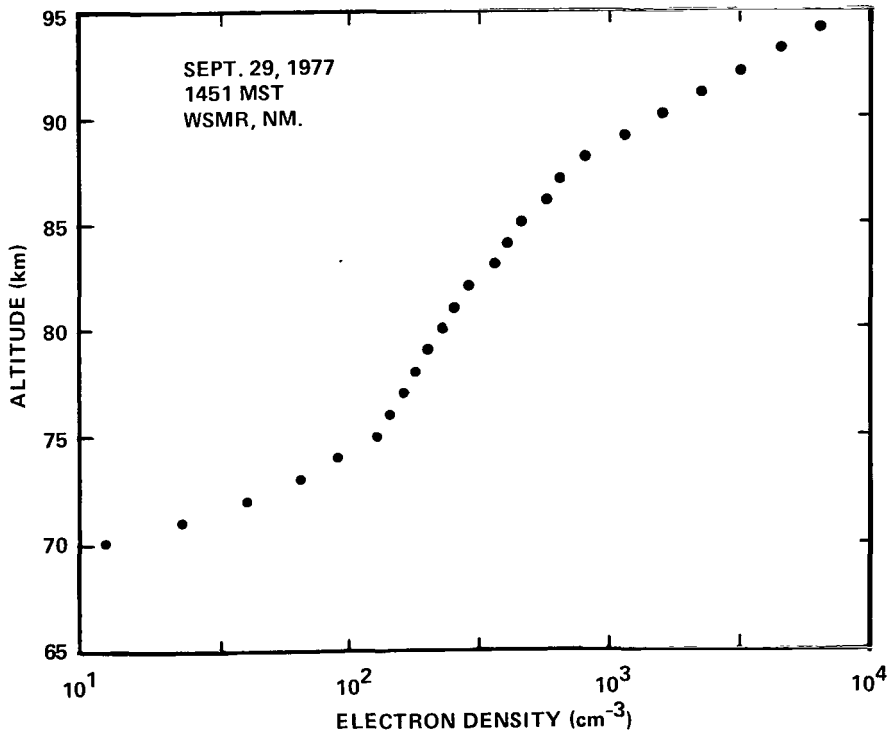

Figure 3. Electron density from the partial reflection sounder – 1451 MST.

BALLOON TRANSIT

During the day of September 29, the balloon passed over the partial-reflection sounder site, providing a unique opportunity for checking our antenna pattern. An observable reflection from the balloon was noted on the radar's A scope from shortly before 1000 MST until shortly after 1400 MST. From balloon position data, it was found that during this period the sub-balloon point moved from approximately 30 km southeast of the sounder site to approximately 30 km northwest, with the balloon altitude approximately 40 km throughout. (Sounder coordinates are 32°39'N, 106°21'W.) These data verify the symmetry of our antenna pattern and indicate that the main, vertical lobe of the antenna array has a cone half-angle of approximately 37°. A theoretical calculation of the antenna pattern places the null-limit of the main lobe at 34° which agrees favorably with the observation. According to the calculation, the half-power point on the main lobe would occur at a cone half-angle of approximately 15°.

REFERENCE

1. Belrose, J. S., and M. J. Burke, *J. Geophys. Res.*, **69**, 1964, pp. 2799–2818.

STRATOSPHERIC AEROSOLS COLLECTED BY U-2 AIRCRAFT

Neil H. Farlow and Guy V. Ferry
National Aeronautics and Space Administration
Ames Research Center
Moffett Field, California 94035

Homer Y. Lem and Dennis M. Hayes
LFE Environmental Analysis Laboratories
Richmond, California 94804

ABSTRACT

Stratospheric aerosols were collected by a U-2 aircraft at 18- and 21-km altitude beneath the flight tracks of two Stratcom VIII balloons, September 29 (GMT), 1977. Particle size distributions, corrected for small particle sampling bias, show bimodal features suggestive of mixtures of young, growing aerosols with mature ones. Heretofore, our studies had indicated the growth of small particles was most prominent in the equatorial zone. Improved techniques used for this study now suggest that aerosol growth occurs at other latitudes as well.

INTRODUCTION

In a recent study (Reference 1), we found considerably more smaller particles in the tropical stratosphere than elsewhere, suggesting that young, growing aerosols were being formed mainly in that region. On the other hand, Lazrus and Gandrud (Reference 2) had suggested that stratospheric aerosol growth might also occur elsewhere, such as on the anticyclonic side of jet streams. Heretofore, the analytical methods we used to determine particle size distributions from stratospheric collections prevented us from accurately assessing the small particle portions. Thus, unless there was an exceptionally large population of small particles, as we found in the tropics, we could easily miss them. Now, with improved methods, we are able to examine particles with radii as small as 0.03 μm, while also correcting for sampling bias inherent in our collection system.

This paper presents the results, using these improved methods, obtained by analyzing collections made with a U-2 aircraft near Holloman Air Force Base, New Mexico, while underflying the Stratcom VIII Balloon systems.

INSTRUMENTATION

Aircraft collections of aerosol particles for size analysis from the upper troposphere and lower stratosphere are made with instruments (Figure 1) developed at Ames Research Center (References 3 and 4). In this approach, particles are collected by direct impaction on very thin carbon-coated palladium wires (0.075 mm diameter) deployed directly into the airstream below the wing and beyond the boundary layer. The collecting wires are inserted into the airstream, then returned to a vacuum-sealable flight module processed before and after flight under clean-room conditions. The carbon coating is used on the wires to prevent fluid particles from spreading out thinly on the surface and complicating the analyses.

Particles are collected at various altitudes from 12 to 21 km, with most collections obtained at 12, 15, and 18 km on each flight. Collection times of 1 to 3 minutes at each altitude are used to obtain adequate samples for determining particle size distributions.

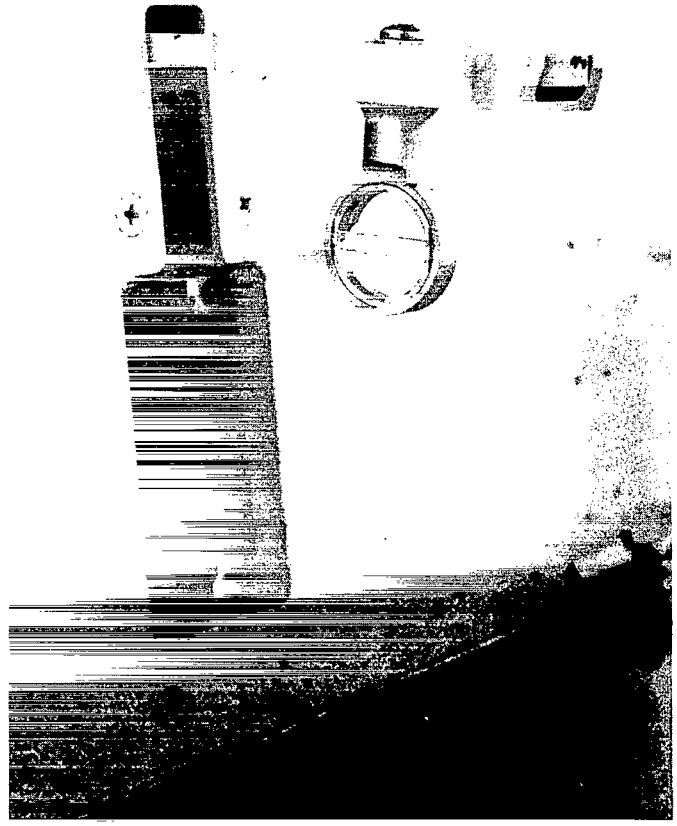

Figure 1. Aerosol collector installed on the U-2 aircraft wing with sampling arm extended (collecting wires are suspended across the circular ring on the arm).

ANALYSIS

A scanning electron microscope (SEM) is used to examine the wire surfaces at magnifications of 10,000X. Consecutive pictures are taken along the stagnation line at this magnification to provide analysts with images of about 100 to 200 particles on which particle radii measurements can be made. The collecting wire is then rotated so that the vertical profile of representative particles can be imaged in the SEM and photographed. This enables an average shape to be defined and a vertical height deduced. Usually the particles are fluid mixtures of crystals and liquid that form into flattened spherical segments on the collecting surfaces. Hence the volume of each collected particle can be calculated from the diameter, shape, and average vertical dimension. These volumes are then equated to equivalent spheres to provide the size distributions presented in this report.

LIMITATIONS

As in all aerosol collection experiments, the accuracy of each size distribution is affected by factors such as configuration of the sampling instrument, analytical procedures, and characteristics of the aerosol material. On our sampling instrument, the thin-wire collecting surfaces are contained in a 2.5-cm-diameter ring that is held in a circular holder affixed to an arm extending 4 cm beyond the integral module cover, and 5 cm beyond the wing pylon. When this array is in the sampling position shown in Figure 1, the sampling wires are well beyond the aerodynamic boundary layers of the instrument pylon, the wing, and the affixed module cover. Only the very central positions on the collecting wires are analyzed to avoid any possible effect due to the ring and supporting holder. Mathematical examination of the collecting efficiency of the wire (Reference 5), which is represented as a long cylinder, yields efficiency curves that show that very small particles are collected with an efficiency less than 100 percent. Table 1 shows the corrections that must be applied in various particle sizes to provide properly adjusted size distributions. Because of the extremely complex procedures required to thoroughly evaluate the aerodynamics of the U-2 aircraft wing, the instrument pylon, module cover, extended arm, ring support and collecting wires in a wind tunnel (including the generation and measurement of test aerosols of known size distributions), we have not evaluated collecting efficiency beyond assessments of the wire efficiency noted above.

In our analytical procedures, we use magnifications of 10,000X to determine the radii of all collected particles, and to evaluate their vertical height and shape. We find that particles with equivalent spherical radii > 0.03 μm can be easily detected and measured on our collection surface at these magnifications. Particles smaller than this are, however, difficult to resolve from imperfections in the wire surface. Hence, unless the particle is positively identifiable, it is not counted. This results in a rapid decrease in the number of particles counted in the extremely small size range. Therefore, for this study we limited our analyses to an assessment of particle sizes > 0.03 μm equivalent sphere radius.

Another analytical procedure which somewhat affects the shapes and absolute values of the size distributions presented in this paper is the method whereby we obtain smooth distribution curves. Usually the plotted data points are quite scattered due to the relatively small sample sizes. Typically,

Table 1
Collection Efficiency Inertial Impaction
on 0.075-mm Wires

Particle Radius (μm)	Fractional Collection Efficiency	
	at 18 km	at 21 km
0.1	1.000	1.000
0.095	1.000	1.000
0.090	1.000	1.000
0.085	0.999	1.000
0.080	0.990	1.000
0.075	0.980	1.000
0.070	0.967	1.000
0.065	0.952	1.000
0.060	0.934	1.000
0.055	0.911	1.000
0.050	0.882	0.987
0.045	0.854	0.970
0.040	0.818	0.947
0.035	0.775	0.914
0.030	0.721	0.870

each data point represents from 1 to 25 particles in each size range. We obtain a smooth curve by drawing an eyeball-fitted line through the scattered data points for each distribution. Thus small differences between size distribution curves should not be given great significance.

Finally, we consider the influence of aerosol composition on the accuracy of the reported distributions. Upper atmosphere aerosols are generally fluid mixtures of liquid and crystals (Reference 6). Portions of the particles are both volatile and hygroscopic; these particles have been observed in the laboratory to grow in size by absorbing moisture, and decrease in size when heated in the electron beam of the SEM under vacuum. Thus the dimensions measured in the microscope are, to some extent, the consequences of how the particles reacted to the various environments. We have conducted several experiments which indicate that size changes of larger particles are probably not drastic, and the resulting size distributions are reasonable estimates of the real sizes in the atmosphere.

These special experiments were conducted on balloons and after U-2 flights, where the collections were either maintained at stratospheric conditions or protected from laboratory moisture in sealed modules (Reference 6). The technique we used involved depositing a thin film of gold obliquely on the collecting surfaces in the sealed containers so that a void in the deposited gold was formed behind each particle. Such a void outlined the particle's shape and size. Analysis later in the SEM showed that little change had occurred in these particles' features after the samples were exposed to laboratory and microscope environments.

RESULTS

The U-2 Aircraft underflew the Stratcom VIII-B Balloon locally on the afternoon of September 28 and the VIII-A Balloon on the morning of September 29, both in the vicinity of Holloman Air Force Base, New Mexico. Precise GMT times and locations of the sample collections are given in Table 2.

Table 2
Location and Time of Aerosol Sample Collections

Altitude (km)	Location (latitude and longitude)	Time (GMT)
18	32°45'N 107°15'W	0040 Sept. 29
18	32°50'N 112° 0'W	0124
18	33°30'N 106°20'W	1616
21	32°30'N 105°30'W	1712

Figures 2 and 3 present the individual size distributions for the two flights. These distributions are corrected and smoothed as discussed above. Observe in Figure 2 that the distributions are quite similar except at the very smallest particle sizes. Some similarity between these collections is to be expected because they were collected at the same altitude and geographically close to each other. Note also the bimodal features of the distributions that suggest the aerosol is a mixture of two populations: a young, growing one and a more mature, larger-particle one. In previous studies we have detected small particle growth in the tropics, but now, these results suggest growth is occurring in temporate regions as well.

In Figure 3, similar bimodal features are seen, except that the bimodal peak occurs at a larger particle size at 21 km than at 18 km. Also, for the pair of collections the concentrations were considerably less at the higher altitude in the smaller size range. These features suggest that aerosol growth is more vigorous at 18 km than above. However, when the 21-km distribution is compared to the 18-km distributions of 16 hours earlier (Figure 2), differences are mainly in the size range > 0.08 μm,

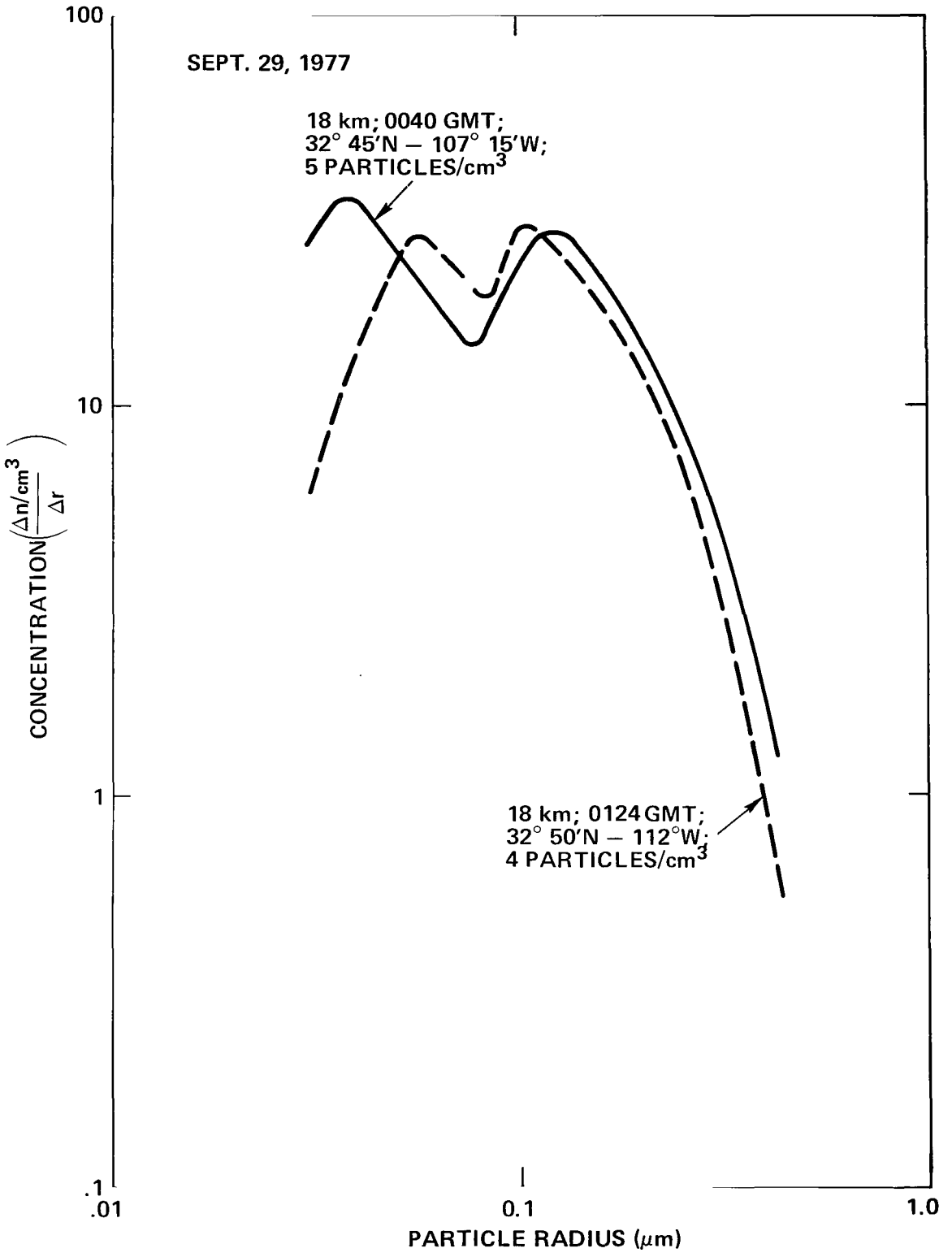

Figure 2. Particle size distributions during the U-2 underflight of the Stratcom VIII-B Balloon.

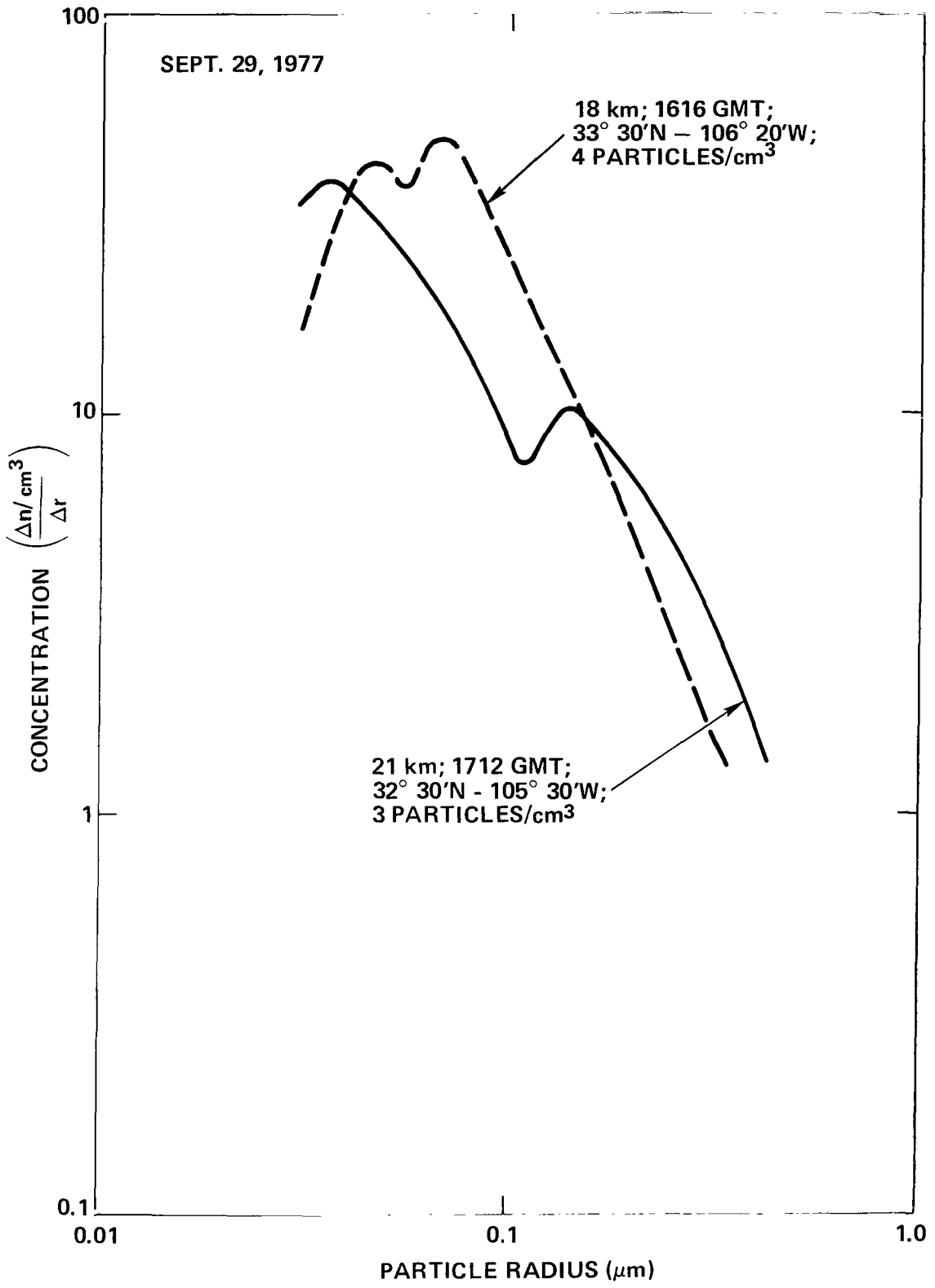

Figure 3. Particle size distributions during the U-2 underflight of the Stratcom VIII-A Balloon.

while the small particle component is not too dissimilar. In fact, the 18-km small particle component from the second flight is considerably larger than on the earlier flight, but fewer large particles are present.

DISCUSSION

Because of the striated nature of the aerosol clouds in the lower stratosphere, consecutive individual size distributions can be quite different. Therefore, it is difficult to draw general conclusions about the aerosol based on a few distributions. We have found that trends can be observed only by averaging together a reasonable number of individual collections. This averaging process, however, can mask interesting features, such as the bimodality observed in the distributions presented here. This is because the bimodal peaks vary in location and tend to average out when curves are combined.

For the first time, we have extended our size analyses to particles as small as 0.03 μm equivalent spherical radius. Heretofore, we had restricted our size analyses to particles larger than 0.1 μm. By improving our methods and extending our observations to the small sizes presented in Figures 2 and 3, we can now begin to observe what appears to be a particle growth component in the mid-latitude stratosphere. Many more observations are needed, however, in this small size range before major conclusions can be drawn.

REFERENCES

1. Ferry, G. V., N. H. Farlow, and H. Y. Lem, "Altitudinal Variations of Stratospheric Aerosols with Latitude," *Trans., AGU,* **58**, 1977, p. 1148.

2. Lazrus, A. L., and B. W. Gandrud, "Stratospheric Sulfate Aerosol," *J. Geophys. Res.*, **79**, 1974, pp. 3424-3431.

3. Ferry, G. V., and H. Y. Lem, "Aerosols in the Stratosphere," (Proceedings of the Third Conference of the Climatic Assessment Program), *Rep.* DOT-TSC-OST-74-15, Department of Transportation, Washington, D.C., 1974.

4. Ferry, G. V., and H. Y. Lem, "Aerosols at 20 Kilometers Altitude," (Proceedings of the Second International Conference on the Environmental Impact of Aerospace Operations in the High Atmosphere), Am. Meteorol. Soc., San Diego, CA, 1974.

5. Wong, J. B., W. E. Ranz, and H. F. Johnstone, "Inertial Impaction of Aerosol Particles on Cylinders," *J. Appl. Phys.*, **26**, 1955, pp. 244-249.

6. Farlow, N. H., D. M. Hayes, and H. Y. Lem, "Stratospheric Aerosols: Undissolved Granules and Physical State," *J. Geophys. Res.*, **82**, 1977, pp. 4921-4929.

CRYOGENIC GAS SAMPLERS

Richard Lueb and Leroy Heidt
National Center for Atmospheric Research
Boulder, Colorado

Two sets of cryogenic sampling cylinders were included on the Stratcom VIII-A Balloon for the purpose of obtaining stratospheric air at altitudes of 25 to 40 km. These would be analyzed for their content of H_2, H_2O, CH_4, CO, CO_2, N_2O, $CFCl_2$, and CF_2Cl_2. The system is described in Reference 1, and techniques for the analysis of the collected samples are discussed in References 2 and 3. To avoid contamination, the inlet tube extended 3 m below the payload and samples were to be taken as the balloon descended at a rate of 30 to 8 m/sec.

However, the helium valves on Balloon VIII-A could not be opened and the balloon did not descend at the desired rate. Samples were taken during the late afternoon and evening of September 29, 1977, as the balloon cooled and descended very slowly to an altitude of 30 km. As expected, the air was markedly contaminated by gases associated with the payload, including remnants of the exhaust fumes from the diesel-driven motor generators that provided power for illumination of the payload during its preparation for a launch at sunrise.

REFERENCES

1. Lueb, R. A., D. H. Ehhalt, and L. E. Heidt, "Balloon-Borne Low Temperature Air Sampler," *Rev. Sci. Instrum.*, **46**, 702-705, 1975.

2. Heidt, L. E., and D. H. Ehhalt, "Gas Chromatographic Measurement of Hydrogen, Methane, and Neon in the Air," *J. Chromatogr.*, **69**, 103-113, 1972.

3. Moore, H., "Isotropic Measurement of Atmospheric Nitrogen Compounds," *Tellus*, **XXVI**, 169-174, 1974.

MEASUREMENTS FROM THE APEX OF THE STRATCOM VIII-A BALLOON

Carlos McDonald
Electrical Engineering Department
University of Texas at El Paso
El Paso, Texas 79968

ABSTRACT

The Top Package, mounted on the apex plate on the top of the Stratcom VIII-A Balloon (September 29, 1977, New Mexico), provided an estimate of thermal and water vapor perturbations due to the balloon, and served as an instrumentation platform for the albedo and Lyman-alpha experiments. Data were obtained for 3 hours, which included the ascent and a short period at the float altitude of about 40 km.

INTRODUCTION

The Top Package, mounted on the apex plate located on the top of the Stratcom VIII-A Balloon, was flown from Holloman Air Force Base, New Mexico, on September 29, 1977. The package was designed to provide information on the extent to which the presence of the balloon modifies the ambient air temperature and water vapor content, and on the flux of radiation from the skyward hemisphere. To accomplish this, sensors were included for air and skin temperatures, water vapor content, ultraviolet flux (121.6 nm), infrared flux (0.2 to 2.8 μm), and temperature of the package itself. The package was entirely self-contained, including batteries and telemetry transmitter.

INSTRUMENTATION

The Top Package included the following sensors:

1. Two balloon skin temperature sensors, each consisting of a 0.25-mm bead thermistor attached to the surface of the balloon by means of Mylar film and tape which served both to hold the thermistors in place and to reinforce the area. The thermistors were mounted 180° apart in azimuth, about 2.5 m from the apex.

2. Air temperature sensor, consisting of film-mounted 0.25-mm bead thermistors, similar to the air temperature sensors on the main gondola.

3. A water vapor sensor consisting of the Panametrics aluminum oxide capacitor operated in a constant temperature mode (Aquamax).

4. A Lyman-alpha radiation sensor (121.6 nm) consisting of an ionization chamber with a MgF_2 window and filled with nitric oxide. Its pass band was 114 to 134 nm.

5. A sensor for the infrared flux from the skyward hemisphere. This was an Epply Precision Infrared Pyranometer (pyrgeometer), Model PIR, sensitive from 0.2 to 2.8 μm.

6. A levelness sensor consisting of a horizontal cylinder, half full of a conductive fluid, with three probes that made contact with fluid. This had a full scale range of $\pm 8°$.

7. Payload monitors, namely, battery voltage and a bead thermistor for container surface temperature.

Mechanical Design

The Top Package was designed to be mounted on the apex plate of the balloon as shown in Figure 1. It met weight and mounting requirements as defined by the launch organization, the Air Force Cambridge Balloon Branch at Holloman Air Force Base. The external surface was a white painted aluminum can; care was taken to ensure that the entire Top Package was free from rough edges and corners. It had a total weight of 14.5 kg including the 15-cm stand. Although the payload was relatively tall, it had a very low center of gravity to ensure the apex plate remained stable.

The package consisted of an aluminum battery box and a Plexiglas module holder insulated by a minimum of 7.5 cm of Styrofoam. The battery box contained four Silvercel Yardley CR100 DC-1 batteries which were maintained at a pressure of 1 atm. The module holder was designed to hold 14, 4- by 5-inch printed circuit boards, a transmitter, the Panametrics water vapor electronics box, a heater, and 19 fuses. An assembly drawing is shown on Figure 2.

The UV sensor and pyranometer were fixed into the top of the Styrofoam insulation. Mounts were provided below the package for a water vapor sensor and a temperature sensor. The transmitter antenna is mounted on the bottom of the apex valve plate, inside the balloon. The Top Package is turned on by means of an external switch shortly prior to inflation of the balloon.

Electrical Design

A block diagram of the electronics is given in Figure 3. Sensor outputs and calibration reference voltages are converted via pulse frequency modulators and transmitted sequentially by the 1680 MHz transmitter to GMD receiving stations at the White Sands MTTR station and at Hatch, New Mexico, where the signals were recorded on magnetic tape along with IRIG-B timing. The sequence and timing of the various items is shown in Table 1. The electronics was designed primarily with CMOS

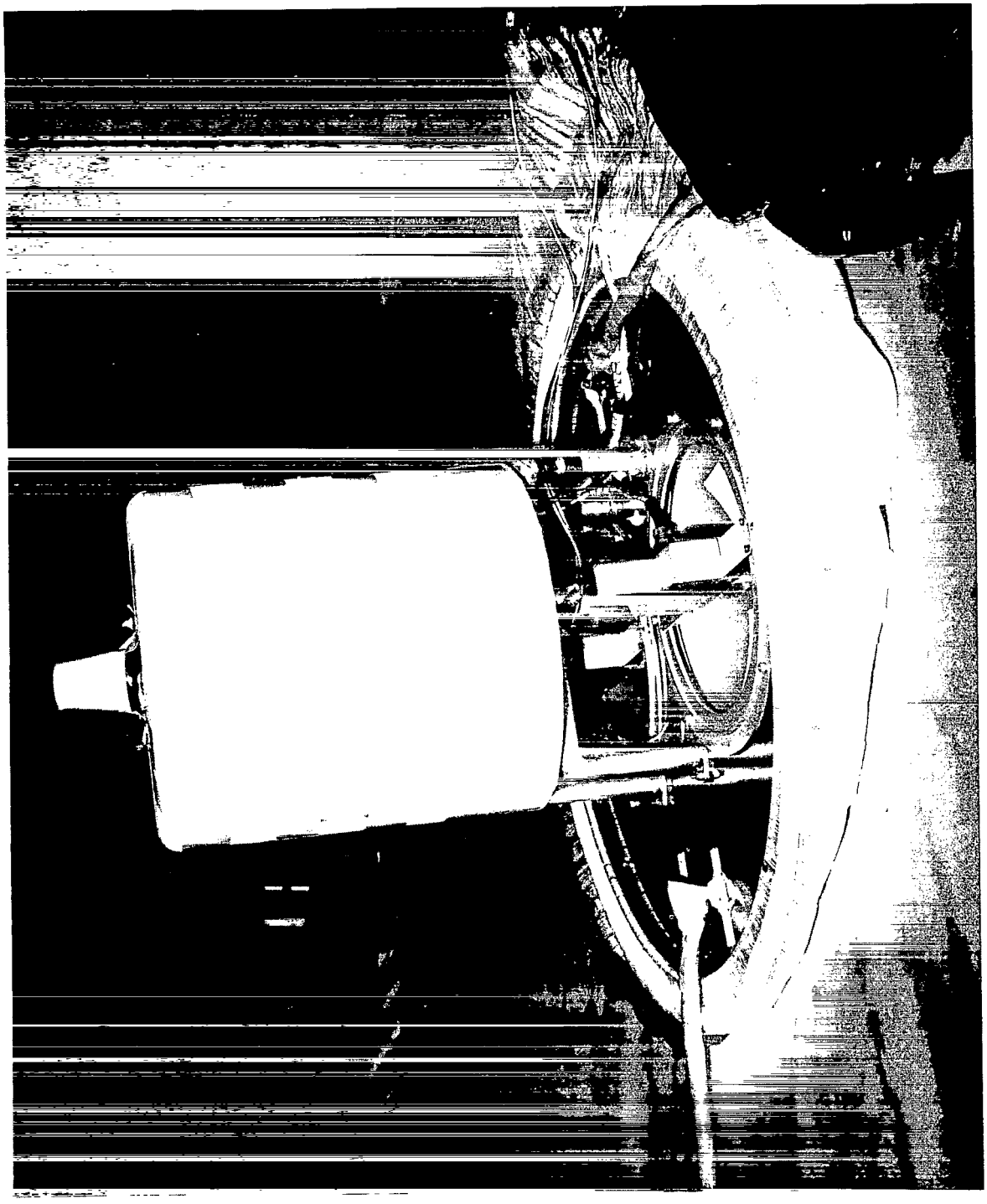

Figure 1. Top Package on the Apex plate.

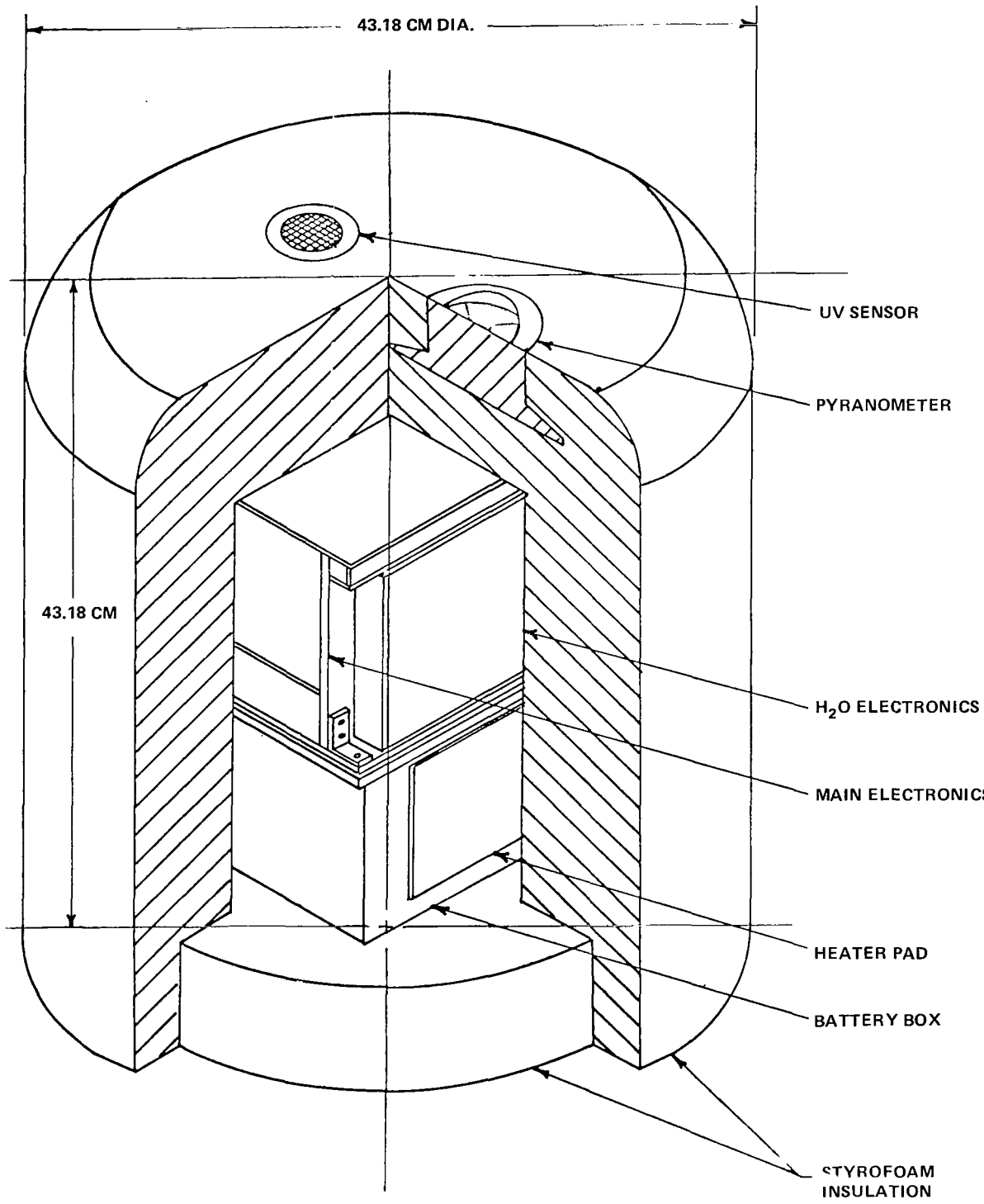

Figure 2. Top Package — physical arrangement.

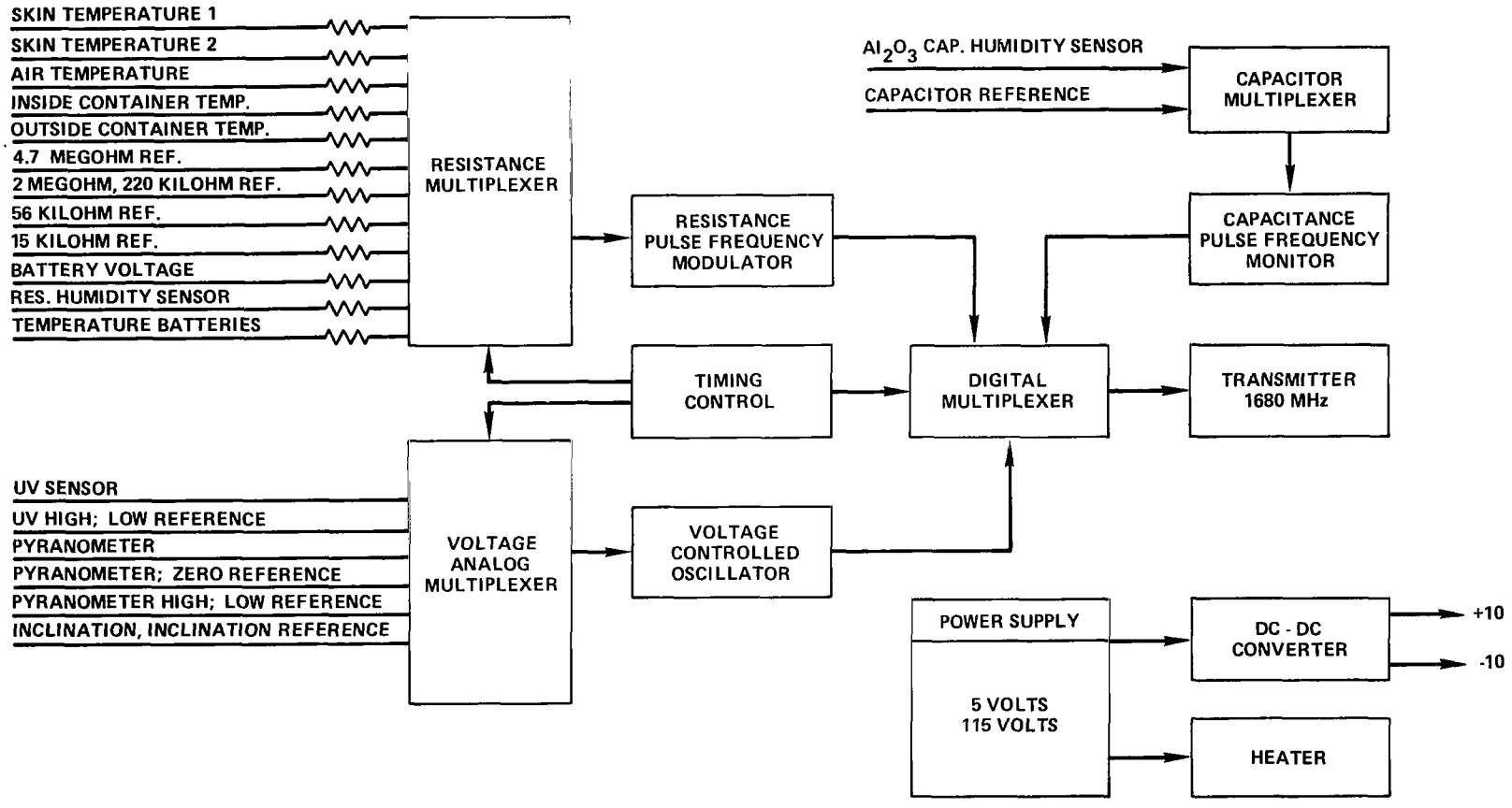

Figure 3. Top Package. Block diagram of electronics and instrumentation.

Table 1
Sampling Sequence of Sensors and References

Channel	Quantity Being Sampled	Time Duration (sec)
1	Skin Temperature #1 and #2	6,6
2	Air Temperature	12
3	4.7- and 2-megohm references	6,6
4	220- and 56-kilohm references	6,6
5	Temperature Electronics	12
6	Temperature of Bottom of Electronics and Temperature of Batteries	6,6
7	Temperature Inside Air and Temperature of Outside Container	6,6
8	Battery Voltage	12
9	Blank	12
10	Inclination, Inclination Ref.	6,6
11	Water Vapor, Water Vapor Ref.	6,6
12	Pryranometer, Pyranometer Ref.	6,6
13	Inclination, Inclination Ref.	6,6
14	UV data	12
15	High and Low Voltage Ref.	6,6
16	UV Ref.	12

devices to conserve power. The power supply uses a 5-V pack of Silvercel batteries adequate for 36 hours continuous operation, with a dc-dc converter to provide the ±12 V for the analog and digital electronics and the 135 V for the transmitter tube. To permit the nighttime operation, a thermistor-controlled heater, operating from the 5-V supply, maintains the electronics modules above -10°C. Details of the circuitry may be found in Reference 1.

FLIGHT DATA

Useful data were received during the period 0613 to 0943 MST, September 29, 1977, from shortly after launch through the initial float period, covering an altitude range of 3.6 km to over 40 km. After this time, the telemetry signal diminished rapidly. The reasons for this are not clear since no failure was evident upon test of the Top Package after recovery.

Data from the various sensors are as follows:

Skin temperature – Data from the skin temperature sensors are given in Figure 4 as a function of time, along with data concerning the altitude of the balloon. Since the two sensors were always within 2°C of each other, the average is used. The skin temperature data may be compared with the air temperature at the same altitudes, as inferred from meteorological sondes launched in the same period. Although the balloon became sunlit shortly after launch (sunrise (upper limb) was at 0557 MST), the skin temperature remained nearly equal to that of the ambient atmosphere. As the solar irradiation increased (see the heat input as observed by the Epply pyranometer, Figure 5) and as the balloon ascended to higher altitudes, the balloon skin temperature rose to approximately 25°C above the surrounding atmosphere.

Air temperature – This sensor broke during launch operations.

Water vapor – The aluminum oxide film capacitor provided data throughout the period. Values were relatively low compared to data from previous Stratcom flights, but still higher than ambient. See the discussion by P. Goodman ("Water Vapor Measurements with Aluminum Oxide Sensors").

Lyman-alpha sensor – Telemetered data indicate that the instrument was operating satisfactorily; however, the signal did not rise above the noise level, corresponding to a flux of 10^6 photons-cm^{-2}-sec^{-1}. Unfortunately, high noon data are not available.

Infrared pyranometer – These data are shown in Figure 5 and discussed by R. Rubio et al. elsewhere in this document ("Measurement of Radiation Energy Transfer").

Levelness sensor – Data from the levelness sensor, along with the altitude of the balloon, are shown in Figure 6 as a function of time. Times of the three parachute drops are also indicated. As can be seen, the excursions are generally less than a degree. The reasons for the 4° tilt seen near 0800 are not immediately evident.

REFERENCE

1. McDonald, C., et al., Upper Atmospheric Research Project V, Final Report, Report No. FR1-78-UA-57, Contract DAAD07-74-0263, The University of Texas at El Paso, June 1978, 109 pages.

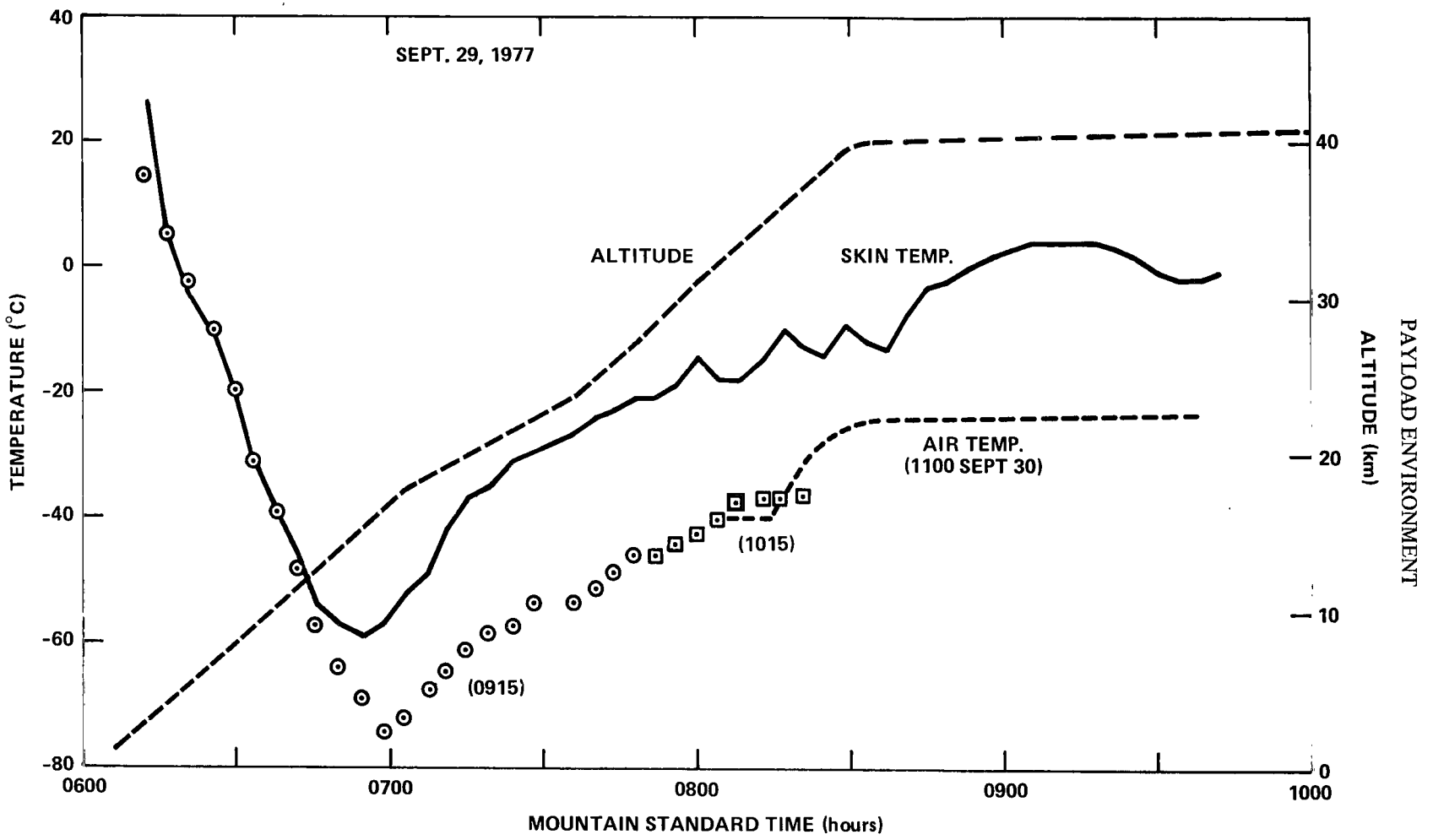

Figure 4. Skin Temperature. Air temperatures are inferred from the three meteorological sondes closest to the time of the Stratcom VIII-A ascent.

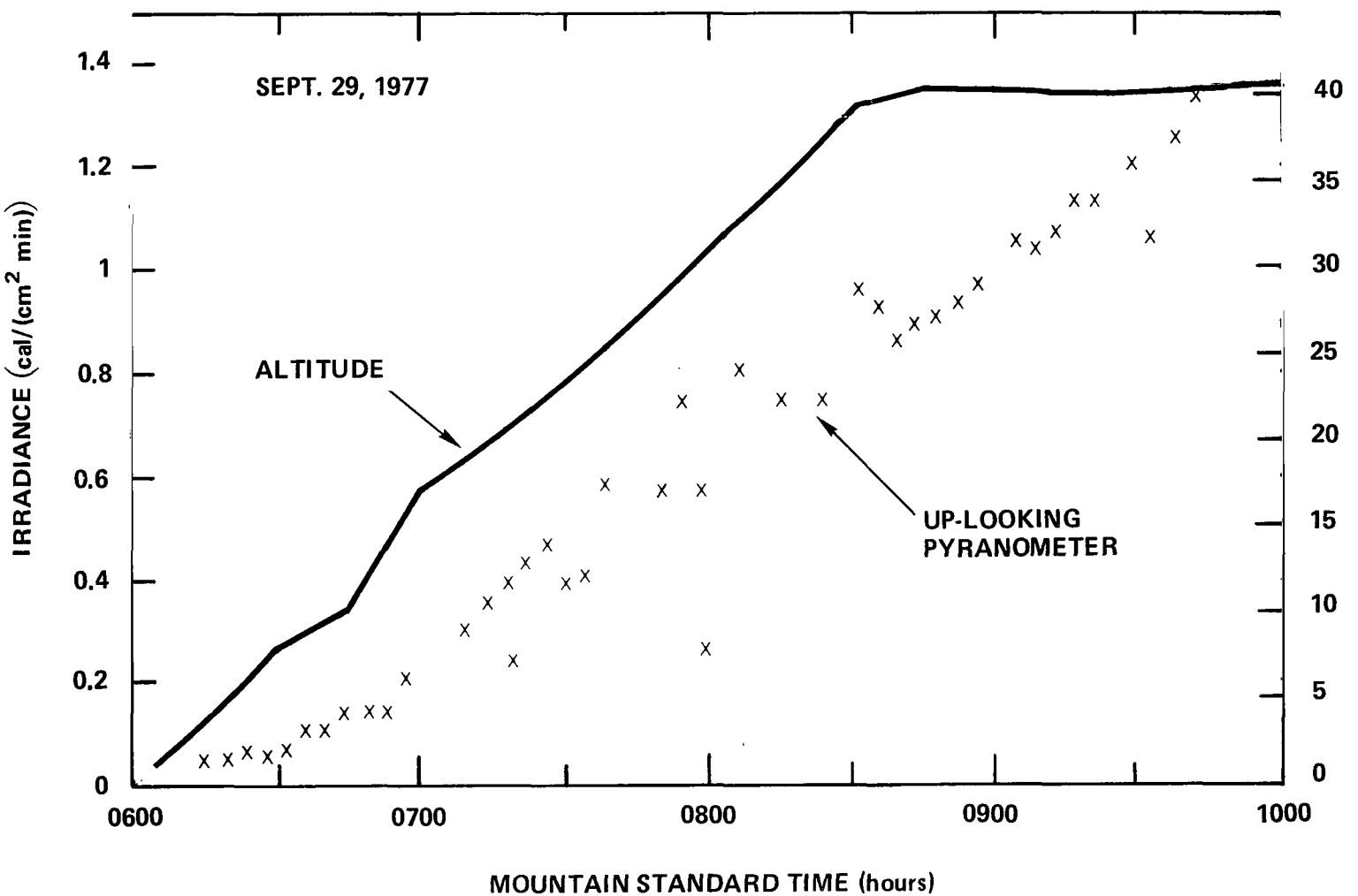

Figure 5. Infrared pyranometer data.

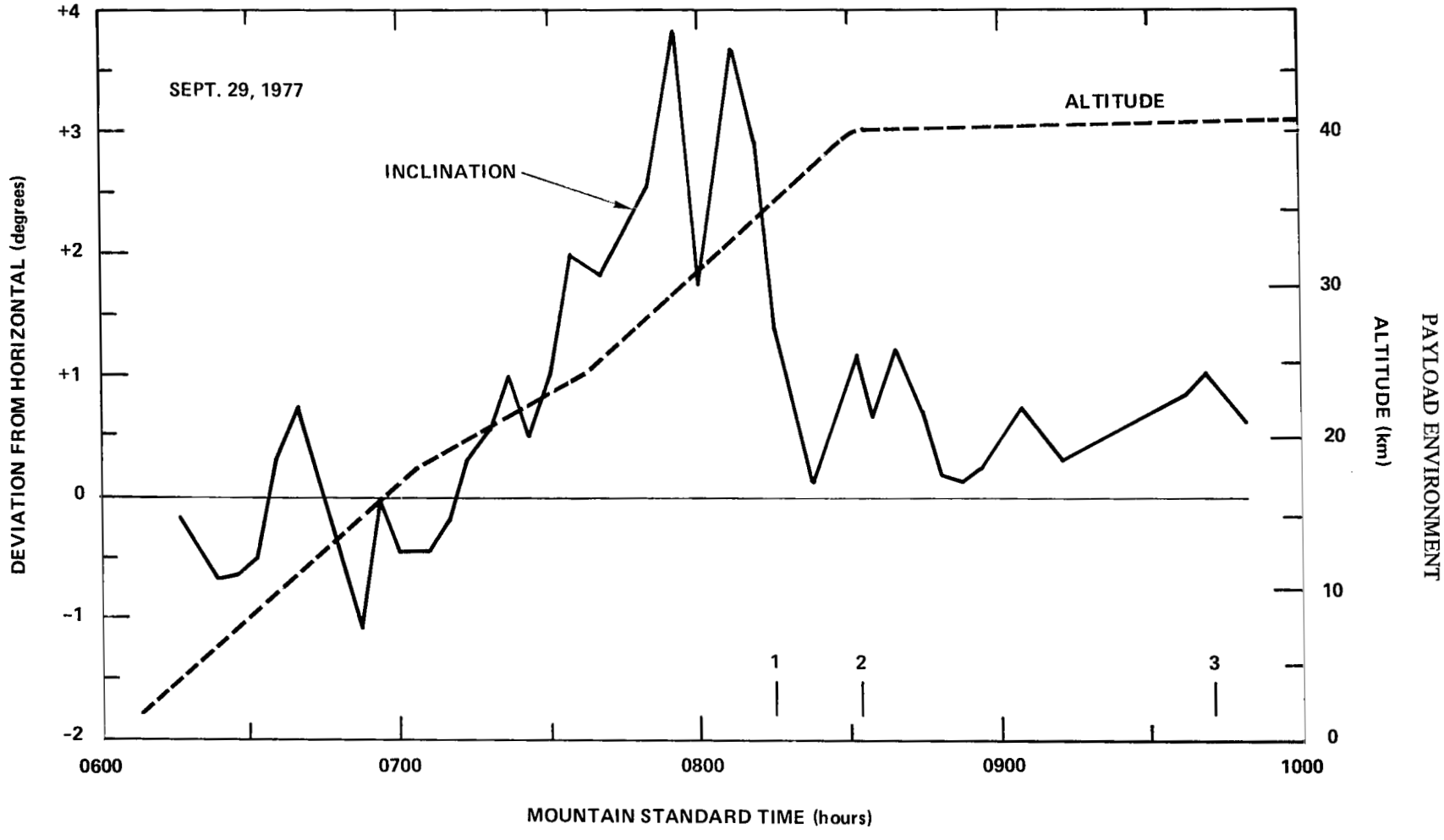

Figure 6. Levelness of the apex plate.

MAIN PAYLOAD MONITORS FOR STRATCOM VIII-A

Preston B. Herrington
Sandia Laboratories
Albuquerque, New Mexico 87185

ABSTRACT

The Stratcom VIII-A Balloon was flown September 29-30, 1977, from Holloman Air Force Base, New Mexico. A portion of the telemetered information was dedicated to the monitoring of various aspects of the main payload. It was found that temperatures at various locations on the payload ranged from more than +40°C to less than -50°C, depending on surface finishes and insulation. The power system functioned as planned. Command receiver monitors showed intermittent and unusual behavior, finally resulting in a loss of command capability. Orientation monitors showed that the payload tilted less than 1° from horizontal and that its rate of rotation about the vertical axis increased to a maximum of nearly one per minute about an hour after launch, then decreased and was variable in direction and rate throughout the remainder of the flight.

INTRODUCTION

A number of parameters were observed primarily for assessing the status of the Stratcom VIII-A main payload. These included bead thermistors for the temperature at selected points, voltage and current monitors in the power system, signal strength monitors, and, for altitude, a two-axis magnetometer and a two-axis pendulum.

TEMPERATURES

To monitor system status, bead thermistors with a range of -50 to +50°C were located as listed in Table 1.

Sensors 1 and 2 were located inside the main electronics housing (TM can), a cylindrical container pressurized at 1 atm (15 psia). The top and sides of the TM can were aluminum and were painted on the outside surfaces with EPO-LUX No. 100 white epoxy paint. Approxiamtely 3.8 cm of styrofoam insulation was used around the inside of the top and sides of the can. The bottom of the TM can was alodyne (conductive chromate) aluminum and internally was about half-covered with 2.5-cm-thick Styrofoam. The extensive insulation kept the temperature excursion to less than 20°C.

Table 1
Temperature Sensors on Main Payload

Sensor	Location	Observed range (°C)
1	TM can near top	+10 to +37.5
2	TM can near base	
3	Frame, near the TM can	less than -50 to +35 (figure 1)
4	Battery 1 container	+15 to +40
5	UV spectrometer electronics	less than -50 to +40 (figure 2)

Sensor 3 was located on the aluminum frame near the base of the TM can. The frame was bare aluminum with no special surface treatment. Its temperature initially followed the air temperatures (which went down to about -75°C at the tropopause) and at higher altitudes was more dependent on the presence or absence of sunlight. Its excursions as a function of time are shown in Figure 1.

Sensor 4 was mounted inside the Battery 1 container, which was mounted on the gondola adjacent to the TM can. This container housed 18 Yardney LR-100 cells which were insulated from the walls of the container by 6.4 cm of Styrofoam. All surfaces of the container were alodyne aluminum. The container was heated (with heating tapes wrapped around the exterior) prior to launch to a sensor reading of 28°C. Very little power (700 mW peak) was dissipated inside the battery container during the flight.

Sensor 5 was located on the electronics package of the UV grating spectrometer located at the top of the gondola. The spectrometer and its electronics were housed in a pressurized aluminum can with an alodyne exterior surface and white-painted top plate. No Styrofoam was included. Its temperature excursions are shown in Figure 2. The instrument was turned off after sunset, and its temperatures probably dropped to somewhat below the -50°C range of the temperature sensor.

POWER SUPPLY

Primary power for the experiments was supplied by three battery packages. Battery 1 was made up of 18 Yardney LR-100 silver-zinc cells, and Batteries 2 and 3 were made up of 18 Yardney LR-20 silver zinc cells. Each LR-100 cell has an average voltage of 1.5 V and a capacity of 100 A-hr. Each LR-20 cell has an average voltage of 1.5 V and a capacity of 20 A-hr.

ATTITUDE MEASUREMENTS

Attitude information is needed for the interpretation of the data from the various ultraviolet-sensing instruments and the two down-looking pyranometers. Spin information is needed for use with the anemometer data.

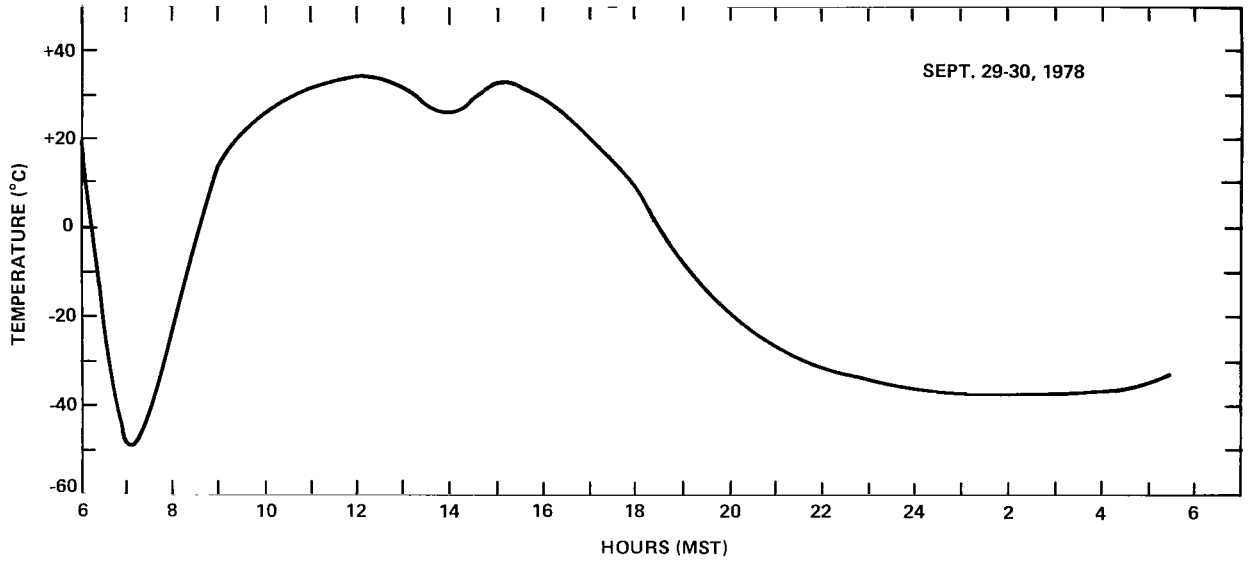

Figure 1. Temperature of the frame of the main instrument package on Stratcom VIII-A.

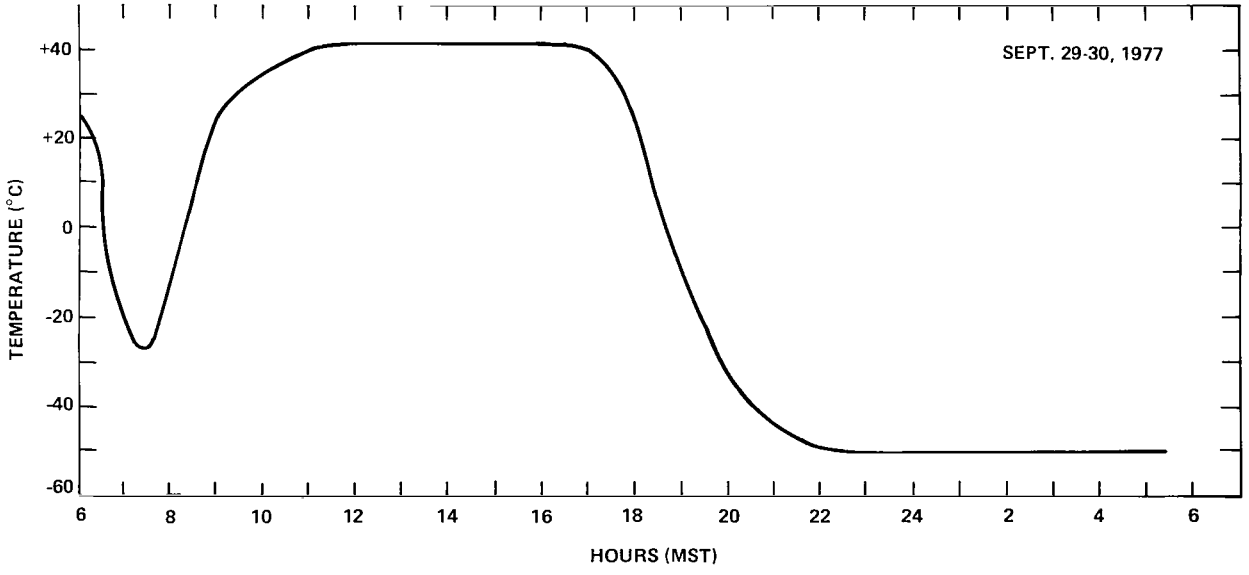

Figure 2. Temperature of the electronics package of the UV spectrometer on Stratcom VIII-A.

Pendulum

A two-axis potentiometric pendulum was used to determine the levelness of the instrument frame. Offsets at significant times during the flight are listed in Table 2.

Table 2
Tilt of Main Payload

Event	X-axis Offset, Degrees	Y-axis Offset, Degrees
Launch 0615 MST, Sept. 29	0.23	0.15
Drop no. 1 (0815 MST)	0.55	0.60
Drop no. 2 (0832 MST)	0.37	0.90
Drop no. 3 (0945 MST)	0.24	0.6 (momentary)
1910 to 2200 MST	Varied linearly to 0.60	No change
0600 MST, Sept. 30	0.60	0.90

Magnetometers

Two Heliflux RAM-5C magnetometers were mounted orthogonally to determine the orientation of the payload relative to magnetic north, in a manner similar to that used for the earlier (Stratcom V, VI, and VII) flights.

The details of the orientation throughout the flight are shown in Figure 3a and b. Initially, the rates were rather high as the suspension of the gondola twisted and untwisted, and slowed gradually. By the early morning of September 30, four hours were required for a single rotation. These same data in terms of rate and magnitude are shown in Figure 4.

The system 28-V monitor shows that the voltage varied from 32 V at launch to 24 V at 0636 on September 30. The power system failed shortly after 0636 because of inability to switch to the second battery pack by remote command.

SIGNAL STRENGTH

The command system in the main gondola received and processed signals as planned on the morning of the flight. In the early afternoon it was found that the separate command system for balloon control (helium valves and ballast release) was of no effect. Later investigation showed that this was due to a short circuit in the explosive squib for activation of the reel-down system, draining the battery for activating the valves and ballast release. The main gondola command system continued to

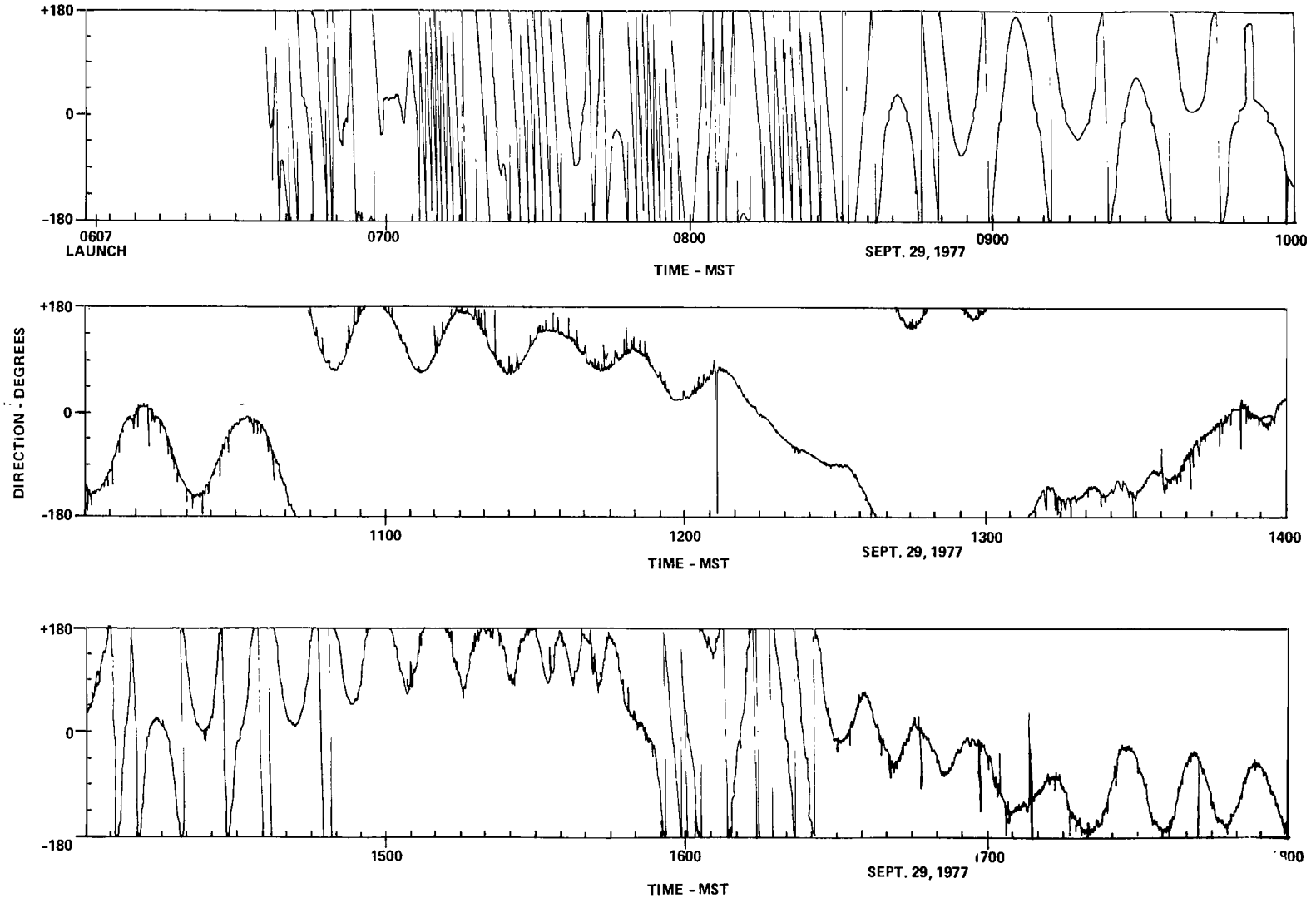

Figure 3a. Azimuth of the Stratcom VIII-A gondola with respect to magnetic north.

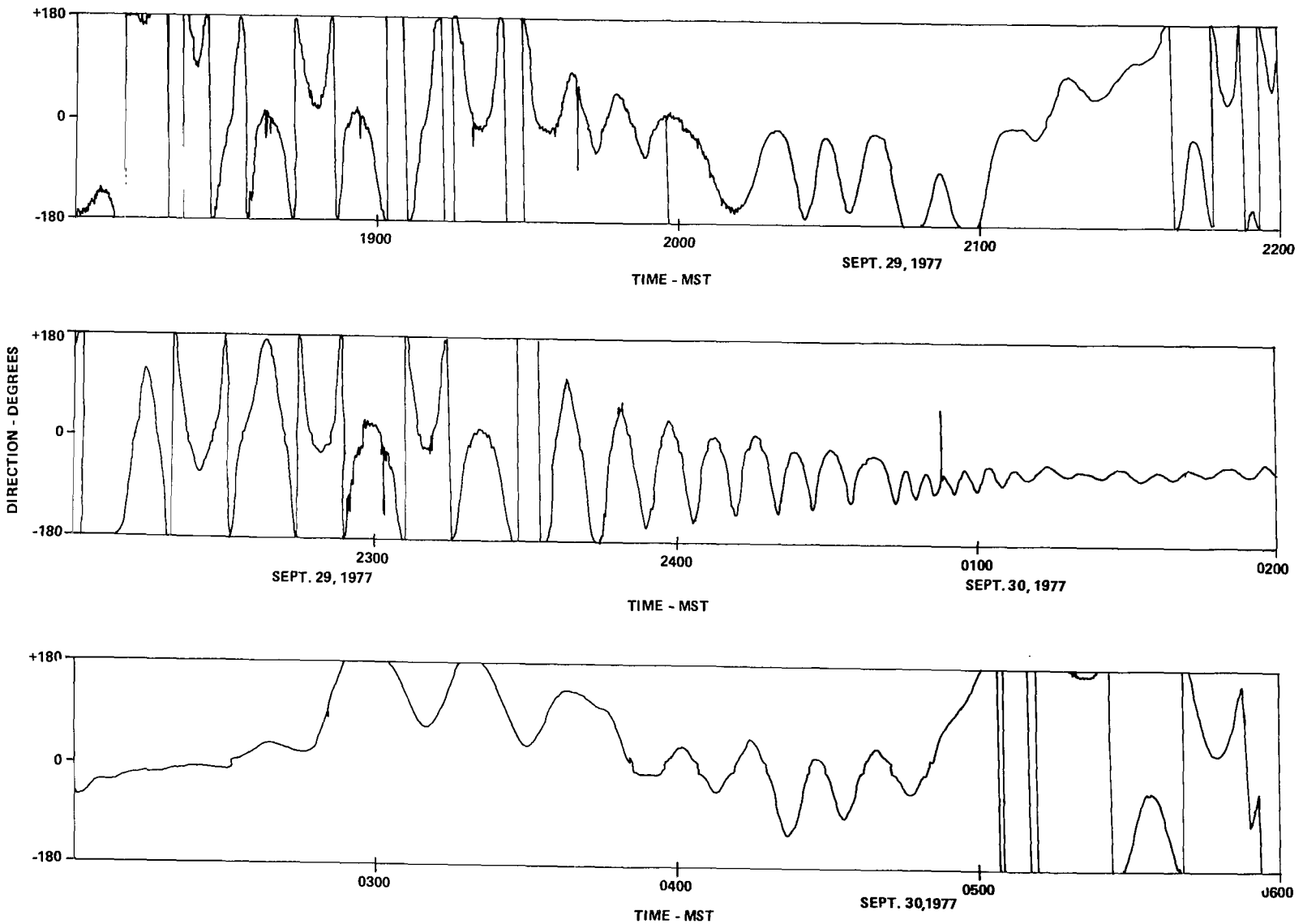

Figure 3b. Azimuth of the Stratcom VIII-A gondola with respect to magnetic north.

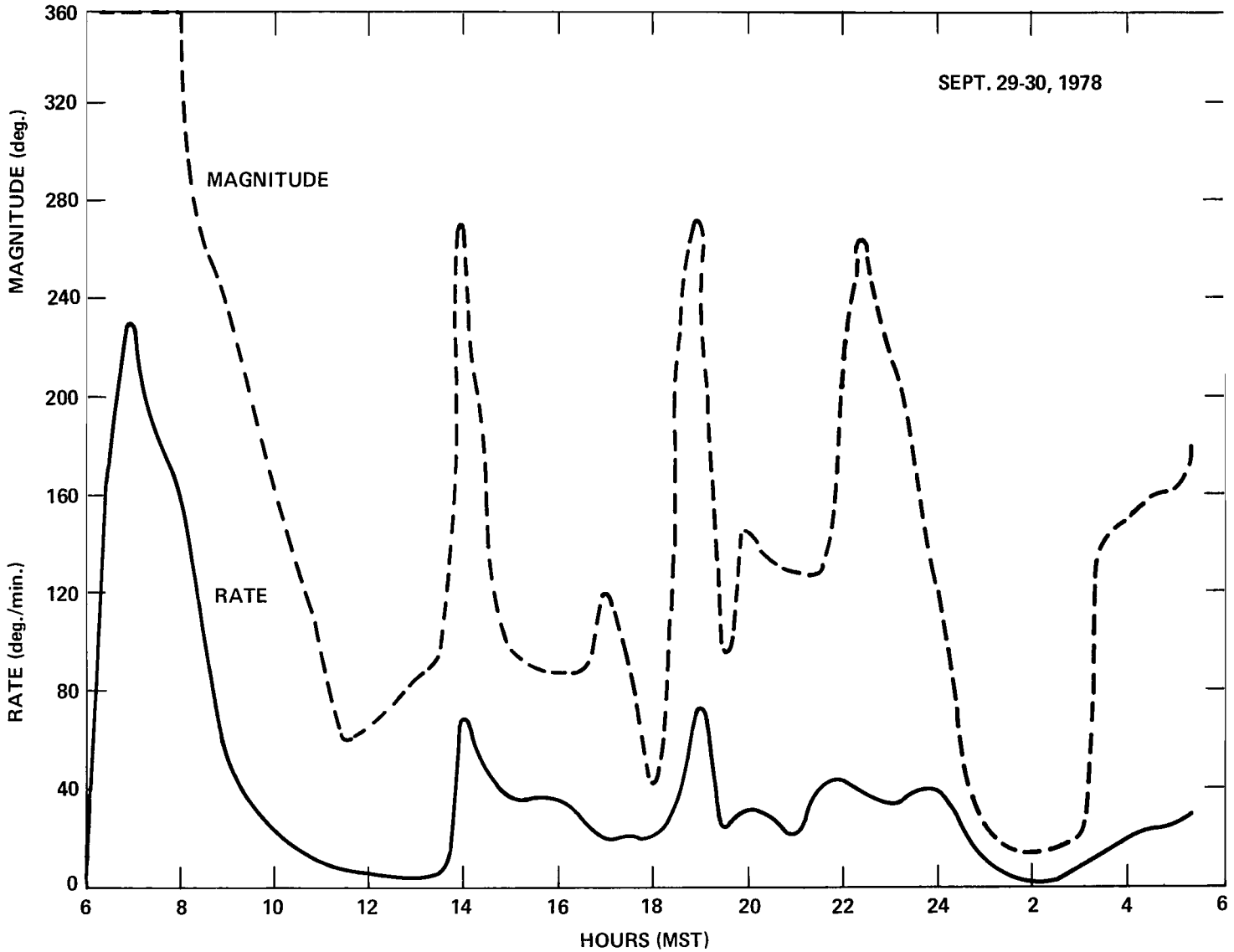

Figure 4. Magnetitude and rate of oscillation of the main instrument package on Stratcom VIII-A as measured by magnetometers.

function generally as expected until the early morning of September 30. At this time the balloon was beyond the San Andreas Mountain Range and was about 100 km from the transmitter. The command receiver signal strength monitor and two other monitors showed intermittent and unusual results, and commands were no longer of any effect. Postflight analysis indicates that the repositioning of the antennas to avoid collision with Dropsonde No. 1 may have been responsible for the reduced range.

ANEMOMETER MEASUREMENT OF AIR FLOW

Carlos McDonald
Electrical Engineering Department
University of Texas at El Paso
El Paso, Texas 79968

ABSTRACT

A three-axis anemometer was included on the Stratcom VIII-A Balloon to measure air flow relative to the instrument platform. Data were obtained for the horizontal and the upward vertical wind components during the flight of this payload September 29, 1977.

INTRODUCTION

Three identical instruments were arranged as a 3-axis anemometer for monitoring the air flow (see Figure 1). Air flow measurements were desired to provide information about the balloon's deviation from a Lagrangian (motionless with respect to air mass) state of the balloon and on boundary layer phenomena. The instruments were flown on Stratcom VIII-A Balloon from Holloman Air Force Base on September 29, 1977.

INSTRUMENTS

Each anemometer uses matched pairs of bead thermistors (0.25 mm diameter) exposed to the wind flow and operated in a constant temperature mode. These matched pairs, operating at different temperatures, are used to eliminate the dependence on ambient temperature and pressure (see Figure 2). Air density dependence is accounted for by use of an enclosed reference pair of thermistors. Calibration is based on the measurement of the difference in the power of the matched thermistors as a function of wind velocity, atmospheric pressure, and temperature. The anemometers were mounted parallel to the x, y, and z axes of the gondola.

RESULTS

Useful data were obtained from the anemometers which measured in one horizontal (x) and the vertical (z) directions. Due to a circuit malfunction, data were not obtained from the other horizontal (y) nor from a second pair of thermistors mounted in the vertical anemometer. Neither were data obtained from the high-sensitivity channels. Data on relative speed of the air flow, corrected for both temperature and density effects, are plotted as a function of time in Figure 3. Ten-second averaging of data was used, and only the ascent and initial float data are shown. Reduction and analysis of the remaining data is in process.

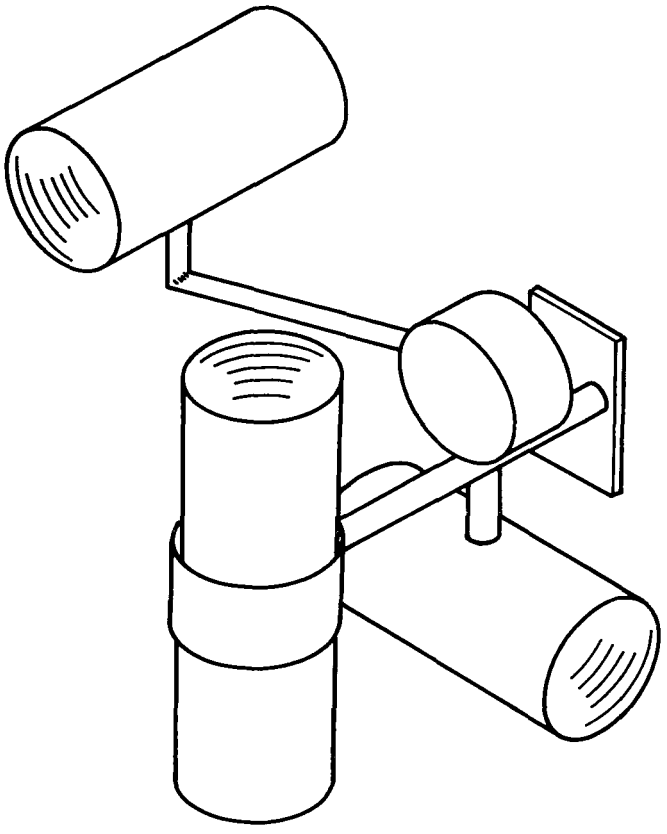

Figure 1. Three-axis anemometer.

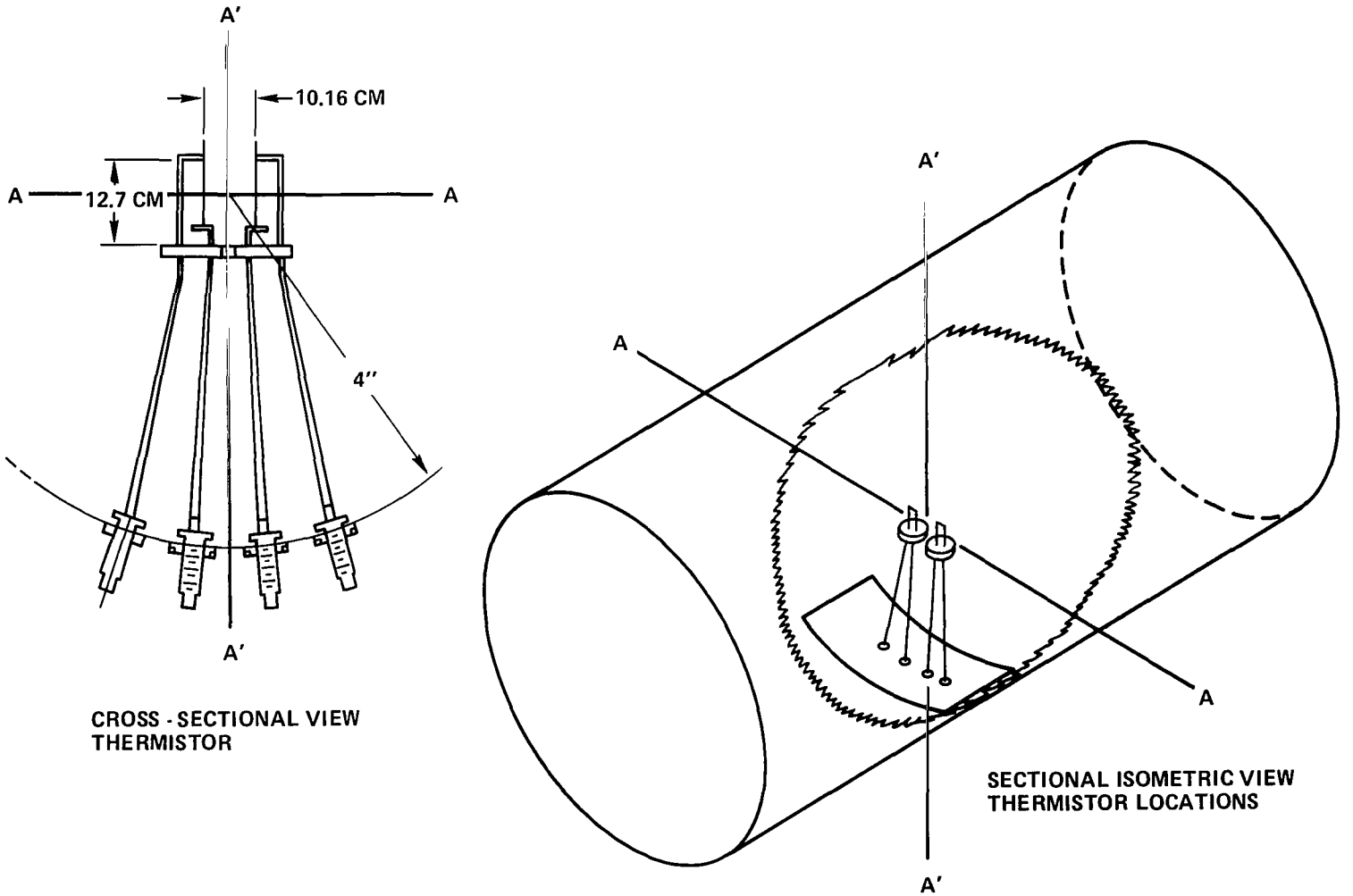

Figure 2. Thermistor detail.

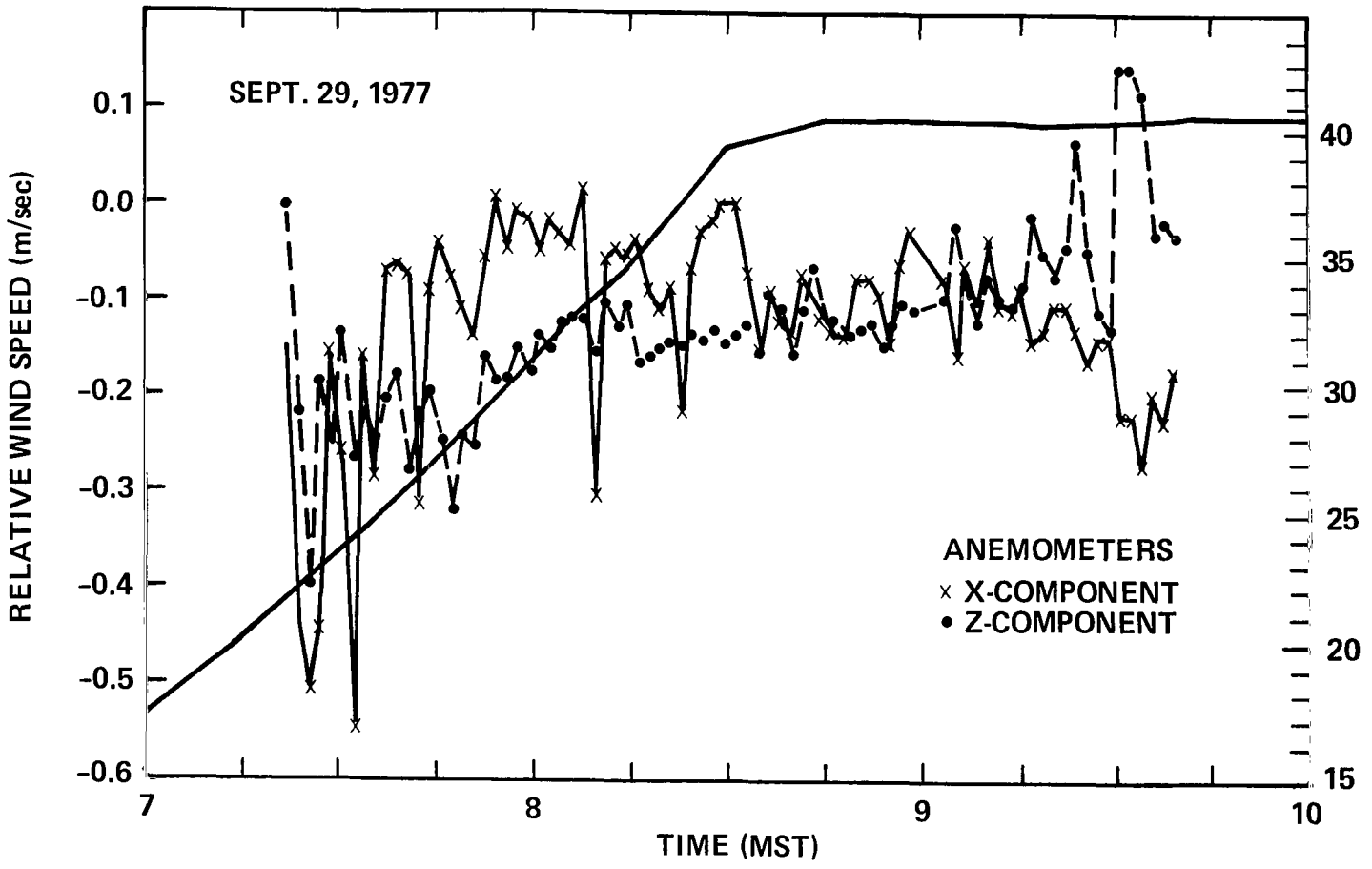

Figure 3. Air flow in the x- and z-direction.

BIBLIOGRAPHY

1969

Randhawa, J. S., "Ozone Measurements from a Stable Platform near the Stratopause," *J. Geophys. Res.*, **74**, 1969, pp. 4588–4590.

1970

Ballard, H. N., N. J. Beyers, and M. Izquierdo, "A Constant-Altitude Balloon Experiment at 48 km," (Proceedings of the Sixth AFCRL Scientific Balloon Symposium), AFCRL-70-0543, L. A. Grass, Editor, October 27, 1970, pp. 33–47.

Ballard, H. N., N. J. Beyers, M. Izquierdo, and J. Whitacre, "A Constant-Altitude Balloon Experiment at 48 km," *J. Geophys. Res.*, **75**, 1970, pp. 3501–3512.

Reynolds, R. D., and A. L. Wallis, Jr., "An Analysis of the Boundary Layer Associated with Floating Balloon System," (Proceedings of the Sixth AFCRL Scientific Balloon Symposium), AFCRL-70-0543, L. A. Grass, Editor, October 27, 1970, pp. 471–476.

1971

Ballard, H. N., N. J. Beyers, B. T. Miers, M. Izquierdo, and J. Whitacre, "Atmospheric Tidal Measurements at 50 km from a Constant-Altitude Balloon," December 1971, ECOM-5417 (U.S. Army Electronics Command, Fort Monmouth, N. J.), AD-739486.

Randhawa, J. S., "Ozone Measurements Near Sunrise," *Nature* (Phys. Sci.), 233, 1971, p. 101.

1972

Ballard, H. N. N. J. Beyers, B. T. Miers, M. Izquierdo, and J. Whitacre, "Atmosphere Tidal Measurements at 50 km from a Constant-Altitude Balloon," *J. Appl. Met.*, **11**, 1972, pp. 1138–1149.

1974

Ballard, H. N., M. Izquierdo, C. McDonald, and J. Whitacre, "Atmospheric Temperatures Measured Near 48 km by Balloon-Borne Thermistors," (Proceedings of the Eighth AFCRL Scientific Balloon Symposium, September 30 to October 3, 1974), AFCRL-TR-74-0393, A. S. Carten, Jr., Editor, pp. 401–416.

Herrington, Preston B., "Balloon Gondola Measurements," (Proceedings of the Eighth AFCRL Scientific Balloon Symposium, September 30 to October 3, 1974), AFCRL-TR-74-0393, A. S. Carten, Jr., Editor, pp. 511-516.

Patel, C. K. N., E. G. Burkhardt, and C. A. Lambert, "Spectroscopic Measurements of Stratospheric Nitric Oxide and Water Vapor," *Science,* **184**, 1974, pp. 1173-1176.

Woods, R. O., "A Cryopump for Balloon-Borne Mass Spectrometer," R. S. I., **45**, 1, January 1974, pp. 136-137.

Woods, R. O., "Flight Mass Spectrometry at Sandia Laboratories," SAND 74-0175, (OUO), October 1974.

Woods, R. O., "Design and Operating Characteristics of a Balloon-Borne Vacuum System," (Proceedings of the Eighth AFCRL Scientific Balloon Symposium, September 30 to October 3, 1974), AFCRL-TR-74-0393, A. S. Carten, Jr., Editor, pp. 495-509.

1975

Ballard, H. N., F. P. Hudson, "Stratospheric Composition Balloon-Borne Experiment, September 18, 1972," ECOM-5554 U.S. Army Electronics Command, Fort Monmouth, N. J., AD-A 008021, January, 1975 contains the following papers:

"Introduction," H. N. Ballard and F. P. Hudson, pp. 1-9.

"Summary of State of Health Measurements, Stratospheric Composition Balloon Experiment," by P. B. Herrington, PP. 10-13.

"Atmospheric Temperatures Measured Near 48 kilometers by Balloon-Borne Thermistors," by H. N. Ballard, M. Izquierdo, C. McDonald, and J. Whitacre, pp. 14-28.

"Stratospheric Balloon Pressure Measurements and Derived Density in the 40- to 48-Kilometer Altitude Interval," by R. Rubio and C. L. Tate, pp. 29-41.

"Ozone Particle Densities Measured by Chemiluminescent Sensors on a Balloon at 48 Kilometers," by J. S. Randhawa and M. Izquierdo, pp. 42-48.

"Solar Ultraviolet Irradiance and Ozone Particle Concentration Observations at 48-Kilometer Balloon-Float Altitude," by R. L. Schellenbaum, pp. 49-58.

"A Comparison of Measured and Calculated Ozone Particle Densities During Sunrise," by J. L. Collins and M. A. Ellis, pp. 59-67.

"Determination of Neutral Constituent Concentrations in 45- to 60-Kilometer Interval with Rocket- and Balloon-Borne Samplers," by H. N. Ballard, R. W. Byrnes, M. Izquierdo, J. Whitacre, and C. McDonald, pp. 68–80.

"Electrical Conductivity Measurements from the September 1972 Stratospheric Balloon Experiment," by J. D. Mitchell and L. C. Hale, pp. 81–89.

"Water Vapor Measurements During a 48-km Balloon Flight," by P. Goodman, pp. 90–97.

"Solar and Cosmic Radiation Prevailing During the September 1972 Stratospheric Balloon Experiment," by R. Rubio, H. N. Ballard, J. Whitacre, and M. Izquierdo, pp. 98–106.

"Mass Spectrometer Data," by R. O. Woods, p. 107.

Burkhardt, E. G., C. A. Lambert, and C. K. N. Patel, "Stratospheric Nitric Oxide: Measurements During Daytime and Sunset," *Science,* **188**, 1975, 1111–1113.

Collins, J. L., "High Latitude Photodissociation Rates, *EOS,* **56**, 1975, 996.

Myers, R. D., and D. K. Werling, "Design of a Linear Ramp Current Supply for Balloon-Borne Instruments SAND-75-0659, Sandia Labs., Albuquerque, New Mexico, 13 pp.

1976

Ballard, H. N., M. Izquierdo, C. McDonald, and J. Whitacre, "Temperature Measurements in the Stratosphere from Balloon-Borne Instrument Platforms, 1968-1975," ECOM-5808, U.S. Army Electronics Command, Fort Monmouth, New Jersey 07703, December 1976, 45 pp. AD-A036-333.

Ballard, H. N., P. B. Herrington, F. P. Hudson, A. O. Korn, "The Stratcom VI Program of Correlated Measurements of Stratospheric Composition and Other Parameters Between 25 and 39 Kilometers; September 24 and 25, 1975," *EOS,* **57**, 1976, p. 156.

Gille, J. C., and P. L. Bailey, "Stratospheric Observations," by Nimbus-6 LRIR Related to Stratcom VI, *EOS,* **57**, 1976, p. 156.

Goodman, P., and M. Izquierdo, "Water Vapor Concentrations in Various Positions in the Balloon Train During the Stratcom VI-A Flight," *EOS,* **57**, 1976, p. 156.

Izquierdo, M., C. McDonald, Z. Salpeter, and H. N. Ballard, "Atmospheric Temperature Measurement During the Stratcom VI-A Flight," *EOS,* **57**,1976, p. 156.

McDonald, C., H. Carrasco, M. Izquierdo, and H. N. Ballard, "Electron Forward-Scatter and α-Particle Absorption Measurements of Atmospheric Density (Stratcom VI)," *EOS*, 57, 1976, p. 156.

Mitchell, J. D., C. L. Croskey, and L. C. Hale, "Electrical Conductivity Measurements in the Middle Stratosphere," *EOS*, 57, 1976, p. 156.

Randhawa, J. S., and M. Izquierdo, "Ozone Measurements at 48 km," *J. Photochemistry*, 6, 1976, p. 148.

Randhawa, J. S., M. Izquierdo, and C. McDonald, "Stratospheric Ozone Density as Measured by Chemiluminescent Sensors," *EOS*, 57, 1976, p. 156.

Rubio, R., and M. Izquierdo, "Measurement of Atmospheric Limb Radiance in the 0.28 to 2.80 Micron Infrared Region on Stratcom VI-A," *EOS*, 57, 1976, p. 156.

Schellenbaum, R. L., B. D. Zak, "Ozone Particle Density Derived from Solar Ultraviolet Absorption Measurements in Stratcom VI," *EOS*, 57, 1956, p. 156.

Sellers, B., F. A. Hanser, J. L. Hunerwadel, "Solar Ultraviolet Fluxes in the 200–400 nm. Range Measured on Stratcom VI-A," *EOS*, 57, 1976, p. 156.

Williams, W. J., J. J. Kosters, A. Goldman, D. G. Murcray, "Simultaneous Stratospheric Measurements of Fluorocarbons and Odd Nitrogen Compounds," *EOS*, 57, 1976, p. 156.

Williams, W. J., J. J. Kosters, A. Goldman, and D. G. Murcray, "Measurements of Stratospheric Fluorocarbon Distributions Using Infrared Techniques," *Geophys. Res. Lett.*, 3, 1976. pp. 379–382.

Williamson, E., C. McDonald, and M. Izquierdo, "Earth Albedo Measurements in the 0.28 to 2.80 Micron Region on Stratcom VI-A," *EOS*, 57, 1976, p. 156.

Zak, B. D., R. L. Schellenbaum, "Stratospheric Solar Ultraviolet Radiation in the Fluorocarbon Dissociation Range: Preliminary Results from Stratcom VI," *EOS*, 57, 1976, p. 156.

1977

Ballard, H. N., F. P. Hudson, "Stratospheric Composition Balloon-Borne Experiment, 23–26 September 1975" ECOM-5830 U.S. Army Electronics Command, Fort Monmouth, N. J. 07703, October 1977 AD-A047030 contains the following papers:

"Experiment Background and Description," H. N. Ballard, F. P. Hudson, and A. Korn, pp. 2-9.

"Summary of System State-of-Health Measurements Stratcom VI-A Balloon Experiment," P. B. Herrington, pp. 10-20.

"Temperature Measurements in the 27-40 km Altitude Interval, Stratcom VI-A Balloon-Borne Experiment," H. N. Ballard, M. Izquierdo, C. McDonald, and J. Whitacre, pp. 21-28.

"Ion Anemometry as a Means of Determining Relative Winds during a Stratospheric Balloon Experiment," R. O. Woods and D. S. Miyoshi, pp. 29-47.

"Measurements of Net Atmospheric Irradiance in the 0.7- to 2.8-micrometer Infrared Region," R. Rubio and M. Izquierdo, pp. 48-57.

"Measurement of 200–400 nm Solar UV Fluxes at Altitudes up to 40 km," F. A. Hanser, B. Sellers, and J. L. Hunerwadel, pp. 59-74.

"Stratospheric Ozone Density as Measured by a Chemiluminescent Sensor during the Stratcom VI-A Flight," J. S. Randhawa, M. Izquierdo, C. McDonald, and Z. Salpeter, pp. 75-86.

"Measurements of Water Vapor Concentrations during the Stratcom VI-A Experiment," P. Goodman, pp. 87-97.

"Cryogenic Collection of Whole Air Aboard Stratcom VI-A," L. E. Heidt, W. H. Pollock, and R. A. Lueb, pp. 98-103.

"Electrical Conductivity Measurements in the Middle Stratosphere," J. D. Mitchell, C. L. Croskey, and L. C. Hale, pp. 104-110.

"Measurements of Stratospheric Fluorocarbon Distributions using Infrared Techniques (Stratcom VI-B)," W. J. Williams, J. J. Kosters, A. Goldman, and D. G. Murcray, pp. 111-119.

Ballard, H. N., M. Izquierdo, F. Hudson, and A. Korn, "Stratcom VII-Experiment Description (Balloon Systems, Instruments, Trajectory, Supporting Measurements)," *EOS,* 58, 1977, 451.

Ballard, H. N., J. N. Serna, and F. P. Hudson, "Calculation of Selected Atmospheric Composition Parameters for the Mid-Latitude September Stratosphere," ECOM-5818, U.S. Army Electronics Command, Fort Monmouth, N. J. 07703, May 1977, 41 pp. AD-A041081.

Buijs, H., and G. Vail, "Measurement of Density Profiles of HF and HCl in the Stratosphere," *EOS,* 58, 1977, 453.

Carrasco, H., G. Cordoba, "Vertical Velocities of the Stratcom VII-A Balloon Calculated from Radar Data," *EOS,* 58, 1977, 451.

Collins, J. L., "Stratcom-Related Photodissociation Rates and Solar Flux Intensities," ECOM-77-1, U.S. Army Electronics Command, Fort Monmouth, N.J. 07703, February 1977, 32 pp. AD-A 037644.

Gildenberg, D., "Analysis of the Meteorological Conditions Associated with the Stratcom VII-A Balloon-Borne Experiment, September 28-29, 1976," *EOS,* 58, 1977, 451.

Goodman, P., "The Water Vapor Environment of the Stratcom VII-A Flight," *EOS,* 58, 1977, 452.

Heidt, L., W. Pollock, and R. Lueb, "Cryogenic Collection of Whole Air Aboard the Stratcom VI-A and VII-A Balloon-Borne Experiments," *EOS,* 58, 1977, 452.

Herrington, P., and R. Meyers, "State of Health Measurements Aboard the Stratcom VII-A Payload," *EOS,* 58, 1977, 451.

Izquierdo, M., H. Ballard, and J. Randhawa, "A Qualitative Interpretation of the Ozone Number Density and Temperature Profiles Measured Aboard Stratcom VII-A as Related to Indicated Atmospheric Vertical Transport," *EOS,* 58, 1977, 452.

McDonald, C., M. Izquierdo, Z. Salpeter, and H. Ballard, "Air Temperature History Associated with the Stratcom VII-A Balloon Flight," *EOS,* 58, 1977, 451.

Megill, R., K. Montierth, K. Baker, and J. Randhawa, "Measurement of Scatter UV Flux in the Stratosphere," *EOS,* 58, 1977, 452.

Mitchell, J. D., K. J. Ho, C. L. Croskey, and L. C. Hale, "Electrical Conductivity Measurements from the Stratcom VII Experiment," *EOS,* 58, 1977, 452.

Murcray, D., A. Goldman, J. Kosters, and W. Williams, "Stratospheric Distribution of Several Minor Constituents and Pollutants as Determined from Infrared Solar Spectra," *EOS,* 58, 1977, 452.

Randhawa, J. G., "Stratospheric Ozone Density as Measured by a Chemiluminescent Sensor During the Stratcom VI-A Flight," ECOM-5816, U.S. Army Electronics Command, Fort Monmouth, N. J. 07703, 1977, 12 pp. AD-A040663.

Randhawa, J., M. Izquierdo, Z. Salpeter, and C. McDonald, "Stratospheric Ozone Density as Measured by Chemiluminescent Sensors During the Stratcom VII-A Flight," *EOS,* 58, 1977, 452.

Reed, E. I., "Stratcom-VIII Scientific Objectives and Mission Organization", GSFC X-624-77-261, Oct. 1977, 104 pp. (N78-11544).

Rubio, R. and M. Izquierdo, "Measurements of Net Atmospheric Irradiance in the 0.7- to 2.8-micrometer Infrared Region", ECOM-5817, U.S. Army Electronics Command, Fort Monmouth, N. J. 07703, May 1977, 11 p. AD-A041076.

Rubio, R., C. McDonald, and Z. Salpeter, "Stratcom VII-A Measurements of Shortwave Radiation in the 10-39 km Altitude Interval," *EOS*, 58, 1977, 452.

Sellers, B., F. Hanser, and J. Hunerwadel, "Solar UV Flux and Total Ozone Measurements from Stratcom VII-A," *EOS*, 58, 1977, 452.

1978

Murcray, D. G., F. H. Murcray, F. I. Murcray, and W. J. Williams, "Infrared Background Measurements," AFGL-TR-78-0249, Sept. 1978, 21 pp. Air Force Geophysics Laboratory, Hanscom AFB, Mass. 01731, Final Report 15 Dec 1976 – 30 June 1978, Contract F19628-C-0016. with Univ. of Denver, Denver, Colorado 80208.

Reed, E. I., "Stratcom VIII Data Workshop, April 13-14, 1978" NASA CP 2043, April 1978, 108 pp.

Woods, R. O., "In-Situ Mass Spectrometry at Stratospheric Altitudes," *Atmospheric Technology*, 9, 20-26, 1978.

1979

Ballard, H.N., M. Izquierdo, A. Korn, D. Murcray, and W. Page, Stratospheric composition balloon, aircraft, and rocket-borne experiments, 28-30 September 1977 (Stratcom VIII). (Systems, instruments, trajectories, supporting measurements), Proceedings, Tenth AFGL Scientific Balloon symposium, 21 August to 23 August 1978, AFGL-TR-79-0053, March 1979, pp. 293-314.

Mitchell, J.D., L.C. Hale, and C.L. Croskey, Stratospheric electrical conductivity measurements by balloon-borne blunt probes, Proceedings, Tenth AFGL Scientific Balloon Symposium, 21 August to 23 August 1978, AFGL-TR-79-0053, March 1979, pp. 281-292.

Rubio, R., C. McDonald, and M. Izquierdo, "Concept for Determination of Earth's Budget and Albedo as a Function of Altitude with Balloon-Borne Pyranometers," *EOS*, 60, 263, 1979.

York, T. M., R. O. Olsen, and J. D. Mitchell, "Electron Density Determination in the Middle Atmosphere Using Rocket Borne Blunt Probes," *EOS*, 60, 338, 1979.

1. Report No. NASA TP-1640	2. Government Accession No.	3. Recipient's Catalog No.
4. Title and Subtitle The Stratcom VIII Effort		5. Report Date April 1980
		6. Performing Organization Code 963
7. Author(s) Edith I. Reed, Editor		8. Performing Organization Report No.
9. Performing Organization Name and Address Goddard Space Flight Center Greenbelt, Maryland 20771		10. Work Unit No. 11. Contract or Grant No.
12. Sponsoring Agency Name and Address National Aeronautics and Space Administration Washington, D.C. 20546		13. Type of Report and Period Covered Technical Paper 14. Sponsoring Agency Code

15. Supplementary Notes

16. Abstract

In the Stratcom VIII effort of September 1977, scientists and engineers from about 20 organizations used nearly 40 kinds of instruments to investigate the stratosphere. The principal objective was to obtain data related to atmospheric photochemistry. This report (1) summarizes the effort, describing balloon, rocket, and aircraft operations; (2) includes detailed lists of organizations, instruments, and parameters; and (3) presents discussions by each participant concerning his experiment and results. Measurements were made of ozone content, solar ultraviolet spectral flux, nitric acid overburden, temperature, aerosol sizes, water vapor content, electron content, positive and negative conductivities, and characteristics of the boundary layer associated with a large balloon and its payload. Data from11 of the ozone sensors are intercompared and noted to differ by as much as a factor of 2 at some altitudes.

17. Key Words (Selected by Author(s))	18. Distribution Statement
Scientific balloons, stratosphere, ozone, nitrogen oxides, water vapor, conductivity, aerosols, ultraviolet spectrometery, infrared spectrometry, cryogenic sampler, chemiluminescent ozone detector	Star Category 47 Unclassified, Unlimited

19. Security Classif. (of this report)	20. Security Classif. (of this page)	21. No. of Pages	22. Price*
Unclassified	Unclassified	219	$9.25

*For sale by the National Technical Information Service, Springfield, Virginia 22161

NASA-Langley, 1980